



Universitat Autònoma de Barcelona

**ADVERTIMENT.** L'accés als continguts d'aquesta tesi queda condicionat a l'acceptació de les condicions d'ús establertes per la següent llicència Creative Commons:  [http://cat.creativecommons.org/?page\\_id=184](http://cat.creativecommons.org/?page_id=184)

**ADVERTENCIA.** El acceso a los contenidos de esta tesis queda condicionado a la aceptación de las condiciones de uso establecidas por la siguiente licencia Creative Commons:  <http://es.creativecommons.org/blog/licencias/>

**WARNING.** The access to the contents of this doctoral thesis it is limited to the acceptance of the use conditions set by the following Creative Commons license:  <https://creativecommons.org/licenses/?lang=en>



Universitat Autònoma  
de Barcelona

---

*Leonardo Pereira Costa da Cruz*

---

Bifurcations of limit cycles  
in planar differential  
and piecewise differential systems

Bellaterra

October 2018



# Bifurcations of limit cycles in planar differential and piecewise differential systems

*Leonardo Pereira Costa da Cruz*

Certifico que aquesta memòria ha estat realitzada per Leonardo Pereira Costa da Cruz sota la meua supervisió i que constitueix la seva tesi per a aspirar al grau de Doctor en Matemàtiques per la Universitat Autònoma de Barcelona.

Bellaterra, Octubre 2018

Dr. Joan Torregrosa i Arús



Dedico aos meus pais, Jailson e Mirna.



# Agradecimentos

---

Particularmente acredito que exista uma relação entre graça e gratidão que trás sentido as nossas vidas e é exatamente essa relação que me motiva a escrever esses agradecimentos. Pelo simples motivo de ser a fonte de toda a minha inspiração e o provedor do ar que respiro gostaria primeiramente de agradecer a Deus.

Aos meus pais *Jailson* e *Mirna* por todo o sacrifício, por sempre colocarem a vida do seus filhos como prioridade, por terem feito do meu ambiente familiar um lugar de bons valores, seguro, agradável e nunca apesar de todos os momentos difíceis da vida terem se rendido. Assim com absoluta certeza diria que o meu núcleo familiar foi fundamental, e essencial para que pudesse ter essa oportunidade e a possibilidade de obtenção desse titulo de Doutor em Matemática. Além desses claro a minha irmã *Natalia*, que me ensinou muito e sou um grande admirador, a minha avó *Florece* que dedicou muito do seu tempo para cuidar de mim, a memória dos meus avos hoje falecidos e também todos os meus familiares.

Em especial gostaria de agradecer ao meu orientador *Joan*, absolutamente não seria possível a obtenção desse titulo sem o seu companheirismo. Recordo nosso primeiro encontro pessoal em um congresso na cidade de Campinas em 2014 no Brasil, onde já sabíamos que iríamos trabalhar juntos, e deis de ali já se mostrou muito atencioso ao demonstrou seu interesse no meu trabalho em uma sessão de pôster através de relevantes perguntas como sempre, nosso segundo contato já seria em terras Catalananas na Espanha no aeroporto onde foi buscar-me. Ao longo desses quatro anos se demonstrou o melhor orientador que poderia ter tido e nos tornamos grande amigos, isso devido ao grau de exigência, sempre questionou, duvidou e colocar a prova os detalhes mais ocultos dos problemas tratado. Na verdade foram muitos questionamentos que levaram a reflexões, discussões, discórdias e concordâncias. Agradeço por todos os “explico?”, para quando notava que não entendia algo, os “mal”, para quando me equivocava e também os “muy bien”, para quando acertava, confesso que esse ultimo foram momentos mais raros e é exatamente por isso que volto a dizer que tive o melhor orientador que particularmente poderia ter tido.

I dedicate this work also to *Valery*, who welcomed me with open arms in Maribor in Slovenia for three months. This period was helpful and a great learning experience. It was the first time that getting all the support (the rides when it was difficult to return home due to snow, the hot teas and etc) had the wonderful experience of being in a place with temperature reached  $-17C^{\circ}$ . I had the opportunity there as well as meet new theories, produce and be reviewer of an article, submit my work, socialize with amazing and thoughtful people.

Agradeço a minha namorada *Tainã*, que sempre esteve ao meu lado apoiando e complementando os meus pensamentos, reconheço que sem a sua agradável companhia, seu admirável exemplo e ajuda teria sido muito mais difícil.

Aos meus pastores *Daniel*, *Ester*, suas filhas *Aida* e *Laia* que verdadeiramente dedicam suas vidas em prol de outras e vivem o verdadeiro evangelho de Jesus. Também, meus irmãos em cristo, *Sergio* e *Viviane* que praticamente me adotaram e foram referências de como valorizar e honrar a Deus, a minha amiga *Lídia* que em bons momentos de conversas e conselhos me ajudou muito, a minha querida amiga *Roberta*, seu marido *Dani* e sua filha amada *Eva* que me fez sentir muito amado, meus amigos mineiros *Gustavo* e *Bruna* por todos os pães de queijo feito com muito carinho, e minha amiga baiana *Sheila* e seu filho amado *Arthur* por todo carinho e lógico os bolos de chocolate inesquecíveis.

Não poderia esquecer os meus amigos de trabalho, *Fernando* meu querido amigo de longa data por todo o companheirismo, *Jackson* que foi o primeiro a me receber e ajudou muito na minha chegada, *Douglas* por levar-me a conhecer os primeiros pontos turísticos em Barcelona, *Murilo* pelo período agradável que convivemos juntos e as discussões matemáticas e *Nathália* sua namorada, *Ricard* por todos os agradáveis almoços juntos, *Alex* e sua esposa *Natália* que chegaram e em pouco tempo nos tornamos grandes amigos, ao meu amigo *Rodrigo* meu conterrâneo por ter sido uma referência acadêmica, *Wilker* e *Regilene* pela ajuda durante o período que passei na Eslovenia, e todos os outros amigos que ganhei nesse período *Durval*, *Lucyjane*, *Camila*, *Paulina*, *Otavio*, *Iván* entre outros que foram muito importante nesse período.

Aos meus amigos de fora do ambiente de trabalho, *Rafael* por todos os churrascos compartilhados, *Nubia*, *Francine*, *Julia*, *Gabi* pela convivência e por passarmos momentos tão agradáveis.

Gostaria de dizer que foi um grande prazer conviver com pessoas tão especiais, vou levar na memória todos os momentos que passamos juntos, foi um tempo de muita aprendizagem. Terminei esse ciclo mais que satisfeito e com o sentimento de dever cumprido pelo fato de ter amadurecido tanto profissionalmente, como pessoalmente. Apenas gostaria de dizer muito obrigado a todos meu coração está cheio de gratidão.

# Contents

---

---

<b>1</b>	<b>Introduction</b>	<b>1</b>
<b>2</b>	<b>Simultaneous bifurcation of limit cycles</b>	<b>9</b>
2.1	Introduction . . . . .	10
2.2	The general case . . . . .	13
2.3	Studying the internal and external regions separately . . . . .	16
2.4	Existence of simultaneous zeros in the internal and external regions . . . . .	24
2.5	Local study of the zero level curves in the bifurcation diagrams . . . . .	33
<b>3</b>	<b>Number of limit cycles in piecewise quadratic systems</b>	<b>39</b>
3.1	Introduction . . . . .	40
3.2	Preliminaries . . . . .	43
3.2.1	Averaging Theory . . . . .	43
3.2.2	ECT-Systems . . . . .	44
3.2.3	Pseudo-Hopf Bifurcation . . . . .	45
3.2.4	Poincaré–Miranda Theorem . . . . .	45
3.3	First order perturbation . . . . .	46
3.4	Second order perturbation . . . . .	54
3.5	Appendix: Explicit computations of the integrals . . . . .	66
<b>4</b>	<b>A Bendixson–Dulac theorem for some piecewise systems</b>	<b>71</b>
4.1	Introduction . . . . .	72
4.2	An extension of the Bendixson–Dulac theory . . . . .	76

---

4.3	The linear and rational families . . . . .	79
4.4	A piecewise version of the classical van der Pol oscillator . . . . .	85
<b>5</b>	<b>The center and cyclicity problems for quartic linear-like reversible systems</b>	<b>97</b>
5.1	Introduction . . . . .	98
5.2	Preliminaries . . . . .	101
5.2.1	The center conditions . . . . .	101
5.2.2	Degenerate Hopf bifurcation . . . . .	103
5.2.3	Darboux integrability . . . . .	104
5.3	Normal forms . . . . .	104
5.4	Centers classification . . . . .	105
5.4.1	Proving the center classification in the aligned case . . . . .	106
5.4.2	Proving the center classification in the triangular case . . . . .	107
5.5	Simultaneous cyclicity . . . . .	116
	<b>Summary</b>	<b>119</b>
	<b>Resum</b>	<b>121</b>
	<b>Resumo</b>	<b>123</b>
	<b>Bibliography</b>	<b>125</b>

# Introduction

---

---

The capacity of men to ask and answer is what pushes science. Taking into account that natural events depend continuously over time, it is clear that understanding natural phenomena of the past, present and future are big concerns of human beings. Mathematics, in turn, is without any doubt the basic language that describes this code behind natural events. Concretely, a field of mathematics that studies this is the so-called differential equations, which provides, for example, the rules for the evolution in time of a particle.

Since the 17th century, when I. Newton and G. Leibniz introduced the *differential calculus* more specifically in 1682, *differential equations* came to be a relevant and efficient tool to model in an abstract language what occurs in the real world, starting with the mechanical problems of bodies. Currently, the study of differential equations have become one of the fundamental pillars of the study of philosophy mathematics, because these equations have a big importance to the development of many areas of science, as well as engineering, biology, electronics, economy, etc.

When the derivation variable just plays an implicit role, the differential equation is said to be autonomous. The autonomous cases can be considered as dynamical systems and the time is taken as the derivation variable.

Ordinary differential equations of order  $n$  take the form

$$F(t, x, x', x'', \dots, x^{(n)}) = 0, \quad (1.1)$$

where  $x^{(n)}$  is the  $n$ th derivative of  $x$  with respect to  $t$ . The autonomous cases take place when  $F$  does not depend on  $t$ . If  $x$  is a vector instead of a real function, the equation (1.1) is called a differential system.

Only after approximately two hundred years of the statements of Newton and Leibniz, in the 19th century and more precisely around 1881, another brilliant mathematician appeared: H. Poincaré, who brought the splendor of the study of differential equations.

He realized that the qualitative properties of the solutions of a differential equation could be investigated, without such solutions having to be determined explicitly. Thus, instead of looking for the solution, he turned to a qualitative approach, using geometric and topological techniques. In his “Mémoire sur les courbes définies par une équation différentielle”, he

introduces these results which were a great breakthrough in the study of differential systems. Currently known as *Qualitative Theory of Differential Equations*.

Despite being applied to higher dimension fields, everything in his work was considered in equations in two variables, which means considering a system of the form (1.1) when the space where  $x$  is considered is  $\mathbb{R}^2$  or any contained open subset, and we refer to it as a planar differential system.

Let  $Z = (X, Y)$  be a first-order autonomous planar differential systems, defined by

$$\begin{cases} \dot{x} = X(x, y), \\ \dot{y} = Y(x, y), \end{cases} \quad (1.2)$$

where  $x(t)$ ,  $y(t)$ ,  $X(x, y)$  and  $Y(x, y)$  are real functions.

In order to understand this geometric point of view, let us consider the velocity field  $Z$ , which is the vector field whose components are  $X$  and  $Y$ , the functions in system (1.2). The solutions of the differential system are the trajectories of the vector field. It means that at any point the tangent vectors to the solution curves and the vector field are parallel. The trajectories are also known as the orbits of the vector field. The advantage of using orbits lies in the fact that if we change the time parametrization, they remain unchanged.

Among the contributions of Poincaré are the introduction of the concept of *phase portrait*, which is the sufficient information to determine the topological structure of the orbits of a differential equation. Moreover, he developed theoretical concepts such as *return map* or the *Annular Region Theorem*, which are fundamental for classifying orbits with particular behaviors. Some of them were characterized by Poincaré, as well as among others the equilibrium points and cycles.

*Equilibrium points* are the points where the vector field vanishes. They are also called singular, critical or fixed points. Cycles are the trajectories of the vector field that repeat themselves along time. Usually, they are also called closed or periodic orbits. Notice that equilibrium points are a particular type of cycles. For a point in a cycle after a finite time  $T$ , its orbit will be again on itself. For a fixed point, its orbit is on itself for every time  $t$  in  $\mathbb{R}$ .

The notion of *limit cycle* was also introduced in the first papers which dealt with qualitative theory. Essentially, a limit cycle,  $\gamma$ , is a periodic orbit such that at least one trajectory of the vector field, different from  $\gamma$ , approaches  $\gamma$  in positive or negative time. Usually, when the vector field is of class  $\mathcal{C}^1$  an alternative definition is given. A closed orbit is named limit cycle if it is isolated from the other periodic orbits. This definition is, in general, more restrictive than the previous one, but both are equivalent in the analytic case.

In the not too distant future in 1926, B. van der Pol provided a differential equation that describes a non-conservative oscillator and used graphical methods to prove the existence of a periodic orbit. Already in 1929, A. Andronov established the relation between the limiting cycles of Poincaré.

Contemporaneous with Poincaré, and using his contributions, I. Bendixon presented in 1901 the well-known Poincaré–Bendixon Theorem. The result states that the solutions

that really matter are called *singular or minimal sets* (critical points, periodic orbits and separatrix) defined a differential equation on a compact set has the property that the other solution goes to a singular solution. Consequently, the phase portrait is now determined by the set of singular solutions.

*Thus, in a more specific way we can say that the qualitative theory aims to make the portrait of a differential equation, using the most significant solutions, that is, the minimal sets.*

Interested in this new approach of the differential equations, the team led by A. Liapunov studied the behavior of solutions in a neighborhood of an equilibrium position, i.e. he founded the modern theory of stability of motion.

In the International Congress of Mathematics in 1900, D. Hilbert proposed 23 problems that in his opinion would motivate advances in mathematics during the 20th century. Among these there is the *16th Hilbert problem*, whose second part asking about the maximum number and the position of the limit cycles of a polynomial planar system in function of its degree, that is a system like (1.2) with  $X$  and  $Y$  being the polynomials of degree  $n$ . By convention, this number is called  $H(n)$ . As expected, these problems motivated many works and the 16th continues inspiring today. Recently it was considered one of the most relevant problems of the 21st century.

The first step in the direction of 16th Hilbert problem was given by H. Dulac in 1923. Currently called the finitude problem, his work goes in the direction of proving the finitude of the number of limit cycles in a polynomial vector field in the plane. This proof was considered valid for many years. It was not until the 1970s that Y. Ilyashenko did prove that it was false. So, some years later and independently, Y. Ilyashenko and J. Écalle provided a correct proof. Although the proof given by Dulac was wrong, the ideas given by him were very fruitful and generated results like the classical Dulac Theorem and its generalization: the Bendixon–Dulac Theorem.

Over the years many other works have been done in this direction of 16th Hilbert problem. But even the simplest case,  $n = 2$ , is still unsolved. N. Bautin (1952) states that  $H(2) \geq 3$ . Later, simultaneously, S. Shi (1979) and L. Chen and M. Wang found an example with  $H(2) \geq 4$ . For the next case,  $n = 3$ , J. Li and Q. Huan (1987) showed that  $H(3) \geq 11$ .

Given the big difficulty of the 16th Hilbert problem, mathematicians began to propose weaker versions of this problem. The more general version is the so-called Arnold–Hilbert problem, however it is still an open problem.

This problem says that: Let  $H$ ,  $P$ , and  $Q$  be polynomials of degree  $n$  and  $R$  an integral factor. Given  $\Gamma(h)$  a level curve  $H(x, y) = h$  of the system

$$\begin{cases} \dot{x} = -\frac{\partial H}{\partial y}, \\ \dot{y} = \frac{\partial H}{\partial x}. \end{cases} \quad (1.3)$$

What is the number of zeroes of the integral

$$M(h) = \int_{\Gamma(h)} \frac{Pdx + Qdy}{R} \quad (1.4)$$

The integral  $M(h)$  is known as an *Abelian integral*, or in a broader context, as a *Melnikov's function*. The maximum number of simple zeros of  $M(h)$  is also related to another problem, the highest multiplicity of a focus, which we call cyclicity (the maximum number of limit cycles that we get from an equilibrium point by a given polynomial perturbation).

The above problem appears when considering the polynomial perturbation of a Hamiltonian system,

$$\begin{cases} \dot{x} = -\frac{\partial H}{\partial y} + \varepsilon P, \\ \dot{y} = \frac{\partial H}{\partial x} + \varepsilon Q. \end{cases} \quad (1.5)$$

More generally the approach to this type of problem is through the *Averaging Theory* this method starts with the classical works of Lagrange and Laplace who provided an intuitive justification of the mechanism. The first formalization of this procedure was given by Fatou in 1928. During the last decade many mathematicians have contributed to this problem. We highlight the works of A. Gasull, J. Libre, A. Varchenko, L. Gavrilov, E. Horozov, C. Li, D. Wang, H. Zoladek and others.

S. Smale also said that the computation of the Hilbert number can be notably difficult. So mathematicians must consider a special class of differential equations where it is proved that finitude is simple, but the upper bounds for  $H(n)$  in this class remains unknown.

For example, considering the differential equations given by A. Liénard, published in a work in “*Révue générale de l'électricité*” in 1928, which has a formulation that has a strong relation with van der Pol oscillators.

He proposes that: Given a Liénard system

$$\begin{cases} \dot{x} = y - F(x), \\ \dot{y} = -x, \end{cases} \quad (1.6)$$

where  $F$  is a real polynomial of degree  $n$  and satisfying  $F(0) = 0$ , which is the number  $H(n)$  for this system? Although much more restricted, this problem also remains open.

Usually when we model a system in nature using differential equations they depend on some free parameters. The study of which phase portraits of a differential equation do not change its topology with small changes in the parameters is what we call *structural stability*. On the other hand, when the phase portrait changes we have a *bifurcation*. In the mid-1930s A. Andronov and L. Pontryagin were the pioneers in this subject. Soon after M. Peixoto, significantly extended the results given by the previous ones. Hence, the structural stability of a differential system is indicated by the stability of the phase portrait by varying the parameters.

The modeling of some systems in nature marked the history of the *applications* of the

differential equations and boosted their development. Among others, three examples are worth mentioning.

Starting with the  $n$ -body problem, this question was motivated by the necessity to understand the movement of the sun, planets and stars. The first mathematical formulation was elaborated by Newton, who expressed the gravitational interactions in terms of differential equations.

Another landmark was the Lotka–Volterra equation proposed independently by the mathematician V. Volterra and the biophysicist A. J. Lotka in 1925. The first one found this model based on the work of U. d’Ancona, who developed its work analyzing the growth of the population of sharks and the decrease of the population of the other fishes in a sea of Italy, and the second studying the prey-predator relationship in a general way. Finally, the last example is the already mentioned modeling of van der Pol oscillators and Liénard equations.

Given a vector field  $F : \mathbb{R}^2 \rightarrow \mathbb{R}^2$  with  $F(0) = 0$ , such that the Jacobian matrix  $JF(0)$  has pure imaginary eigenvalues. In these conditions the *center-focus* problem is based on finding conditions to the parameters to distinguish the equilibrium point between focus and center. From the return maps, Liapunov considers the importance of the terms of the series expansion of this application, which are the *Liapunov constants*. Thus, when all constants are identically zero we obtain the sufficient condition for a center. The problem however is extremely difficult due to the facts that the calculations of these quantities usually requires complex algebraic calculations and finding the points where all of them vanish is also very difficult.

The problem of *global stability*, both in points of equilibrium and in periodic orbits, has a special relevance in applications since it ensures the asymptotic tendency of any flow of a vector field that tends to a given singular solution or state of equilibrium. In 1960, L. Markus and H. Yamabe established the conjecture: Let  $F : \mathbb{R}^n \rightarrow \mathbb{R}^n$  be a vector field of class  $\mathcal{C}^1$  with  $F(0) = 0$ , such that for every  $x \in \mathbb{R}^n$  the proper values of the Jacobian matrix  $JF(x)$  have negative real part. Then,  $x = 0$  is a globally asymptotically stable point. This conjecture was proved for  $n = 2$  by C. Gutiérrez and R. Fessler in 1993. Years later in 1997 for  $n = 3$ , A. Gasull, A. Cima, F. Mañosa, A. van den Essen. and E. Hubbers gave a counterexample to the conjecture.

Considering the *local stability* of an equilibrium point, we can affirm that in general we have three types of singularities. The ones that are called hyperbolic, in which the Groebner–Hartman Theorem applies. The cases associated to the center-focus problem which are non-hyperbolic. And the rest of the points where usually the technique of blowing-up is used, which consists in exploding the critical point to others for which we can explore the local behavior of the orbits around them and so find the types of sectors of the original critical point. The works of F. Dumortier, R. Roussarie and J. Sotomayor from 1977 are fundamental to understand this technique.

Although the study of *piecewise systems* came from the first half of the last century, it was around 1950 that F. Filippov completely formalized this branch of qualitative theory by considering and defining the flow of the simultaneous systems on the manifold of separation.

We define a  $\Sigma$ -piecewise vector field as follows. Let  $h : \mathbb{R}^n \rightarrow \mathbb{R}$  be a function. We denote the discontinuity boundary by  $\Sigma = h^{-1}(0)$ , being 0 a regular point and  $\Sigma^\pm = \{\pm h > 0\}$ . We consider the  $\Sigma$ -piecewise vector field by  $Z^\pm = (X^\pm, Y^\pm)$ , where  $X^\pm, Y^\pm : \mathbb{R}^n \rightarrow \mathbb{R}^n$  are real functions and the vector field  $Z^\pm$  is defined on  $\Sigma$  following Filippov's terminology.

In last years, emerged a big interest for the study of piecewise systems has emerged, due to the fact that many real phenomena can be modeled with this class of systems. In particular in electrical and mechanical systems, in control theory, and even genetic networks, among others.

Motivated by the importance of piecewise systems, to extending the tools and classic problems of Qualitative Theory in analytical systems to this kind of systems, became a relevant and interesting question. A large set of classical theorems are not satisfied by the piecewise systems. Among others, we can cite the Existence and Uniqueness Theorem or the Hartman–Grobman Theorem.

For piecewise systems, similarly as for analytical differential systems, a *limit cycle* is an isolated periodic orbit. On  $\Sigma$ , Filippov defined the regions of escaping, sliding, crossing and tangency points. Consequently, a limit cycle here can have points in those regions. Periodic orbits that contain only crossing points are the ones closest to that given by analytical systems.

For piecewise systems, the classical *Poincaré–Bendixson theorems* are not satisfied due to the fact that there exist different minimal sets. However recently in 2018 C. A. Buzzi, T. Carvalho, and R. D. Euzébio presented an extension of this theorem for piecewise systems. Over some extra hypothesis they proved a larger number of minimal sets by adding the pseudo-cycle, the pseudo-graph and the singular tangencies.

Assuming that  $Z^\pm$  are polynomials, we can consider an *extension of the Hilbert's 16th problem* to piecewise systems restricting, if necessary, the studied family.

That is, for  $n = 1$ . Considering the hypothesis that  $\Sigma$  is a straight line and the system is continuous ( $Z^+(x, y) = Z^-(x, y)$  with  $(x, y) \in \Sigma$ ), in 1998, E. Freire, E. Ponce, F. Rodrigo and F. Torres proved that  $H(1) = 1$ .

For the non-continuous but linear case and also when  $\Sigma$  is a straight line we have that  $H(1) \geq 3$ . This number was firstly detected numerically by Huan and Yang. Later, it was analytically proved by Llibre and Ponce. Other authors have also proved the same. For analytical systems one of the most used tools to find limit cycles is the Average Theory, which in general way applies in a very similar way to piecewise systems.

For piecewise  $\Sigma$  systems, the study of the hyperbolicity of minimal sets (equilibrium points, limit cycles, ...) is even more complicated. First, the classification of equilibrium points in  $\Sigma$ , because among the hyperbolic, non-hyperbolic and the other cases, the combination of two or more equilibria is needed to study. Furthermore, in piecewise systems the so-called tangency points also fulfill this role.

The study of hyperbolicity of limit cycles and other minimal sets also depends on the behavior of the systems on the manifold separation,  $\Sigma$ . It is worth quoting Llibre for his contributions in this subject and also M. A. Teixeira. Teixeira is known for the  $T$ -singularity that shows that the behavior of singularities given by tangencies has a really interesting

behavior and very different from the analytic cases.

Due to the difficulties on the computations of the Liapunov constants on piecewise systems, the center-focus problem for these type of systems has not been completely developed, as well as many other results and problems that we can extend to piecewise systems but were not developed due to the fact that they have a very high degree of difficulty. This thesis is our contribution to this recent and interesting field.

The work has been developed in collaboration with J. Torregrosa, and it is structured in an introduction as the first chapter and then four chapters where the results and proofs are developed. The main techniques in each chapter are different and so they are written in an independent form. As it is explained in the title, the main results are concerning to limit cycles in differential and piecewise differential systems in the plane. Basically, almost all the studied vector fields are polynomial or piecewise polynomial.

In Chapter 2 we use the averaging technique to study the simultaneous bifurcation of isolate periodic orbits in a polynomial cubic planar system that has two period annuli. Although the unperturbed system is analytic and also its perturbation is considered inside the piecewise class of two zones separated by a straight line, the  $x$ -axis. We consider two different type of problems. First we study the number of limit cycles up to first order polynomial perturbation of degree  $n$ . More concretely, we prove that the inner and outer Abelian integrals are rational functions and we provide an upper bound for the number of simple zeros. Second, for a cubic perturbation, we can improve the general result by obtaining the maximum number of these periodic solutions, always up to first order perturbation. This maximum number is 9 and 8, for the inner and outer regions, respectively. Finally, the simultaneous bifurcation problem is also considered. Then, 12 limit cycles exist and they appear in three different types of configurations: (9,3), (6,6) and (4,8). We remark that, in the non-piecewise scenario, only 5 limit cycles were found. The results on this chapter are already published in [CT18b].

The aim of Chapter 3 is to provide the best lower bound known up to now for the Hilbert number in the quadratic polynomial piecewise vector fields defined in two zones separated by a straight line. We prove that, in this class, at least 16 limit cycles appear. We study, using first and second order averaging method, the perturbation of all isochronous quadratic polynomial vector fields having a birational linearization. For the first order we provide some upper bounds that are reached. For the second order, we study the Taylor developments near the origin to provide the 16 limit cycles. The result is proved by doing a careful study of the intersection of second order varieties. The Poincaré–Miranda theorem and some computer assisted proofs have been necessary to complete the proof. This work has been developed together with D. Novaes and it is submitted to be published, see [CNT18].

The Bendixson–Dulac Theorem provides a criterion to find upper bounds to the number of limit cycles in analytic differential systems. In Chapter 4 we extend this classical result to some classes of piecewise differential systems. We apply it to three different Liénard piecewise differential systems. In all cases, the systems present regions in the parameter space with no limit cycles and others having at most one. The results are submitted to be

published, see [CT18a].

In Chapter 5 we study the family of quartic linear-like time reversible polynomial systems having a nondegenerate center at the origin. This family is defined by quartic vectors fields having only degree one in one variable. In this class, we classify all systems having two extra non-degenerate centers out of the symmetry line. There are only two configuration types, when the three centers are aligned or when they are located at the vertex of an isosceles triangle. Next, we are interested in the simultaneous bifurcation of small limit cycles in these systems. This work is not finished yet. We have studied all the limit cycles appearing with first order Taylor developments. We have obtained five different configurations of limit cycles surrounding the three centers. The highest number has been 13 in two configurations. We are still working in the high order analysis to improve our results. The results has been done in collaborations with V. Romanovsky and can be found in [CRT18].

# Simultaneous bifurcation of limit cycles from a cubic piecewise center with two period annuli

---

---

## Abstract

In this chapter we study the number of periodic orbits that bifurcate from a cubic polynomial vector field having two period annuli via piecewise perturbations. The cubic planar system  $(x', y') = (-y((x-1)^2 + y^2), x((x-1)^2 + y^2))$  has simultaneously a center at the origin and at infinity. We study, up to first order averaging analysis, the bifurcation of periodic orbits from the two period annuli, first separately and second simultaneously. This problem is a generalization of [PGT14] to the piecewise systems class. When the polynomial perturbation has degree  $n$ , we prove that the inner and outer Abelian integrals are rational functions and we provide an upper bound for the number of zeros. When the perturbation is cubic, the same degree as the unperturbed vector field, the maximum number of limit cycles, up to first order perturbation, from the inner and outer annuli is 9 and 8, respectively. When the simultaneous bifurcation problem is considered, 12 limit cycles exist. These limit cycles appear in three types of configurations: (9,3), (6,6) and (4,8). In the non-piecewise scenario, only 5 limit cycles were found.

## 2.1 Introduction

The knowledge of the existence of periodic solutions is very important for understanding the dynamics of differential systems. The method of averaging has a long history that starts with the classical works of Lagrange and Laplace who provided an intuitive justification of the mechanism. The first formalization of this procedure was given by Fatou in 1928, see [Fat28]. Nevertheless, Buica and Llibre [BL04] extended the averaging theory for studying periodic orbits to continuous differential systems using mainly the Brouwer degree theory. Recently, the averaging theory for studying periodic orbits to piecewise differential systems has been developed, see [LMN15, LNT15b] for example. Here we use the same approach as [BPT13].

Consider the perturbed polynomial piecewise differential system

$$Z^\pm = \begin{cases} \dot{x} = -y((x-1)^2 + y^2) + \varepsilon P_n^\pm(x, y), \\ \dot{y} = x((x-1)^2 + y^2) + \varepsilon Q_n^\pm(x, y), \end{cases} \quad \text{if } (x, y) \in \Sigma^\pm, \quad (2.1)$$

with  $P_n^\pm$  and  $Q_n^\pm$  polynomials of degree  $n$  and  $\Sigma^\pm = \{(x, y) : \pm y > 0\}$ . An example of the phase portrait of the above system, for  $\varepsilon$  small, is drawn in Figure 2.1.

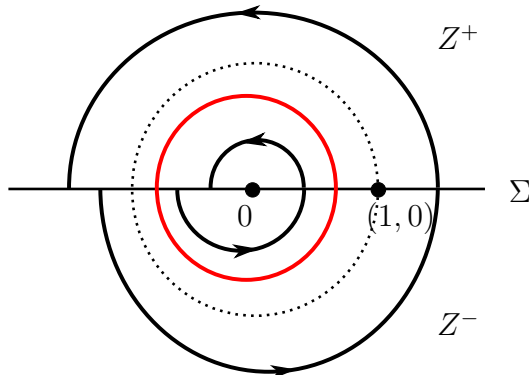


Figure 2.1: A possible phase portrait of system (2.1)

Following [BPT13], the limit cycles of (2.1) correspond to the zeros of the difference map  $\Pi^+(r) - (\Pi^-)^{-1}(r)$ , see Figure 2.2. Moreover, for  $\varepsilon$  small enough and doing a time rescaling, the simple zeros of  $I(r) = I^+(r) - I^-(r)$ , where

$$I^\pm(r) = \int_{\gamma_r^\pm} \frac{P_n^\pm(x, y)dy - Q_n^\pm(x, y)dx}{(x-1)^2 + y^2}, \quad (2.2)$$

gives limit cycles for (2.1), bifurcating from  $\gamma_r^\pm = \{x^2 + y^2 = r^2 : \pm y > 0\}$ . The above integrals defined over closed curves are known as Abelian integrals, see [CL07]. We can say that the expression (2.2) are the piecewise version of them. See more details in [GT03] or

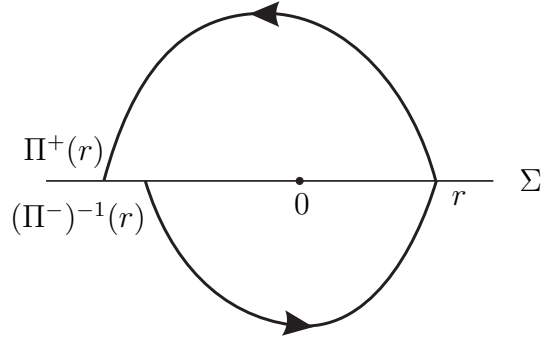


Figure 2.2: Return map for system (2.1)

[LP03]. In our case both components of the unperturbed system have a common factor that appears in the denominator of the integrand. This expression appears in [LPdRR01] (in polar coordinates) or in [GLT12]. As we will see in Theorem 2.2 the explicit expression of (2.2) is different in the two period annuli associated to (2.1):

$$\mathcal{R}_i = \{r \in \mathbb{R} : 0 < r < 1\} \quad \text{and} \quad \mathcal{R}_e = \{r \in \mathbb{R} : r > 1\}.$$

As we have commented before, the function  $I(r)$  is also called the Abelian integral associated to system (2.1). By similarity we define the *inner and outer Abelian integrals* as

$$\begin{aligned} I_i(r) &= I_i^+(r) - I_i^-(r), \quad 0 < r < 1, \\ I_e(r) &= I_e^+(r) - I_e^-(r), \quad r > 1, \end{aligned} \tag{2.3}$$

where  $I_j^\pm$  are the upper and lower inner ( $j = i$ ) and outer ( $j = e$ ) integrals.

The study of the number limit cycles that bifurcate from a linear center, also called harmonic oscillator, is very relevant in the qualitative theory of differential equations. Over the last two decades, there have been papers showing that when we add a curve of singularities the number of limit cycles appearing by perturbation increases. In [LPdRR01], only doing a first-order analysis, it was proved that this number is doubled, adding a straight line of singularities to the unperturbed system, in comparison with the perturbation of the linear center. Similar results have been done adding curves with a fixed degree. See, for example, [GLT12] for the study of a fixed number of straight lines or [Xio16] for a circle of singularities. But, there are not so many papers focused on the study of simultaneous bifurcation of limit cycles from centers with different period annuli. Some of them are [CLP09, GGJ08] that deal with the simultaneity in two different regions, or [DL03] where three separated period annuli appear. A study of the bifurcation of limit cycles from different period annuli of polynomial Hamiltonian systems to obtain lower bounds for the Hilbert number is done in [CL95] and, more recently, in [Li03]. Although the most common technique to study simultaneity is the  $Z_n$  symmetry, see for example [MH09, MHL09], when it is not considered, see for example [Chr05], more periodic orbits appear. This is the case done in [PGT14] where non-symmetric

perturbations are considered. Following the same procedure we consider now a piecewise polynomial perturbation of the two nested period annuli. The main goals are consequence of the explicit expressions for the Abelian integrals that we have obtained. From this fact, we can study the upper bound of the number of zeros in both regions separately and the existence of some configurations of simultaneity. We will show also that, in some sense, there are no others.

The explicit expression obtained for the functions (2.2) allow us to use the classical theory of Chebyshev systems to provide an upper bound for the number of zeros. Now we recall the main definitions and properties. Let  $\mathcal{F} = [f_0, \dots, f_n]$  be an ordered set of functions of class  $\mathcal{C}^n$  defined in a closed interval  $[a, b]$ . We consider only elements in  $\text{Span}(\mathcal{F})$ , that is, functions such as  $f = a_0 f_0 + a_1 f_1 + \dots + a_n f_n$  where  $a_j$  for  $j = 0, 1, \dots, n$  are real numbers. We say that  $\mathcal{F}$  is an Extended Chebyshev system, ET-system in short, on  $[a, b]$  if the maximum number of zeros, taking into account its multiplicity, is  $n$ . For a sufficient condition we can introduce the Extended Complete Chebyshev systems. We say that  $\mathcal{F}$  is an Extended Chebyshev system, ECT-system in short, on  $[a, b]$ , if any set  $[f_0, \dots, f_j]$ , for  $j = 0, \dots, n$  is an ET-system on  $[a, b]$ . When all the Wronskians,  $W_j = W(f_0, \dots, f_j)$   $j = 0, \dots, n$ , are different from zero in  $[a, b]$  the family  $\mathcal{F}$  is an ECT-system. More details on ET-systems and ECT-system can be found in [KS66]. Here we use an extension of this theory, the extended Chebyshev systems with accuracy (see [NT17]), because some Wronskians vanish.

Before presenting our results we state a definition about what we consider that a configuration of limit cycles is.

**Definition 2.1.** *We say that the system (2.1) presents a configuration with exactly  $(k, \ell)$  limit cycles when it has  $k$  and  $\ell$  limit cycles in  $\mathcal{R}_i$  and  $\mathcal{R}_e$ , respectively.*

Next result provides the general expressions for the first averaged functions in the inner and outer period annuli. Moreover, writing these functions using an Extended Complete Chebyshev system we can also find an upper bound for the number of zeros and, consequently, for the number of limit cycles, up to a first order analysis in  $\varepsilon$ , that system (2.1) has.

**Theorem 2.2.** *Let  $P_n^\pm$  and  $Q_n^\pm$  be polynomials of degree  $n$  in (2.1). Then, the inner and outer Abelian integrals (2.3) associated to (2.1) are*

$$\begin{cases} I_i(r) = \frac{rR_{2n+1}(r)}{r^2 - 1} + H_n(r^2) \log\left(\frac{1-r}{1+r}\right) & \text{if } 0 < r < 1, \\ I_e(r) = \frac{rS_{2n+1}(r)}{r^2 - 1} + H_n(r^2) \log\left(\frac{r-1}{1+r}\right) & \text{if } r > 1, \end{cases} \quad (2.4)$$

where  $R_m$ ,  $S_m$  and  $H_m$  are polynomials of degree  $m$ . Moreover, the maximum number of zeros of each  $I_i$  and  $I_e$  is  $4n + 8$ .

For fixed (small) values of  $n$ , the above upper bound is far to be optimal. A more precise study can be done for the cubic family when both period annuli are considered separately and also when the simultaneity is taken into account. Next theorem gives our main result for cubic perturbations.

**Theorem 2.3.** *For  $n = 3$ , the functions  $I_i(r)$  and  $I_e(r)$ , defined in (2.4), have at most 9 and 8 zeros, respectively. Moreover, there exist polynomial perturbations such that (2.1) exhibits configurations with 12 limit cycles. In particular it presents configurations with (9, 3), (6, 6) and (4, 8) limit cycles.*

The perturbation inside the piecewise polynomial class of degree  $n$ , including the proof of Theorem 2.2, is presented in Section 2.2. The rest of the chapter is devoted to the cubic family. In Section 2.3 we study each region,  $\mathcal{R}_i$  and  $\mathcal{R}_e$  separately. The first statement of Theorem 2.3 is also proved here. The simultaneity study and the rest of the proof of Theorem 2.3 is done in Section 2.4. Additionally, also in Section 2.4, we study some bifurcation diagrams where the different configurations can appear. Moreover, we also provide other configurations with less number of limit cycles. In particular, as we are working in a 10-dimensional space of parameters, the technique used in Section 2.4 provides all the configurations  $(k, \ell)$  with  $k + \ell = 10$ ,  $0 \leq k \leq 8$  and  $0 \leq \ell \leq 7$ . Finally, in Section 2.5, we study the local behavior of the bifurcation curves near the boundary of the domain of definition.

## 2.2 The general case

This section is devoted to the proof of Theorem 2.2. The first statement follows from the explicit computation of the Abelian integrals defined in the two annular regions  $\mathcal{R}_i$  and  $\mathcal{R}_e$ . The second statement is proved using ECT-systems, see [KS66].

As in [PGT14], the integrals (2.2), in the usual polar coordinates  $(x, y) = (r \cos \theta, r \sin \theta)$ , can be written, for  $j \in \{i, e\}$ , as

$$\begin{aligned} I_j^\pm(r) &= \sum_{m=1}^{n+1} r^m \int_0^{\pm\pi} \frac{\sum_{k=0}^m (\alpha_{k,m}^\pm \cos(k\theta) + \beta_{k,m}^\pm \sin(k\theta))}{r^2 - 2r \cos \theta + 1} d\theta \\ &= \sum_{k=0}^{n+1} r^k R_k^\pm(r^2) C_{j,k}^\pm(r) + \sum_{k=1}^{n+1} r^k T_k^\pm(r^2) S_{j,k}^\pm(r), \end{aligned} \quad (2.5)$$

where

$$\begin{aligned} C_{i,k}^\pm(r) &= \int_0^{\pm\pi} \frac{\cos(k\theta) d\theta}{r^2 - 2r \cos \theta + 1}, \quad 0 < r < 1, \\ S_{i,k}^\pm(r) &= \int_0^{\pm\pi} \frac{\sin(k\theta) d\theta}{r^2 - 2r \cos \theta + 1}, \quad 0 < r < 1, \\ C_{e,k}^\pm(r) &= \int_0^{\pm\pi} \frac{\cos(k\theta) d\theta}{r^2 - 2r \cos \theta + 1}, \quad r > 1, \\ S_{e,k}^\pm(r) &= \int_0^{\pm\pi} \frac{\sin(k\theta) d\theta}{r^2 - 2r \cos \theta + 1}, \quad r > 1. \end{aligned} \quad (2.6)$$

Moreover,  $\alpha_{k,m}^\pm = \beta_{k,m}^\pm = 0$  when  $k$  and  $m$  do not have the same parity and  $R_k^\pm(r^2)$  and  $T_k^\pm(r^2)$  are polynomials of degree at most  $[(n+1-k)/2]$  with arbitrary coefficients for all  $k = 0, \dots, n+1$ .

We start proving Lemma 2.4, that provides the recurrence to compute the integrals given in (2.5). In Lemma 2.5 we provide the explicit expressions for (2.6).

**Lemma 2.4.** *Let  $k \geq 1$  be an integer number. If  $C_k(r) = \int_a^b \frac{\cos(k\theta)}{r^2 - 2r \cos \theta + 1} d\theta$  and  $S_k(r) = \int_a^b \frac{\sin(k\theta)}{r^2 - 2r \cos \theta + 1} d\theta$ , for  $r \neq 0$  and  $r \neq 1$ , then*

$$C_{k+1}(r) = \frac{\sin(kb) - \sin(ka)}{kr} + \frac{r^2 + 1}{r} C_k(r) - C_{k-1}(r) \quad (2.7)$$

and

$$S_{k+1}(r) = \frac{\cos(kb) - \cos(ka)}{kr} + \frac{r^2 + 1}{r} S_k(r) - S_{k-1}(r). \quad (2.8)$$

*Proof.* The recurrence (2.7), for the function  $C_k$ , follows doing the next computations:

$$\begin{aligned} \int_a^b \cos(k\theta) d\theta &= \int_a^b \cos(k\theta) \frac{r^2 - 2r \cos \theta + 1}{r^2 - 2r \cos \theta + 1} d\theta \\ &= (r^2 + 1)C_k(r) - 2r \int_a^b \frac{\cos(k\theta) \cos \theta}{r^2 - 2r \cos \theta + 1} d\theta \\ &= (r^2 + 1)C_k(r) - r \int_a^b \frac{\cos((k+1)\theta)}{r^2 - 2r \cos \theta + 1} d\theta + r \int_a^b \frac{\cos((k-1)\theta)}{r^2 - 2r \cos \theta + 1} d\theta \\ &= (r^2 + 1)C_k(r) - rC_{k+1}(r) - rC_{k-1}(r). \end{aligned}$$

The recurrence (2.8), for  $S_k$ , follows similarly.  $\square$

**Lemma 2.5.** *Let  $k \geq 0$  be an integer number. The functions defined in (2.6) satisfy the next relations:*

$$(a) \ C_{i,k}^\pm(r) = \mp \frac{r^k \pi}{r^2 - 1} \text{ and } S_{i,k}^\pm(r) = \frac{-p_{k-1}(r^2)}{r^k} L(r) + \frac{q_{i,k-2}^\pm(r^2)}{r^{k-1}}, \text{ when } 0 < r < 1,$$

$$(b) \ C_{e,k}^\pm(r) = \pm \frac{\pi}{r^k(r^2 - 1)} \text{ and } S_{e,k}^\pm(r) = \frac{-p_{k-1}(r^2)}{r^k} L\left(\frac{1}{r}\right) + \frac{q_{e,k-2}^\pm(r^2)}{r^{k-1}}, \text{ when } r > 1,$$

where  $L(r) = \log\left(\frac{1-r}{1+r}\right)$  is defined in the interval  $(0, 1)$ . Moreover,  $p_{k-1}(r^2) = \sum_{j=0}^{k-1} r^{2j}$ , for  $k \geq 1$ ,  $q_{j,k-2}^\pm(r^2)$  are polynomials of degree  $k-2$ , for  $k \geq 2$ , and  $j \in \{i, e\}$ ; and, for compactness,  $p_{-1} \equiv 0$  and  $q_{j,-2}^\pm \equiv q_{j,-1}^\pm \equiv 0$ , for  $j \in \{i, e\}$ .

*Proof.* We prove only item (a). Item (b) follows similarly.

(a<sub>1</sub>) Straightforward computations show the cases  $k = 0, 1$ . Assuming the recurrence relation (2.7) in the intervals  $(0, \pi)$  and  $(0, -\pi)$  we have that

$$C_{i,k}^\pm = \frac{(r^2 + 1)}{r} \left( \mp \frac{r^{k-1} \pi}{r^2 - 1} \right) - \left( \mp \frac{r^{k-2} \pi}{r^2 - 1} \right) = \mp \frac{r^k \pi}{r^2 - 1}.$$

(a<sub>2</sub>) As in the above case, straightforward computations show the cases  $k = 0, 1$ . From the recurrence (2.8), for  $S_{i,k}^\pm$ , we have

$$\begin{aligned} \frac{p_{k-1}(r^2)}{r^k} L(r) &= \left( \frac{r^2 + 1}{r} \frac{p_{k-2}(r^2)}{r^{k-1}} - \frac{p_{k-3}(r^2)}{r^{k-2}} \right) L(r), \\ \frac{q_{k-2}(r^2)}{r^{k-1}} &= \frac{(-1)^{k-1} - 1}{(k-1)r} + \frac{r^2 + 1}{r} \frac{q_{k-3}(r^2)}{r^{k-2}} - \frac{q_{k-4}(r^2)}{r^{k-3}}. \end{aligned}$$

The above expressions provide the next recurrence relations:

$$\begin{aligned} p_{k-1}(r^2) &= (r^2 + 1)p_{k-2}(r^2) - r^2 p_{k-3}(r^2), \\ q_{k-2}(r^2) &= \frac{(-1)^{k-1} - 1}{k-1} r^{k-2} + (r^2 + 1)q_{k-3}(r^2) - r^2 q_{k-4}(r^2). \end{aligned}$$

The proofs of the expressions of  $S_{i,k}^\pm$  given in the statement follow by induction taking into account that, in the last expression, the term  $r^{k-2}$  vanishes when  $k$  is odd. We have not indicated the dependence of the polynomials  $q_k$  in terms of the inner region, only that they are of degree  $k$ .  $\square$

*Proof of Theorem 2.2.* We consider only  $r \in (0, 1)$ . When  $r > 1$  the proof follows analogously.

The inner Abelian integral (2.5), using Lemma 2.5 when  $0 < r < 1$ , writes as

$$\begin{aligned} I_i(r) &= \sum_{k=0}^{n+1} r^k R_k^+(r^2) C_{i,k}^+(r) + \sum_{k=1}^{n+1} r^k T_k^+(r^2) S_{i,k}^+(r) \\ &\quad - \sum_{k=0}^{n+1} r^k R_k^-(r^2) C_{i,k}^-(r) - \sum_{k=1}^{n+1} r^k T_k^-(r^2) S_{i,k}^-(r) \\ &= \left( \sum_{k=1}^{n+1} r^k T_k^+(r^2) \frac{p_{k-1}(r^2)}{r^k} - \sum_{k=1}^{n+1} r^k T_k^-(r^2) \frac{p_{k-1}(r^2)}{r^k} \right) L(r) \\ &\quad - \sum_{k=0}^{n+1} r^k R_k^+(r^2) \frac{r^k \pi}{r^2 - 1} + \sum_{k=1}^{n+1} r^k T_k^+(r^2) \frac{q_{i,k-2}^+(r^2)}{r^{k-1}} \\ &\quad - \sum_{k=0}^{n+1} r^k R_k^-(r^2) \frac{r^k \pi}{r^2 - 1} - \sum_{k=1}^{n+1} r^k T_k^-(r^2) \frac{q_{i,k-2}^-(r^2)}{r^{k-1}}. \end{aligned}$$

Therefore we obtain that the coefficient of  $L(r)$  is a polynomial of degree  $n$ . Because each term in the sum

$$H_n(r^2) = \sum_{k=1}^{n+1} T_k^+(r^2) p_{k-1}(r^2) - \sum_{k=1}^{n+1} T_k^-(r^2) p_{k-1}(r^2),$$

has degree  $s_k = [n + 1 - k/2] + k - 1$ , which is a nondecreasing sequence in  $k$ . So the greatest degree is achieved for  $k = n + 1$ . Consequently  $s_{n+1} = n$ , as we wanted to prove. For the

independent term we can argue similarly to prove that it has degree  $2n + 1$ . In particular, we can write

$$\begin{aligned} R_{2n+1}(r) = & -\pi \sum_{k=0}^{n+1} r^{2k-1} R_k^+(r^2) - \pi \sum_{k=0}^{n+1} r^{2k-1} R_k^-(r^2) \\ & + \sum_{k=1}^{n+1} (r^2 - 1) T_k^+(r^2) q_{i,k-2}^+(r^2) - \sum_{k=1}^{n+1} (r^2 - 1) T_k^-(r^2) q_{i,k-2}^-(r^2). \end{aligned}$$

Therefore, the highest degree term in each of the above sums is  $t_k = [n+1-k/2] + (2k-1)/2$ , which is also a nondecreasing sequence in  $k$ . So when  $k = n+1$  we have that the degree of  $R_{2n+1}$  is  $t_{n+1} = 2n+1$ . This finishes the proof of the first part of the statement.

For the second part, we use the change of variables  $r = (1-s)/(1+s)$  in (2.4), for  $0 < r < 1$ . Now, the Abelian integral  $I_i$  writes as

$$\tilde{I}_i(s) = \frac{\tilde{R}_{2n+4}(s) + \tilde{H}_{2n+3}(s) \log s}{4s(1+s)^{2n+3}},$$

where  $\tilde{R}_m$  and  $\tilde{H}_m$  are polynomials of degree  $m$ . The proof finishes because the ordered family  $\{1, \log s, s, s \log s, s^2, s^2 \log s, \dots\}$  is an ECT-system. Because the total terms in the numerator of  $\tilde{I}_i$  is  $4n+9 = (2n+4+1) + (2n+3+1)$  and, consequently, it has  $4n+8$  simple zeros.  $\square$

## 2.3 Studying the internal and external regions separately

This section is devoted to study the case  $n = 3$ . With the change  $r \rightarrow 1/r$  in the outer region, the functions  $I_i$  and  $I_e$  share the interval of definition, that is  $r \in (0, 1)$ . In fact, we will use  $I_e(1/r) = \tilde{I}_e(r)$  for  $r \in (0, 1)$ . The first part of Theorem 2.3 provides the number of zeros of the functions  $I_i$  and  $I_e$  separately. Its proof follows directly from the results of this section. In the first two we provide the expressions of  $I_i$  and  $I_e$  in terms of independent functions and which is the maximum number of simple zeros. As we will see, these functions are not an ECT-system. Consequently, we can not give a direct proof that the upper bounds are achieved. The last two explain which is the highest value for the multiplicity of a zero and how the maximum number of zeros varies when a zero of the highest multiplicity moves along the interval of definition.

**Lemma 2.6.** *For  $n = 3$ , the inner Abelian integral (2.4) can be written as*

$$I_i(r; \beta) = \sum_{j=0}^8 \beta_j f_j(r), \tag{2.9}$$

where

$$\begin{aligned} f_0(r) &= \frac{r^2}{r^2 - 1}, & f_1(r) &= \frac{r^4}{r^2 - 1}, & f_2(r) &= \frac{r^6}{r^2 - 1}, \\ f_3(r) &= \frac{r^8}{r^2 - 1}, & f_4(r) &= r, & f_5(r) &= \frac{1}{2}r^4L(r) + r^3, \\ f_6(r) &= \frac{1}{6}r^4(3r^2 - 1)L(r) + r^5, & f_7(r) &= L(r), & f_8(r) &= r^2L(r), \\ L(r) &= \log\left(\frac{1-r}{1+r}\right), \end{aligned}$$

and  $\beta = (\beta_0, \dots, \beta_8)$ . For  $r \in (0, 1)$ , the function  $I_i(r; \beta)$ , has at most 9 zeros.

*Proof.* From the proof of Theorem 2.3, also using Lemma 2.5, the function  $I_i$  can be written as (2.9), in fact it writes as a linear combination of 9 different functions  $\{f_0, f_1, \dots, f_8\}$ . First we change the order of the functions to  $[f_0, f_1, f_2, f_3, f_4, f_6, f_5, f_7, f_8]$ . The proof follows showing that, with this new order, the first 8 Wronskian are non vanishing and the last has exactly one simple zero. Then, from [NT17], the statement is proved.

We show only why the last Wronskian has exactly one zero. The others follow similarly. Straightforward computations show that  $W_8(r) = 5218385264640(H_0(r)L(r) + H_1(r))/(r^2 - 1)^{25}$  with

$$\begin{aligned} H_0(r) &= 15(3r^{14} - 13r^{12} + 63r^{10} + 63r^8 + 553r^6 - 231r^4 + 1365r^2 + 245)(r^2 - 1), \\ H_1(r) &= 2r(45r^{14} - 225r^{12} + 301r^{10} + 5495r^8 - 7665r^6 + 17605r^4 - 18025r^2 - 3675). \end{aligned}$$

As  $H_0(r) \neq 0$  in  $(0, 1)$  we can consider  $\overline{W}_8(r) = W_8(r)/H_0(r) = L(r) + H_1(r)/H_0(r)$ . Hence its first derivative is

$$\overline{W}'_8(r) = \frac{512r^8(3r^{10} - 21r^8 + 70r^6 - 210r^4 - 105r^2 + 7)(5r^8 - 28r^6 + 70r^4 - 140r^2 - 35)}{5(r^2 - 1)^2(3r^{14} - 13r^{12} + 63r^{10} + 63r^8 + 553r^6 - 231r^4 + 1365r^2 + 245)^2}.$$

Clearly  $\overline{W}'_8$  has only one zero in  $(0, 1)$ . The proof finishes because the series of  $W_8$  starts with a positive term and  $\lim_{r \rightarrow 1^-} W_8(r) = -\infty$ .  $\square$

We remark that we have not reordered the functions in the statement of the above and next result because the crossed relation between the perturbed coefficients when we consider also the simultaneous bifurcation in next sections.

**Lemma 2.7.** For  $n = 3$  the outer Abelian integral (2.4), after the change  $r \rightarrow 1/r$ , can be written as

$$\tilde{I}_e(r; \gamma) = \sum_{j=0}^7 \gamma_j g_j(r), \quad (2.10)$$

where

$$\begin{aligned} g_0(r) &= \frac{r^4}{r^2 - 1}, & g_1(r) &= r^5, & g_2(r) &= \frac{1}{2}r^2L(r) + r^3, \\ g_3(r) &= \frac{1}{6}(3 - r^2)L(r) + r, & g_4(r) &= r^6L(r), & g_5(r) &= r^4L(r), \\ g_6(r) &= r^4(r^2 + 1), & g_7(r) &= r^4, & L(r) &= \log\left(\frac{1-r}{1+r}\right), \end{aligned}$$

and  $\gamma = (\gamma_0, \dots, \gamma_7)$ . For  $r \in (0, 1)$ , the function  $\tilde{I}_e(r; \gamma)$  has at most 8 zeros.

*Proof.* We follow the same scheme as in Lemma 2.6 but for the function  $\tilde{I}_e(r) = I_e(1/r)$  that can be obtained from (2.10). The ordered family to be considered now is  $[g_7/r^4, g_1/r^4, (g_6 - g_7)/r^4, g_5/r^4, g_2/r^4, g_3/r^4, g_4/r^4, g_0/r^4]$ . We have divided all by  $r^4$  to simplify the computations.

As in the previous proof, the first Wronskians are non vanishing but the last,  $W_7$ , has exactly one simple zero. Then, using [NT17], the statement follows.

Straightforward computations show that the first four Wronskians,  $W_0, W_1, W_2$ , and  $W_3$ , have no zeros and  $W_4(r) = (H_0(r)L(r) + H_1(r))/(r^6(r^2 - 1)^6)$  with

$$\begin{aligned} H_0(r) &= 96(3r^4 - 22r^2 - 5)(r^2 - 1)^2, \\ H_1(r) &= -64r(51r^6 - 111r^4 + 41r^2 + 15). \end{aligned}$$

As  $H_0(r) \neq 0$  in  $(0, 1)$  and the first derivative of  $\overline{W}_4(r) = L(r) + H_1(r)/H_0(r)$ ,

$$\overline{W}'_4(r) = \frac{8r^6(3r^2 + 1)(5r^4 + 2r^2 + 1)}{(r^2 - 1)^3(3r^4 - 22r^2 - 5)^2},$$

does not vanish, we have that  $W_4$  is non vanishing.

The next Wronskians need a more accurate analysis because they are polynomials of degree 2 in  $L(r)$ . We follow the same approach as in [MT15], that uses [Kho84]. More concretely, the corresponding Wronskian writes as  $W_5(r) = 256(H_0(r)(L(r))^2 + H_1(r)L(r) + H_2(r))/(r^{15}(r^2 - 1)^9)$  with

$$\begin{aligned} H_0(r) &= 45(r^2 - 1)^4(9r^6 + 55r^4 + 203r^2 + 35), \\ H_1(r) &= 12r(r^2 - 1)(10r^{12} - 422r^{10} + 3631r^8 - 8767r^6 + 7790r^4 - 1645r^2 - 525), \\ H_2(r) &= 4r^2(60r^{12} + 5983r^{10} - 25701r^8 + 41052r^6 - 26870r^4 + 3885r^2 + 1575), \end{aligned}$$

and  $H_0(r)$  has no zeros in  $(0, 1)$ . Then the solutions of  $W_5(r) = 0$  correspond with the intersections of the two curves  $f(r, s) = 0$  and  $g(r, s) = 0$  defined by

$$\begin{aligned} f(r, s) &= s - L(r), \\ g(r, s) &= H_0(r)s^2 + H_1(r)s + H_2(r), \end{aligned} \tag{2.11}$$

in the region  $r \in (0, 1)$  and  $s < 0$ . In fact we use the derivative of  $g$  with respect to  $f$ ,  $h(r, s) = \frac{\partial g}{\partial s} \frac{2}{r^2 - 1} + \frac{\partial g}{\partial r}$ , because we are considering the intersections of two algebraic curves.

Straightforward computations show that the curves  $g$  and  $h$ ,

$$\begin{aligned} h(r, s) = & 18r((315r^{12} - 2730r^{10} + 11925r^8 - 22860r^6 + 19605r^4 - 6570r^2 + 315)s^2 \\ & + (100r^{13} - 3654r^{11} + 28902r^9 - 70438r^7 + 69786r^5 - 25860r^3 + 1260r)s \\ & + (200r^{12} + 15392r^{10} - 52272r^8 + 61292r^6 - 25440r^4 + 1260r^2)), \end{aligned} \quad (2.12)$$

have no intersection for  $r \in (0, 1)$ . This is due to the fact that the resultant of both polynomials with respect to  $s$ ,

$$\begin{aligned} \text{Res}(g, h, s) = & 59719680r^{30}(r^2 - 1)^4(30r^6 + 23r^4 + 16r^2 + 3) \\ & (350r^{10} + 295r^8 + 240r^6 + 194r^4 + 58r^2 + 15), \end{aligned}$$

never vanishes for  $r \in (0, 1)$ . The curves  $f$  and  $g$  coincide at  $(0, 0)$ , where they are tangent. Thus, using the generalized Rolle's Theorem for curves, see [Kho84], we have proved that  $f$  and  $g$  have no intersection points with  $r \in (0, 1)$ . Consequently,  $W_5(r) \neq 0$  in  $r \in (0, 1)$ .

The proof that  $W_6$  is non vanishing follows similarly. In this case, the nonintersection property, except the tangent point at  $(0, 0)$ , is even simpler to prove. Because the corresponding resultant,  $\text{Res}(g, h, s)$ , is  $r^{38}(1 - r^2)^2$ , modulus a multiplicative constant.

Finally, it remains only the study of the last Wronskian, that needs a more accurate analysis. It writes as  $W_7 = -84934656(H_0(r)(L(r))^2 + H_1(r)L(r) + H_2(r))/(r^{19}(r^2 - 1)^{20})$  with

$$\begin{aligned} H_0(r) = & 15(r^2 - 1)^2(35r^{14} - 315r^{12} + 651r^{10} - 6523r^8 + 18193r^6 \\ & - 12201r^4 - 10815r^2 + 735), \\ H_1(r) = & 4r(40r^{18} - 1475r^{16} + 9680r^{14} - 64320r^{12} + 301680r^{10} \\ & - 662534r^8 + 492240r^6 + 93240r^4 - 180600r^2 + 11025), \\ H_2(r) = & 4r^2(80r^{16} + 2013r^{14} - 36257r^{12} + 174713r^{10} - 504557r^8 \\ & + 488775r^6 + 35245r^4 - 176925r^2 + 11025). \end{aligned}$$

Using the same procedure as in the previous cases we have that the corresponding function  $h(r, s) = \frac{r^2-1}{2r}(\frac{\partial g}{\partial s} \frac{2}{r^2-1} + \frac{\partial g}{\partial r})$  writes as

$$\begin{aligned} h(r, s) = & 15(1 - r^2)^2(315r^{14} - 2765r^{12} + 6447r^{10} - 42393r^8 + 117057r^6 \\ & - 103383r^4 - 8043r^2 + 12285)s^2 - 4r(1 - r^2)(380r^{16} - 12275r^{14} + 69975r^{12} \\ & - 410835r^{10} + 1605435r^8 - 2796033r^6 + 1494885r^4 + 243495r^2 - 184275)s \\ & + 4r^2(760r^{16} + 13909r^{14} - 260223r^{12} + 1237757r^{10} - 3269383r^8 + 3815351r^6 \\ & - 1357125r^4 - 366345r^2 + 184275) \end{aligned}$$

and the resultant as

$$\begin{aligned} \text{Res}(g, h, s) = & 5033164800r^{36}(r^2 - 1)^2(5r^{14} - 40r^{12} + 135r^{10} + 782r^8 + 243r^6 \\ & - 132r^4 + 33r^2 - 2)(35r^{18} - 350r^{16} + 1540r^{14} + 12656r^{12} \\ & + 5346r^{10} - 4620r^8 + 2340r^6 - 640r^4 + 83r^2 - 6). \end{aligned} \quad (2.13)$$

But now  $H_0$  has a zero,  $r_1 \approx 0.25258$ , and  $\text{Res}(g, h, s)$  has two,  $r_2 \approx 0.28749$  and  $r_3 \approx 0.47708$ . The algebraic system,  $\{g = 0, h = 0\}$ , defined in (2.11) and (2.12), of degree 2 in  $s$  can be rewritten, using Groebner basis, as an equivalent one of degree 1 in  $s$ . This new system has only two intersection points  $(r_2, s_2)$  and  $(r_3, s_3)$ , with  $s_2 \approx -0.59167$  and  $s_3 \approx -1.03840$ , in the region where we are interested,  $r \in (0, 1)$  and  $s < 0$ . Moreover solving  $W_7 = 0$  with respect to  $L$ , we can write both solutions as

$$L_{\pm} = \frac{-H_1 \pm \sqrt{H_1^2 - 4H_0H_2}}{2H_0}.$$

Notice that in  $r_1$ , one of the roots has an asymptote and the other not. This is due to the fact that  $H_0(r_1) = 0$ ,  $H'_0(r_1) \neq 0$ ,  $H_1(r_1) \neq 0$  and  $H_2(r_1) \neq 0$ . Furthermore,  $H_0 = (r - r_1)\tilde{H}_0$  and  $H'_0 = \tilde{H}_0 + (r - r_1)\tilde{H}'_0$ , that is  $H'_0(r_1) = \tilde{H}'_0(r_1)$ . From these conditions we have the first terms of the series expansion of  $L_{\pm}$  at  $r_1$ :

$$\begin{aligned} L_+ &= -\frac{H_1(r_1)}{\tilde{H}_0(r_1)(r - r_1)} + \dots = -\frac{H_1(r_1)}{H'_0(r_1)(r - r_1)} + \dots, \\ L_- &= -\frac{H_2(r_1)}{H_1(r_1)} + \dots. \end{aligned}$$

Additionally, the function  $L$ , in the interval  $(0, 1/2)$ , is between the next two functions:

$$\begin{aligned} M_{\pm} &= -2r - \frac{2}{3}r^3 - \frac{2}{5}r^5 - \frac{2}{7}r^7 - \frac{2}{9}r^9 - \frac{2}{11}r^{11} - \frac{2}{13}r^{13} - \frac{2}{15}r^{15} - \frac{2}{17}r^{17} \\ &\quad - \frac{2}{19}r^{19} - \frac{2}{21}r^{21} - \frac{2}{23}r^{23} - \frac{2}{25}r^{25} \pm \frac{1}{4}r^{27}. \end{aligned}$$

This last property follows studying the series expansion of  $L$  in the neighborhood of the origin. In fact,  $M_+ - L = 35r^{27}/108 + O(r^{29})$  and  $L - M_- = 19r^{27}/108 + O(r^{29})$ . Thus  $d(M_+ - L)/dr$  and  $d(L - M_-)/dr$  does not have zeros in  $(0, 1/2)$ . Now replacing  $M_{\pm}$  in  $W_7$  instead of  $L$ , we have that  $W_7(M_{\pm})$  in the interval  $(0, 1/2)$  is non vanishing. Moreover, in the neighborhood of  $r = 0$  we have  $L - L_+ = -704r^9/11025 + \dots$  and  $L - L_- = 1024r^{13}/7630623 + \dots$ . And, in the neighborhood of  $r = 1$ , we have  $L_-(1) = -23/4$ , and  $L - L_+ = 1/(r - 1)^2 - \log((1 - r)/2) + \dots$ .

We finish the proof applying Rolle's Theorem separately in the intervals  $(0, r_1)$  and  $(r_1, 1)$ , where the functions  $L$  and  $L_{\pm}$  are well defined and smooth. As the tangency points satisfy  $r_2 < 1/2$  and  $r_3 < 1/2$ , we can conclude that only one intersection point can exist and it is between  $L$  and  $L_-$ . So  $W_7$  vanishes at most once. All these properties can be seen in Figure 2.3. □

**Remark 2.8.** *In the above proof, as the resultant (2.13) vanishes three times, the results of [NT17] provide a worst upper bound than if an accurate analysis is done. The main difficulty has been to provide an analytic argument showing which are the tangent points providing intersection points and which not.*

Following also the ideas of [NT17], and because we will need in the following section,

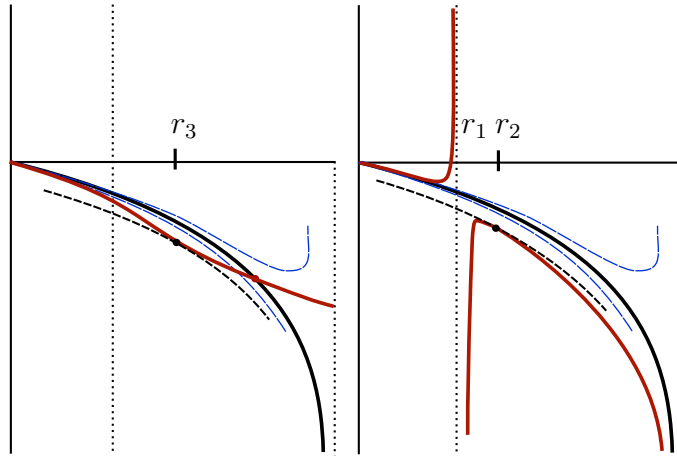


Figure 2.3: Graphs of  $L$  (in black),  $L_+(r)$  (in red on the left),  $L_-(r)$  (in red on the right) and  $M_{\pm}(r)$  (in blue) on  $(0, 1)$ . The values  $r_1$ ,  $r_2$  and  $r_3$  are depicted also.

the next two results study which are the maximal multiplicity zeros of the inner and outer Abelian integrals (2.3) and the corresponding unfolding of simple zeros bifurcating from them.

**Proposition 2.9.** (a) Let  $\rho^\circ \approx 0.27055$  be the zero in  $(0, 1)$  of the function

$$\begin{aligned} w_{i,8}(r) = & 15(1 - r^2)(3r^{14} - 13r^{12} + 63r^{10} + 63r^8 + 553r^6 - 231r^4 \\ & + 1365r^2 + 245)L(r) - 2r(45r^{14} - 225r^{12} + 301r^{10} + 5495r^8 \\ & - 7665r^6 + 17605r^4 - 18025r^2 - 3675). \end{aligned} \quad (2.14)$$

Let  $\hat{\beta}$  be a point in the parameters space such that the function  $I_i(r; \hat{\beta})$ , defined in (2.9), has a zero of multiplicity  $k$  at  $\rho$ . Then  $1 \leq k \leq 8$  for  $\rho \neq \rho^\circ$  and  $k = 9$  when  $\rho = \rho^\circ$ . Moreover, for these values of  $k$ , there exist  $\beta$  in a neighborhood of  $\hat{\beta}$  such that  $I_i(r; \beta)$  has  $k$  simple zeros in a small enough neighborhood of  $\rho^\circ$ .

(b) Let  $\eta^\circ \approx 0.5143$  be the zero in  $(0, 1)$  of the function

$$\begin{aligned} w_{e,7}(r) = & 15(1 - r^2)^2(35r^{14} - 315r^{12} + 651r^{10} - 6523r^8 + 18193r^6 - 12201r^4 \\ & - 10815r^2 + 735)(L(r))^2 + 4r(40r^{18} - 1475r^{16} + 9680r^{14} - 64320r^{12} \\ & + 301680r^{10} - 662534r^8 + 492240r^6 + 93240r^4 - 180600r^2 + 11025)L(r) \\ & + 4r^2(80r^{16} + 2013r^{14} - 36257r^{12} + 174713r^{10} - 504557r^8 + 488775r^6 \\ & + 35245r^4 - 176925r^2 + 11025). \end{aligned}$$

Let  $\tilde{\beta}$  be a point in the parameters space such that the function  $\tilde{I}_e(r; \tilde{\beta})$ , defined in (2.10), has a zero of multiplicity  $\ell$  at  $\eta$ . Then  $1 \leq \ell \leq 7$  for  $\eta \neq \eta^\circ$  and  $\ell = 8$  when  $\eta = \eta^\circ$ . Moreover, for these values of  $\ell$ , there exist  $\beta$  in a neighborhood of  $\tilde{\beta}$  such that  $\tilde{I}_e(r; \beta)$  has  $\ell$  simple zeros in a small enough neighborhood of  $\eta^\circ$ .

*Proof.* We prove only the maximal multiplicity cases for  $I_i$ , that are  $k = 8, 9$ . The other

cases follow similarly.

First we show how the parameters  $\beta_j$ , for  $j = 0, \dots, 7$ , of the function  $I_i$  can be written in terms of  $\rho$ , when  $\rho$  is a zero of multiplicity eight of it. Hence, this function writes only using  $r, \rho, L(r), L(\rho)$ . We recall that  $0 < r < 1$  and, consequently,  $0 < \rho < 1$ .

Assume that  $\rho$  is a root of multiplicity eight. We consider the linear system of 8 equations and 8 variables  $\beta_j$ ,  $j = 0, \dots, 7$ , defined by  $\frac{d^j I_i}{dr^j}(\rho) = 0$  for  $j = 0, \dots, 7$ . As the Wronskian defined by  $[f_0, f_1, \dots, f_7]$  does not vanish for  $\rho \in (0, 1)$ , the variables  $\beta_j$ ,  $j = 0, \dots, 7$ , can be written as  $\beta_j = \hat{f}_j(\rho)\beta_8$ , with  $\hat{f}_j(\rho)$  functions of  $\rho$  and  $L(\rho)$ . See (2.9) for the definition of the functions  $f_j$ . Then, see for instance [NT17], the eighth derivative of  $I_i$  at  $\rho$  is

$$\frac{d^8 I_i}{dr^8}(\rho) = \frac{W([f_0, f_1, f_2, f_3, f_4, f_6, f_5, f_7, f_8], r)}{W([f_0, f_1, f_2, f_3, f_4, f_6, f_5, f_7], r)} \Big|_{r=\rho}, \quad (2.15)$$

where  $W$  denotes the Wronskian function. In particular

$$W([f_0, f_1, f_2, f_3, f_4, f_6, f_5, f_7, f_8], r)|_{r=\rho} = -5218385264640 w_{i,8}(\rho)/(1 - \rho^2)^{25},$$

where  $w_{i,8}(\rho)$  is defined in (2.14). When  $\rho \neq \rho^o$  clearly the multiplicity is eight and it can be checked that when  $\rho = \rho^o$  the multiplicity is nine.

Finally, the unfolding of zeros of any perturbation (moving the parameters  $\beta_j$ ) of  $I_i$ , in a small neighborhood of  $r = \rho$ , follows from the ECT-system (ECT-system with accuracy one) property for  $\rho \neq \rho^o$  ( $\rho = \rho^o$ ), see [NT17]. Consequently, the statement follows.  $\square$

**Proposition 2.10.** (a) *Let  $\rho^* \approx 0.3029$  be the positive solution of*

$$\begin{aligned} & 3(\rho^{12} - 75\rho^8 + 200\rho^6 - 645\rho^4 + 600\rho^2 + 175)L(\rho) \\ & + 2\rho(3\rho^{10} - 95\rho^8 + 390\rho^6 - 1230\rho^4 + 1975\rho^2 + 525) = 0. \end{aligned} \quad (2.16)$$

*Let  $\hat{\beta}$  be a point in the parameters space such that  $I_i$ , defined in (2.9), has a zero of multiplicity eight at  $\rho$ . The maximum number of zeros of  $I_i(r; \beta)$  in  $(0, 1)$  is 9 or 8 if  $\rho \in (0, \rho^*)$  or  $\rho \in (\rho^*, 1)$ , respectively, for all  $\beta$  in a small neighborhood of  $\hat{\beta}$ . Moreover, these maximal numbers are achieved as simple ones.*

(b) *Let  $\eta^* \approx 0.57704$  be the positive solution of*

$$\begin{aligned} & -135(1 - \eta^2)^4(35\eta^{10} - 147\eta^8 + 174\eta^6 + 378\eta^4 + 735\eta^2 + 105)(L(\eta))^3 - 9\eta(1 - \eta^2) \\ & (5\eta^{18} - 615\eta^{16} + 6615\eta^{14} - 25425\eta^{12} + 25305\eta^{10} - 22047\eta^8 + 91605\eta^6 - 123795\eta^4 \\ & + 40950\eta^2 + 9450)(L(\eta))^2 + 12\eta^2(1 - \eta^2)(177\eta^{16} - 1136\eta^{14} + 6090\eta^{12} + 5226\eta^{10} \\ & + 18762\eta^8 - 126900\eta^6 + 165690\eta^4 - 66150\eta^2 - 14175)L(\eta) - 12\eta^3(369\eta^{16} - 4358\eta^{14} \\ & + 28517\eta^{12} - 30268\eta^{10} - 76323\eta^8 + 178010\eta^6 - 143325\eta^4 + 37800\eta^2 + 9450) = 0. \end{aligned}$$

*Let  $\hat{\gamma}$  be a point in the parameters space such that  $\tilde{I}_e$ , defined in (2.10), has a zero of multiplicity seven at  $\eta$ . The maximum number of zeros of  $\tilde{I}_e(r; \gamma)$  in  $(0, 1)$  is 8 or 7 if*

$\eta \in (0, \eta^*)$  or  $\eta \in (\eta^*, 1)$ , respectively, for all  $\gamma$  in a small neighborhood of  $\hat{\gamma}$ . Moreover, these maximal numbers are achieved as simple ones.

*Proof.* We prove only the statement (a), the other case follows similarly.

As nine is the upper bound of the number of zeros of  $I_i$ , see Lemma 2.6, the distribution and the number of zeros, in terms of  $\rho$ , can be studied from the graph of  $I_i$  in the full interval  $(0, 1)$ . In fact, it only depends on the local plot near  $r = 0$ ,  $r = \rho$ , and  $r = 1$ . We start studying how is this local behavior in terms of  $\rho$  and we finish drawing the graph of the function  $I_i$ .

For the local behavior, first we consider  $\rho \neq \rho^o$ , see Proposition 2.9. Consequently  $r = \rho$  is a zero of multiplicity 8 (of  $I_i$ ) for  $\beta = \hat{\beta}$ . Also from the proof of Proposition 2.9 we can assume that  $\beta_8 = 1$  and, consequently,  $I_i$  writes as a rational function in  $\{r, \rho, L(r), L(\rho)\}$ . The series expansions are denoted by  $I_{i,0}$ ,  $I_{i,\rho}$ , and  $I_{i,1}$ , respectively. Straightforward computations show that

$$\begin{aligned} I_{i,0} &= h_{i,0}(\rho)r + \mathcal{O}(r^2), \\ I_{i,\rho} &= h_{i,\rho}(\rho)(r - \rho)^8 + \mathcal{O}((r - \rho)^9), \\ I_{i,1} &= h_{i,1}(\rho)\frac{1}{1 - r} + \mathcal{O}(r^0), \end{aligned}$$

where  $h_{i,\xi} = N_{i,\xi}/D_{i,\xi}$  for  $\xi \in \{0, \rho, 1\}$  and

$$N_{i,\xi}(\rho) = p_0^\xi(\rho) + p_1^\xi(\rho)L(\rho), \quad D_{i,\xi}(\rho) = q_0^\xi(\rho) + q_1^\xi(\rho)L(\rho),$$

for  $\xi \in \{0, \rho, 1\}$ , with  $p_j^\xi, q_j^\xi$  given polynomials. In fact, the denominators are related by the expressions  $D_{i,\rho}(\rho) = 7\rho(\rho^2 - 1)^5 D_{i,0}(\rho)$ ,  $D_{i,1}(\rho) = \rho D_{i,0}(\rho)/5$ , and

$$\begin{aligned} D_{i,0}(\rho) &= 225(3\rho^{14} - 3\rho^{12} - 165\rho^{10} + 77\rho^8 - 1071\rho^6 - 609\rho^4 - 175\rho^2 - 105)(\rho^2 - 1)^2 L(\rho) \\ &\quad + 30\rho(45\rho^{16} - 960\rho^{14} + 3480\rho^{12} - 13248\rho^{10} + 23170\rho^8 - 2240\rho^6 - 5600\rho^4 - 1575). \end{aligned}$$

We remark that the three denominators do not vanish for  $\rho \in (0, 1)$ . Now, we can draw  $h_{i,0}$ , first studying the local behavior near the endpoints of the interval of definition and second studying when it vanishes. The series of  $h_{i,0}$  at  $\rho = 0$  is

$$h_{i,0}(\rho) = \frac{512}{4725}\rho^8 - \frac{985088}{779625}\rho^{10} + \frac{140819456}{152026875}\rho^{12} + \mathcal{O}(\rho^{14})$$

and  $\lim_{\rho \rightarrow 1^-} h_{i,0}(\rho) = -\infty$ . When  $\rho \in (0, 1)$  the zeros of  $h_{i,0}(\rho)$  are obtained solving equation (2.16). Hence, as the coefficient of  $L$  in (2.16) does not vanish, the number of zeros of it is given by the zeros of

$$\Lambda(\rho) = L(\rho) + \frac{2\rho(3\rho^{10} - 95\rho^8 + 390\rho^6 - 1230\rho^4 + 1975\rho^2 + 525)}{3(\rho^{12} - 75\rho^8 + 200\rho^6 - 645\rho^4 + 600\rho^2 + 175)}.$$

As  $L'(\rho)$  only has a zero, the drawing of  $h_{i,0}$  in  $(0, 1)$  is sketched in Figure 2.4. Clearly, equation (2.16) only has one positive zero which defines the bifurcation point  $\rho^* \approx 0.3029$ .

From (2.15) we know that  $h_{i,\rho} = 8!(d^8 I_i/dr^8)(\rho)$  that only has a positive zero at  $\rho^\circ$ , see equation (2.14). Consequently the drawing of  $h_{i,\rho}$  in  $(0, 1)$  is sketched in Figure 2.4 because  $\lim_{\rho \rightarrow 1^-} h_{i,\rho}(\rho) = -\infty$  and its series expansion at  $\rho = 0$  is

$$h_{i,\rho}(\rho) = \frac{512}{4725}\rho - \frac{118784}{111375}\rho^3 - \frac{714041344}{152026875}\rho^5 + \mathcal{O}(\rho^7).$$

Arguing as in the above cases and using that  $\lim_{\rho \rightarrow 1^-} h_{i,1}(\rho) = 0$  and

$$h_{i,1}(\rho) = -\frac{2048}{4725}\rho + \frac{2220032}{779625}\rho^3 - \frac{1308176384}{152026875}\rho^5 + \mathcal{O}(\rho^7),$$

the drawing of  $h_{i,1}$  is sketched in Figure 2.4.

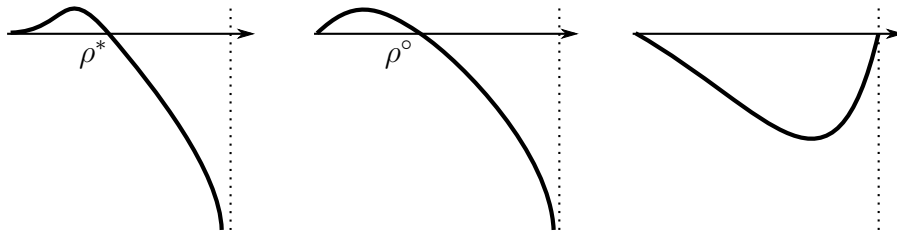


Figure 2.4: Graph of  $h_{i,0}(\rho)$ ,  $h_{i,\rho}(\rho)$ , and  $h_{i,1}(\rho)$  on  $(0,1)$ , respectively

From the above description, it is clear that the graph of  $I_i(r, \hat{\beta})$  for  $r \in (0, 1)$  depends on  $\rho$ . In particular, it can be seen that, when  $\rho \in (0, \rho^*)$  and  $\rho \neq \rho^\circ$ ,  $I_i$  has a zero of multiplicity eight at  $r = \rho$  and an extra simple zero in  $(0, 1)$ . Moreover, when  $\rho = \rho^*$   $I_i$  has a zero of multiplicity nine and when  $\rho \in (\rho^*, 1)$ ,  $I_i$  has no other zeros except the zero of multiplicity eight at  $r = \rho$ . The different plots of  $I_i(r, \hat{\beta})$  for  $r \in (0, 1)$  when  $\rho$  varies in  $(0, 1)$  can be seen in Figure 2.5.

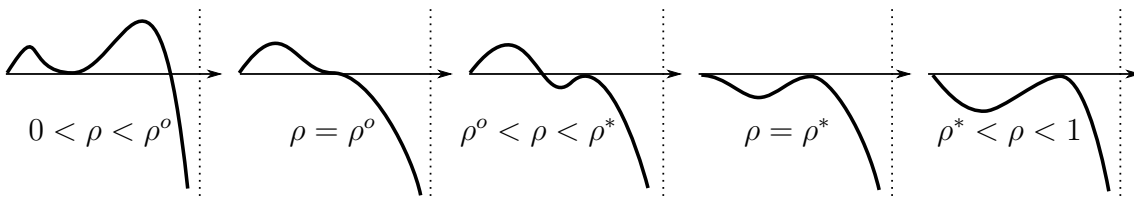


Figure 2.5: Graphs of  $I_i(r, \hat{\beta})$  for  $r \in (0, 1)$  for different values of  $\rho$ .

Finally, the proof follows, also using also Proposition 2.9, choosing values of  $\beta$  close enough to  $\hat{\beta}$ .  $\square$

## 2.4 Existence of simultaneous zeros in the internal and external regions

This section is devoted to prove the second part of Theorem 2.3, which provides a partial result about the simultaneous bifurcation of limit cycles in the inner and outer period annuli

regions. Following the change of variable in the outer period annuli,  $r \rightarrow 1/r$ , introduced in Lemma 2.7, we study the simultaneous zeros of the functions  $I_i$  and  $\tilde{I}_e$ , see (2.9) and (2.10). In Section 2.3, we have proved that the maximum number of zeros, separately, of the inner and outer Abelian integrals, is 9 and 8, respectively. Moreover, except for some special values of the perturbation parameters, the maximum multiplicity of each zero is 8 and 7, respectively. We remark that, while the number of parameters in the inner and outer annuli regions is 9 and 8, see Lemmas 2.6 and 2.7, we will see, in Lemma 2.11, that the total number of independent parameters is 11. But the dimension of the essential parameter space is 10, because it is not restrictive to assume that one of them is different from zero. A complete study of all possible configurations of zeros of both Abelian integrals is very difficult due to the high dimension of the parameter space. For this reason we study some special zones in this 10-dimensional space. More concretely, we will study all possible configurations of simultaneous zeros near zeros of multiplicities  $(k, \ell)$  such that  $k + \ell = 10$ , that is  $(8, 2)$ ,  $(7, 3)$ ,  $(6, 4)$ ,  $(5, 5)$ ,  $(4, 6)$ , and  $(3, 7)$ , see Propositions 2.12, 2.13, 2.14, 2.15, 2.16, and 2.17, respectively. Theorem 2.3 follows from them.

Straightforward computations show, see the next result, the relation between the parameters that appear in the definition of the inner and outer Abelian integrals, when we study the configuration of simultaneous zeros.

**Lemma 2.11.** *When the zeros of the functions  $I_i$  and  $\tilde{I}_e$  are considered simultaneously, the parameters  $\beta$  and  $\gamma$ , defined in (2.9) and (2.10), can be written as  $\beta_j = \alpha_j$  for  $j = 0, \dots, 8$  and  $\gamma_0 = \alpha_0 + \alpha_1 + \alpha_2 + \alpha_3$ , and  $\gamma_j = \alpha_{j+3}$  for  $j = 1, \dots, 7$ .*

Our interest in this section will be not only the study of the number of zeros that have the functions  $I_i$  and  $\tilde{I}_e$  simultaneously. We deal also with a partial study of the bifurcation diagram of them. As we have mentioned above, this is done by taking two simultaneous zeros  $(\rho, \eta)$  with multiplicities  $(k, \ell)$ , in the inner and outer regions, such that  $k + \ell = 10$ . Hence, as in the previous section, every point  $(\rho, \eta) \in (0, 1)^2$  corresponds with a line of points  $\alpha = (\alpha_0, \dots, \alpha_{10}) \in \mathbb{R}^{11}$ . In some sense, we have compactified the parameter space transforming the 11-dimensional space to a compact region of a 2-dimensional space, in fact the unit square. The following results provide the different regions in  $(0, 1)^2$  corresponding with all possible configurations of simultaneous zeros of the functions  $I_i$  and  $\tilde{I}_e$  in the full interval  $(0, 1)$  in a neighborhood of the full line defined by  $\alpha$ .

**Proposition 2.12.** *Let  $\rho, \eta$  be zeros of multiplicity 8 and 2 of  $I_i$  and  $\tilde{I}_e$ , respectively. There exist two curves  $\Upsilon = \{\rho = \rho^*\}$  and  $\Psi = \{N_{e,0}(\rho, \eta) = 0\}$  such that the square  $(0, 1)^2$  is divided in four regions, see Figure 2.6. In particular,  $\rho^*$  is the unique zero of (2.16) and the function  $N_0^e(\rho, \eta)$  writes as*

$$N_{e,0}(\rho, \eta) = p_0^0 + p_1^0 L(\rho) + p_2^0 L(\eta) + p_3^0 L(\rho)L(\eta),$$

with  $p_0^0$ ,  $p_1^0$ ,  $p_2^0$ , and  $p_3^0$  polynomials in  $\rho$  and  $\eta$  of degrees 29, 28, 30, and 29, respectively. Then, the configurations of simple zeros of  $I_i$  and  $\tilde{I}_e$ , in a neighborhood of  $(\rho, \eta)$ , are  $(9, 3)$ ,

$(9, 2)$ ,  $(8, 3)$ , and  $(8, 2)$ , respectively. Moreover, each of them is realizable only in one of the four regions.

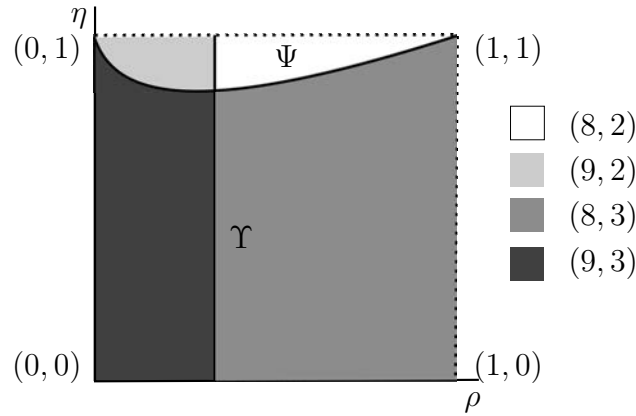


Figure 2.6: Bifurcation diagram of configuration of simultaneous zeros for the maximum multiplicity case  $(8, 2)$

*Proof.* The proof follows similarly as the proof of Proposition 2.9 studying the different plots of the functions  $I_i(r)$  and  $\tilde{I}_e(r)$  in  $r \in (0, 1)$ , but in terms of the parameters  $\rho$  and  $\eta$ . We only show the main differences.

Let  $\rho$  and  $\eta$  be zeros of multiplicity 8 and 2 of the functions  $I_i$  and  $\tilde{I}_e$ , respectively, defined in Lemma 2.11. Straightforward computations provide the coefficients  $\alpha_j$ , for  $j = 0, \dots, 10$ , in terms of  $\rho$  and  $\eta$ . We denote this special value as  $\hat{\alpha}$ . In fact, the function  $I_i(r, \alpha(\rho))$  coincides with the obtained in Propositions 2.9 and 2.10. So,  $\alpha_j = \beta_j$ , for  $j = 0, \dots, 7$ , and  $I_i$  is a function of  $\{r, \rho, L(r), L(\rho)\}$  with  $0 < r, \rho < 1$ . Moreover the other components  $\alpha_8, \alpha_9$ , and  $\alpha_{10}$  are functions of  $\rho$  and  $\eta$ . Consequently, the function  $\tilde{I}_e$  writes in terms of  $\{r, \rho, \eta, L(r), L(\rho), L(\eta)\}$  with  $0 < r, \rho, \eta < 1$ .

The local and global studies for the function  $I_i$  are, in fact, the same. Consequently, only remains the study of  $\tilde{I}_e$ . Its series expansions at  $r = 0$ , at  $r = \eta$  and  $r = 1$  write as

$$\begin{aligned}\tilde{I}_{e,0} &= h_{e,0}(\rho, \eta)r^4 + \mathcal{O}(r^5), \\ \tilde{I}_{e,\eta} &= h_{e,\eta}(\rho, \eta)(r - \eta)^2 + \mathcal{O}((r - \eta)^3), \\ \tilde{I}_{e,1} &= h_{e,1}(\rho, \eta)\frac{1}{1 - r} + \mathcal{O}(1),\end{aligned}$$

respectively. For each value  $\xi \in \{0, \eta, 1\}$ , we denote the numerators and denominators by  $N_{e,\xi}(\rho, \eta) = \text{num}(h_{e,\xi})$  and  $D_{e,\xi}(\rho, \eta) = \text{den}(h_{e,\xi})$ . As  $D_{e,0} = D_{e,1}$ ,  $D_{e,\eta} = D_{e,1}/(\eta^2 - 1)$  and  $N_{e,1} < 0$  with  $0 < \rho, \eta < 1$ , essentially, there are only three different functions to be studied:

$$\begin{aligned}N_{e,0}(\rho, \eta) &= p_0^0 + p_1^0 L(\rho) + p_2^0 L(\eta) + p_3^0 L(\rho)L(\eta), \\ N_{e,\eta}(\rho, \eta) &= p_0^\eta + p_1^\eta L(\rho) + p_2^\eta L(\eta) + p_3^\eta L(\rho)L(\eta), \\ D_{e,1}(\rho, \eta) &= q_0^1 + q_1^1 L(\rho) + q_2^1 L(\eta) + q_3^1 L(\rho)L(\eta),\end{aligned}\tag{2.17}$$

with  $p_0^0, p_1^0, p_2^0$  and  $p_3^0$  polynomials in  $\rho$  and  $\eta$  of degrees 29, 30, 28, and 29;  $p_0^\eta, p_1^\eta, p_2^\eta$  and  $p_3^\eta$  polynomials in  $\rho$  and  $\eta$  of degrees 33, 34, 30, and 31; and  $q_0^1, q_1^1, q_2^1$  and  $q_3^1$  polynomials in  $\rho$  and  $\eta$  with rational coefficients of degrees 29, 30, 28, and 29. We do not write here the explicit expressions of that polynomials because of the size of them.

The signs of the functions (2.17) define the topologically different plots of  $\tilde{I}_e(r, \hat{\alpha})$ . The zero level curves of  $N_{e,0}$ ,  $N_{e,\eta}$  and  $D_{e,1}$  are depicted in Figure 2.7 as black, red and blue dots lines, respectively. Moreover, they define six different regions denoted by  $I$ ,  $II$ ,  $III$ ,  $IV$ ,  $V$ , and  $VI$  in Figure 2.7. In Section 2.5 we do a more detailed study of that zero level curves near the corners of the domain of definition.

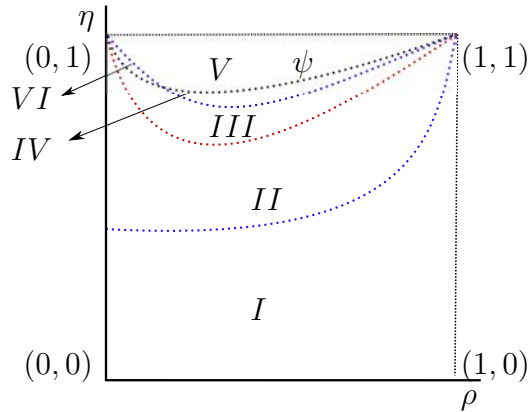


Figure 2.7: The zero level curves of  $N_{e,0}$ ,  $N_{e,\eta}$  and  $D_{e,1}$  in black, red, and blue dotted lines, respectively

Now, analyzing the sign of the functions (2.17), it can be shown that in regions  $I$ ,  $II$ ,  $III$ , and  $IV$  the function  $\tilde{I}_e(r, \hat{\alpha})$  has a point of multiplicity 2 at  $r = \eta$  and an extra simple zero in  $(0, 1)$ . Moreover in regions  $V$  and  $VI$  only a zero of multiplicity 2 exits at  $r = \eta$ . Examples of both situations are drawn in Figure 2.8. Arguing as in the inner Abelian integral we can obtain that the outer Abelian integral has two or three simple zeros depending on the values of  $(\rho, \eta)$ .

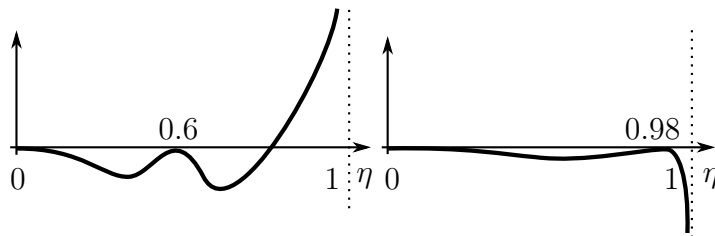


Figure 2.8: The graphs of  $I_e(r, \hat{\alpha})$  for  $(\rho, \eta) = (0.1, 0.6)$  and  $(\rho, \eta) = (0.4, 0.98)$ , respectively

All the above results, together with the obtained in Proposition 2.10.(a), can be summarized in the bifurcation diagram given in the statement. See Figure 2.6. More concretely, the dark gray region corresponds to the maximal number of 12 simple zeros in configuration  $(9, 3)$ . The region with 11 simple zeros correspond with the medium gray and the light gray in

configurations (8, 3) and (9, 2), respectively. The cases with 10 simple zeros in configuration (8, 2) correspond to the white region.  $\square$

From the above proof we have seen that the bifurcation curves are the numerators and denominators of the series expansions in  $\rho$  and  $\eta$ . In particular they are functions of the form (2.17). To simplify the reading, we have unified how the bifurcation curves that will appear in the following results are written,

$$\begin{aligned} N_{j,\xi}(\rho, \eta) &= p_0^{j,\xi} + p_1^{j,\xi}L(\eta) + p_2^{j,\xi}L(\rho) + p_3^{j,\xi}(L(\eta))^2 + p_4^{j,\xi}L(\rho)L(\eta), \\ &\quad + p_5^{j,\xi}L(\rho)(L(\eta))^2 + p_6^{j,\xi}(L(\eta))^3 + p_7^{j,\xi}L(\rho)(L(\eta))^3, \\ D_{j,\xi}(\rho, \eta) &= q_0^{j,\xi} + q_1^{j,\xi}L(\eta) + q_2^{j,\xi}L(\rho) + q_3^{j,\xi}(L(\eta))^2 + q_4^{j,\xi}L(\rho)L(\eta), \\ &\quad + q_5^{j,\xi}L(\rho)(L(\eta))^2 + q_6^{j,\xi}(L(\eta))^3 + q_7^{j,\xi}L(\rho)(L(\eta))^3, \end{aligned} \quad (2.18)$$

where  $p_k^{j,\xi}$  and  $q_k^{j,\xi}$  are polynomials in  $\rho, \eta$  for  $j \in \{i, e\}$ ,  $\xi \in \{0, \rho, 1\}$  and  $k = 0, \dots, 7$ . As in the last proof all  $p_k^{j,\xi}$  and  $q_k^{j,\xi}$  are polynomials of high degrees with rational coefficients. In the next propositions we only get explicitly the sequence of degrees of them because of their sizes. We will say that a polynomial has degree  $\hat{0}$  when it vanishes identically.

**Proposition 2.13.** *Let  $\rho, \eta$  be zeros of multiplicity 7 and 3 of  $I_i$  and  $\tilde{I}_e$ , respectively. There exist three zero level curves  $\Theta = \{N_{i,\rho}(\rho, \eta) = 0\}$ ,  $\Lambda = \{N_{i,0}(\rho, \eta) = 0\}$ , and  $\Psi = \{N_{e,0}(\rho, \eta) = 0\}$  such that the square  $(0, 1)^2$  is divided in four regions, see Figure 2.9. Moreover, the functions  $N_{i,\rho}$ ,  $N_{i,0}$  and  $N_{e,0}$  write as (2.18) and the sequences of degrees of  $p_k^{i,\rho}$ ,  $p_k^{i,0}$ , and  $p_k^{e,0}$  are  $\{29, 30, 26, \hat{0}, 27, \hat{0}, \hat{0}, \hat{0}\}$ ,  $\{29, 30, 38, \hat{0}, 29, \hat{0}, \hat{0}, \hat{0}\}$ , and  $\{36, 37, 37, 34, 38, 25, \hat{0}, \hat{0}\}$  for  $k = 0, \dots, 7$ , respectively. Then, the configurations of simple zeros of  $I_i$  and  $\tilde{I}_e$ , in a neighborhood of  $(\rho, \eta)$ , are (9, 3), (7, 4), (8, 3), and (7, 3), respectively. Moreover, each of them is realizable only in one of the four regions.*

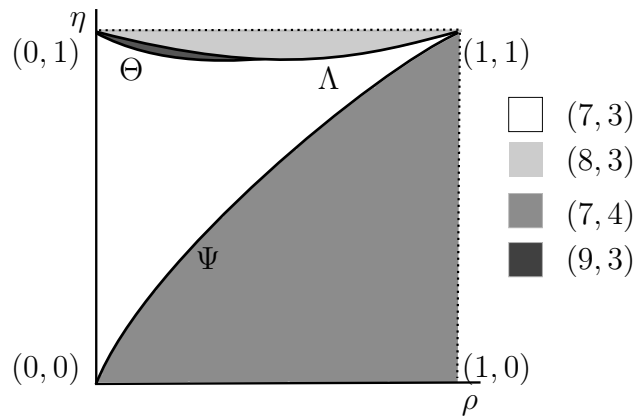


Figure 2.9: Bifurcation diagram of configuration of simultaneous zeros for the maximum multiplicity case (7, 3)

*Proof.* The proof follows similarly as the proof of Proposition 2.12. The main changes are the multiplicities at  $\rho$  and  $\eta$  that are 7 and 3 and the local behaviors of  $I_i$  and  $\tilde{I}_e$  are also

necessary to be done. This study, similar to the one performed for the outer function of the previous proposition, gives relations between the numerators and the denominators of the series expansions near  $r = 0$ ,  $r = \rho$ ,  $r = \eta$ , and  $r = 1$ . Therefore, we have only three zero level curves corresponding to  $I_i$  and another three to  $\tilde{I}_e$ . They are drawn in Figure 2.10 as dashed and dotted lines, respectively. All these curves are defined as zero level curves of functions of type (2.18). The remaining sequences of the degrees of the polynomials in (2.18), among the given in the statement, are  $\{31, 28, 32, \hat{0}, 29, \hat{0}, \hat{0}, \hat{0}\}$ ,  $\{41, 40, 42, 35, 41, 36, \hat{0}, \hat{0}\}$ , and  $\{36, 37, 37, 34, 38, 35, \hat{0}, \hat{0}\}$  for  $D_{i,1}(\rho, \eta)$ ,  $N_{e,\eta}(\rho, \eta)$  and  $D_{e,1}(\rho, \eta)$ , respectively. The proof finishes studying the plot of the functions  $I_i$  and  $\tilde{I}_e$  in each region depicted in Figure 2.10.

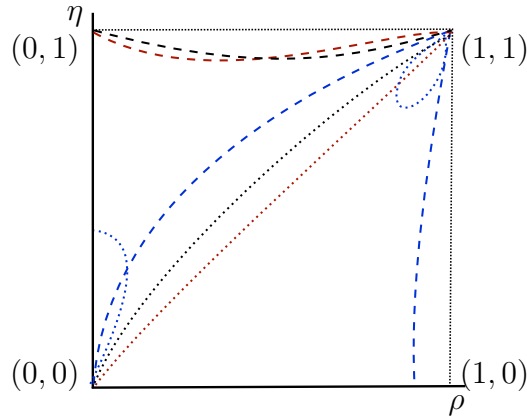


Figure 2.10: The zero level curves of  $N_{i,0}$ ,  $N_{i,\rho}$ ,  $D_{i,1}$  (dashed line) and  $N_{e,0}$ ,  $N_{e,\eta}$ ,  $D_{e,1}$  (dotted line) in black, red, and blue, respectively

□

**Proposition 2.14.** *Let  $\rho, \eta$  be zeros of multiplicity 6 and 4 of  $I_i$  and  $\tilde{I}_e$ , respectively. There exist three level curves  $\Lambda = \{N_{i,0}(\rho, \eta) = 0\}$ ,  $\Psi = \{N_{e,0}(\rho, \eta) = 0\}$ , and  $\Phi = \{N_{e,\eta}(\rho, \eta) = 0\}$ , such that the square  $(0, 1)^2$  is divided in four regions, see Figure 2.11. Moreover, the functions  $N_{i,0}$ ,  $N_{e,0}$ , and  $N_{e,\eta}$ , write as (2.18) and the list of degrees of the polynomials  $p_k^{i,0}$ ,  $p_k^{e,0}$ , and  $p_k^{e,\eta}$  are  $\{34, 35, 35, 32, 32, 31, \hat{0}, \hat{0}\}$ ,  $\{38, 39, 39, 38, 38, 33, 33, 32\}$ , and  $\{42, 43, 43, 40, 40, 33, \hat{0}, \hat{0}\}$ , for  $k = 0, \dots, 7$ , respectively. Then, the configurations of simple zeros of  $I_i$  and  $\tilde{I}_e$ , in a neighborhood of  $(\rho, \eta)$ , are  $(6, 6)$ ,  $(7, 4)$ ,  $(6, 5)$ , and  $(6, 4)$ , respectively. Each of them is realizable only in one of the four regions.*

*Proof.* The proof follows as the proof of Proposition 2.13 changing only the multiplicities, that are 6 and 4, and the zero level curves. In particular, the sequences of degrees, among the ones detailed in the statement, are  $\{38, 37, 39, 32, 38, 33, \hat{0}, \hat{0}\}$ ,  $\{38, 37, 37, 32, 32, 31, \hat{0}, \hat{0}\}$ , and  $\{38, 39, 37, 38, 38, 33, 33, 32\}$ , for  $N_{i,\rho}(\rho, \eta)$ ,  $D_{i,1}(\rho, \eta)$ , and  $D_{e,1}(\rho, \eta)$ , respectively. The zero level curves for this case are drawn in Figure 2.12.

□

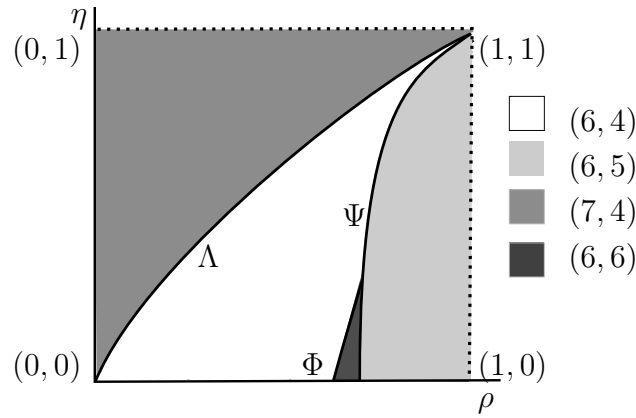


Figure 2.11: Bifurcation diagram of configuration of simultaneous zeros for the maximum multiplicity case (6, 4)

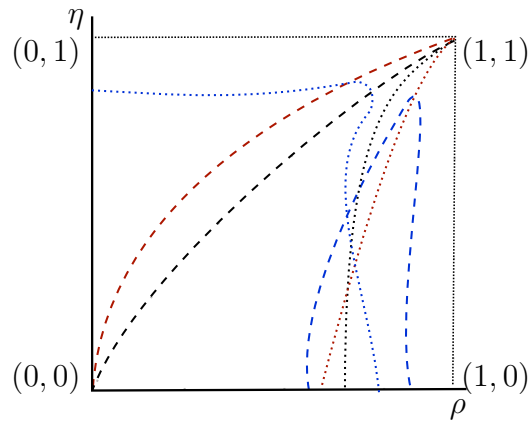


Figure 2.12: The zero level curves of  $N_{i,0}$ ,  $N_{i,\rho}$ ,  $D_{i,1}$  (dashed line) and  $N_{e,0}$ ,  $N_{e,\eta}$ ,  $D_{e,1}$  (dotted line) in black, red, and blue, respectively

**Proposition 2.15.** *Let  $\rho, \eta$  be zeros of multiplicity 5 of  $I_i$  and  $\tilde{I}_e$ , respectively. There exist two level curves  $\Lambda = \{N_{i,0}(\rho, \eta) = 0\}$  and  $\Psi = \{N_{e,0}(\rho, \eta) = 0\}$ , such that the square  $(0, 1)^2$  is divided in four regions, see Figure 2.13. Moreover, the functions  $N_{0,i}$  and  $N_{0,e}$  write as (2.18) and the sequences of degrees of  $p_k^{i,0}$  and  $p_k^{e,0}$  are  $\{30, 31, 31, 30, 30, 25, \hat{0}, \hat{0}\}$  and  $\{33, 34, 34, 35, 35, 32, 32, 25\}$  for  $k = 0, \dots, 7$ , respectively. Then, the configurations of simple zeros of  $I_i$  and  $\tilde{I}_e$ , in a neighborhood of  $(\rho, \eta)$ , are (6, 6), (6, 5), (6, 5), and (5, 5), respectively. Each of them is realizable only in one of the four regions.*

*Proof.* The proof follows as the proof of Proposition 2.13. Here the multiplicities are 5 in both inner and outer regions. Moreover, the sequences of degrees, among the ones detailed in the statement, are  $\{38, 39, 39, 36, 36, 29, \hat{0}, \hat{0}\}$ ,  $\{34, 35, 35, 32, 32, 25, \hat{0}, \hat{0}\}$ ,  $\{36, 37, 37, 36, 36, 31, \hat{0}, \hat{0}\}$ , and  $\{33, 34, 34, 35, 35, 32, 30, 25\}$ , for  $N_{i,\rho}(\rho, \eta)$ ,  $D_{i,1}(\rho, \eta)$ ,  $N_{e,\eta}(\rho, \eta)$ , and  $D_{e,1}(\rho, \eta)$ , respectively. The zero level curves for this case are depicted in Figure 2.14.

□

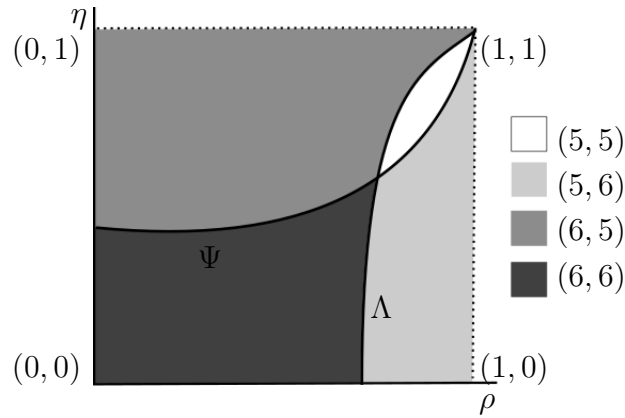


Figure 2.13: Bifurcation diagram of configuration of simultaneous zeros for the maximum multiplicity case (5, 5)

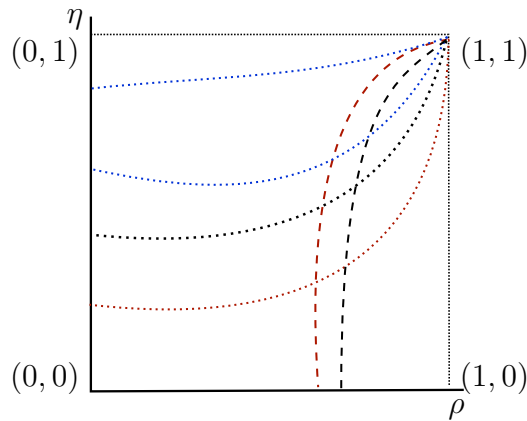


Figure 2.14: The zero level curves of  $N_{i,0}$ ,  $N_{i,\rho}$ ,  $D_{i,1}$  (dashed line) and  $N_{e,0}$ ,  $N_{e,\eta}$ ,  $D_{e,1}$  (dotted line) in black, red and blue, respectively

**Proposition 2.16.** *Let  $\rho, \eta$  be zeros of multiplicity 4 and 6 of  $I_i$  and  $\tilde{I}_e$ , respectively. There exist four level curves  $\Theta = \{N_{i,\rho}(\rho, \eta) = 0\}$ ,  $\Lambda = \{N_{i,0}(\rho, \eta) = 0\}$ ,  $\Phi = \{N_{e,\eta}(\rho, \eta) = 0\}$ , and  $\Psi = \{N_{e,0}(\rho, \eta) = 0\}$ , such that the square  $(0, 1)^2$  is divided in five regions, see Figure 2.15. Moreover, the functions  $N_{i,\rho}$ ,  $N_{i,0}$ ,  $N_{e,\eta}$ , and  $N_{e,0}$ , write as (2.18) and the sequences of degrees of  $p_k^{i,\rho}$ ,  $p_k^{i,0}$ ,  $p_k^{e,\eta}$ , and  $p_k^{e,0}$ , are  $\{32, 33, 33, 32, 32, 27, \hat{0}, \hat{0}\}$ ,  $\{24, 25, 23, 22, 24, 21, \hat{0}, \hat{0}\}$ ,  $\{31, 32, 30, 29, 31, 28, \hat{0}, \hat{0}\}$ , and  $\{27, 28, 28, 29, 29, 28, 24, 23\}$  are  $k = 0, \dots, 7$ , respectively. Then, the configurations of simple zeros of  $I_i$  and  $\tilde{I}_e$ , in a neighborhood of  $(\rho, \eta)$ , are (4, 8), (6, 6), (4, 7), (5, 6), and (4, 6), respectively. Each of them is realizable only in one of the five regions.*

*Proof.* The proof follows, changing the multiplicities to 4 and 6, as the proof of Proposition 2.13. The sequences of degrees, among the ones detailed in the statement, are  $\{30, 29, 29, 24, 28, 23, \hat{0}, \hat{0}\}$ , and  $\{29, 30, 28, 29, 29, 28, 22, 23\}$  for  $D_{i,1}(\rho, \eta)$  and  $D_{e,1}(\rho, \eta)$ , respectively. The zero level curves for this case are drawn in Figure 2.16.

□

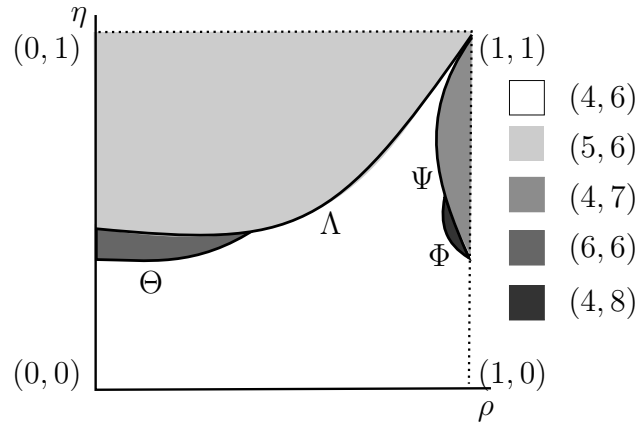


Figure 2.15: Bifurcation diagram of configuration of simultaneous zeros for the maximum multiplicity case (4, 6)

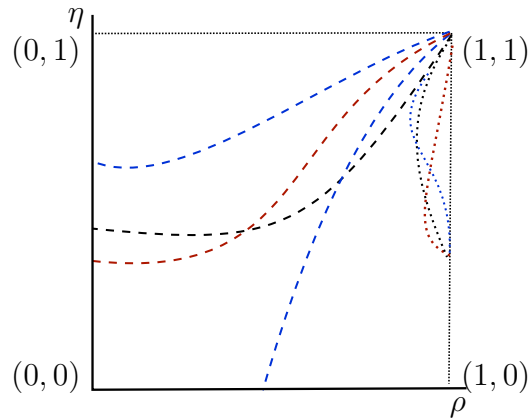


Figure 2.16: The zero level curves of  $N_{i,0}$ ,  $N_{i,\rho}$ ,  $D_{i,1}$  (dashed line) and  $N_{e,0}$ ,  $N_{e,\eta}$ ,  $D_{e,1}$  (dotted line) in black, red, and blue, respectively

**Proposition 2.17.** *Let  $\rho, \eta$  be zeros of multiplicity 3 and 7 of  $I_i$  and  $\tilde{I}_e$ , respectively. There exists one level curve  $\Gamma = \{\eta^* \approx 0.57704\}$ , such that the square  $(0, 1)^2$  is divided in two regions, see Figure 2.17. Then, the configurations of simple zeros of  $I_i$  and  $\tilde{I}_e$ , in a neighborhood of  $(\rho, \eta)$ , are (4, 8) and (4, 7), respectively. Each of them is realizable only in one of the two regions, see also Figure 2.17.*

*Proof.* The proof follows as the proof of Proposition 2.13 changing only the multiplicities, that in this case are 3 and 7, and the zero level curves. The sequences of degrees are  $\{29, 30, 28, 27, 29, 26, \hat{0}, \hat{0}\}$ ,  $\{14, 15, \hat{0}, 14, \hat{0}, \hat{0}, \hat{0}, \hat{0}\}$ , and  $\{20, 21, \hat{0}, 18, \hat{0}, \hat{0}, \hat{0}, \hat{0}\}$ , for  $N_{i,\rho}(\rho, \eta)$ ,  $N_{i,0}(\rho, \eta)$ , and  $D_{i,1}(\rho, \eta)$ , respectively. The zero level curves are depicted in Figure 2.18. In fact in the square  $(0, 1)^2$  only appear two curves.  $\square$

Finally we summarize the configurations given in all the above results in the next corollary.

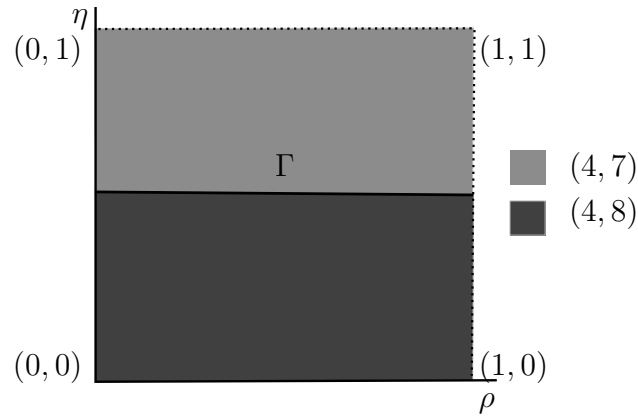


Figure 2.17: Bifurcation diagram of configuration of simultaneous zeros for the maximum multiplicity case  $(3, 7)$

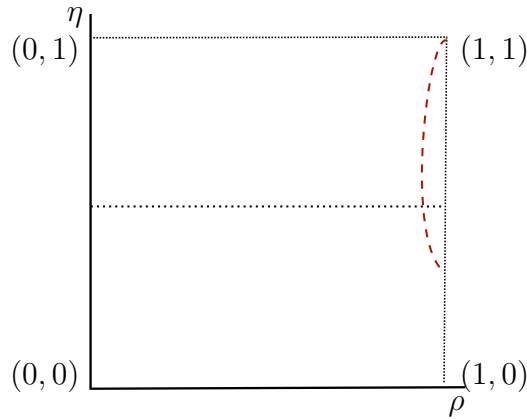


Figure 2.18: The zero level curves of  $N_{i,\rho}$  (dashed line) in red and  $N_{e,0}$  (dotted line) in black, respectively

**Corollary 2.18.** *There exist polynomial perturbation of degree 3 such that (2.1) exhibits 10, 11, and 12 limit cycles in configurations  $\{(8, 2), (7, 3), (6, 4), (5, 5), (4, 6), (3, 7)\}$ ,  $\{(9, 2), (8, 3), (7, 4), (6, 5), (5, 6), (4, 7)\}$ , and  $\{(9, 3), (6, 6), (4, 8)\}$ , respectively.*

From the technique used in this section it is clear that, as there are 10 essential parameters, there exist perturbations such that system (2.1) exhibits all the configurations of limit cycles of type  $(k, \ell)$  with  $k + \ell < 10$ ,  $0 \leq k \leq 8$  and  $0 \leq \ell \leq 7$ . For that reason we have concentrated our efforts in the configurations exhibiting more limit cycles and how they can appear.

### 2.5 Local study of the zero level curves in the bifurcation diagrams

Finally, we explain how the zero levels curves (2.17) can be studied near the boundary of the domain of definition and the difficulties, that we have found, when they are non analytic. We make the analysis in the neighborhood of the corners of  $[0, 1]^2$  where they can be extended. Before the description of them, we present a general result about how to obtain the branches of a curve with only one logarithm function.

**Lemma 2.19.** *Consider the zero level curve*

$$f(u, v) + g(u, v) \log v = 0, \quad (2.19)$$

with  $f$  and  $g$  analytical functions such that  $f(0, 0) = g(0, 0) = 0$ . Then, it is a solution of the differential equation

$$(\dot{u}, \dot{v}) = (h(u, v), v), \quad (2.20)$$

where  $h = (v(fg_v - f_vg) - g^2)/(f_u g - f g_u)$ . Furthermore, if  $h$  is analytical,  $h(0, 0) = 0$ , and  $\frac{\partial h}{\partial u}(0, 0) = k$ , with  $k$  a natural bigger than one, then there exists a  $C^\infty$  function  $U(u, v)$  such that  $u(v) = U(v^k \log v, v)$  satisfies (2.19).

*Proof.* Firstly, we consider a  $t$ -parameterization,  $(u(t), v(t))$ , of the level curve (2.19) such that  $v \neq 0$ . As it satisfies  $\frac{d}{dt}(f(u(t), v(t)) + g(u(t), v(t)) \log(v(t))) = 0$  for every  $t$ , we can write

$$f_u \dot{u} + f_v \dot{v} + (g_u \dot{u} + g_v \dot{v}) \log v + g \frac{1}{v} \dot{v} = f_u \dot{u} + f_v \dot{v} - (g_u \dot{u} + g_v \dot{v}) \frac{f}{g} + g \frac{1}{v} \dot{v} = 0,$$

or equivalently,

$$v(f_u g - f g_u) \dot{u} + (v(f_v g - f g_v) + g^2) \dot{v} = 0.$$

So, we have written the level curve as a solution of system (2.20).

Secondly, under the conditions of the statement, the origin is an equilibrium point of (2.20) such that the matrix of its linear part has eigenvalues  $k$  and 1. The study of the normal form of (2.20) can be done using the resonance theory. In fact, only the first component,  $h(u, v)$ , has resonances. As the equation  $(k, 1)(n, m) - k = 0$  has solution only when  $(n, m) = (0, k)$ , then there exists a diffeomorphism  $(u, v) = (U(x, y), y)$  that transforms system (2.20) to its normal form

$$\begin{cases} \dot{x} = kx - y^k, \\ \dot{y} = y. \end{cases} \quad (2.21)$$

The proof finishes using  $(x(t), y(t)) = ((x_0 - y_0^k t)e^{kt}, y_0 e^t)$  as the solution of the above differential equation and changing  $t = \log(y/y_0) = \log(v/y_0)$ .  $\square$

**Proposition 2.20.** *Let  $N_{e,0}$ ,  $N_{e,\eta}$ , and  $D_{e,1}$  be the zero level curves defined in (2.17). Then,*

- (a) *there are only two branches passing through  $(0, 0)$  and they are  $\rho = \eta = 0$ ,*
- (b) *there is only one branch passing through  $(1, 0)$  and it is  $\eta = 0$ ,*
- (c) *for each  $N_{e,0}$ ,  $N_{e,\eta}$ , and  $D_{e,1}$ , there is only one branch passing through  $(0, 1)$ . Their series expansions are*

$$0 = \rho + \frac{945}{32} L(\eta) \left( \frac{1-\eta}{1+\eta} \right)^2 - \frac{315}{64} \left( \frac{1-\eta}{1+\eta} \right) + \frac{315}{64} \left( \frac{1-\eta}{1+\eta} \right)^2 + \frac{2835}{16} L(\eta) \left( \frac{1-\eta}{1+\eta} \right)^3 + \dots,$$

$$0 = \rho + \frac{945}{32} L(\eta) \left( \frac{1-\eta}{1+\eta} \right)^3 - \frac{315}{128} \left( \frac{1-\eta}{1+\eta} \right) + \frac{315}{64} \left( \frac{1-\eta}{1+\eta} \right)^2 + \frac{945}{4} L(\eta) \left( \frac{1-\eta}{1+\eta} \right)^4 + \dots,$$

$$0 = \rho + \frac{315}{8} L(\eta) \left( \frac{1-\eta}{1+\eta} \right)^2 - \frac{315}{64} \left( \frac{1-\eta}{1+\eta} \right) + \frac{105}{2} \left( \frac{1-\eta}{1+\eta} \right)^2 + \frac{945}{16} L(\eta) \left( \frac{1-\eta}{1+\eta} \right)^3 + \dots,$$

respectively.

(d) for each  $N_{e,0}$ ,  $N_{e,\eta}$  there is only one branch passing through  $(1,1)$  and two for  $D_{e,1}$ . Their series expansion are

$$\begin{aligned} 0 &= \frac{1-\eta}{1+\eta} - \frac{1}{2} \frac{\sqrt{10}}{\sqrt{-L(\rho)}} \left( \frac{1-\rho}{1+\rho} \right)^2 + \dots, \\ 0 &= \frac{1-\eta}{1+\eta} - \frac{1}{2} \frac{\sqrt[3]{20}}{\sqrt[3]{-L(\rho)}} \left( \frac{1-\rho}{1+\rho} \right)^{4/3} + \dots, \\ 0 &= \frac{1-\eta}{1+\eta} - \sqrt{3} \left( \frac{1-\rho}{1+\rho} \right)^2 + \dots, \\ 0 &= \frac{1-\eta}{1+\eta} + \frac{5}{12} \frac{1}{L(\rho)} + \dots, \end{aligned}$$

respectively.

*Proof.* (a) All curves in (2.17) are analytic in  $(\rho, \eta) = (0, 0)$  and, in order to unify notation along the proof, we write  $(\rho, \eta) = (u, v)$ . Now, at the origin, they write as  $f(u, v) = u^i v^j \tilde{f}(u, v)$  with  $\tilde{f}(0, 0) \neq 0$ . More concretely, we have

$$\begin{aligned} \tilde{N}_{e,0} &= \frac{4096}{21} u^8 v^7 (63 + 224 u^2 - 90 v^2 + \dots), \\ \tilde{N}_{e,\eta} &= -\frac{4096}{21} u^8 v^9 (63 + 224 u^2 - 81 v^2 + \dots), \\ \tilde{D}_{e,1} &= -\frac{4096}{21} u^8 v^5 (63 + 224 u^2 - 297 v^2 + \dots). \end{aligned}$$

So, moving to the original coordinates, all curves has only the branches  $\rho = \eta = 0$  at the origin.

(b) The study near  $(\rho, \eta) = (1, 0)$  will be done near the origin, as in the previous case, but using the change  $(\rho, \eta) = (\frac{1-u}{1+u}, v)$ . Although the curves are analytic only with respect to  $\eta$ , or  $v$ , the series, using the logarithmic function, can be extended to the origin. They write as  $f(u, v) = v^j \tilde{f}(u, v)$  with  $\tilde{f}(u, v)$  different from zero near the origin. More concretely, we have

$$\begin{aligned} \tilde{N}_{e,0} &= 4096 v^7 (-12 \log u - 25 + 24 v^2 \log u + \dots), \\ \tilde{N}_{e,\eta} &= -4096 v^9 (-12 \log u - 25 + 36 v^2 \log u + \dots), \\ \tilde{D}_{e,1} &= 4096 v^5 (-12 \log u - 25 + 36 v^2 \log u + \dots). \end{aligned}$$

The proof of this statement finishes because, in the above curves only  $v = 0$ , or  $\eta = 0$ , passes through the point  $(1, 0)$ .

(c) As in the above cases, we study the neighborhood of the point  $(\rho, \eta) = (0, 1)$  with an adequate change of variables,  $(\rho, \eta) = (u, \frac{1-v}{1+v})$ , that moves it to the origin. But in this case we use also Lemma 2.19 for each function  $N_{e,0}$ ,  $N_{e,\eta}$  and  $D_{e,1}$ , writing them in the form  $f(u, v) = u^i \tilde{f}(u, v)$ , where  $\tilde{f}(u, v) = \tilde{f}_0(u, v) + \tilde{f}_1(u, v) \log v$  and  $\tilde{f}_0(0, 0) = \tilde{f}_1(0, 0) = 0$ .

Firstly, we detail the computations for  $N_{e,0}$ , in (2.17). For this function, we have

$$\begin{aligned}\tilde{f}_0(u, v) &= 704u - 3465v + 72765v^2 - 14080uv + \dots, \\ \tilde{f}_1(u, v) &= 9v^2 - 126v^3 + 936v^4 + 4u^2v^2 + \dots.\end{aligned}$$

Hence, applying Lemma 2.19, we get (2.20) with  $k = 2$  and

$$h(u, v) = 2u - \frac{315}{64}v - \frac{5985}{128}v^2 + \frac{3}{2}uv + \dots.$$

Consequently, there exists a diffeomorphism  $(u, v) = (U(x, y), y)$  such that the normal form associated to (2.20) is

$$(\dot{x}, \dot{y}) = \left( 2x - \frac{5985}{128}y^2, y \right),$$

which has the solution

$$(x(t), y(t)) = \left( \left( -\frac{5985}{128}y_0^2t + x_0 \right) e^{2t}, y_0 e^t \right).$$

Notice that, the above normal form is equivalent, after a rescaling in  $y$ , to (2.21). Then, we get  $u = U \left( \left( -\frac{5985}{128}y_0^2t + x_0 \right) e^{2t}, y_0 e^t \right)$  and  $u = U(v^2 \log v, v)$ . From this normal form we can write also the series expansion near the origin, that is

$$u = \frac{315}{64}v - \frac{945}{32}v^2 \log v - \frac{315}{64}v^2 - \frac{2835}{16}v^3 \log v + \dots.$$

The expression in the statement follows recovering the original coordinates,  $(\rho, \eta)$ .

Secondly, for  $N_{e,\eta}$ , the resonance corresponding to the normal form for equation (2.20) is  $k = 3$  and the series expansion writes as

$$u = \frac{315}{128}v - \frac{315}{64}v^2 - \frac{945}{32}v^3 \log v - \frac{945}{4}v^4 \log v + \dots.$$

Finally, as in the above cases, for  $D_{e,1}$  we obtain  $k = 2$  and

$$u = -\frac{315}{64}v + \frac{315}{8}v^2 \log v + \frac{105}{2}v^2 + \frac{945}{16}v^3 \log v + \dots.$$

(d) The last case is the study of the behavior of  $(\rho, \eta) = (1, 1)$ . The translation to the origin now is done by the change of variables  $(\rho, \eta) = (\frac{1-u}{1+u}, \frac{1-v}{1+v})$ . But for this last case is more difficult to find a general local development of all the curves. So, we will find only the first terms using a generalized Newton's diagram, using the powers in the variables  $u, v, \log u$ , and

$\log v$ , see [LR97]. In fact we depict the terms of the form  $u^{n_1}v^{m_1}$ ,  $u^{n_2}v^{m_2} \log u$ ,  $u^{n_3}v^{m_3} \log v$  and  $u^{n_4}v^{m_4} \log u \log v$  for our three curves to see which of them are enough to describe the series expansion near the origin. The corresponding generalized Newton's diagrams for the functions  $\tilde{N}_{e,0}$ ,  $\tilde{N}_{e,\eta}$ , and  $\tilde{D}_{e,1}$  are drawn in Figure 2.19. Hence, from them, the first terms

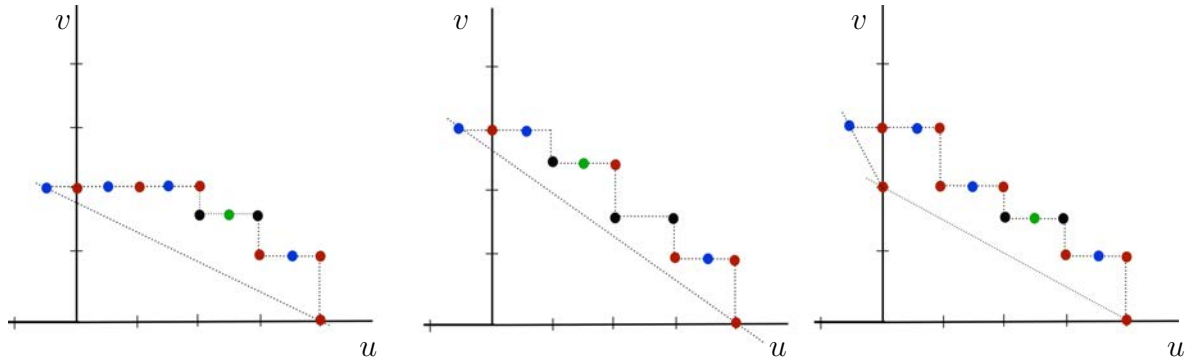


Figure 2.19: The red, blue, black and green are points represent the monomials of  $N_{e,0}$ (left),  $N_{e,\eta}$ (middle), and  $D_{e,1}$ (right) associated to  $(u^{n_1}v^{m_1})$ ,  $(u^{n_2}v^{m_2} \log u)$ ,  $(u^{n_3}v^{m_3} \log v)$  and  $(u^{n_4}v^{m_4} \log u \log v)$ , respectively.

for studying the different branches of the level zero curve are

$$\begin{aligned}\tilde{N}_{e,0} &= -393216(2v^2 \log u + 5u^4) + \dots, \\ \tilde{N}_{e,\eta} &= 1572864(2v^3 \log u + 5u^4) + \dots, \\ \tilde{D}_{e,1} &= -262144(12v^3 \log u + 5v^2 - 15u^4) + \dots.\end{aligned}$$

Then, the branches of  $\tilde{N}_{e,0} = 0$  follow studying a series expansion of the form

$$v = A_0 u^2 / \sqrt{-\log u} + \dots.$$

Straightforward computations give us two possible values for  $A_0$ ,  $\pm\sqrt{10}/2$ , but, as we are interested only in the branches in the first quadrant ( $u, v > 0$ ), we get  $A_0 = \sqrt{10}/2$ . The branches of  $\tilde{N}_{e,\eta} = 0$  follow in a similar way, but with series expansion of the form  $v = A_\eta u^{4/3} / (-\log u)^{1/3} + \dots$ . In this case we have only one possible real value for  $A_\eta = 20^{1/3}/2$ . For  $\tilde{D}_{e,1} = 0$ , we have to study two type of different branches  $v = A_{1,1}u^2 + \dots$  and  $v = A_{1,2}/\log u + \dots$ . The possible values for  $A_{1,1}$  and  $A_{1,2}$  are  $\pm\sqrt{3}$  and  $5/12$ , respectively. But, restricting to the first quadrant, we have only one for each,  $A_{1,1} = \sqrt{3}$  and  $A_{1,2} = 5/12$ . The expressions that appear in the statement follow recovering the original coordinates.  $\square$

Finally, we show the existence of an intersection point for the level zero curves  $N_{e,0}$  and  $D_{e,1}$ , defined in (2.17), as we have depicted in Figure 2.7. This fact follows just comparing their series expansions near the points  $(0, 1)$  and  $(1, 1)$ . Numerically it is not so easy to find

this intersection point. But, transforming the system to the equivalent one

$$\begin{aligned} \frac{q_0^1(\rho, \eta)}{q_3^1(\rho, \eta)} - \frac{p_0^0(\rho, \eta)}{p_3^0(\rho, \eta)} + \left( \frac{q_1^1(\rho, \eta)}{q_3^1(\rho, \eta)} - \frac{p_1^0(\rho, \eta)}{p_3^0(\rho, \eta)} \right) L(\rho) + \left( \frac{q_2^1(\rho, \eta)}{q_3^1(\rho, \eta)} - \frac{p_2^0(\rho, \eta)}{p_3^0(\rho, \eta)} \right) L(\eta) &= 0, \\ \frac{q_0^1(\rho, \eta)}{q_1^1(\rho, \eta)} - \frac{p_0^0(\rho, \eta)}{p_1^0(\rho, \eta)} + \left( \frac{q_2^1(\rho, \eta)}{q_1^1(\rho, \eta)} - \frac{p_2^0(\rho, \eta)}{p_1^0(\rho, \eta)} \right) L(\eta) + \left( \frac{q_3^1(\rho, \eta)}{q_1^1(\rho, \eta)} - \frac{p_3^0(\rho, \eta)}{p_1^0(\rho, \eta)} \right) L(\rho)L(\eta) &= 0, \end{aligned}$$

we numerically can find the intersection point  $(\rho, \eta) \approx (0.0325224964, 0.9889101365)$ .

# Number of limit cycles in piecewise quadratic systems

---

---

## Abstract

This chapter is devoted to the study of the number of limit cycles bifurcating from a piecewise quadratic system. All the differential systems considered are piecewise in two zones separated by a straight line. We prove the existence of 16 crossing limit cycles in this class of systems. If we denote by  $H_p(n)$  the extension of the Hilbert number to degree  $n$  piecewise polynomial differential systems, then  $H_p(2) \geq 16$ . As far as we are concerned, this is the best lower bound for the quadratic class. Moreover, all the limit cycles appear in one nest bifurcating from the period annulus of some isochronous quadratic centers.

### 3.1 Introduction

Consider the class of polynomial differential systems of degree  $n$ . The maximum number of isolated periodic orbits, the so-called *limit cycles*, that a polynomial differential system of degree  $n$  can have is called *Hilbert number*,  $H(n)$ . It is well known that linear systems have no limit cycles, then  $H(1) = 0$ . For  $n = 2$ , the problem of estimating  $H(2)$  has been studied intensively during the last century. Lower bounds for  $H(2)$  can be given by providing concrete examples of polynomial differential systems of degree 2. Up to now, the best result was given by Shi in [Shi80], where he proved the existence of a quadratic system with 4 limit cycles in configuration (3, 1), that is  $H(2) \geq 4$ . We call by  $M(n)$  the maximum number of limit cycles bifurcating from a singular point as a degenerate Hopf bifurcation. Clearly,  $M(n)$  is a lower bound for  $H(n)$ . Bautin showed in [Bau54] that  $M(2) = 3$ ; in [Ž95, Ž16], Żoładek proved that  $M(3) \geq 11$ ; a simpler proof was provided by Christopher in [Chr05]. For  $n = 3$ , Li, Liu, and Yang proved in [LLY09] that  $H(3) \geq 13$ .

In the last few years there has been an increasing interest in piecewise smooth systems. This interest has been mainly motivated by their wider range of application in modeling real phenomena (see, for instance, [ABB11, dBBC08]). In this chapter we shall deal with the following class of piecewise vector fields

$$Z(x, y) = \begin{cases} Z^+(x, y), & h(x, y) > 0, \\ Z^-(x, y), & h(x, y) < 0, \end{cases} \quad (3.1)$$

where  $Z^\pm = (X^\pm, Y^\pm)$  are smooth vector fields and  $h : \mathbb{R}^2 \rightarrow \mathbb{R}$  is a  $\mathcal{C}^1$  function for which 0 is a regular value. In the above vector field, the discontinuity curve and the regions where  $Z^\pm$  are denoted by  $\Sigma = h^{-1}(0)$  and  $\Sigma^\pm = \{(x, y) \in \mathbb{R}^2 : \pm h(x, y) > 0\}$ , respectively. The local trajectories of  $Z$  on  $\Sigma$  was stated by Filippov in [Fil88] (see Figure 3.1). The points on  $\Sigma$  where both vectors fields simultaneously point outward or inward from  $\Sigma$  define the *escaping* ( $\Sigma^e$ ) and *sliding region* ( $\Sigma^s$ ), respectively. The interior of its complement on  $\Sigma$  defines the *crossing region* ( $\Sigma^c$ ), and the boundary of these regions is constituted by tangential points of  $Z^\pm$  with  $\Sigma$ . Let  $Z^\pm h$  denote the derivative of the function  $h$  in the direction of the vector  $Z^\pm$

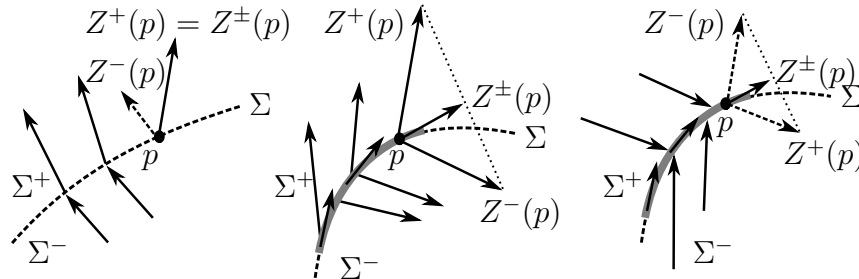


Figure 3.1: Definition of the vector field on  $\Sigma$  following Filippov's convention in the sewing, escaping, and sliding regions.

that is,  $Z^\pm h(p) = \langle \nabla h(p), Z^\pm(p) \rangle$ . Notice that  $p \in \Sigma^c$  provided that  $Z^+ h(p) \cdot Z^- h(p) > 0$ ,

$p \in \Sigma^e \cup \Sigma^s$  provided that  $Z^+h(p) \cdot Z^-h(p) < 0$ , and  $p$  in  $\Sigma$  is a tangential point of  $Z^\pm$  provided that  $Z^+h(p)Z^-h(p) = 0$ . We say that  $p \in \Sigma$  is a *singularity* of  $Z$ , if  $p$  is either a tangential point or a singularity of  $Z^+$  or  $Z^-$ . We call  $p \in \Sigma$  an *invisible fold* of  $Z^+$  (resp.  $Z^-$ ) if  $p$  is a tangential point of  $Z^+$  (resp.  $Z^-$ ) and  $(Z^+)^2h(p) < 0$  (resp.  $(Z^-)^2h(p) > 0$ ).

Analogously to the smooth case, we denote by  $H_p^c(n)$  the maximum number of crossing limit cycles that piecewise polynomial differential systems of degree  $n$  admit when the curve of discontinuity is a straight line. We also denote by  $M_p^c(n)$  the maximum number of crossing limit cycles bifurcating from a singular point or sliding set. Up to now, for piecewise linear systems in two zones separated by a straight line, there are no examples with more than 3 limit cycles. An example with 3 limit cycles was firstly detected numerically in [HY12] by Huan and Yang. Later, it was analytically proved by Llibre and Ponce in [LP12]. The existence of 3 limit cycles was also obtained from perturbations of a center. For instance, Buzzi et al. in [BPT13] obtained 3 limit cycles after a seventh order piecewise linear perturbation of a linear center, and Llibre et al. in [LNT15a] obtained the same result through a first order perturbation of a piecewise linear center. We may also quote Freire et al. [FPT14]. Consequently, for piecewise linear systems in two zones separated by a straight line we have  $H_p^c(1) \geq 3$ .

The averaging theory of order five for studying piecewise perturbations of the linear center was used by Llibre and Tang in [LT16] who provided that  $H_p^c(2) \geq 8$  and  $H_p^c(3) \geq M_p^c(3) \geq 13$ . These are the best results so far for piecewise quadratic and cubic systems in two zones separated by a straight line. Previously, using the averaging theory of first order for studying piecewise perturbations of some quadratic isochronous systems, Llibre and Mereu in [LM14] obtained only 5 limit cycles. Recently, in [CLYZ18] the authors study this perturbation problem, only up to first order but for degree  $n$ . It is worthwhile to say that for quadratic polynomial systems Chicone and Jacobs in [CJ91] proved that at most 2 limit cycles can bifurcate from any period annulus.

In this chapter we shall use the averaging theory of first and second order to provide better lower bounds for the maximum number of limit cycles that piecewise quadratic systems can have. More specifically, we shall give examples satisfying  $M_p^c(2) \geq 16$ . Consequently,  $H_p^c(3) \geq H_p^c(2) \geq 16$ . Table 3.1 summarizes the results about the Hilbert numbers for lower degree vector fields.

**Theorem 3.1.** *There exists a piecewise planar quadratic differential system in two zones separated by a straight line with 16 crossing limit cycles.*

In order to prove our main result we shall proceed with a first and second order perturbation analysis of quadratic isochronous centers. In [Lou64] the quadratic isochronous centers are classified in four families, namely  $S_1$ ,  $S_2$ ,  $S_3$ , and  $S_4$ . In [MRT95] their isochronicity properties were proved as well as their linearizations. In this chapter we consider the first three classes of centers, which are birational equivalent to the linear one. This property does not hold for  $S_4$ . It is proved in [CS99] that any center of families  $S_1$ ,  $S_2$ , and  $S_3$  can be

deg	PVF	PPVF
$n = 1$	$H(1) = 0$	$H_p^c(1) \geq 3$
$n = 2$	$H(2) \geq 4$	$H_p^c(2) \geq 16(8)$
$n = 3$	$H(3) \geq 13$	$H_p^c(3) \geq 16(13)$

Table 3.1: Summary of Hilbert numbers for polynomial and piecewise polynomial systems of degree  $n$ . Listed in parenthesis the known Hilbert numbers so far.

transformed, after a birational change of variables, in one of the following centers:

$$S_1 : \begin{cases} \dot{x} = -y + x^2 - y^2, \\ \dot{y} = x + 2xy. \end{cases} \quad S_2 : \begin{cases} \dot{x} = -y + x^2, \\ \dot{y} = x + xy. \end{cases} \quad S_3 : \begin{cases} \dot{x} = -y - \frac{4}{3}x^2, \\ \dot{y} = x - \frac{16}{3}xy. \end{cases} \quad (3.2)$$

Here, the dot denotes the derivative with respect to time. The phase portraits of these systems are depicted in Figure 3.2.

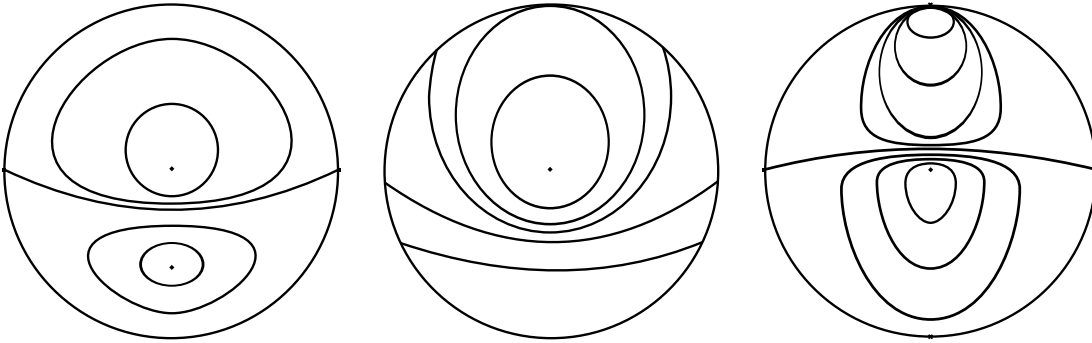


Figure 3.2: Phase portrait of systems  $S_1$ ,  $S_2$ , and  $S_3$  from left to right.

The first order averaging method was used in [LM14] to get 4 and 5 limit cycles by perturbing, respectively, the centers  $S_1$  and  $S_2$  inside the class of piecewise quadratic systems with two zones separated by the straight line  $y = 0$ . Here, due to restrictions of the employed technique, we take  $\{x = 0\}$  as the curve of discontinuity for the centers  $S_1$  and  $S_3$ . The first and second order analysis for  $S_1$  are performed in Propositions 3.6 and 3.11, where we get 5 and 11 limit cycles, respectively. Analogously, for  $S_3$  Propositions 3.7 and 3.13 provide 5 and 10 limit cycles, respectively. We shall see that for the center  $S_2$  the employed technique works whenever the curve of discontinuity is a straight line passing through the origin. This allows to reach the best result, namely  $H_p^c(2) \geq 16$ . In fact, proceeding with a first order analysis Proposition 3.8 provides 5, 6, and 8 limit cycles when the curve of discontinuity is  $\{x = 0\}$ ,  $\{y = 0\}$ , and  $\{y + \sqrt{3}x = 0\}$ , respectively. Due to the difficulties in the massive computations, the second order analysis has been performed only for the case of highest cyclicity at the first order analysis, namely when the curve of discontinuity is given

by  $\{y + \sqrt{3}x = 0\}$ . In this case, Proposition 3.17 provides 16 limit cycles bifurcating from the origin, that is  $M_p^c(2) \geq 16$ . This proves our main result, Theorem 3.1.

This chapter is structured as follows. In Section 3.2, we present some basic notions and preliminary tools. In Sections 3.3 and 3.4, the first and second order analysis are performed, respectively. Finally, last section contains the integrals used in this chapter.

## 3.2 Preliminaries

This section is devoted to present some basic notions and preliminary tools needed to prove our main result. Firstly, we introduce some results on averaging theory of first and second orders. In fact, the limit cycles will appear from the simple zeros of some integrals (see, for instance, [ILN17, LMN15]). Secondly, we recall the concepts of Extended Complete Chebyshev system (ECT-system) and Chebyshev system with accuracy (see, for instance, [NT17]). Then, we introduce the concept of pseudo-Hopf bifurcation, which is the birth of a limit cycle when the sliding set changes stability (see, for instance, [Fil88, FPT12]). Finally, we state the Poincaré–Miranda theory, which is an extension of the intermediate value theorem, see [Kul97].

### 3.2.1 Averaging Theory

Assume that the origin is a center equilibrium point for system (3.1). Consider the following perturbed piecewise polynomial vector field

$$Z_\varepsilon^\pm = \begin{cases} Z^+(x, y) + \varepsilon (P_1^+(x, y), Q_1^+(x, y)) + \varepsilon^2 (P_2^+(x, y), Q_2^+(x, y)), & \text{if } h(x, y) > 0, \\ Z^-(x, y) + \varepsilon (P_1^-(x, y), Q_1^-(x, y)) + \varepsilon^2 (P_2^-(x, y), Q_2^-(x, y)), & \text{if } h(x, y) < 0, \end{cases} \quad (3.3)$$

where  $\varepsilon$  is sufficiently small,  $P_k^\pm, Q_k^\pm$  are polynomials of degree  $n$  in  $(x, y)$ , for  $k = 1, 2$ , and  $h(x, y) = y - \tan(\alpha)x$ . After changing to polar coordinates,  $(x, y) = (r \cos \theta, r \sin \theta)$ , system (3.3) writes

$$\tilde{Z}_\varepsilon(\theta, r) = \begin{cases} \tilde{Z}_\varepsilon^+(\theta, r), & \text{if } \alpha < \theta < \alpha + \pi, \\ \tilde{Z}_\varepsilon^-(\theta, r), & \text{if } \alpha - \pi < \theta < \alpha. \end{cases} \quad (3.4)$$

Taking  $\theta$  as the new independent variable, the differential system associated to the vector field (3.4) becomes the piecewise differential equation

$$r'(\theta) = \frac{dr}{d\theta} = \varepsilon F_1(\theta, r) + \varepsilon^2 F_2(\theta, r) + \mathcal{O}(\varepsilon^3), \quad (3.5)$$

with

$$F_i(\theta, r) = \begin{cases} F_i^+(\theta, r) & \text{if } \alpha < \theta < \alpha + \pi, \\ F_i^-(\theta, r) & \text{if } \alpha - \pi < \theta < \alpha, \end{cases}$$

where  $F_i^\pm : [\alpha - \pi, \alpha + \pi] \times (0, \rho^*) \rightarrow \mathbb{R}$  are analytical functions  $2\pi$ -periodic in the variable  $\theta$  for  $i = 1, 2$ .

We define  $\mathcal{F}_1, \mathcal{F}_2 : (0, \rho^*) \rightarrow \mathbb{R}$  as

$$\begin{aligned}
\mathcal{F}_1(r) &= \int_{\alpha}^{\alpha+\pi} (F_1^+(\theta, r) + F_1^-(\theta - \pi, r)) d\theta, \\
\mathcal{F}_2(r) &= \int_{\alpha}^{\alpha+\pi} (F_2^+(\theta, r) + F_2^-(\theta - \pi, r)) d\theta \\
&\quad + \int_{\alpha}^{\alpha+\pi} \left( \frac{\partial}{\partial r} F_1^+(\theta, r) r_1^+(\theta, r) + \frac{\partial}{\partial r} F_1^-(\theta - \pi, r) r_1^-(\theta - \pi, r) \right) d\theta.
\end{aligned} \tag{3.6}$$

Here, the functions  $r_1^{\pm} : (-\pi, \pi) \times \mathbb{R}^+ \rightarrow \mathbb{R}$  are defined as

$$r_1^{\pm}(\theta, r) = \int_{\alpha}^{\alpha+\theta} F_1^{\pm}(\phi, r) d\phi. \tag{3.7}$$

**Theorem 3.2** ([LMN15]). *Consider the piecewise differential equation (3.5).*

(a) *Suppose that for  $\rho \in (0, \rho^*)$  with  $\mathcal{F}_1(\rho) = 0$  and  $\mathcal{F}'_1(\rho) \neq 0$ . Then, for  $|\varepsilon| > 0$  sufficiently small, there exists a  $2\pi$ -periodic solution  $r(\theta, \varepsilon)$  of (3.5) such that  $r(0, \varepsilon) \rightarrow \rho$  when  $\varepsilon \rightarrow 0$ .*

(b) *Assume that  $\mathcal{F}_1 = 0$ . Suppose that for  $\rho \in (0, \rho^*)$  with  $\mathcal{F}_2(\rho) = 0$  and  $\mathcal{F}'_2(\rho) \neq 0$ . Then, for  $|\varepsilon| > 0$  sufficiently small, there exists a  $2\pi$ -periodic solution  $r(\theta, \varepsilon)$  of (3.5) such that  $r(0, \varepsilon) \rightarrow \rho$  when  $\varepsilon \rightarrow 0$ .*

### 3.2.2 ECT-Systems

Let  $\mathcal{F} = [u_0, \dots, u_n]$  be an ordered set of functions of class  $\mathcal{C}^{\infty}$  on the closed interval  $[a, b]$ . We denote by  $\mathcal{Z}(\mathcal{F})$  the maximum number of zeros counting multiplicity that any nontrivial function  $v \in \text{Span}(\mathcal{F})$  can have. Here,  $\text{Span}(\mathcal{F})$  is the set of functions generated by linear combinations of elements of  $\mathcal{F}$ , that is  $v(s) = a_0 u_0(s) + a_1 u_1(s) + \dots + a_n u_n(s)$  where  $a_i$ , for  $i = 0, 1, \dots, n$ , are real numbers.

The theory of Chebyshev systems is a classical tool to study the quantity  $\mathcal{Z}(\mathcal{F})$ . In fact, when  $\mathcal{Z}(\mathcal{F}) \leq n$ ,  $\mathcal{F}$  is called an *Extended Chebyshev system* or ET-system on  $[a, b]$ , see [KS66]. We say that  $\mathcal{F}$  is an *Extended Complete Chebyshev system* or an ECT-system on a closed interval  $[a, b]$  if and only if for any  $k$ ,  $0 \leq k \leq n$ ,  $[u_0, u_1, \dots, u_k]$  is an ET-system. In order to prove that  $\mathcal{F}$  is a ECT-system on  $[a, b]$  it is sufficient and necessary to show that  $W(u_0, u_1, \dots, u_k)(t) \neq 0$  on  $[a, b]$  for  $0 \leq k \leq n$ , see also [KS66]. Here,  $W(u_0, u_1, \dots, u_n)(t)$  denotes the Wronskian of  $\mathcal{F}$  with respect to  $t$ . That is,

$$W_n(t) = W(u_0, \dots, u_n)(t) = \det \begin{pmatrix} u_0(t) & \cdots & u_n(t) \\ u'_0(t) & \cdots & u'_n(t) \\ \vdots & \ddots & \vdots \\ u_0^{(n)}(t) & \cdots & u_n^{(n)}(t) \end{pmatrix}.$$

Furthermore, the sufficient condition to be an ECT-system also provides that each configuration of  $m \leq n$  zeros, taking into account their multiplicity, is realizable.

The next theorem, proved in [NT17], extends the results for ECT-systems when some of the Wronskian vanish.

**Theorem 3.3** ([NT17]). *Let  $\mathcal{F} = [u_0, u_1, \dots, u_n]$  be an ordered set of analytic functions on  $[a, b]$ . Assume that all the  $\nu_i$  zeros of the Wronskian  $W_i$  are simple for  $i = 0, \dots, n$ . Then, the number of isolated zeros for every element of  $\text{Span}(\mathcal{F})$  does not exceed*

$$n + \nu_n + \nu_{n-1} + 2(\nu_{n-2} + \dots + \nu_0) + \nu_{n-1} + \dots + \nu_3$$

where  $\nu_i = \min(2\nu_i, \nu_{i-3} + \dots + \nu_0)$ , for  $i = 3, \dots, n - 1$ .

### 3.2.3 Pseudo-Hopf Bifurcation

In the well-known Hopf bifurcation (see, for instance, [HK91]) a limit cycle arises from an equilibrium point when it changes its stability. In piecewise differential systems, the pseudo-Hopf bifurcation describes the same phenomenon but when the sliding segment changes its stability. Analogously to the classical Hopf bifurcation, the proof is a direct consequence of the generalized Poincaré–Bendixson Theorem for piecewise differential systems (see, for instance, [BCE18]).

**Proposition 3.4.** *Let  $Z^\pm = (X^\pm(x, y), Y^\pm(x, y))$  be a  $\mathcal{C}^1$  piecewise differential system in two zones separated by the straight line  $y = 0$ . Additionally, the origin is a stable monodromic equilibrium point and  $a = (\partial Y^+ / \partial x)|_{(0,0)} > 0$ . Given a real number  $b$ , we consider the perturbed system  $Z_b^\pm = (X_b^\pm(x, y), Y_b^\pm(x, y))$  defined by  $X_b^\pm(x, y) = X^\pm(x, y)$ , and  $Y_b^-(x, y) = Y^-(x, y)$  and  $Y_b^+ = Y^+ + b$ . Then, for  $b$  small enough, the system  $Z_b^\pm$  exhibits a pseudo-Hopf bifurcation at  $b = 0$  when  $ab > 0$ . See Figure 3.3.*

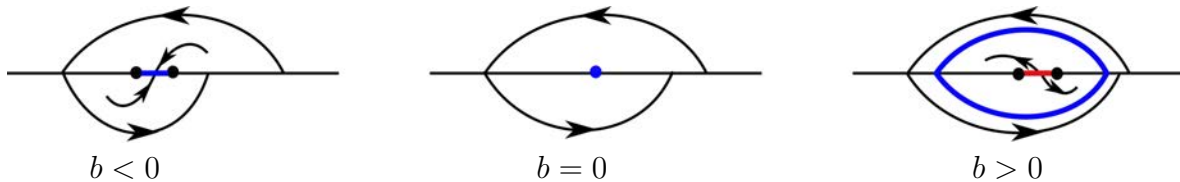


Figure 3.3: Pseudo-Hopf bifurcation.

### 3.2.4 Poincaré–Miranda Theorem

The next result is a generalization of the intermediate value theorem. It was conjectured by Poincaré in 1883 and proved by Miranda in 1940 (see, for instance, [Kul97] and the references therein).

**Theorem 3.5** ([Kul97]). *Let  $a$  be a positive real number and  $B = [-a, a]^n$  the  $n$ -dimensional cube. Let  $f = (f_1, \dots, f_n) : B \rightarrow \mathbb{R}^n$  be a continuous function such that  $f_i(B_i^-) < 0$  and  $f_i(B_i^+) > 0$ , for each  $i \leq n$ , where  $B_i^\pm = \{(x_1, \dots, x_n) \in B : x_i = \pm a\}$ . Then, there exists a point  $c \in B$  such that  $f(c) = 0$ .*

### 3.3 First order perturbation

In this section the first order averaging method is used to study the limit cycles of the perturbed piecewise vector field (3.3) when the unperturbed vector field  $Z_0$  is a quadratic isochronous center in one of the families  $S_1$ ,  $S_2$ , or  $S_3$ . Regarding (3.3) we shall denote  $Z_\varepsilon = Z_{i,\varepsilon}$  and  $Z_\varepsilon^\pm = Z_{i,\varepsilon}^\pm$  in order to indicate that  $Z_0 \in S_i$ , for  $i = 1, 2, 3$ . Here, it is only considered quadratic polynomial perturbations, that is

$$P_k^\pm(x, y) = \sum_{j=0}^2 \sum_{i=0}^j p_{k,i,j-i}^\pm x^i y^{j-i} \quad \text{and} \quad Q_k^\pm(x, y) = \sum_{j=0}^2 \sum_{i=0}^j q_{k,i,j-i}^\pm x^i y^{j-i}.$$

The first order analyses for families  $S_1$ ,  $S_3$ , and  $S_2$  are performed in Propositions 3.6, 3.7, and 3.8, respectively. For the families  $S_1$  and  $S_2$ , we shall also use the ECT-system properties to study the bifurcation of limit cycles in the global interval of definition. Accordingly, Propositions 3.6 and 3.7 are concerned about upper bounds (up to a first order analysis) for the maximum number of limit cycles bifurcating from the period annulus (the so-called medium amplitude limit cycles). In the third result, Proposition 3.8, a local analysis is performed around the center point. In this case, we also see how the number of limit cycles changes when we consider different lines of discontinuity.

Before stating the main results of this section we briefly discuss the choosing of the lines of discontinuity. The birational linearizations of families  $S_1$  and  $S_3$  (see, for instance, [CS99]) transform the straight line  $\{x = 0\}$  into another straight line passing through the origin. Moreover,  $\{x = 0\}$  is the unique straight line for which this happens. This is the main reason for choosing  $\Sigma = \{x = 0\}$  as the curve of discontinuity. The birational linearization of the family  $S_2$  transforms straight lines passing through the origin into straight lines passing through the origin, so that we are allowed to choose any straight line passing through the origin as the curve of discontinuity. Nevertheless, in this last case, since the computations are more intricate we only study the limit cycles bifurcating from the origin. We anticipate that all the conclusions of this section will be improved by results of the next section.

**Proposition 3.6.** *For  $|\varepsilon| > 0$  sufficiently small the averaging method of first order predicts at most 5 crossing limit cycles for the piecewise quadratic vector field  $Z_{1,\varepsilon}$  when the curve of discontinuity is the straight line  $\{x = 0\}$ . Moreover, this number is reached.*

*Proof.* In order to apply Theorem 3.2, we have to write the vector field (3.4) as a differential equation (3.5). So, we first proceed with the change of variables (see, for instance, [CS99])

$$x = -\frac{v}{v^2 + (u-1)^2} \quad \text{and} \quad y = -\frac{u^2 + v^2 - u}{v^2 + (u-1)^2}, \quad (3.8)$$

which has the following rational inverse

$$u = \frac{x^2 + y^2 + y}{x^2 + y^2 + 2y + 1} \quad \text{and} \quad v = -\frac{x}{x^2 + y^2 + 2y + 1}. \quad (3.9)$$

With this change of variables the differential equation  $S_1$  becomes the linear center  $(u', v') = (-v, u)$  and the line of discontinuity becomes  $v = 0$ .

Then, we change to polar coordinates  $u = r \cos \theta$  and  $v = r \sin \theta$ . Taking  $\theta$  as the new independent variable, (3.4) becomes

$$r'(\theta) = \frac{\dot{r}}{\dot{\theta}} = \varepsilon \frac{\mathcal{A}(r \cos \theta, r \sin \theta)}{\mathcal{C}(\theta, r)} + \mathcal{O}(\varepsilon^2), \quad (3.10)$$

where  $\mathcal{C}(\theta, r) = (2r \cos \theta - r^2 - 1)^2$  and  $\mathcal{A}$  is the piecewise function

$$\mathcal{A}(r \cos \theta, r \sin \theta) = \begin{cases} \mathcal{A}^+(r \cos \theta, r \sin \theta) & \text{if } 0 < \theta \leq \pi, \\ \mathcal{A}^-(r \cos \theta, r \sin \theta) & \text{if } \pi < \theta \leq 2\pi, \end{cases} \quad (3.11)$$

being  $\mathcal{A}^\pm$  polynomials of degree 3.

From here we want to use the integral formulas of Section 3.5 to compute the averaged function  $\mathcal{F}_1$ , as stated in (3.6), for  $\alpha = 0$ . The denominators of  $F_1^+(\theta, r)$  and  $F_1^-(\theta - \pi, r)$  write  $(2r \cos \theta - r^2 - 1)^2$  and  $(2r \cos \theta + r^2 + 1)^2$ , respectively. In order to use the integrals we must apply a transformation on  $r$  in order to get the denominators written in a standard form.

Firstly, take  $r = (-1 + \sqrt{1 - R^2})/R$ . The denominator of  $F_1^+(\theta, r)$  is transformed into  $2R^2(R \cos \theta + 1)^2(R^2 + 2\sqrt{1 - R^2} - 2)$ . Hence, the first part of the first averaged function

$$\int_0^\pi F_1^+(\theta, (-1 + \sqrt{1 - R^2})/R) d\theta$$

can be computed using the integrals (3.25) for  $\alpha = 0$ ,  $\ell = 2$ , and  $k \in \{0, 1, 2, 3\}$ . We shall suppress it here. The original variable  $r$  is recovered by taking  $R = -2r/(r^2 + 1)$ .

Secondly, take  $r = (1 - \sqrt{1 - R^2})/R$ . The denominator of  $F_1^-(\theta - \pi, r)$  is transformed into  $2R^2(R \cos \theta + 1)^2(R^2 + 2\sqrt{1 - R^2} - 2)$ . Hence, the second part of the first averaging function

$$\int_0^\pi F_1^-(\theta - \pi, (1 - \sqrt{1 - R^2})/R) d\theta$$

can be computed also using the integrals (3.25) for  $\alpha = 0$ ,  $\ell = 2$ , and  $k \in \{0, 1, 2, 3\}$ . The original variable  $r$  is recovered by taking  $R = 2r/(r^2 + 1)$ .

Adding up the above integrals, we get the averaged function  $\mathcal{F}_1(r)$ . Proceeding with the

change of parameters

$$\begin{aligned}
p_{1,0,0}^- &= p_{1,0,0}^+ - 2k_4 + \frac{k_0}{2}, \\
p_{1,0,1}^- &= p_{1,0,2}^- + p_{1,0,1}^+ - p_{1,0,2}^+ - 2k_4 + 2k_5 + \frac{k_2 + k_0}{2}, \\
p_{1,1,0}^- &= -p_{1,1,0}^+ + 2(q_{1,0,0}^- + q_{1,0,0}^+) - \frac{q_{1,0,2}^- + q_{1,2,0}^- + q_{1,0,2}^+ + q_{1,2,0}^+}{2} + \frac{k_1 - k_3}{\pi}, \\
p_{1,2,0}^- &= p_{1,2,0}^+ + \frac{q_{1,1,1}^- - q_{1,1,1}^+}{2} - 2k_4 - 2k_5, \\
q_{1,0,1}^- &= 2q_{1,0,0}^- + 2q_{1,0,0}^+ - q_{1,0,1}^+ + \frac{q_{1,0,2}^- + q_{1,2,0}^- + q_{1,0,2}^+ + q_{1,2,0}^+}{2} + \frac{k_1 + 2k_3}{\pi}, \\
q_{1,1,0}^+ &= q_{1,1,0}^- + \frac{q_{1,1,1}^+ - q_{1,1,1}^- + k_2 + k_0}{2},
\end{aligned} \tag{3.12}$$

we get

$$\mathcal{F}_1(r) = \sum_{n=0}^5 k_n f_n(r), \tag{3.13}$$

where

$$\begin{aligned}
f_0(r) &= 1, & f_1(r) &= r, & f_2(r) &= r^2, \\
f_3(r) &= r^3, & f_4(r) &= \frac{1-r^2}{r} L(r), & f_5(r) &= r(1-r^2) L(r),
\end{aligned}$$

and

$$L(r) = \log \left( \frac{1-r}{1+r} \right). \tag{3.14}$$

Clearly, from (3.12), the parameters  $k_n$  can be chosen arbitrarily.

The maximum number of simple zeros that (3.13) can have follows by studying the Wronskians of the ordered set  $[f_0, f_1, \dots, f_5]$ . Straightforward computations show that

$$\begin{aligned}
W_0(r) &= 1, & W_1(r) &= 1, & W_2(r) &= 2, \\
W_3(r) &= 12, & W_4(r) &= \frac{288}{r^5} \overline{W}_4(r), & W_5(r) &= \frac{9216(r^2+5)}{(1-r^2)^4 r^6} \overline{W}_5(r),
\end{aligned}$$

where

$$\overline{W}_4 = L(r) - \frac{2}{3} \frac{r(7r^2 - 8r^2 + 3)}{(r^2 - 1)^3}, \quad \overline{W}_5 = L(r) - \frac{2}{3} \frac{r(3r^2 - 22r^2 + 15)}{(r^2 - 1)^2(r^2 + 5)}.$$

Clearly,  $W_0, W_1, W_2$ , and  $W_3$  do not vanish in  $(0, 1)$ . Now, computing the derivative

$$\overline{W}_4'(r) = \frac{4r^4(5r^2 + 1)}{(r^2 - 1)^4} > 0,$$

as  $\overline{W}_4(0) = 0$ , also  $W_4(r)$  does not vanish in  $(0, 1)$ . The same argument applies for  $W_5(r)$ ,

but using

$$\overline{W}'_5(r) = \frac{64r^6}{(r^2 - 1)^3(r^2 + 5)^2}.$$

So, the proof follows by noticing that the ordered set of functions  $[f_0, \dots, f_5]$  is an ECT-system.  $\square$

**Proposition 3.7.** *For  $|\varepsilon| > 0$  sufficiently small the averaging method of first order predicts at most 5 crossing limit cycles for the piecewise quadratic vector field  $Z_{3,\varepsilon}$  when the curve of discontinuity is the straight line  $\{x = 0\}$ . Moreover, this number is reached .*

*Proof.* We shall follow the same procedure of the proof of Proposition 3.6. The linearization stated in [CS99] is given by

$$x = \frac{3u}{8v + 1} \quad y = \frac{3(4u^2 + 8v^2 + v)}{(8v + 1)^2},$$

which has the following rational inverse

$$u = \frac{3x}{32x^2 - 24y + 9} \quad \text{and} \quad v = \frac{-4x^2 + 3y}{32x^2 - 24y + 9}.$$

Then, applying the change of variables  $u = r \sin \theta$  and  $v = -r \cos \theta$ , and taking  $\theta$  as the new independent variable, equation (3.5) becomes

$$r'(\theta) = \frac{\dot{r}}{\dot{\theta}} = \varepsilon \frac{\mathcal{A}(\theta, r)}{\mathcal{C}(\theta, r)} + \mathcal{O}(\varepsilon^2),$$

where  $\mathcal{C}(\theta, r) = 8r \cos \theta - 1$  and  $\mathcal{A}$  is the piecewise function

$$\mathcal{A}(\theta, r) = \begin{cases} \mathcal{A}^+(r \sin \theta, -r \cos \theta) & \text{if } 0 < \theta \leq \pi, \\ \mathcal{A}^-(r \sin \theta, -r \cos \theta) & \text{if } \pi < \theta \leq 2\pi, \end{cases}$$

being  $\mathcal{A}^\pm$  polynomials of degree 6.

Now we compute the averaged function (3.6) for  $\alpha = 0$ . As in the proof of Proposition 3.6, the denominators of  $F_1^+(\theta, r)$  and  $F_1^-(\theta - \pi, r)$  are not written in a standard form in order to use directly the integrals of Section 3.5.

Firstly, take  $r = -R/8$ . The denominator of  $F_1^+(\theta, r)$  in (3.6) becomes  $(R \cos \theta + 1)^4$ . Hence, the integral

$$\int_0^\pi F_1^+(\theta, -R/8) d\theta$$

can be computed using (3.25) for  $\alpha = 0$ ,  $\ell = 4$ , and  $k \in \{0, 1, \dots, 6\}$ . The original variable  $r$  is recovered taking  $R = -8r$ .

Secondly, take  $r = R/8$ . The denominator of  $F_1^-(\theta - \pi, r)$  in (3.6) also becomes  $(R \cos \theta + 1)^4$ . Hence, the integral

$$\int_0^\pi F_1^-(\theta - \pi, R/8) d\theta,$$

can be also computed using (3.25) for  $\alpha = 0$ ,  $\ell = 4$ , and  $k \in \{0, 1, \dots, 6\}$ . The original variable  $r$  is recovered taking  $R = 8r$ .

Adding up the above integrals we obtain the first averaged function  $\mathcal{F}_1(r)$ , which depends on  $r$ ,  $\sqrt{1-r^2}$ , and  $L(r)$  defined in (3.14). Proceeding with the change

$$r = 2\rho/(1 + \rho^2), \quad (3.15)$$

the averaged function writes

$$\tilde{\mathcal{F}}_1(\rho) = \sum_{n=0}^5 k_n f_n(\rho), \quad (3.16)$$

where

$$\begin{aligned} f_0(\rho) &= \rho, & f_1(\rho) &= \rho^2, & f_2(\rho) &= \rho^3, \\ f_3(\rho) &= \rho^4 + 1, & f_4(\rho) &= \rho^5, & f_5(\rho) &= \frac{L(\rho)}{\rho}. \end{aligned}$$

We remark that  $L(r) = 2L(\rho)$ .

The maximum number of simple zeros that (3.16) can have follows by studying the Wronskians of the ordered set  $[f_0, f_1, \dots, f_5]$ . Straightforward computations show that.

$$\begin{aligned} W_0(\rho) &= \rho, & W_1(\rho) &= \rho^2, & W_2(\rho) &= 2\rho^3, \\ W_3(\rho) &= 12(\rho^4 - 1), & W_4(\rho) &= 288\rho(\rho^4 - 5), & W_5(\rho) &= \frac{207360(1 - \rho^4)}{\rho^5} \overline{W}_5(\rho), \end{aligned}$$

where

$$\overline{W}_5(\rho) = L(\rho) - \frac{\rho(75\rho^{12} - 175\rho^{10} + 61\rho^8 + 95\rho^6 - 230\rho^4 + 140\rho^2 - 30)}{15(\rho^2 - 1)^6(\rho^2 + 1)}.$$

Clearly  $W_0, W_1, W_2, W_3$ , and  $W_4$  do not vanish in  $(0, 1)$ . The last Wronskian does not vanish either because  $\overline{W}_5(0) = 0$  and the derivative

$$\overline{W}'_5(\rho) = \frac{\rho^4(\rho^4 - 5)(105\rho^8 + 105\rho^6 + 175\rho^4 - 5\rho^2 + 4)}{15(\rho^2 - 1)^7(\rho^2 + 1)^2}$$

is positive for every  $\rho \in (0, 1)$ . So, the proof follows by noticing that the ordered set of functions  $[f_0, \dots, f_5]$  is an ECT-system.  $\square$

The global analysis performed in the previous results cannot be performed in a straightforward way for the family  $S_2$ . Hence, for this family we provide only a local analysis around the origin.

**Proposition 3.8.** *For  $|\varepsilon| > 0$  sufficiently small and under the condition  $P^\pm(0, 0) = Q^\pm(0, 0) = 0$ , the averaging method of first order predicts at most 4, 5, or 7 limit cycles bifurcating from the origin for the quadratic vector field  $Z_{2,\varepsilon}$  when the curve of discontinuity is the straight line  $\{x = 0\}$ ,  $\{y = 0\}$ , or  $\{y + \sqrt{3}x = 0\}$ , respectively. Moreover, these numbers are reached.*

*Proof.* The linearization stated in [CS99] for family  $S_2$  is given by

$$x = -\frac{u}{v-1} \quad \text{and} \quad y = -\frac{v}{v-1},$$

which has the following rational inverse

$$u = \frac{x}{y+1} \quad \text{and} \quad v = \frac{y}{y+1}.$$

As we have commented before, straight lines passing through the origin are transformed into straight lines passing through the origin.

Firstly, assume that  $\Sigma = \{x = 0\}$ . Applying the change  $(u, v) = (r \sin \theta, -r \cos \theta)$  and taking  $\theta$  as the new independent variable we obtain the equivalent functions (3.10) and (3.11). Here,  $\mathcal{A}^\pm$  are cubic polynomials and the denominator becomes  $\mathcal{C}(\theta, r) = 1 + r \cos \theta$ . For this case, the first averaged function  $\mathcal{F}_1$  is given by (3.6) for  $\alpha = 0$ . Since  $\mathcal{C}(\theta, r) = 1 + r \cos \theta$  is the denominator of  $F_1^+(\theta, r)$  in (3.6), the integrals (3.25) can be used directly. Nevertheless, the denominator of  $F_1^-(\theta - \pi, r)$  in (3.6) is given by  $\mathcal{C}(\theta - \pi, r) = 1 - r \cos \theta$ , so it is necessary to proceed with the change  $r = -R$  in order to use the integrals (3.25). Applying the integrals (3.25) for  $\ell = 1$  and  $k \in \{0, 1, 2, 3\}$ , and going back to the original variable  $r$  we have computed the first averaged function  $\mathcal{F}_1(r)$ . Finally, with the change (3.15) and after some algebraic manipulations, we get

$$\tilde{\mathcal{F}}_1(\rho) = \sum_{n=0}^4 k_n f_n(\rho),$$

with

$$\begin{aligned} f_0(\rho) &= \frac{\rho}{(\rho^2 + 1)^2}, & f_1(\rho) &= \frac{\rho^2}{(\rho^2 + 1)^2}, \\ f_2(\rho) &= \frac{3\rho^4 + 3\rho^3 + \rho^2 + 3}{3(\rho^2 + 1)^2} + \frac{\rho^4 - \rho^2 + 1}{2(\rho^2 + 1)\rho} L(\rho), & f_3(\rho) &= -\frac{3\rho^2}{4(\rho^2 + 1)^2} - \frac{3\rho}{8(\rho^2 + 1)} L(\rho), \\ f_4(\rho) &= \frac{\rho^5}{(\rho^2 + 1)^2}, \end{aligned}$$

and  $L$  is defined in (3.14). Moreover, the parameters  $k_n$  can be chosen arbitrarily. The first part of the statement follows because, in a neighborhood of the origin,  $f_i(\rho) = \rho^{i+1} + \mathcal{O}(\rho^{i+2})$ .

Now, assume that  $\Sigma = \{y = 0\}$ . The procedure for this case is similar to the previous case. We only detail the differences. The functions  $\mathcal{F}_1$  and  $\tilde{\mathcal{F}}_1$  are obtained from (3.6) and (3.25), but now for  $\alpha = -\pi/2$ . Thus, after some algebraic manipulations we get

$$\tilde{\mathcal{F}}_1(\rho) = \sum_{n=0}^5 k_n f_n(\rho),$$

with

$$\begin{aligned}
f_0(\rho) &= \frac{\rho}{(\rho^2 + 1)^2}, & f_1(\rho) &= \frac{\rho^2}{(\rho^2 + 1)^2}, & f_2(\rho) &= \frac{\rho^3}{(\rho^2 + 1)^2}, \\
f_3(\rho) &= \frac{3\rho^2}{4(\rho^2 + 1)^2} - \frac{3\rho(\rho^2 - 1)^2}{8(\rho^2 + 1)^3} \phi\left(\rho, \frac{\pi}{2}\right), & f_4(\rho) &= \frac{\rho^5}{(\rho^2 + 1)^2}, \\
f_5(\rho) &= \frac{525\rho^4 - 490\rho^2 + 525}{768(\rho^2 + 1)^2} - \frac{(175\rho^4 + 70\rho^2 + 175)(\rho^2 - 1)^2}{512\rho(\rho^2 + 1)^3} \phi\left(\rho, \frac{\pi}{2}\right).
\end{aligned} \tag{3.17}$$

Here, the function  $\phi$  is defined as

$$\phi(r, \theta) = \frac{1}{\sqrt{1-r^2}} \left( \theta - 2 \arctan \left( \sqrt{\frac{1-r}{1+r}} \tan \left( \frac{\theta}{2} \right) \right) \right),$$

and the parameters  $k_n$ ,  $n = 0, 1, \dots, 5$ , are arbitrary real numbers. The functions (3.17) also write  $f_i(\rho) = \rho^{i+1} + \mathcal{O}(\rho^{i+2})$ . Consequently, the second part of the proof follows.

Finally, assume that  $\Sigma = \{y + \sqrt{3}x = 0\}$ . Again, the procedure for this case is similar to the previous cases and we shall only detail the differences. The functions  $\mathcal{F}_1$  and  $\tilde{\mathcal{F}}_1$  are obtained from (3.6) and (3.25), but now for  $\alpha = -\pi/3$ . Thus, after some algebraic manipulations we get

$$\tilde{\mathcal{F}}_1(\rho) = \sum_{n=0}^7 k_n f_n,$$

with

$$\begin{aligned}
f_0(\rho) &= \frac{\rho}{\rho^2 + 1}, & f_1(\rho) &= \frac{\rho^2}{(\rho^2 + 1)^2}, & f_2(\rho) &= \frac{\rho^3}{(\rho^2 + 1)^2}, \\
f_3(\rho) &= \frac{5(54733\rho^4 + 94452\rho^2 + 54733)}{6912(\rho^2 + 1)^2} + \frac{15(1366\rho^4 + 1847\rho^2 + 1366)}{1024(\rho^2 + 1)\rho} \tilde{L}(\rho) \\
&\quad + \frac{25\sqrt{3}(236\rho^4 - 247\rho^2 + 236)(\rho^2 - 1)^2}{82944\rho(\rho^2 + 1)^3} \tilde{\phi}(\rho), \\
f_4(\rho) &= \frac{\rho^5}{(\rho^2 + 1)^2}, \\
f_5(\rho) &= -\frac{35(21835\rho^4 + 40596\rho^2 + 21835)}{6912(\rho^2 + 1)^2} - \frac{105(550\rho^4 + 797\rho^2 + 550)}{1024(\rho^2 + 1)\rho} \tilde{L}(\rho) \\
&\quad - \frac{175\sqrt{3}(176\rho^4 - 181\rho^2 + 176)(\rho^2 - 1)^2}{82944\rho(\rho^2 + 1)^3} \tilde{\phi}(\rho), \\
f_6(\rho) &= \frac{245(227\rho^4 + 444\rho^2 + 227)}{768(\rho^2 + 1)^2} + \frac{315(122\rho^4 + 181\rho^2 + 122)}{1024(\rho^2 + 1)\rho} \tilde{L}(\rho) \\
&\quad + \frac{35\sqrt{3}(116\rho^4 - 115\rho^2 + 116)(\rho^2 - 1)^2}{9216\rho(\rho^2 + 1)^3} \tilde{\phi}(\rho),
\end{aligned} \tag{3.18}$$

$$f_7(\rho) = -\frac{385(77\rho^4 + 156\rho^2 + 77)}{2304(\rho^2 + 1)^2} - \frac{3465(2\rho^4 + 3\rho^2 + 2)}{1024(\rho^2 + 1)\rho} \tilde{L}(\rho) \\ - \frac{385\sqrt{3}(8\rho^4 - 7\rho^2 + 8)(\rho^2 - 1)^2}{27648\rho(\rho^2 + 1)^3} \tilde{\phi}(\rho).$$

Here,

$$\tilde{L}(\rho) = \log\left(\frac{\rho^2 - \rho + 1}{\rho^2 + \rho + 1}\right), \quad \tilde{\phi}(\rho) = \phi\left(\frac{2\rho}{\rho^2 + 1}, \frac{2\pi}{3}\right) - \phi\left(-\frac{2\rho}{\rho^2 + 1}, \frac{2\pi}{3}\right).$$

Analogously to the previous cases,  $k_n$ ,  $n = 0, 1, \dots, 7$ , are arbitrary real numbers. Here,  $f_i(\rho) = \rho^{i+1} + \mathcal{O}(\rho^{i+2})$  for  $i = 0, 1, \dots, 5$ ,  $f_6(\rho) = \rho^8 + \mathcal{O}(\rho^9)$ , and  $f_7(\rho) = \rho^{10} + \mathcal{O}(\rho^{11})$ . Therefore, the ordered set of functions  $[f_0, f_1, \dots, f_7]$  is an ECT-system in a neighborhood of the origin. This completes the proof of the last case.  $\square$

Following the ideas of [CT18b], the previous local result can be numerically improved to a global one. Taking linear combinations of the functions (3.18) one may try to get an ordered set of 8 functions which is an ECT-system with accuracy (see, for instance, [NT17]). For instance, it can be checked numerically that the ordered set  $[f_0, f_1, f_2, f_3, f_4, f_6 + f_7, f_7, f_5]$  has all Wronskians non-vanishing except  $W_5, W_6$  which vanish once. From Theorem 3.3, we conclude that  $\mathcal{F}$  has at most 9 simple zeros. We shall see that a second order analysis allow us to overcome this number of limit cycles.

The next result is a technical lemma describing the existence of a pseudo-Hopf bifurcation for  $Z_{2,\varepsilon}$ .

**Lemma 3.9.** *Consider the piecewise vector fields  $Z_{i,\varepsilon}$ ,  $i = 1, 2, 3$ , under the assumption  $P^\pm(0, 0) = Q^\pm(0, 0) = 0$ . For all curve of discontinuity given by  $\{h(x, y) = Ax + By = 0\}$ , there exists a constant perturbation such that a small limit cycle bifurcates from the origin in a pseudo-Hopf bifurcation.*

*Proof.* The unperturbed vector fields have a monodromic equilibrium point. This property remains under the assumption  $P^\pm(0, 0) = Q^\pm(0, 0) = 0$ . Then, the proof follows directly from Proposition 3.4.  $\square$

The conclusions on hyperbolic limit cycles of  $Z_{2,\varepsilon}$  provided by Proposition 3.8 have assumed that  $P^\pm(0, 0) = Q^\pm(0, 0) = 0$ . So, from Lemma 3.9, the parameters  $P^\pm(0, 0)$  and  $Q^\pm(0, 0)$  can be used to get a pseudo-Hopf bifurcation for  $Z_{2,\varepsilon}^\pm$ , which adds an extra limit cycle to each case of Proposition 3.8. This is the content of the next result. It is worthwhile to say that this is the best result so far obtained after a first order analysis for piecewise quadratic system in two zones separated by a straight line.

**Corollary 3.10.** *For  $|\varepsilon| > 0$  sufficiently small, the maximum number of limit cycles that the system  $Z_{2,\varepsilon}$  can have in any neighborhood of origin is at least 5, 6, and 8 when the curve of discontinuity is  $\{x = 0\}$ ,  $\{y = 0\}$ , and  $\{y + \sqrt{3}x = 0\}$ , respectively.*

### 3.4 Second order perturbation

In this section, in order to extend the previous results, we perform a second order analysis on piecewise quadratic perturbations of quadratic isochronous centers from the families  $S_1$ ,  $S_2$ , and  $S_3$  (see (3.2)). More specifically, we shall apply the averaging method of second order to study the limit cycles of  $Z_{i,\varepsilon}$ ,  $i = 1, 2, 3$ . Due to the difficulties in the massive second order computations, we only perform a local study. Despite this, we shall get the best lower bounds so far for the maximum number of limit cycles of  $Z_{i,\varepsilon}$ ,  $i = 1, 2, 3$ , which are 11, 16, and 10, respectively. This proves our main result, Theorem 3.1.

In Propositions 3.11 and 3.13, we provide conditions such that the second averaged functions associated to  $Z_{1,\varepsilon}$  and  $Z_{3,\varepsilon}$  are linear with respect to the parameters and have the highest possible rank. Under these conditions the origin is a zero of maximal finite multiplicity for  $\mathcal{F}_2$ . Moreover, we shall see that  $\mathcal{F}_2$  satisfies the versal unfolding property at the origin guaranteeing then the existence of the highest possible number of simple zeros near the origin and, consequently, limit cycles for  $Z_{1,\varepsilon}$  and  $Z_{3,\varepsilon}$ . The second order analysis for centers of the family  $S_2$  is much more difficult and the procedure used for the families  $S_1$  and  $S_3$  cannot be followed straightly for  $S_2$ . In this case, some computer assisted analyses will be needed in order to use the Poincaré–Miranda theorem, that is Theorem 3.5, to obtain analytically the existence of 16 limit cycles of  $Z_{2,\varepsilon}$  bifurcating from the origin. This is the content of Proposition 3.17.

**Proposition 3.11.** *For  $|\varepsilon| > 0$  sufficiently small, the maximum number of limit cycles that  $Z_{1,\varepsilon}$  can have in any neighborhood of the origin is at least 11 when the curve of discontinuity is  $\{x = 0\}$ .*

*Proof.* Assume that  $P^\pm(0,0) = Q^\pm(0,0) = 0$ . Under such condition, as in Proposition 3.4 or Lemma 3.9, an extra limit cycle can always be obtained from a pseudo-Hopf bifurcation. So, the rest of the proof consists in applying the second order averaging method, Theorem 3.2(b), to get at least 10 limit cycles bifurcating from the origin. We notice that such special condition on the perturbation will guarantee that the averaged functions  $\mathcal{F}_1$  and  $\mathcal{F}_2$  are well defined at the origin.

The proof is structured in two parts. Firstly, we provide the expression of the function  $\mathcal{F}_2(r)$ . Secondly, we study the Taylor series of  $\mathcal{F}_2$  around  $r = 0$  in order to obtain the highest number of independent monomials.

The first part will follow the same steps as in the proof of Proposition 3.6. In fact, the function  $\mathcal{F}_1$  is given by (3.13). Then, imposing conditions such that  $\mathcal{F}_1 \equiv 0$ , that is  $k_0 = \dots = k_5 = 0$  in (3.12), we compute the second averaged function  $\mathcal{F}_2$  from (3.6) for  $\alpha = 0$ . Proceeding with the changes of variables (3.8) and (3.9) the denominators of the functions  $F_1^\pm$  and  $F_2^\pm$  write  $(1 + R \cos \psi)^2$ . Hence, the integrals

$$\begin{aligned} r_1^+(\theta, R) &= \int_0^\theta F_1^+(\theta, (-1 + \sqrt{1 - R^2})/R) d\theta, \\ r_1^-(\theta - \pi, R) &= \int_0^\theta F_1^-(\theta - \pi, (1 - \sqrt{1 - R^2})/R) d\theta, \end{aligned}$$

can be computed using the expressions  $\{\mathcal{S}, \mathcal{C}\}_{k,\ell}^{\alpha=0}$  (see (3.25)) for  $\ell = 2$ , and  $k \in \{0, 1, 2, 3\}$ . We notice that  $\mathcal{F}_2 = \mathcal{F}_2^{(1)} + \mathcal{F}_2^{(2)}$  in (3.6) has two summands. The first one, which depends linearly on the parameters of second order terms ( $p_{2,i,j}^{\pm}, q_{2,i,j}^{\pm}$  in  $F_2^{\pm}$ ), has the same form as  $\mathcal{F}_1$ . Indeed, changing the first index 1 to 2 of all the parameters  $p_{1,i,j}^{\pm}, q_{1,i,j}^{\pm}$  in (3.12) we see that  $\mathcal{F}_2^{(1)}$  becomes  $\mathcal{F}_1$ . Consequently,  $\mathcal{F}_2^{(1)}$  writes as (3.13) for some new parameters  $k_0, k_1, \dots, k_5$ . The second summand, which depends quadratically on the remaining parameters of first order terms ( $p_{1,i,j}^{\pm}, q_{1,i,j}^{\pm}$  in  $F_1$ ), can also be obtained using the integrals from Section 3.5. Indeed, in order to get  $\mathcal{F}_2^{(2)}$  the integrals

$$\begin{aligned}\mathcal{G}^+(R) &= \int_0^\pi \left( \frac{\partial}{\partial R} F_1^+(\theta, (-1 + \sqrt{1-R^2})/R) r_1^+(\theta, R) \right) d\theta, \\ \mathcal{G}^-(R) &= \int_0^\pi \left( \frac{\partial}{\partial R} F_1^-(\theta - \pi, (1 - \sqrt{1-R^2})/R) r_1^-(\theta - \pi, R) \right) d\theta,\end{aligned}$$

can be computed using the expressions  $\{s, c\}_{k,\ell}^\lambda, \{s, c\}_{k,\ell}^\phi, \{s, c\}_{k,\ell}^\theta, \{s, c\}_{k,\ell}^{\alpha=0}$ , for  $\ell = 3$  with  $k \in \{0, 1, 2, 3, 4\}$ , and  $\{s, c\}_{k,\ell}^{\alpha=0}$  for  $\ell = 4$  with  $k \in \{0, 1, 2, 3, 4, 5, 6\}$ . Finally, taking  $R = -2r/(1+r^2)$  and  $R = 2r/(1+r^2)$  in  $\mathcal{G}^+(R)$  and  $\mathcal{G}^-(R)$ , respectively, we get back the original variable  $r$ . Hence, the second averaged function writes

$$\mathcal{F}_2(r) = \mathcal{F}_2^{(1)}(r) + \mathcal{F}_2^{(2)}(r) = \mathcal{F}_2^{(1)}(r) + \mathcal{G}^+(-2r/(1+r^2)) + \mathcal{G}^-(2r/(1+r^2)). \quad (3.19)$$

Now, from Lemma 3.18, expression (3.13), and applying the change of parameters

$$\begin{aligned}c_0 &= p_{1,1,1}^- + p_{1,1,1}^+ + 2q_{1,2,0}^- + 2q_{1,2,0}^+, \\ c_1 &= 2p_{1,0,1}^+ - 2p_{1,0,2}^+ - 2p_{1,2,0}^+ + 2q_{1,1,0}^- - q_{1,1,1}^- + q_{1,1,1}^+, \\ c_2 &= p_{1,1,0}^+ + q_{1,0,1}^+, \\ c_3 &= -2p_{1,1,0}^+ + 2q_{1,0,1}^+ - 2q_{1,0,2}^+ - 2q_{1,2,0}^+, \end{aligned}$$

the second averaged function (3.19) writes

$$\begin{aligned}\mathcal{F}_2(r) &= \frac{H_0(r)}{r^2} + \frac{(1-r^2)H_1(r)}{r^3} \log\left(\frac{1-r}{1+r}\right) \\ &\quad + H_2(r) \log\left(\frac{(1-r^2)^2(1+r^2)}{(1+6r^2+r^4)^3}\right) + H_3(r)\Phi_0^0\left(\frac{2r}{r^2+1}\right),\end{aligned} \quad (3.20)$$

where  $\Phi_0^0$  is defined in (3.27),  $H_0(r)$  and  $H_1(r)$  are polynomials of degrees 7 and 6, respectively, satisfying

$$\begin{aligned}H_0(0) &= 2H_1(0), \\ H_0'(0) &= 2H_1'(0), \\ H_0''(0) &= -\frac{8}{3}H_1(0) + 2H_1''(0).\end{aligned} \quad (3.21)$$

Moreover,  $H_0$  and  $H_1$  depend quadratically on the parameters  $c_i, p_{1,i,j}^{\pm}, q_{1,i,j}^{\pm}$  and linearly on

the new parameters  $k_i$ . The other two functions write

$$H_2(r) = -\frac{(r^2 - 1)^2 \pi}{16r} c_0 c_1,$$

$$H_3(r) = \frac{r^2 - 1}{8r(r^2 + 1)} c_0 (c_3 r^4 - 2c_3 r^2 - 2c_2).$$

The above conditions imply that  $\mathcal{F}_2(r) = \mathcal{O}(r)$ . This concludes the first part of this proof.

Now, we compute the Taylor series of  $\mathcal{F}_2$  given in (3.20) around  $r = 0$ . So,

$$\mathcal{F}_2(r) = \sum_{i=0}^n f_i r^{i+1} + \mathcal{O}(r^{n+2}).$$

Here, the coefficients  $f_i$  are quadratic functions in the variables  $c_i, p_{1,i,j}^+, q_{1,i,j}^+$  and linear in the variables  $k_i, p_{1,0,1}^+, q_{1,0,2}^+, q_{1,2,0}^-, \dots$ . Assuming that

$$\begin{aligned} c_0 &= 1, \\ 2c_2 + c_3 - 2p_{1,1,1}^+ - 4q_{1,0,2}^- - 4q_{1,0,2}^+ &= 1, \\ 116c_2 + 58c_3 - 116p_{1,1,1}^+ - 230q_{1,2,0}^- - 230q_{1,2,0}^+ - 59 &= 1, \\ -2c_2 - c_3 + 2p_{1,1,1}^+ + 5 &= 1, \end{aligned}$$

the system of equations

$$\{f_0 = c_4, f_1 = c_5, f_2 = c_6, f_3 = c_7, f_4 = c_9, f_5 = c_8, f_7 = c_{10}, f_9 = c_{11}\}$$

has a unique solution. Accordingly, all the perturbation parameters depend only on the new parameters  $\{c_1, \dots, c_{11}\}$ . So, the second order averaged function writes

$$\mathcal{F}_2(r) = \sum_{i=0}^{13} g_i r^{i+1} + \mathcal{O}(r^{15}),$$

with  $g_0 = c_4, g_1 = c_5, g_2 = c_6, g_3 = c_7, g_4 = c_9, g_5 = c_8, g_7 = c_{10}, g_9 = c_{11}$

$$\begin{aligned} g_6 &= 3517699860675\pi c_1 + c_4 - c_6 + c_9, \\ g_8 &= -12593243758095\pi c_1, \\ g_{10} &= 61075412843445\pi c_1, \\ g_{11} &= -786432c_2 + \frac{63045632}{3}c_3 + \frac{3632}{1287}c_5 - \frac{3632}{1287}c_7 + \frac{1211}{429}c_8 - \frac{109}{39}c_{10} + \frac{7}{3}c_{11}, \\ g_{12} &= -304692133550805\pi c_1, \\ g_{13} &= -2484794504c_2 + 16745167364c_3 + \frac{7088319}{36608}c_5 - \frac{7088319}{36608}c_7 \\ &\quad + \frac{56833457}{292864}c_8 - \frac{1230915}{6656}c_{10} + \frac{209569}{2048}c_{11}. \end{aligned}$$

Notice that  $(g_0, g_1, \dots, g_{13})$  is a linear function on the variable  $(c_1, \dots, c_{11})$ . Since its rank with respect to  $(c_1, \dots, c_{11})$  is 11, there exists a change of variables  $(c_1, \dots, c_{11}) \mapsto (d_1, \dots, d_{11})$  such that

$$\mathcal{F}_2(r) = r \left( \sum_{i=1}^{11} d_i U_{a_i}(r) + \mathcal{O}(r^{14}) \right),$$

where  $U_{a_i}(r) = r^{a_i} + \mathcal{O}(r^{14})$ ,  $a_i = i - 1$ ,  $i = 1, 2, \dots, 8$ ,  $a_9 = 9$ ,  $a_{10} = 11$ , and  $a_{11} = 13$ . Since  $\mathcal{F}_2$  is analytic at  $r = 0$ , the Weierstrass Preparation Theorem (see, for instance, [CH82]) implies that there exists an analytic function  $F$  such that  $F(0) \neq 0$  and

$$\mathcal{F}_2(r) = rF(r) \sum_{i=1}^{11} d_i r^{a_i},$$

This proof follows by noticing that the parameters  $d_i$ ,  $i = 1, 2, \dots, 11$ , can be chosen (small) in order that the function  $\mathcal{F}_2(r)$  has 10 simple zeros near the origin.  $\square$

**Remark 3.12.** *There are two main difficulties in studying the maximum number of simple zeros of (3.20). First,  $\Phi_0^0$  is an integral function that cannot be expressed with simple functions. Second, the parameter coefficients of the polynomials  $H_0$  and  $H_1$  have a quadratic dependence on the parameters of  $Z_{1,\varepsilon}$ , consequently the ECT-systems theory cannot be directly applied.*

Similar difficulties as pointed out by Remark 3.12 will also appear in the next two propositions.

**Proposition 3.13.** *For  $|\varepsilon| > 0$  sufficiently small, the maximum number of limit cycles that  $Z_{3,\varepsilon}$  can have in any neighborhood of the origin is at least 10 when the curve of discontinuity is  $\{x = 0\}$ .*

*Proof.* The proof follows the same steps as the proof of Proposition 3.11. We recall that the first order analysis has been performed in Proposition 3.7. Again, an extra limit cycle can be obtained from a pseudo-Hopf bifurcation, so we may assume that  $P^\pm(0, 0) = Q^\pm(0, 0) = 0$ . Then, the proof will consist in applying the second order averaging method to get at least 9 limit cycles bifurcating from the origin.

Firstly, using (3.7) for  $\alpha = 0$ , the functions  $r_1^+(\theta, R)$  and  $r_1^-(\theta - \pi, R)$  write

$$\begin{aligned} r_1^+(\theta, R) &= \int_0^\theta F_1^+(\theta, -R/8) d\theta, \\ r_1^-(\theta - \pi, R) &= \int_0^\theta F_1^-(\theta - \pi, R/8) d\theta. \end{aligned}$$

The above integrals can be computed using the expressions from Section 3.5,  $\{\mathcal{S}, \mathcal{C}\}_{k,\ell}^{\alpha=0}$  for  $\ell = 4$ , and  $k = 0, 1, \dots, 6$ . Then, the second summand of the second averaged function,  $\mathcal{F}_2^{(2)}$ ,

follows from the integrals

$$\begin{aligned}\mathcal{G}^+(R) &= \int_0^\pi \left( \frac{\partial}{\partial R} F_1^+(\theta, -R/8) r_1^+(\theta, R) \right) d\theta, \\ \mathcal{G}^-(R) &= \int_0^\pi \left( \frac{\partial}{\partial R} F_1^-(\theta - \pi, R/8) r_1^-(\theta - \pi, R) \right) d\theta,\end{aligned}$$

which can be computed using the expressions from Section 3.5,  $\{s, c\}_{k,\ell}^\lambda$ ,  $\{s, c\}_{k,\ell}^\phi$ ,  $\{s, c\}_{k,\ell}^\theta$ ,  $\{s, c\}_{k,\ell}^{\alpha=0}$  for  $\ell = 5$  with  $k = 0, 1, \dots, 7$ , and  $\{s, c\}_{k,\ell}^{\alpha=0}$  with  $\ell = 8$  and  $k = 0, 1, \dots, 12$ . So, going back to the original variable  $r$  we get

$$\mathcal{F}_2(r) = \mathcal{F}_2^{(1)}(r) + \mathcal{F}_2^{(2)}(r) = \mathcal{F}_2^{(1)}(r) + \mathcal{G}^+(-8r) + \mathcal{G}^-(8r).$$

Again, from Lemma 3.18 and expression (3.16) we get

$$\mathcal{F}_2(r) = \frac{H_0(r)}{r^2(1-r^4)^2} + \frac{H_1(r)}{r^3(1+r^2)} \log \left( \frac{1-r}{1+r} \right).$$

Here,  $H_0$  and  $H_1$  are polynomials of degree 13 and 8, respectively, and satisfy the relations (3.21). As previously, with these conditions, we have  $\mathcal{F}_2(r) = \mathcal{O}(r)$ .

Now, computing the Taylor series of  $\mathcal{F}_2$  around  $r = 0$  we get

$$\mathcal{F}_2(r) = \sum_{i=1}^n f_i r^i + \mathcal{O}(r^{n+1}). \quad (3.22)$$

In order to simplify the expression of  $\mathcal{F}_2(r)$ , we introduce the new parameters,

$$\begin{aligned}c_1 &= 16 q_{1,1,0}^- + 3 q_{1,1,1}^- - 16 q_{1,1,0}^+ - 3 q_{1,1,1}^+, \\ c_2 &= -16 q_{1,1,0}^- + 4 p_{1,0,2}^+ - 3 q_{1,1,1}^- + 16 q_{1,1,0}^+ + 3 q_{1,1,1}^+, \\ c_3 &= -48 q_{1,1,0}^- + 12 p_{1,0,2}^+ + 8 p_{1,2,0}^+ - 9 q_{1,1,1}^- + 48 q_{1,1,0}^+ + 7 q_{1,1,1}^+, \\ c_4 &= 184 p_{1,1,1}^+ + 21 q_{1,0,2}^- + 71 q_{1,0,2}^+, \\ c_5 &= q_{1,0,2}^- + q_{1,0,2}^+, \\ c_6 &= q_{1,2,0}^- + q_{1,2,0}^+, \\ c_7 &= 200 p_{1,1,0}^+ + 579 p_{1,1,1}^+ - 825 q_{1,2,0}^- - 1300 q_{1,0,1}^+, \\ c_8 &= 16 p_{1,0,1}^- - 16 p_{1,0,1}^+ - 3 q_{1,1,1}^- + 3 q_{1,1,1}^+, \\ c_9 &= 16 p_{1,0,1}^+ - 3 q_{1,1,1}^+, \\ c_{10} &= q_{1,1,0}^+ + p_{1,0,1}^+, \\ c_{11} &= 800 p_{1,1,0}^+ - 1413 p_{1,1,1}^+ - 800 q_{1,0,1}^+, \\ c_{12} &= -\frac{789}{6125} p_{1,1,1}^+ - \frac{1}{24500} c_4 + \frac{71}{24500} c_5 + \frac{184}{18375} c_6 + \frac{4}{67375} c_7 - \frac{2}{28875} c_{11}.\end{aligned}$$

We see that the coefficients  $f_i$  in (3.22) depend linearly on the second order parameters,  $p_{2,i,j}^\pm$

and  $q_{2,i,j}^{\pm}$ , and quadratically on the new parameters  $c_i$ . Under the assumption  $P^{\pm}(0,0) = Q^{\pm}(0,0) = 0$ , the first averaged function, studied in Proposition 3.7, provides only the first 5 linearly independent coefficients. Thus, there exists a transformation on the parameters space such that  $f_i = d_i$  for  $i = 1, \dots, 5$ , and, under the condition  $c_1 = 1, c_5 = c_6 = c_8 = c_{10} = 0$ , the system

$$\{f_6 = d_6, f_7 = d_7, f_8 = d_8, f_9 = d_9, f_{10} = d_{10}\}$$

has a unique solution with respect to  $\{c_2, c_3, c_4, c_7, c_9\}$ . Therefore, we get

$$\mathcal{F}_2(r) = \sum_{i=1}^{10} d_i r^i + \mathcal{O}(r^{11}).$$

In this case, the multiplicity of the origin cannot be increased because the coefficients  $d_{11}$  and  $d_{12}$  depend linearly on the parameters  $\{d_1, \dots, d_{10}\}$ . In fact,

$$\begin{aligned} d_{11} &= d_5 + d_7 - d_9 \\ d_{12} &= -\frac{76}{715}d_2 - \frac{37}{65}d_4 + \frac{502}{715}d_6 + \frac{116}{65}d_8 - \frac{2}{5}d_{10}. \end{aligned}$$

Finally, this proof follows by noticing that the parameters  $d_i, i = 1, 2, \dots, 9$ , can be chosen (small) in order that the function  $\mathcal{F}_2(r)$  has 9 simple zeros near the origin.  $\square$

Next technical results, whose proofs are straightforward, provide lower and upper bounds for the values that a polynomial of  $n$  variables take in a  $n$  dimensional polyhedron. Moreover, they will be useful for proving the last proposition of this section concerning the second order analysis of the system  $Z_{2,\varepsilon}$ .

**Lemma 3.14.** *Consider  $h > 0, p > 0, q$  real numbers such that  $p \in [\underline{p}, \bar{p}]$ , with  $\underline{p}\bar{p} > 0$ , and  $q \in [\underline{q}, \bar{q}]$ , with  $\underline{q}\bar{q} > 0$ .*

(a) *Then,  $\sigma^{\ell}(q, p) \leq qp \leq \sigma^r(q, p)$ ,*

$$\text{where } \sigma^{\ell}(q, p) = \begin{cases} q\underline{p}, & \text{if } q > 0, \\ q\bar{p}, & \text{if } q < 0, \end{cases} \text{ and } \sigma^r(q, p) = \begin{cases} q\bar{p}, & \text{if } q > 0, \\ q\underline{p}, & \text{if } q < 0. \end{cases}$$

(b) *If  $u_j \in [-h, h]$ , for  $j = 1, \dots, n$ , and denoting  $u^i = u_1^{i_1} u_2^{i_2} \cdots u_n^{i_n}$  for  $i = (i_1, \dots, i_n) \neq 0$ , we have  $\chi^{\ell}(q, u^i) \leq qu^i \leq \chi^r(q, u^i)$ , where*

$$\chi^{\ell}(q, u^i) = \begin{cases} 0, & \text{if } q > 0 \text{ and } i_k \text{ even for all } k = 1, \dots, n, \\ -\bar{q} h^{i_1 + \dots + i_n}, & \text{if } q > 0 \text{ and } i_k \text{ odd for some } k = 1, \dots, n, \\ \underline{q} h^{i_1 + \dots + i_n}, & \text{if } q < 0, \end{cases}$$

and

$$\chi^r(q, u^i) = \begin{cases} \bar{q} h^{i_1 + \dots + i_n}, & \text{if } q > 0, \\ 0, & \text{if } q < 0 \text{ and } i_k \text{ even for all } k = 1, \dots, n, \\ -\underline{q} h^{i_1 + \dots + i_n}, & \text{if } q < 0 \text{ and } i_k \text{ odd for some } k = 1, \dots, n. \end{cases}$$

Furthermore,  $\chi^\ell(q, 1) = \underline{q}$  and  $\chi^r(q, 1) = \bar{q}$ .

**Lemma 3.15.** *Let  $h > 0$  and  $p_j$  be a positive non rational numbers such that  $p_j \in [\underline{p}_j, \bar{p}_j]$  with  $\underline{p}_j, \bar{p}_j$  rational numbers satisfying  $\underline{p}_j \bar{p}_j > 0$ , for  $j = 1, \dots, m$ . Consider the polynomial*

$$\mathcal{U}(u_1, \dots, u_n) = \sum_{i_1 + \dots + i_n = 0}^M \left( \sum_{j=1}^m U_{j,i} p_j \right) u^i, \quad (3.23)$$

with  $u^i = u_1^{i_1} \cdots u_n^{i_n}$ ,  $i = (i_1, \dots, i_n)$ , and  $U_{j,i}$  rational numbers. Then,

$$U_i^\ell \leq \sum_{j=1}^m U_{j,i} p_j \leq U_i^r$$

with  $U_i^\ell = \sum_{j=1}^m U_{j,i} \cdot \sigma^\ell(U_{j,i}, p_j)$  and  $U_i^r = \sum_{j=1}^m U_{j,i} \cdot \sigma^r(U_{j,i}, p_j)$ . Moreover, if  $u_j \in [-h, h]$ , for  $j = 1, \dots, n$ , and  $U_i^\ell \cdot U_i^r > 0$  then

$$\underline{\mathcal{U}} = \sum_{i_1 + \dots + i_n = 0}^M \chi^\ell(U_i^\ell, u^i) \leq \mathcal{U}(u_1, \dots, u_n) \leq \sum_{i_1 + \dots + i_n = 0}^M \chi^r(U_i^r, u^i) = \bar{\mathcal{U}}.$$

The next example shows how the above two technical lemmas can be used to get rational lower and upper bounds for the values that a function takes in a given 3D-polyhedron. In this example the lower and upper bounds for the values of  $\pi$  and  $\sqrt{3}$  are chosen from their continued fraction.

**Example 3.16.** *Consider the polynomial*

$$P(u, v, w) = P_0 + P_1 u + P_2 v^2 w^2 + P_3 uv^2 w^4, \quad (3.24)$$

with  $P_0 = \pi - 5\sqrt{3} + 4$ ,  $P_1 = -\pi^2 + 3\sqrt{3} - 3$ ,  $P_2 = -2\pi^3 - \sqrt{3} + 70$ , and  $P_3 = 4\pi + \sqrt{3} + 7$ . Consider the following intervals containing  $\pi$  and  $\sqrt{3}$ ,

$$\pi \in [\underline{p}, \bar{p}] = \left[ \frac{333}{106}, \frac{355}{113} \right] \quad \text{and} \quad \sqrt{3} \in [\underline{s}, \bar{s}] = \left[ \frac{5}{3}, \frac{7}{4} \right].$$

Then, for  $u, v, w \in [-1/9, 1/9]$ , we have

$$P(u, v, w) \in \left[ -\frac{8036904331130}{3236907751533}, -\frac{5753192708807927}{18184947748112394} \right].$$

*Proof.* Following the notation of Lemma 3.15, we take  $p_1 = \pi$ ,  $p_2 = \pi^2$ ,  $p_3 = \pi^3$ , and  $p_4 = \sqrt{3}$ . Then, the coefficients of (3.24) write as  $P_0 = p_1 - 5p_4 + 4$ ,  $P_1 = -p_2 + 3p_4 - 3$ ,  $P_2 = -2p_3 - p_4 + 70$ , and  $P_3 = 4p_1 + p_4 + 7$ .

The intervals given in the statement provide that  $\{p_1, p_4, p_2\} \subset [\underline{p}^2, \bar{p}^2]$  and  $p_3 \in [\underline{p}^3, \bar{p}^3]$ . So, these new variables allow us to define the coefficients  $U_{j,i}$  in (3.23). From Lemma 3.14(a)

we have

$$\begin{aligned} -\frac{341}{212} &= \underline{p} - 5\underline{s} + 4 = U_{000}^\ell \leq P_0 \leq U_{000}^r = \bar{p} - 5\bar{s} + 4 = -\frac{404}{339}, \\ -\frac{100487}{12769} &= -\bar{p}^2 + 3\underline{s} - 3 = U_{100}^\ell \leq P_1 \leq U_{100}^r = -\underline{p}^2 + 3\bar{s} - 3 = -\frac{21402}{2809}, \\ \frac{35999881}{5771588} &= -2\underline{p}^3 - \bar{s} + 70 = U_{022}^\ell \leq P_2 \leq U_{022}^r = -2\bar{p}^3 - \underline{s} + 70 = \frac{11301029}{1786524}, \\ \frac{3376}{159} &= 4\underline{p} + \underline{s} + 7 = U_{124}^\ell \leq P_3 \leq U_{124}^r = 4\bar{p} + \bar{s} + 7 = \frac{9635}{452}. \end{aligned}$$

Finally, applying Lemma 3.14(b) we get the following lower and upper bounds for  $P$ ,

$$U_{000}^\ell + U_{100}^\ell h - U_{124}^r h^7 = \underline{U} \leq P(u, v, w) \leq \bar{U} = U_{000}^r - U_{100}^\ell h + U_{022}^r h^4 + U_{124}^r h^7.$$

The proof follows by substituting  $h = 1/2$  in the above expression.  $\square$

The last proposition deals with second order perturbation of family  $S_2$ , which exhibits the highest number of limit cycles found in this chapter. Theorem 3.1 is a direct consequence of it. In Proposition 3.8 we have studied the zeros of the first averaged function for three different straight lines of discontinuity. The best result was obtained when  $\Sigma = \{y + \sqrt{3}x = 0\}$ . So, we shall perform the second order analysis only in this case.

**Proposition 3.17.** *For  $|\varepsilon| > 0$  sufficiently small, the maximum number of limit cycles that  $Z_{2,\varepsilon}$  can have in any neighborhood of the origin is at least 16 when the curve of discontinuity is  $\{y + \sqrt{3}x = 0\}$ .*

*Proof.* The proof follows basically the same steps as the proofs of Propositions 3.11 and 3.13. Nevertheless, in this case, some of the integrals of  $\mathcal{F}_2$  cannot be explicitly obtained. Then, since the functions are analytic near the origin, we compute the Taylor series of the integrand before integrating. We recall that the first order analysis has been performed in Proposition 3.8. Again, an extra limit cycle can be obtained from a pseudo-Hopf bifurcation, so we may assume that  $P^\pm(0, 0) = Q^\pm(0, 0) = 0$ . Then, the proof will consist in applying the second order averaging method to get at least 15 limit cycles bifurcating from the origin.

Using (3.7) for  $\alpha = -\pi/3$ , the functions  $r_1^+(\theta, R)$  and  $r_1^-(\theta - \pi, R)$  write

$$r_1^+(\theta, R) = \int_{-\pi/3}^{-\pi/3+\theta} F_1^+(\theta, R) d\theta,$$

and

$$r_1^-(\theta - \pi, R) = \int_{-\pi/3}^{-\pi/3+\theta} F_1^-(\theta - \pi, -R) d\theta.$$

The above integrals can be computed using the expressions for  $\{\mathcal{S}, \mathcal{C}\}_{k,\ell}^{\alpha=-\pi/3}$ , for  $\ell = 1$  and  $k = 0, 1, 2, 3$ , from Section 3.5. The second summand of the second averaged function,  $\mathcal{F}_2^{(2)}$ ,

follows from the integrals

$$\begin{aligned}\mathcal{G}^+(R) &= \int_{-\pi/3}^{2\pi/3} \left( \frac{\partial}{\partial R} F_1^+(\theta, R) r_1^+(\theta, R) \right) d\theta, \\ \mathcal{G}^-(R) &= \int_{-\pi/3}^{2\pi/3} \left( \frac{\partial}{\partial R} F_1^-(\theta - \pi, -R) r_1^-(\theta - \pi, -R) \right) d\theta.\end{aligned}$$

We point out that the integrands of the above integrals are rational functions with denominators  $(1 + R \cos \theta)^2$  and numerators depending on

$$\{R, \theta, \cos \theta, \sin \theta, \lambda(R, -\pi/3 + \theta), \lambda(R, -4\pi/3 + \theta), \phi(R, -\pi/3 + \theta), \phi(R, -4\pi/3 + \theta)\}.$$

Computing the Taylor series around  $R = 0$ , integrating on the interval  $[-\pi/3, 2\pi/3]$ , and going back to the original variable  $r$ , we get the Taylor series around  $r = 0$  of  $\mathcal{F}_2^{(2)}(r)$ . The Taylor series of  $\mathcal{F}_2^{(1)}(r)$  is obtained analogously to the series of  $\mathcal{F}_1(r)$  in Proposition 3.8. Accordingly, the second averaged function writes

$$\mathcal{F}_2(r) = \sum_{i=1}^n f_i r^i + \mathcal{O}(r^{n+1}).$$

The coefficients  $f_i$ 's depend linearly on  $\{p_{2,i,j}^\pm, q_{2,i,j}^\pm\}$  and quadratically on  $\{p_{1,i,j}^\pm, q_{1,i,j}^\pm\}$ .

The rest of the proof is devoted to show that there exists a transformation on the parameters such that the above function becomes

$$\mathcal{F}_2(r) = \sum_{i=1}^{16} d_i r^i + \mathcal{O}(r^{n+1}),$$

where  $d_1, \dots, d_{16}$  are independent parameters. In fact, we shall prove the existence of a transversal curve of weak foci of order 16. The transversality also guarantees the unfolding of 15 simple zeros near the origin because our function, also the perturbed one, vanishes at zero. The existence of such curve is obtained in two steps. Firstly, we analyse the maximal rank  $(f_1, \dots, f_n)$  with respect to the linear parameters  $\{p_{2,i,j}^\pm, q_{2,i,j}^\pm\}$ . Secondly, proceeding with a change of parameters, which eliminates the linear terms, we study the quadratic terms regarding  $\{p_{1,i,j}^\pm, q_{1,i,j}^\pm\}$  from  $(f_1, \dots, f_n)$ . We shall see that these quadratic terms are homogeneous and we show the existence of a transversal straight line such that these terms vanish on it. The described procedure is detailed in [Chr05, Theorems. 2.1 and 3.1]. These ideas have been originally introduced in [CJ89, CJ91] for quadratic vector fields and have also been employed in [Han99] for Liénard families.

Firstly, we see that the system of equations

$$\{f_1 = d_1, \dots, f_6 = d_6, f_8 = d_8, f_{10} = d_{10}\}$$

has a unique solution with respect to the variables  $p_{2,1,0}^+, p_{2,0,2}^+, p_{2,1,1}^+, p_{2,2,0}^+, q_{2,2,0}^+, q_{2,0,1}^+, p_{2,1,1}^-$ ,

and  $q_{2,2,0}^-$ . Hence, after this change, the rest of coefficients remains quadratic.

Secondly, assuming  $f_{16} \neq 0$  we shall obtain a transversal solution of the quadratic system

$$\mathcal{S} : \{f_7 = f_9 = f_{11} = f_{12} = f_{13} = f_{14} = f_{15} = 0\}.$$

Since there are more parameters than necessary, we impose that  $\{p_{1,2,0}^- = p_{1,1,1}^+ = q_{1,0,1}^- = q_{1,0,2}^- = q_{1,1,0}^- = q_{1,1,1}^- = q_{1,2,0}^- = q_{1,0,1}^+ = q_{1,0,2}^+ = q_{1,1,0}^+ = q_{1,1,1}^+ = q_{1,2,0}^+ = 0, p_{1,2,0}^+ = 1\}$ . Furthermore, it is not restrictive to assume that the first parameters  $d_1, d_2, \dots, d_6, d_8$ , and  $d_{10}$  vanish. For the sake of simplicity, we change the names of the remaining parameters  $[p_{1,0,1}^-, p_{1,1,0}^-, p_{1,0,1}^+, p_{1,1,0}^+, p_{1,0,2}^-, p_{1,1,1}^-, p_{1,0,2}^+]$  to  $[z_1, \dots, z_7]$ . In order to solve the quadratic system  $\mathcal{S}$  we consider two quadratic subsystems, namely  $\mathcal{S}_1 = \{f_7 = f_9 = f_{11} = f_{13} = f_{15} = 0\}$  and  $\mathcal{S}_2 = \{f_{12} = f_{14} = f_{15} = 0\}$ . Then, we study the intersection between their solutions.

Using the condition  $f_{15} = 0$ , the subsystem  $\mathcal{S}_1$  can be rewritten in order that all the equations depend linearly on  $z_1, z_2, z_3$ , and  $z_4$ . So, solving  $\mathcal{S}_1$  in these parameters we get

$$z_i = \frac{\zeta_i(z_5, z_6, z_7)}{\eta(z_5, z_6, z_7)}, \quad \text{for } i = 1, 2, 3, 4,$$

where  $\zeta_i$  are polynomials of degree 5 and  $\eta$  is a polynomial of degree 4. Later on, we shall see that  $\eta$  does not vanish at the intersection point. Accordingly, the parameters  $f_{12}, f_{14}$ , and  $f_{15}$  write

$$f_{12} = \frac{\tilde{f}_{12}(z_5, z_6, z_7)}{(\eta(z_5, z_6, z_7))^2}, \quad f_{14} = \frac{\tilde{f}_{14}(z_5, z_6, z_7)}{(\eta(z_5, z_6, z_7))^2}, \quad f_{15} = \frac{\tilde{f}_{15}(z_5, z_6, z_7)}{(\eta(z_5, z_6, z_7))^2}.$$

where  $\tilde{f}_{12}, \tilde{f}_{14}$ , and  $\tilde{f}_{15}$  are polynomials of degree 10. So, on the variety provided by  $\mathcal{S}_1$ , the subsystem  $\mathcal{S}_2$  is equivalent to

$$\tilde{\mathcal{S}}_2 : \{\tilde{f}_{12}(z_5, z_6, z_7) = 0, \tilde{f}_{14}(z_5, z_6, z_7) = 0, \tilde{f}_{15}(z_5, z_6, z_7) = 0\},$$

provided that  $\eta(z_5, z_6, z_7) \neq 0$ . Consequently, the system  $\mathcal{S}$  is reduced to  $\tilde{\mathcal{S}}_2$  whenever  $\eta(z_5, z_6, z_7) \neq 0$ . Although  $\tilde{\mathcal{S}}_2$  has only 3 equations and 3 unknowns, the high degree of these equations is a barrier for solving the system. Furthermore, the algebraic varieties provided by each equation of  $\tilde{\mathcal{S}}_2$  are numerically close to each other (see Figure 3.4), which adds an extra numerical difficulty.

In order to overcome these difficulties, we shall first work with numerical approximations of the solutions. Then, using Lemmas 3.14 and 3.15, and Theorem 3.5 we prove analytically the numerical results. Working with enough precision we get the following numerical solution of the system  $\tilde{\mathcal{S}}_2$ ,

$$(z_5^*, z_6^*, z_7^*) \approx (-0.260976000571, 0.111582119099, -0.84487667629841).$$

We can check that  $\eta(z_5^*, z_6^*, z_7^*) \approx 1.8531749845 \cdot 10^{-11}$  and  $\tilde{f}_{16}(z_5^*, z_6^*, z_7^*) \approx 8.876706245 \cdot 10^{-26}$ , so  $f_{16} = \tilde{f}_{16}(z_5, z_6, z_7)/(\eta(z_5, z_6, z_7))^2 \neq 0$ . Additionally, the intersection is transver-

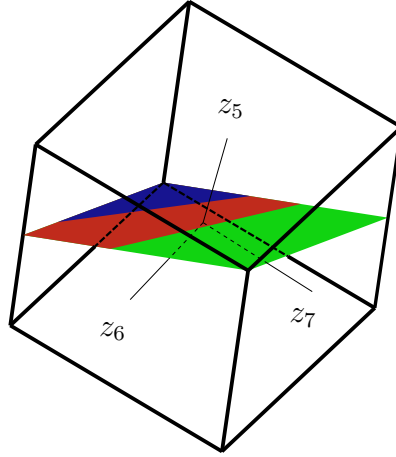


Figure 3.4: Plot of the varieties  $\tilde{f}_{12} = 0$ ,  $\tilde{f}_{14} = 0$ , and  $\tilde{f}_{15} = 0$  in a cube centered at  $(z_5^*, z_6^*, z_7^*)$  with edges of length  $10^{-2}$ . They are depicted in red, blue, and green, respectively.

sal because the determinant of the Jacobian matrix of  $f = (\tilde{f}_{12}, \tilde{f}_{14}, \tilde{f}_{15})$  with respect to  $(z_5, z_6, z_7)$  evaluated at the solution  $(z_5^*, z_6^*, z_7^*)$  does not vanish. In fact,  $J_f(z_5^*, z_6^*, z_7^*) \approx -5.379835263496 \cdot 10^{-67}$ . It is worthwhile to mention that although the values for  $\eta$ ,  $\tilde{f}_{16}$ , and  $J_f$  are very small at  $(z_5^*, z_6^*, z_7^*)$ , we were able to observe that they remain fixed when we increase the precision of the computations, while the values for  $\tilde{f}_{12}$ ,  $\tilde{f}_{14}$ , and  $\tilde{f}_{15}$  decrease to zero.

Finally, we shall prove analytically the existence of such transversal intersection point  $(z_5^*, z_6^*, z_7^*)$ . In order to apply Lemmas 3.14 and 3.15, we make the following change of variables,

$$\begin{aligned} z_5 &= -\frac{102563793961}{75692301} u_1 + \frac{93673471843}{117235838} u_2 - \frac{5228323783}{13687494949} u_3 - \frac{1104348344}{4231608813}, \\ z_6 &= -\frac{114951879798}{118751113} u_1 + \frac{66846520379}{116131808} u_2 + \frac{1728113446}{4218432187} u_3 + \frac{859801297}{7705547304}, \\ z_7 &= \frac{131538341646}{188147809} u_1 - \frac{23870722389}{57947275} u_2 + \frac{1387092713}{5464980203} u_3 - \frac{2790022856}{3302284149}. \end{aligned}$$

Then,

$$\begin{aligned} \tilde{f}_{12} &= \xi_1(u_1, u_2, u_3), & \tilde{f}_{14} &= \xi_2(u_1, u_2, u_3), & \tilde{f}_{15} &= \xi_3(u_1, u_2, u_3), \\ \tilde{f}_{16} &= \xi_4(u_1, u_2, u_3), & \eta &= \xi_5(u_1, u_2, u_3), & J_f &= \xi_6(u_1, u_2, u_3). \end{aligned}$$

Now, the problem is to check that the varieties defined by  $\xi_1 = 0$ ,  $\xi_2 = 0$ , and  $\xi_3 = 0$  intersect transversally near the origin (see Figure 3.5).

We notice that the functions  $\xi_i$ ,  $i = 1, \dots, 6$ , are polynomials in  $(u_1, u_2, u_3)$ . Moreover,  $\xi_i$ ,  $i = 1, \dots, 4$  have degree 10,  $\xi_5$  has degree 4, and  $\xi_6$  has degree 27. We see that the coefficients of the previous polynomials depend on the irrational numbers  $\pi$  and  $\sqrt{3}$ . More specifically, the coefficients of  $\xi_i$ ,  $i = 1, \dots, 4$ , depend on  $\pi$  up to power 12,  $\xi_5$  depends on  $\pi$  up to power 5, and  $\xi_6$  depends on  $\pi$  up to power 37. The number  $\sqrt{3}$  appears in

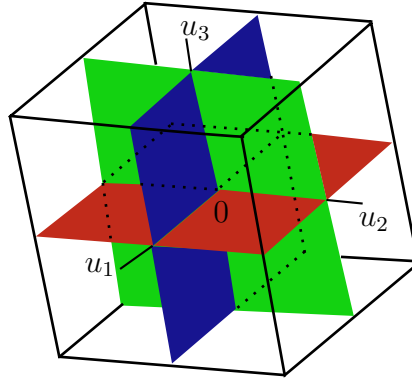


Figure 3.5: Plot of the varieties  $\xi_1 = \xi_2 = \xi_3 = 0$  in a neighborhood of the origin. The varieties are drawn in green, blue, and red, respectively. The length of the edges of the 3d-cube is  $10^{-10}$ .

these coefficients with no exponent. For each function  $\xi_i$ , let  $\mu_i$  denote the degree with respect to  $\pi$ . Then, substituting  $\sqrt{3}, \pi, \pi^2, \dots, \pi^{\mu_i}$  by  $p_1, p_2, \dots, p_{\mu_i+1}$ , respectively, all the coefficients of the polynomial  $\xi_i(p_1, p_2, \dots, p_{\mu_i+1}, u_1, u_2, u_3)$  are now rational numbers defined as the quotient of two big integers, around 1000 figures each. Moreover, they have 6292, 6292, 6006, 6292, 220 and 234668 monomials.

Finally, we can apply Theorem 3.5 to  $(\xi_1, \xi_2, \xi_3)$  in  $B = [-h, h]^3$ , with  $h = 10^{-10}$ , because

$$\begin{aligned} \xi_1(B_1^-) &\subset [a_1^-, b_1^-] \approx [-3.58842524 \cdot 10^{-32}, -3.20226086 \cdot 10^{-32}], \\ \xi_1(B_1^+) &\subset [a_1^+, b_1^+] \approx [3.28009013 \cdot 10^{-32}, 3.66625367 \cdot 10^{-32}], \\ \xi_2(B_2^-) &\subset [a_2^-, b_2^-] \approx [-3.70185379 \cdot 10^{-32}, -3.04215854 \cdot 10^{-32}], \\ \xi_2(B_2^+) &\subset [a_2^+, b_2^+] \approx [3.16666084 \cdot 10^{-32}, 3.82635712 \cdot 10^{-32}], \\ \xi_3(B_3^-) &\subset [a_3^-, b_3^-] \approx [-4.72369496 \cdot 10^{-32}, -1.41476503 \cdot 10^{-32}], \\ \xi_3(B_3^+) &\subset [a_3^+, b_3^+] \approx [2.14481860 \cdot 10^{-32}, 5.45375151 \cdot 10^{-32}]. \end{aligned}$$

We notice that the values for  $a_i^\pm$  and  $b_i^\pm$ , for  $i = 1, 2, 3$ , are all rational numbers explicitly computed using Lemmas 3.14, 3.15, and

$$\pi \in \left[ \frac{21053343141}{6701487259}, \frac{1783366216531}{567663097408} \right], \quad \sqrt{3} \in \left[ \frac{716035}{413403}, \frac{978122}{564719} \right].$$

Hence, we conclude that there exists a point  $(\xi_1^*, \xi_2^*, \xi_3^*)$  in  $B$  such that  $\xi_1 = \xi_2 = \xi_3 = 0$ . Additionally,  $\xi_4, \xi_5, \xi_6$  do not vanish on  $B$ . Indeed,

$$\begin{aligned} \xi_4(B) &\subset [a_4^-, b_4^-] \approx [8.87669600 \cdot 10^{-26}, 8.87671664 \cdot 10^{-26}], \\ \xi_5(B) &\subset [a_5^-, b_5^-] \approx [1.85317477 \cdot 10^{-11}, 1.85317520 \cdot 10^{-11}], \\ \xi_6(B) &\subset [a_6^+, b_6^+] \approx [-5.37983643 \cdot 10^{-67}, -5.37983443 \cdot 10^{-67}], \end{aligned}$$

Again, the values for  $a_i^\pm$  and  $b_i^\pm$ ,  $i = 4, 5, 6$ , are rational numbers explicitly computed using

Lemmas 3.14 and 3.15. So, we conclude that the solution provided by Theorem 3.5 is a transversal solution of  $\mathcal{S}$ .  $\square$

### 3.5 Appendix: Explicit computations of the integrals

This section is devoted to provide explicit expressions for some of the integrals necessary to compute the averaged functions. We also introduce new special integral functions as well as some of their properties and relations. The proofs follow closely the results from [PT14].

For each pair of natural numbers  $k$  and  $\ell$ , we define the following functions:

$$\begin{aligned}
\mathcal{S}_{k,\ell}^\alpha(r, \theta) &= \int_\alpha^{\alpha+\theta} \frac{\sin(k\psi)}{(1+r\cos\psi)^\ell} d\psi, & \mathcal{C}_{k,\ell}^\alpha(r, \theta) &= \int_\alpha^{\alpha+\theta} \frac{\cos(k\psi)}{(1+r\cos\psi)^\ell} d\psi, \\
s_{k,\ell}^\alpha(r) &= \int_\alpha^{\alpha+\pi} \frac{\sin(k\theta)}{(1+r\cos\theta)^\ell} d\theta, & c_{k,\ell}^\alpha(r) &= \int_\alpha^{\alpha+\pi} \frac{\cos(k\theta)}{(1+r\cos\theta)^\ell} d\theta, \\
s_{k,\ell}^\lambda(r) &= \int_0^\pi \frac{\sin(k\theta) \lambda(r, \theta)}{(1+r\cos\theta)^\ell} d\theta, & c_{k,\ell}^\lambda(r) &= \int_0^\pi \frac{\cos(k\theta) \lambda(r, \theta)}{(1+r\cos\theta)^\ell} d\theta. \\
s_{k,\ell}^\phi(r) &= \int_0^\pi \frac{\sin(k\theta) \phi(r, \theta)}{(1+r\cos\theta)^\ell} d\theta, & c_{k,\ell}^\phi(r) &= \int_0^\pi \frac{\cos(k\theta) \phi(r, \theta)}{(1+r\cos\theta)^\ell} d\theta, \\
s_{k,\ell}^\theta(r) &= \int_0^\pi \frac{\theta \sin(k\theta)}{(1+r\cos\theta)^\ell} d\theta, & c_{k,\ell}^\theta(r) &= \int_0^\pi \frac{\theta \cos(k\theta)}{(1+r\cos\theta)^\ell} d\theta.
\end{aligned} \tag{3.25}$$

Here,  $r \in (-1, 1)$ ,  $\theta \in [-\pi, \pi]$ , and  $\phi, \lambda$  are the two periodic functions

$$\begin{aligned}
\phi(r, \theta) &= \frac{1}{\sqrt{1-r^2}} \left( \theta - 2 \arctan \left( \sqrt{\frac{1-r}{1+r}} \tan \left( \frac{\theta}{2} \right) \right) \right), \\
\lambda(r, \theta) &= \log(1+r\cos\theta).
\end{aligned} \tag{3.26}$$

**Lemma 3.18.** *Let  $\phi, \lambda$  be the functions defined by (3.26). Then,  $\phi(r, 0) = \phi(-r, 0) = 0$ ,  $\phi(r, \pi) = \phi(r, -\pi) = 0$ , and  $\phi(-r, t + \pi) = \phi(r, t)$ . Moreover,*

$$\frac{\partial}{\partial r} \phi(r, \theta) = \frac{r\phi(r, \theta)}{1-r^2} + \frac{\sin\theta}{(1-r^2)(1+r\cos\theta)}, \quad \frac{\partial}{\partial r} \lambda(r, \theta) = \frac{\cos\theta}{1+r\cos\theta}.$$

*Proof.* The first properties follow simply by substituting  $\theta = 0, \pi$  in the definition of  $\phi$ . The last is satisfied because  $F(r, 0) = 0$  and the derivative, with respect to  $\theta$ , of  $F(r, \theta) = \phi(-r, \theta + \pi) - \phi(r, \theta)$  vanishes identically. The expressions of their derivatives are easily to be checked.  $\square$

We notice that not all the above integrals can be explicitly obtained. So, next lemma introduce some new functions. They, together with their derivatives, are useful for the proofs of the results.

**Lemma 3.19.** *Let  $\Phi_0^0(r)$ ,  $\Lambda_0^0(r)$ , and  $\Lambda_1^0(r)$  be the functions*

$$\begin{aligned}\Phi_0^0(r) &= \int_0^\pi \phi(r, \theta) d\theta, \\ \Lambda_0^0(r) &= \int_0^\pi \lambda(r, \theta) d\theta = -\pi \log \left( \frac{2(1 - \sqrt{1 - r^2})}{r^2} \right), \\ \Lambda_1^0(r) &= \int_0^\pi \frac{\lambda(r, \theta)}{1 + r \cos \theta} d\theta = \frac{\pi \log(1 - r^2) - \Lambda_0^0(r)}{\sqrt{1 - r^2}}.\end{aligned}\tag{3.27}$$

Then, their derivatives can be expressed explicitly as functions of (3.26) and (3.27),

$$\begin{aligned}\frac{d}{dr} \Phi_0^0(r) &= \frac{r^2 \Phi_0^0(r) + \lambda(r, 0) - \lambda(-r, 0)}{r(1 - r^2)} \\ \frac{d}{dr} \Lambda_0^0(r) &= -\frac{\pi(1 - \sqrt{1 - r^2})}{r\sqrt{1 - r^2}}, \\ \frac{d}{dr} \Lambda_1^0(r) &= \frac{1}{1 - r^2} \left( r \Lambda_1^0(r) - \frac{(1 + r^2 - \sqrt{1 - r^2})\pi}{r\sqrt{1 - r^2}} \right).\end{aligned}$$

The following results give recurrent formulas in terms of  $k$  and  $\ell$  for all the functions defined at the beginning of this section.

**Proposition 3.20.** *The functions  $\mathcal{S}_{k,\ell}^\alpha$  and  $\mathcal{C}_{k,\ell}^\alpha$ , defined in (3.25), write as*

$$\mathcal{S}_{k,\ell}^\alpha(r, \theta) = \begin{cases} 0 & k = 0, \ell \geq 0, \\ (\cos(k\alpha) - \cos(k(\theta + \alpha)))k^{-1} & k \geq 1, \ell = 0, \\ (\lambda(r, \alpha) - \lambda(r, \theta + \alpha))r^{-1} & k = 1, \ell = 1, \\ \frac{(1 + r \cos(\theta + \alpha))^{1-\ell} - (1 + r \cos \alpha)^{1-\ell}}{r(\ell - 1)} & k = 1, \ell \geq 2, \\ 2(\mathcal{S}_{k-1,\ell-1}^\alpha(r, \theta) - \mathcal{S}_{k-1,\ell}^\alpha(r, \theta))r^{-1} - \mathcal{S}_{k-2,\ell}^\alpha(r, \theta) & k \geq 2, \ell \geq 1, \end{cases}$$

$$\mathcal{C}_{k,\ell}^\alpha(r, \theta) = \begin{cases} \theta & k = 0, \ell = 0, \\ (\sin(k(\theta + \alpha)) - \sin(k\alpha))k^{-1} & k \geq 1, \ell = 0, \\ \phi(r, \alpha) - \phi(r, \theta + \alpha) + \theta(1 - r^2)^{-\frac{1}{2}} & k = 0, \ell = 1, \\ \mathcal{C}_{0,\ell-1}^\alpha(r, \theta) + \frac{r}{\ell - 1} \frac{\partial}{\partial r} \mathcal{C}_{0,\ell-1}^\alpha(r, \theta) & k = 0, \ell \geq 2, \\ (\mathcal{C}_{0,\ell-1}^\alpha(r, \theta) - \mathcal{C}_{0,\ell}^\alpha(r, \theta))r^{-1} & k = 1, \ell \geq 1, \\ 2(\mathcal{C}_{k-1,\ell-1}^\alpha(r, \theta) - \mathcal{C}_{k-1,\ell}^\alpha(r, \theta))r^{-1} - \mathcal{C}_{k-2,\ell}^\alpha(r, \theta) & k \geq 2, \ell \geq 1, \end{cases}$$

when  $r \neq 0$ . Furthermore,  $\mathcal{S}_{k,\ell}^\alpha(0, \theta) = \mathcal{S}_{k,0}^\alpha(r, \theta)$  and  $\mathcal{C}_{k,\ell}^\alpha(0, \theta) = \mathcal{C}_{k,0}^\alpha(r, \theta)$ .

*Proof.* The expressions of  $\mathcal{S}_{k,\ell}^\alpha(r, \theta)$  for  $k = 0, 1$  follow by direct integration. When  $k \geq 2$

and  $\ell \geq 2$ , from its definition and by using elementary transformations, we get

$$\begin{aligned} \mathcal{S}_{k-1,\ell-1}^\alpha(r, \theta) &= \int_\alpha^{\alpha+\theta} \frac{\sin((k-1)\psi)}{(1+r \cos \psi)^{\ell-1}} d\psi = \int_\alpha^{\alpha+\theta} \frac{\sin((k-1)\psi)(1+\cos \psi)}{(1+r \cos \psi)^\ell} d\psi \\ &\quad \int_\alpha^{\alpha+\theta} \frac{\sin((k-1)\psi)}{(1+r \cos \psi)^\ell} d\psi + r \int_\alpha^{\alpha+\theta} \frac{\sin((k-1)\psi) \cos \psi}{(1+r \cos \psi)^\ell} d\psi. \end{aligned} \quad (3.28)$$

Using the identity  $2 \sin((k-1)\psi) \cos \psi = \sin(k\psi) + \sin((k-2)\psi)$  the above expression writes

$$\mathcal{S}_{k-1,\ell-1}^\alpha(r, \theta) = \mathcal{S}_{k-1,\ell}^\alpha(r, \theta) + \frac{1}{2}r \mathcal{S}_{k,\ell}^\alpha(r, \theta) + \frac{1}{2}r \mathcal{S}_{k-2,\ell}^\alpha(r, \theta).$$

Then, solving  $\mathcal{S}_{k,\ell}^\alpha(r, \theta)$  in this expression we recover the one appearing in the statement.

The expression for  $\mathcal{C}_{k,0}^\alpha(r, \theta)$  follows by a direct integration, whereas  $\mathcal{C}_{0,1}^\alpha$  follows from the definition of  $\phi$  given in (3.26) and the change of variables  $\tan(\psi/2) = \varphi$ . The expression of  $\mathcal{C}_{0,\ell}^\alpha(r, \theta)$ , for  $\ell \geq 2$ , follows deriving with respect to  $r$ . The expression for  $\mathcal{C}_{k,\ell}^\alpha(r, \theta)$  can be obtained analogously to  $\mathcal{S}_{k,\ell}^\alpha(r, \theta)$ .  $\square$

The next corollary follows straightaway by evaluating  $\theta = \pi$  in the last result.

**Corollary 3.21.** *The functions  $s_{k,\ell}^\alpha$  and  $c_{k,\ell}^\alpha$  defined in (3.25) write as*

$$s_{k,\ell}^\alpha(r) = \begin{cases} 0 & k = 0, \ell \geq 0, \\ (\lambda(r, \alpha) - \lambda(r, \alpha + \pi)) r^{-1} & k = 1, \ell = 1, \\ \frac{(1 - (-1)^k)}{k} \cos(k\alpha) & k \geq 1, \ell = 0, \\ \frac{(1 + r \cos \alpha)^{1-\ell} - (1 - r \cos \alpha)^{1-\ell}}{r(1-\ell)} & k = 1, \ell \geq 2, \\ 2 (s_{k-1,\ell-1}^\alpha(r) - s_{k-1,\ell}^\alpha(r)) r^{-1} - s_{k-2,\ell}^\alpha(r) & k \geq 2, \ell \geq 1, \end{cases}$$

$$c_{k,\ell}^\alpha(r) = \begin{cases} \pi & k = 0, \ell = 0, \\ \phi(r, \alpha) - \phi(r, \alpha + \pi) + \frac{\pi}{\sqrt{1-r^2}} & k = 0, \ell = 1, \\ \frac{r}{\ell-1} \frac{d}{dr} c_{0,\ell-1}^\alpha(r) + c_{0,\ell-1}^\alpha(r) & k = 0, \ell \geq 2, \\ \frac{-1 + (-1)^k}{k} \sin(k\alpha) & k \geq 1, \ell = 0, \\ (c_{0,\ell-1}^\alpha(r) - c_{0,\ell}^\alpha(r)) r^{-1} & k = 1, \ell \geq 1, \\ 2 (c_{k-1,\ell-1}^\alpha(r) - c_{k-1,\ell}^\alpha(r)) r^{-1} - c_{k-2,\ell}^\alpha(r) & k \geq 2, \ell \geq 1, \end{cases}$$

when  $r \neq 0$ . Furthermore,  $s_{0,\ell}^\alpha(0) = 0$ ,  $c_{0,\ell}^\alpha(0) = \pi$  for  $\ell \geq 0$  and

$$s_{k,\ell}^\alpha(0) = \frac{1 - (-1)^k}{k} \cos(k\alpha), \quad c_{k,\ell}^\alpha(0) = \frac{-1 + (-1)^k}{k} \sin(k\alpha),$$

for  $k \geq 1$  and  $\ell \geq 0$ .

**Proposition 3.22.** *The functions  $s_{k,\ell}^\lambda$  and  $c_{k,\ell}^\lambda$ , defined in (3.25), write as*

$$s_{k,\ell}^\lambda(r) = \begin{cases} 0 & k = 0, \ell \geq 0, \\ \frac{\lambda(r, 0) - (-1)^k \lambda(-r, 0)}{\lambda(r, 0)^2 - \lambda(-r, 0)^2} + \frac{r}{2k} (s_{k-1,1}(r) - s_{k+1,1}(r)) & k \geq 1, \ell = 0, \\ \frac{1}{r(\ell-1)} \left( \frac{2r}{(1-r)^{\ell-1}} - \frac{\lambda(r, 0) + (\ell-1)^{-1}}{(1+r)^{\ell-1}} \right) & k = 1, \ell \geq 2, \\ 2(s_{k-1,\ell-1}^\lambda(r) - s_{k-1,\ell}^\lambda(r)) r^{-1} - s_{k-2,\ell}^\lambda(r) & k \geq 2, \ell \geq 1, \end{cases}$$

$$c_{k,\ell}^\lambda(r) = \begin{cases} \Lambda_\ell^0(r) & k = 0, \ell = 0, 1, \\ \frac{r}{\ell-1} \left( \frac{d}{dr} c_{0,\ell-1}^\lambda(r) - c_{1,\ell}(r) \right) + c_{0,\ell-1}^\lambda(r) & k = 0, \ell \geq 2, \\ \frac{r}{2k} (c_{k-1,1}(r) - c_{k+1,1}(r)) & k \geq 1, \ell = 0, \\ (c_{0,\ell-1}^\lambda(r) - c_{0,\ell}^\lambda(r)) r^{-1} & k = 1, \ell \geq 1, \\ 2(c_{k-1,\ell-1}^\lambda(r) - c_{k-1,\ell}^\lambda(r)) r^{-1} - c_{k-2,\ell}^\lambda(r) & k \geq 2, \ell \geq 1, \end{cases}$$

when  $r \neq 0$ . Furthermore,  $s_{k,\ell}^\lambda(0) = s_{k,\ell}(0)$  and  $c_{k,\ell}^\lambda(0) = 0$  for  $k \geq 0$  and  $\ell \geq 0$ .

*Proof.* The general expression for  $k \geq 1, \ell \geq 1$  follows similarly to (3.28). The other cases follow straightforward. In some of them, the integration by parts rule is necessary and also the fact that  $c_{k,\ell}^\lambda$  is an even function.  $\square$

**Proposition 3.23.** *The functions  $s_{k,\ell}^\phi$  and  $c_{k,\ell}^\phi$ , defined in (3.25), write as*

$$s_{k,\ell}^\phi(r) = \begin{cases} 0 & k = 0, \ell \geq 0, \\ -\frac{c_{k,1}(r)}{r\sqrt{1-r^2}} & k \geq 1, \ell = 0, \\ \frac{\Lambda_0^0(r)}{r\sqrt{1-r^2}} - \frac{\Lambda_1^0(r)}{r} & k = 1, \ell = 1, \\ \frac{1}{r(\ell-1)} \left( c_{0,\ell} - \frac{c_{0,\ell-1}}{\sqrt{1-r^2}} \right) & k = 1, \ell \geq 2, \\ 2(s_{k-1,\ell-1}^\phi(r) - s_{k-1,\ell}^\phi(r)) r^{-1} - s_{k-2,\ell}^\phi(r) & k \geq 2, \ell \geq 1, \end{cases}$$

$$c_{k,\ell}^\phi(r) = \begin{cases} \Phi_0^0(r) & k = 0, \ell = 0, \\ \frac{c_{0,1}^\phi(r)}{\sqrt{1-r^2}} - \frac{1}{2} \left( \frac{\pi}{\sqrt{1-r^2}} \right)^2 & k = 0, \ell = 1, \\ \frac{r}{\ell-1} \left( \frac{d}{dr} c_{0,\ell-1}^\phi(r) - \frac{s_{1,\ell}(r)}{1-r^2} \right) + \frac{\ell(1-r^2) - 1}{(\ell-1)(1-r^2)} c_{0,\ell-1}^\phi(r) & k = 0, \ell \geq 2, \\ \frac{s_{k,1}(r)}{k} + \frac{(-1)^k - 1}{k^2 \sqrt{1-r^2}} & k \geq 1, \ell = 0, \\ (c_{0,\ell-1}^\phi(r) - c_{0,\ell}^\phi(r)) r^{-1} & k = 1, \ell \geq 1, \\ 2(c_{k-1,\ell-1}^\phi(r) - c_{k-1,\ell}^\phi(r)) r^{-1} - c_{k-2,\ell}^\phi(r) & k \geq 2, \ell \geq 1, \end{cases}$$

when  $r \neq 0$ . Furthermore,  $s_{k,\ell}^\phi(0) = c_{k,\ell}^\phi(0) = 0$ .

*Proof.* The expression of  $s_{k,\ell}^\phi$  follows from the fact that it is an even function and the results in [PT14]. For  $k = 1, \ell \geq 1$  and  $k \geq 2, \ell \geq 1$ , proceeding analogously to the previous proofs, we get  $c_{k,\ell}^\phi$ . Finally, for  $k = 0, \ell \geq 2$ , we compute directly the derivative, with respect to  $r$ , of  $c_{0,\ell-1}^\phi$ . The other cases follow using the integration by parts rule.  $\square$

The last result follows similarly as all the previous results.

**Proposition 3.24.** *The functions  $s_{k,\ell}^\theta$  and  $c_{k,\ell}^\theta$  defined in (3.25) write as*

$$s_{k,\ell}^\theta(r) = \begin{cases} 0 & k = 0, \ell \geq 0, \\ \frac{-(-1)^k \pi}{k} & k \geq 1, \ell = 0, \\ (-\pi \lambda(-r, 0) + \Lambda_0^0(r)) r^{-1} & k = 1, \ell = 1, \\ \frac{1}{r(\ell-1)} \left( \frac{\pi}{(1-r)^{\ell-1}} - c_{0,\ell-1}(r) \right) & k = 1, \ell \geq 2, \\ 2 \left( s_{k-1,\ell-1}^\theta(r) - s_{k-1,\ell}^\theta(r) \right) r^{-1} - s_{k-2,\ell}^\theta(r) & k \geq 2, \ell \geq 1, \end{cases}$$

$$c_{k,\ell}^\theta(r) = \begin{cases} \frac{\pi^2}{2} & k = 0, \ell = 0, \\ \Phi_0^0(r) + \frac{\pi^2}{2\sqrt{1-r^2}} & k = 0, \ell = 1, \\ \frac{r}{\ell-1} \frac{d}{dr} c_{0,\ell-1}^\theta(r) + c_{0,\ell-1}^\theta(r) & k = 0, \ell \geq 2, \\ \frac{-1 + (-1)^k}{k^2} & k \geq 1, \ell = 0, \\ \left( c_{0,\ell-1}^\theta(r) - c_{0,\ell}^\theta(r) \right) r^{-1} & k = 1, \ell \geq 1, \\ 2 \left( c_{k-1,\ell-1}^\theta(r) - c_{k-1,\ell}^\theta(r) \right) r^{-1} - c_{k-2,\ell}^\theta(r) & k \geq 2, \ell \geq 1, \end{cases}$$

when  $r \neq 0$ . Furthermore,  $s_{0,\ell}^\theta(0) = 0$ ,  $c_{0,\ell}^\theta(0) = \pi^2/2$  for  $\ell \geq 0$  and

$$s_{k,\ell}^\theta(0) = \frac{-(-1)^k \pi}{k}, \quad c_{k,\ell}^\theta(0) = \frac{-1 + (-1)^k}{k^2}.$$

for  $k \geq 1$  and  $\ell \geq 0$ .

---

## A Bendixson–Dulac theorem for some piecewise systems

---

---

### Abstract

The Bendixson–Dulac Theorem provides a criterion to find upper bounds for the number of limit cycles in analytic differential systems. We extend this classical result to some classes of piecewise differential systems. We apply it to three different Liénard piecewise differential systems  $\ddot{x} + f^\pm(x)\dot{x} + x = 0$ . The first is linear, the second is rational and the last corresponds to a particular extension of the cubic van der Pol oscillator. In all cases, the systems present regions in the parameter space with no limit cycles and others having at most one.

## 4.1 Introduction

The study of the number of isolated periodic orbits, the so called *limit cycles*, is a very relevant problem in the qualitative theory of differential equations. This question, known as the 16th Hilbert problem, was proposed by Hilbert in a list of 23 problems in the International Congress of Mathematics in 1900. In his opinion the study of them would motivate advances in mathematics during the 20th century. The 16th Hilbert problem is one of the few that remain open, see [Ily02]. Now, this problem consists in two different questions: The first asks about the relative positions of the branches of real algebraic curves of some degree. The second asks about the existence of an upper bound for the number of limit cycles in planar polynomial vector fields of degree  $n$  besides their relative position. This maximum number depending only on  $n$  is usually known as the Hilbert number  $H(n)$ . There are a lot of published works in relation with this problem. As linear systems have no limit cycles, the most simple case to start with is the quadratic family. But even in this case the problem remains open. The highest value, found in 1980, for this number in quadratic vector fields, which is conjectured that will be the maximum, is  $H(2) \geq 4$ , see [Shi80]. Recently, this problem has been extended also to piecewise differential equations. In this field, denoting it by  $H_p(n)$  when the discontinuity line is a straight line, the best result for the simplest case, found in 2012, says that  $H_p(1) \geq 3$ , see [BPT13, HY12, LP12].

There are few specific families that this problem is totally solved. One of the most useful tools to address this question has been the well-known Bendixson–Dulac Theory. It comes to the end of the 19th century, and it appears in most textbooks on differential equations; see for example [DLA06]. Analogously to Lyapunov functions, the main difficulty in this theory is how the so called Dulac function is obtained for the region where the result applies. The recent work [GG13] presents an interesting extension of the Bendixson–Dulac theory to regions with holes, where the problem of knowing these Dulac functions is translated to control the sign of a polynomial of one variable in a suitable domain. These ideas can be also found in [Che97].

With the same aim that Hilbert, in 1998, Smale proposed a list of mathematical problems for the 21st century, see [Sma98]. He also includes a modern version of 16th Hilbert problem, saying that the computation of the Hilbert number can be notably difficult. So, he suggests to prove it for some special class of differential equations where the finiteness, even the upper bounds, could be simpler. This is the case of the second order polynomial Liénard equation,  $\ddot{x} + f(x)\dot{x} + x = 0$ , that we can write as the planar system

$$\begin{cases} \dot{x} = y - F(x), \\ \dot{y} = -x. \end{cases} \quad (4.1)$$

Here  $F(x) = \int_0^x f(s)ds$  is also a real polynomial. These systems are so relevant because many areas, as biology, chemistry, engineering, . . . , use it for modeling real situations. In particular, they were intensely studied to model oscillating circuits. Some elegant results concerning the existence of limit cycles for Liénard’s equation were obtained by Filippov in

[Fil52]. Bendixson–Dulac theory is a classical approach to provide non existence periodic orbit results. But usually, the most common way to prove uniqueness for these type of equations is the study of the stability of such periodic orbits, via Green’s Theorem. Some results providing conditions for  $F$  assuring that the limit cycle, when it exists, is unique can be found in [ZDHD92]. Only for  $n = 3$  and  $n = 4$  the 16th Hilbert problem for (4.1) is solved, see [LL12, LdMP77]. But in general this is still an open problem.

The study of piecewise differential systems has been extremely effective in helping to understand the behavior of many important physical phenomena such as fluid flows, elastic deformation, nonlinear optical and biological systems, see [dBCK08]. One of the important applications are the impact oscillators that also are to describe by second order differential equations. The aim of this chapter is to present an extension of the classical results of Bendixson and Dulac to some classes of piecewise Liénard systems.

Let 0 be a regular value of a function  $h : \mathbb{R}^2 \rightarrow \mathbb{R}$ . We denote the discontinuity line by  $\Sigma = h^{-1}(0)$  and the two regions by  $\Sigma^\pm = \{\pm h(x, y) > 0\}$ . Thus, we consider the  $\Sigma$ -piecewise differential system

$$Z^\pm = \begin{cases} \dot{x} = X^\pm(x, y), \\ \dot{y} = Y^\pm(x, y), \end{cases} \quad \text{if } (x, y) \in \Sigma^\pm, \quad (4.2)$$

where  $X^\pm$  and  $Y^\pm$  are  $\mathcal{C}^1$  functions in  $\Sigma^\pm$ . Moreover, it is defined on  $\Sigma$  following Filippov’s convention, see [Fil88] and Figure 4.1. That is, the points on  $\Sigma$  where both vectors fields simultaneously point outward or inward from  $\Sigma$  define the *escaping* or *sliding region*. The complement in  $\Sigma$  defines the *crossing region*. In fact, the boundary of the escaping/sliding regions is defined by the tangential points of  $Z^\pm$  in  $\Sigma$ .

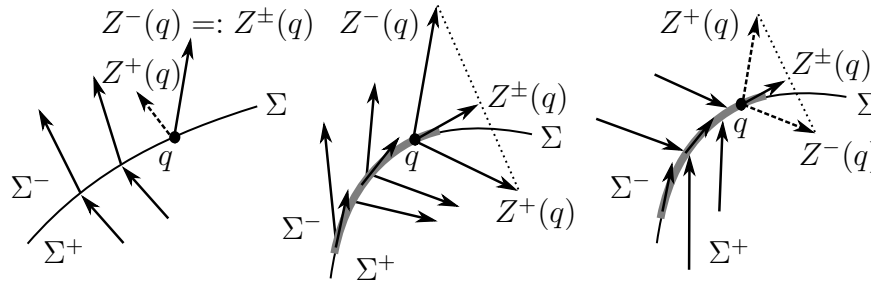


Figure 4.1: Definition of the vector field on  $\Sigma$  following Filippov’s convention in the crossing, escaping, and sliding regions.

In this chapter, we are interested only in the *crossing limit cycles*. They are isolated periodic orbit intersecting the discontinuity line on the crossing region. Moreover, we introduce a class of piecewise differential vector fields. They have the next special property on the discontinuity line  $\Sigma$ .

**Definition 4.1.** We say that (4.2) is a  $\Sigma_P$ -continuous piecewise differential system if it satisfies  $Z^+(q) \cdot \nabla h(q) = Z^-(q) \cdot \nabla h(q)$  for  $q \in \Sigma$ . Where  $\nabla h = (\partial h / \partial x, \partial h / \partial y)$ . See Figure 4.2.

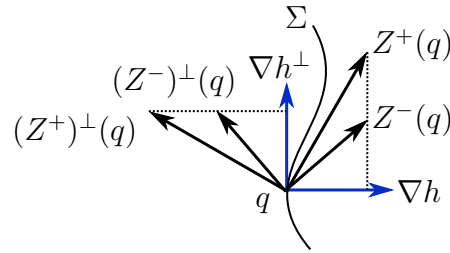


Figure 4.2: The system (4.2), and its orthogonal. Both are  $\Sigma_P$ -continuous piecewise system.

In Section 4.2 we will use such property but with the respective orthogonal vectors fields,  $(Z^+(q) \cdot \nabla h(q))^\perp = (Z^-(q) \cdot \nabla h(q))^\perp$ . Because, sometimes is simpler to check the  $\Sigma_P$ -continuous property with the tangent vector of the discontinuity line. See also Figure 4.2.

The following result provide conditions to bound the number of limit cycles for some piecewise systems (4.2). It will be a generalization of the classical Bendixon–Dulac Theorem to piecewise differential systems.

We say, as in [GG13], that  $S \subset \mathbb{R}^2$  is an  $\ell$ -connected region if its fundamental group,  $\pi_1(S)$ , is  $\mathbb{Z} * \dots * \mathbb{Z}$ , or in other words, if  $S$  has  $\ell$  holes.

**Theorem 4.2.** *Let  $S \subset \mathbb{R}^2$  be an  $\ell$ -connected region with a boundary defined by a finite number of smooth pieces and  $S^\pm = S \cap \Sigma^\pm$ . Consider system (4.2) defined in the region  $S$ ,  $B^\pm : S^\pm \rightarrow \mathbb{R}$  a  $C^1$ -piecewise function, and  $Z_B^\pm$  the  $\Sigma_P$ -continuous piecewise vector field*

$$Z_B^\pm = (B^\pm(x, y)X^\pm(x, y), B^\pm(x, y)Y^\pm(x, y)) \text{ if } (x, y) \in \Sigma^\pm. \quad (4.3)$$

*If  $\operatorname{div}(Z_B^+) \cdot \operatorname{div}(Z_B^-) \geq 0$  and  $(\operatorname{div}(Z_B^+))^2 + (\operatorname{div}(Z_B^-))^2 \neq 0$  in  $S$ , then, system (4.2) has at most  $\ell$  limit cycles in  $S$ . We say that  $B^\pm$  is a  $C^1$ -Dulac piecewise function for system (4.2). Moreover, if  $B^\pm$  is continuous on  $\Sigma$  and  $\operatorname{sgn} B^+ = \operatorname{sgn} B^-$  in  $S$ , then each limit cycle is hyperbolic and its stability is given by the sign of  $B^\pm \cdot \operatorname{div}(Z_B^\pm)$  over it.*

In the following applications of the above theorem, we prove that at most one crossing limit cycle can appear. All of them can be considered in the Liénard class.

**Proposition 4.3.** *Consider, for  $\beta > 0$ , the piecewise differential system*

$$Z^\pm = \begin{cases} \dot{x} = y, \\ \dot{y} = \beta(\alpha^\pm - x) - \lambda^\pm y, \end{cases} \quad (4.4)$$

*defined in  $\Sigma^\pm = \{(x, y) : \pm x > 0\}$ . Then,*

- (a) *when  $\lambda^+ \lambda^- \geq 0$  and  $(\lambda^+)^2 + (\lambda^-)^2 \neq 0$ , system (4.4) has no limit cycles,*
- (b) *when  $\lambda^+ \lambda^- < 0$  and  $(\alpha^+)^2 + (\alpha^-)^2 \neq 0$  then, if  $\alpha^\pm \geq 0$  and  $(\lambda^+)^2 - 4\beta < 0$  or  $\alpha^\pm \leq 0$  and  $(\lambda^-)^2 - 4\beta < 0$ , system (4.4) has at most one limit cycle being*

$$B_1^\pm = (y^2 + \beta(x^2 - 2\alpha^\pm x) + \lambda^\pm xy)^{-1} \quad (4.5)$$

a  $\mathcal{C}^1$ -Dulac piecewise function, otherwise it has no limit cycles. Moreover, when the limit cycle exists it is hyperbolic and stable (resp. unstable) when  $\lambda^+\alpha^+ < 0$  or  $\lambda^+\alpha^- < 0$  (resp.  $\lambda^+\alpha^+ > 0$  or  $\lambda^+\alpha^- > 0$ ).

This problem, taking  $\beta = \varepsilon$  small enough,  $\alpha^+ = \alpha^- = a$ , and  $\lambda^\pm = k^\pm$ , is also considered in [LL17]. The uniqueness of limit cycle follows from the continuity of the piecewise vector field, see [LPT08]. Moreover, a classification of all phase portraits is also obtained. We remark that, our generalized system (4.4) is only  $\Sigma_P$ -continuous and the original proof does not work.

The next application is a piecewise generalization of the classical van der Pol oscillator, which is a dynamical system which includes a non-linear damping term. Under some conditions on the parameters, the Dulac function discovered by Cherkas (see [Che97, Chi06]) can also be used here to prove the uniqueness of limit cycle. We provide also a partial result about the bifurcation diagram of the phase portraits in the Poincaré disk. More details on this theory can be found in [DLA06].

**Proposition 4.4.** *Consider the piecewise system*

$$Z^\pm = \begin{cases} \dot{x} = y, \\ \dot{y} = -x + \lambda^\pm(1 - x^2)y, \end{cases} \quad (4.6)$$

defined in  $\Sigma^\pm = \{(x, y) : \pm x > 0\}$ . Then, when  $\lambda^+\lambda^- \geq 0$  and  $(\lambda^+)^2 + (\lambda^-)^2 \neq 0$ , system (4.6) has exactly one limit cycle, which is hyperbolic and stable (resp. unstable) when  $\lambda^+ + \lambda^- > 0$  (resp.  $\lambda^+ + \lambda^- < 0$ ), with the associated  $\mathcal{C}^1$ -Dulac piecewise function

$$B_2^\pm = (x^2 + y^2 - 1)^{-1/2}. \quad (4.7)$$

Moreover, the phase portraits in the Poincaré disk are topologically conjugated to Figure 4.3 (left) when  $\lambda^+\lambda^- > 0$  or to Figure 4.3 (right) when  $\lambda^+\lambda^- = 0$ , but  $(\lambda^+)^2 + (\lambda^-)^2 \neq 0$ .

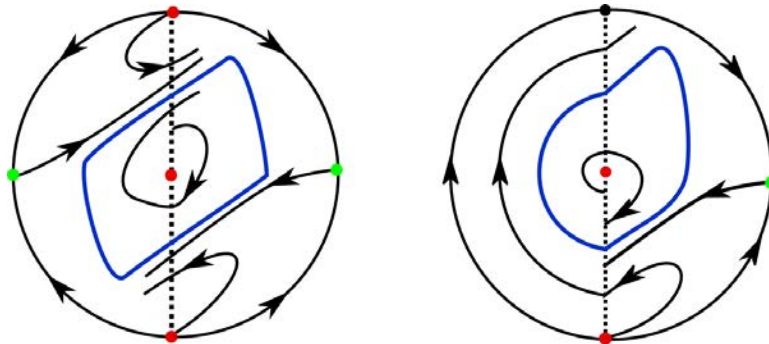


Figure 4.3: Phase portraits in the Poincaré disk for system (4.6)

The next differential system is also written in the classical Liénard form but being  $F$  in (4.1) a rational function instead of a polynomial, as in the previous results. Here we also provide a Dulac function to prove the uniqueness of the limit cycle.

**Proposition 4.5.** *Consider the rational piecewise system*

$$Z^\pm = \begin{cases} \dot{x} = y - \frac{x(x^2 + \lambda^\pm)}{(x \pm 1)^2 + 1}, \\ \dot{y} = -x, \end{cases} \quad (4.8)$$

defined in  $\Sigma^\pm = \{(x, y) : \pm x > 0\}$ . Then, when  $\lambda^\pm < 0$ , system (4.8) has exactly one limit cycle, which is hyperbolic and stable, with the  $\mathcal{C}^1$ -Dulac piecewise function

$$B_3^\pm = \left( y^2 - \frac{(x^2 + \lambda^\pm)}{(x \pm 1)^2 + 1} xy + x^2 \right)^{-1}. \quad (4.9)$$

We remark that, in Proposition 4.4, the function  $B_2^\pm$  is, in fact, a Dulac function if we consider each system (4.6) separately but in the full plane. This is not the case for Propositions 4.3 and 4.5. But both together, each one considered in a different semiplane, define a  $\mathcal{C}^1$ -Dulac piecewise function for systems (4.4) and (4.8), respectively.

This chapter is structured as follows, Section 4.2 is devoted to study the properties such that the Green's Theorem applies for piecewise vector fields and how the stability of a period orbit can be computed, because the classical divergence Theorem does not apply. Consequently, the definition of  $\Sigma_P$ -continuous piecewise differential systems has been necessary to be introduced. Furthermore, we also provide the proof of Theorem 4.2. In the rest of the chapter, we prove the uniqueness of limit cycles for the Liénard families described above. In Section 4.3, we prove the statements of Propositions 4.3 and 4.5. In last Section 4.4, besides proving Proposition 4.4, we study the bifurcation diagram of the phase portraits of system (4.6) in the Poincaré disc.

## 4.2 An extension of the Bendixson–Dulac theory

This section is devoted to the proof of Theorem 4.2, a generalization of the classical Bendixson–Dulac result on the non-existence and uniqueness of periodic orbits for piecewise vector fields. We will use the Green's Theorem on domains with smooth and piecewise smooth boundaries.

We start recalling the Bendixson and Dulac Theorems. See for example the textbooks [Chi06, DLA06].

**Theorem 4.6.** *Let  $Z$  be a  $\mathcal{C}^1$ -planar vector field defined in some open simply connected region  $S \subset \mathbb{R}^2$ , such that*

$$\operatorname{div}(Z)|_S \geq 0 \quad (\text{or } \leq 0)$$

*and vanishing only on a set of zero Lebesgue measure. Then, it has no limit cycles contained in  $S$ .*

**Theorem 4.7.** *Let  $Z$  be a  $\mathcal{C}^1$ -planar vector field defined in some open simply connected region  $S \subset \mathbb{R}^2$ . If there exists a  $\mathcal{C}^1$ -Dulac function  $B : S \rightarrow \mathbb{R}$ , such that*

$$\operatorname{div}(BZ)|_S \geq 0 \quad (\text{or } \leq 0), \quad (4.10)$$

vanishing only on a set of zero Lebesgue measure, then  $Z$  has no limit cycles contained in the region  $S$ .

In the above two results, the cases with null divergence are not considered because the vectors fields are integrable and have no limit cycles. In this special case, the function  $B$  is called an *inverse integrating factor*. Later, we will show that this is not the case in the piecewise world.

The above two results can be extended to  $\ell$ -connected regions. For a proof of the next result see [GG10, GG13].

**Theorem 4.8.** *Let  $Z$  be a  $C^1$ -planar vector field defined in some  $S \subset \mathbb{R}^2$   $\ell$ -connected region. If there exists a  $C^1$ -Dulac function  $B : S \rightarrow \mathbb{R}$  such that in this region it satisfies condition (4.10), then  $Z$  has at most  $\ell$  limit cycles in  $S$ .*

It is well-known that, for planar analytical differential systems, the integral of the divergence along a periodic orbit determines its stability, see [DLA06]. But, for planar piecewise differential systems, this property cannot be used for crossing limit cycles. This is the main difference between these areas of research.

Let  $\gamma = \gamma^+ \cup \gamma^-$  be a crossing periodic orbit passing through  $q^\pm \in \Sigma$ , with  $\gamma^\pm$  two solutions of  $Z^\pm$ . If  $\tau_0, \tau_1 \subset \Sigma$  are transversal sections to  $\gamma$  at  $q^+$  and  $q^-$ , respectively, then the derivative of the Poincaré map at  $q = q^+$  is given by

$$\Pi'(q) = \Gamma(Z^\pm, h) \exp \left( \int_{\gamma^+} \operatorname{div} Z^+ + \int_{\gamma^-} \operatorname{div} Z^- \right), \quad (4.11)$$

where

$$\Gamma(Z^\pm, h) = \frac{Z^+(q^+) \cdot \nabla h(q^+) Z^-(q^-) \cdot \nabla h(q^-)}{Z^-(q^+) \cdot \nabla h(q^+) Z^+(q^-) \cdot \nabla h(q^-)}, \quad (4.12)$$

see [MT15].

As a simple application of the above stability formula, we can check that the system

$$\begin{aligned} Z^+ : (\dot{x}, \dot{y}) &= (-3y^2 + 8y - 4, -1), \\ Z^- : (\dot{x}, \dot{y}) &= (y - a, -x), \end{aligned} \quad (4.13)$$

defined in  $\Sigma^\pm = \{(x, y) \in \mathbb{R}^2 : \pm x \geq 0\}$ , and studied in [BGT18], has a unique stable crossing limit cycle when  $2/3 < a < 1$ . Straightforward computations shows that the limit cycle passes through the points  $q^\pm = (0, \mu^\pm)$  with  $\mu^\pm = a \pm \sqrt{3a^2 + 8a - 4}$  and it can be explicitly written as

$$\begin{cases} x^2 + y^2 - 2ay + 4(a-1)^2 = 0 & \text{for } x < 0, \\ y^3 - 4y^2 - x + 4y + 8(a-2)(a-1)^2 = 0 & \text{for } x > 0. \end{cases}$$

Moreover, system (4.13) has null divergence, but it exhibits an stable limit cycle because,

by (4.11),

$$\Pi'(q) = \Pi'(q^+) = \Gamma(Z^\pm, h) = \frac{3a^2 - 8a + 6 + (3a - 4)\sqrt{3a^2 + 8a - 4}}{2(a - 1)(3a - 5)} < 1.$$

In this chapter, we are interested in  $\Sigma_P$ -continuous piecewise differential systems. They satisfy, by Definition 4.1, that the derivative of the Poincaré map only depends on the integral of the divergence along a crossing periodic orbit. That is,  $\Gamma(Z^\pm, h) = 1$ , see (4.12).

*Proof of Theorem 4.2.* We will only prove the non-existence case and when system (4.2) has at most one limit cycle. The other cases follow similarly.

First, consider  $B^\pm$  a  $\mathcal{C}^1$ -Dulac piecewise function defined in  $S$ , a 0-connected region, see Figure 4.4 left. We will do a proof by contradiction. Assume that  $\gamma^\pm$  is a crossing periodic orbit passing through the points  $q^\pm \in \Sigma$ . We denote by  $L$  the segment between them and by  $A^\pm$  the interior of  $\gamma^\pm$ . So, applying the Green's Theorem to  $(Z_B^\pm)^\perp$  (orthogonal to system (4.3)), we have

$$\int_{L^\pm} (-(BY)^\pm dx + (BX)^\pm dy) = \iint_{A^\pm} \left( \frac{\partial(BX)^\pm}{\partial x} + \frac{\partial(BY)^\pm}{\partial y} \right) dx dy. \quad (4.14)$$

Where the line integral on  $\gamma^\pm$  vanishes, because it is a solution of the vector field  $Z_B^\pm$ . We have denoted by  $L^\pm$  the segment  $L$  such that the boundary path of  $A^\pm$  is clock-wise oriented, see Figure 4.4 right. As  $Z_B^\pm$  is  $\Sigma_P$ -continuous, the integrands of the left hand side of equalities

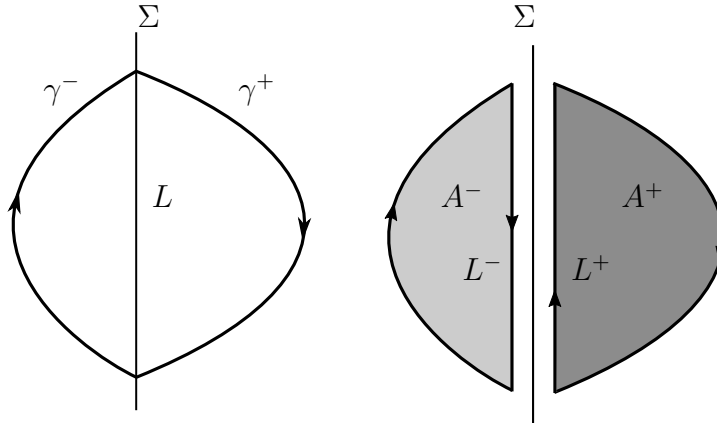


Figure 4.4: The regions and oriented paths chosen to apply Green's Theorem for one crossing periodic orbit.

(4.14) coincide, but  $L^\pm$  have opposite orientation. Hence, adding both equalities, we get

$$0 = \int_{A^+} \operatorname{div}(Z_B^+) dx dy + \int_{A^-} \operatorname{div}(Z_B^-) dx dy.$$

Therefore, by hypotheses on the divergence of  $Z_B^\pm$  we have a contradiction.

Second, we consider the system (4.3) with a  $\mathcal{C}^1$ -Dulac piecewise function  $B^\pm$  defined in the 1-connected region  $S$ . The proof follows by contradiction assuming that there are two crossing periodic orbits,  $\gamma_i^\pm$  for  $i = 1, 2$ , arguing similarly as the previous case, see Figure 4.5 left. The key point is, as above, the selection of a good oriented path defined in the boundary of the annular region  $A^\pm$ . See Figure 4.5 right. Here, the  $\Sigma_P$ -continuity is also necessary in order that the integral over  $L_i^+$  is compensated by the integral over  $L_i^-$ , for  $i = 1, 2$ . We notice that the integral over the other pieces of the boundary vanishes because the curves  $\gamma_i^\pm$  are defined by solutions of the corresponding differential systems.

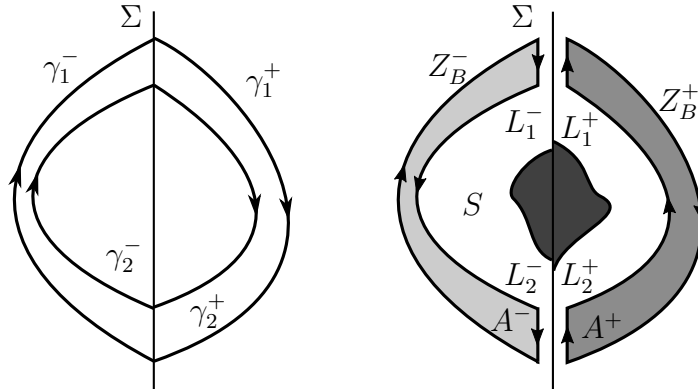


Figure 4.5: The regions and oriented paths chosen to apply Green's Theorem for two crossing periodic orbits.

Finally, we prove the hyperbolicity and stability properties of each limit cycle,  $\gamma^\pm$ , from expression (4.11), showing that the integral of the divergence over it is non zero. This follows from the equality

$$\operatorname{div}(Z^\pm) = \frac{\operatorname{div}(Z_{B^\pm}^\pm)}{B^\pm} - \frac{\frac{\partial B^\pm}{\partial x} X^\pm + \frac{\partial B^\pm}{\partial y} Y^\pm}{B^\pm}$$

and the fact that the second summand, as in [GG13], writes  $\frac{d}{dt}(\log |B^\pm(x(t), y(t))|)$ . It is important to remark that we have used that the functions  $B^\pm$  are continuous on  $\Sigma$ .  $\square$

### 4.3 The linear and rational families

This section is devoted to prove Propositions 4.3 and 4.5. These results study two different piecewise differential systems in the Liénard class. The first, which is a linear, is a generalization of the continuous family introduced in [LL17]. We provide conditions on the parameter space such that the system has no limit cycles or it has at most one. For the second, which the nonlinearities are defined by rational functions, we can prove the existence of a unique limit cycle in a region of the parameter space.

The following technical lemma shows the condition about  $\Sigma_P$ -continuity on piecewise vector fields when the separation line is the  $x$ -axis. The proof is straightforward.

**Lemma 4.9.** *When  $h(x, y) = x$ , the piecewise system (4.2) is  $\Sigma_P$ -continuous if the first component of the associated vector field coincides on both sides, i.e.  $X^+(0, y) = X^-(0, y)$ .*

Next proof is a direct application of Theorem 4.2. Only for the second statement we need to find a  $\mathcal{C}^1$ -Dulac piecewise function.

*Proof of Proposition 4.3.* (a) System (4.4) is defined in  $\mathbb{R}^2$ , that is a simple connected region, and, by Lemma 4.9, it is  $\Sigma_P$ -continuous. The statement follows, applying Theorem 4.2, because the sign of the divergence,  $\text{div}(Z^\pm) = -\lambda^\pm$ , coincides in both regions  $\Sigma^\pm$ .

(b) This statement will be proved in three steps. In the first, we prove that a periodic orbit of (4.4) can not cross the pieces of the curves  $\{\Lambda^\pm(x, y) = 0\} \cap \Sigma^\pm$ , where

$$\Lambda^\pm(x, y) = (B_1(x, y))^{-1} = y^2 + \lambda^\pm xy + \beta(x^2 - 2\alpha^\pm x) \quad (4.15)$$

is defined from (4.5). Because, these curves are without contact with the vector field associated to system (4.4). Then, the regions where the limit cycles can exist are completely determined. In the second, we discuss the different kind of regions defined by the zero level curves  $\{\Lambda^\pm(x, y) = 0\}$ . More concretely, we obtain only 0-connected or 1-connected regions. Finally, the proof finishes applying Theorem 4.2.

It is not restrictive to assume  $\lambda^+ > 0$ ,  $\lambda^- < 0$ ,  $\alpha^+ \geq 0$  and  $\alpha^- > 0$ . Because, the other cases can be moved to it, doing in system (4.4) the next changes of variables: (i)  $(x, y, t) \rightarrow (-x, y, -t)$  when  $\lambda^+ > 0$ ,  $\lambda^- < 0$ ,  $\alpha^+ \leq 0$  (ii)  $(x, y, t) \rightarrow (x, -y, -t)$ , when  $\lambda^+ < 0$ ,  $\lambda^- > 0$ ,  $\alpha^+ \geq 0$ , or (iii)  $(x, y, t) \rightarrow (-x, -y, t)$  when  $\lambda^+ < 0$ ,  $\lambda^- > 0$ ,  $\alpha^+ \leq 0$ .

We notice that, with these sign assumptions, the divergence has different sign in regions  $\Sigma^\pm$ , see Figure 4.6 left.

In the first step, using the notation (4.2) for system (4.4) and considering  $\psi_1^\pm(x) = \lambda^\pm \beta \alpha^\pm x$ , we have that

$$\begin{aligned} \left( \frac{\partial \Lambda^\pm}{\partial x} X^\pm + \frac{\partial \Lambda^\pm}{\partial y} Y^\pm \right) \Big|_{\Lambda^\pm=0} &= \left( \frac{\partial \Lambda^\pm}{\partial x} X^\pm + \frac{\partial \Lambda^\pm}{\partial y} Y^\pm + \lambda^\pm \Lambda^\pm \right) \Big|_{\Lambda^\pm=0} \\ &= (-\lambda^\pm \beta \alpha^\pm x) \Big|_{\Lambda^\pm=0} \leq 0. \end{aligned} \quad (4.16)$$

Because, clearly,  $\psi_1^\pm$  is a nonnegative function, see Figure 4.6 right. Then, the zero level curve  $\{\Lambda^\pm(x, y) = 0\}$  is without contact for the vector field associated to system (4.4), when  $\alpha^+ \neq 0$ , or it contains solutions, when  $\alpha^+ = 0$ . In this last situation we refer the reader to the work [GLV96].

In the second step, we study the draws of the pieces of the conics  $\{\Lambda^\pm(x, y) = 0\}$ , for  $\Lambda^\pm$  in (4.15), when they remain on  $\Sigma^\pm$ .

When  $\alpha^+ > 0$ , the zero level curve of  $\Lambda^+$ , is a nondegenerate conic: a hyperbola ( $(\lambda^+)^2 - 4\beta > 0$ ), a parabola ( $(\lambda^+)^2 - 4\beta = 0$ ) or an ellipse ( $(\lambda^+)^2 - 4\beta < 0$ ). Moreover, it has a branch passing through the origin as  $2\alpha^+ \beta x - y^2 + \mathcal{O}(y^3) = 0$  and another at the point  $(2\alpha^+, 0)$ . When  $\alpha^+ = 0$ , the conic degenerates to two straight lines ( $(\lambda^+)^2 - 4\beta > 0$ ), to a double straight line ( $(\lambda^+)^2 - 4\beta = 0$ ) or to a point ( $(\lambda^+)^2 - 4\beta < 0$ ). Additionally, the origin

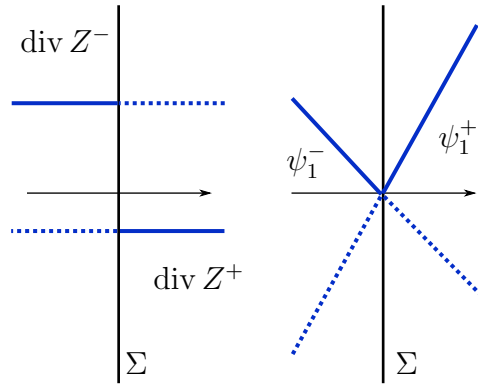


Figure 4.6: Plots of the sign of the divergence of system (4.4) (left) and the function  $\psi_1^\pm(x)$  (right) which appear in  $\text{div}(Z_{B_1}^\pm)$ .

is the unique intersection point with the coordinates axis. Finally, when  $(\lambda^+)^2 - 4\beta \geq 0$ , as  $-\lambda^+ \pm \sqrt{(\lambda^+)^2 - 4\beta} < 0$ , because  $\lambda^+ > 0$ , the branches of the conic arrive to infinity in the second or fourth quadrant. Consequently, all the possible the zero level curves are depicted in Figure 4.7 (right). The zero level curves of  $\Lambda^-$ , can be drawn, doing a symmetry with respect to the  $x$ -axis, from the previous study, because  $\lambda^- < 0$ , instead of  $\lambda^+ > 0$ . See Figure 4.7 (left).

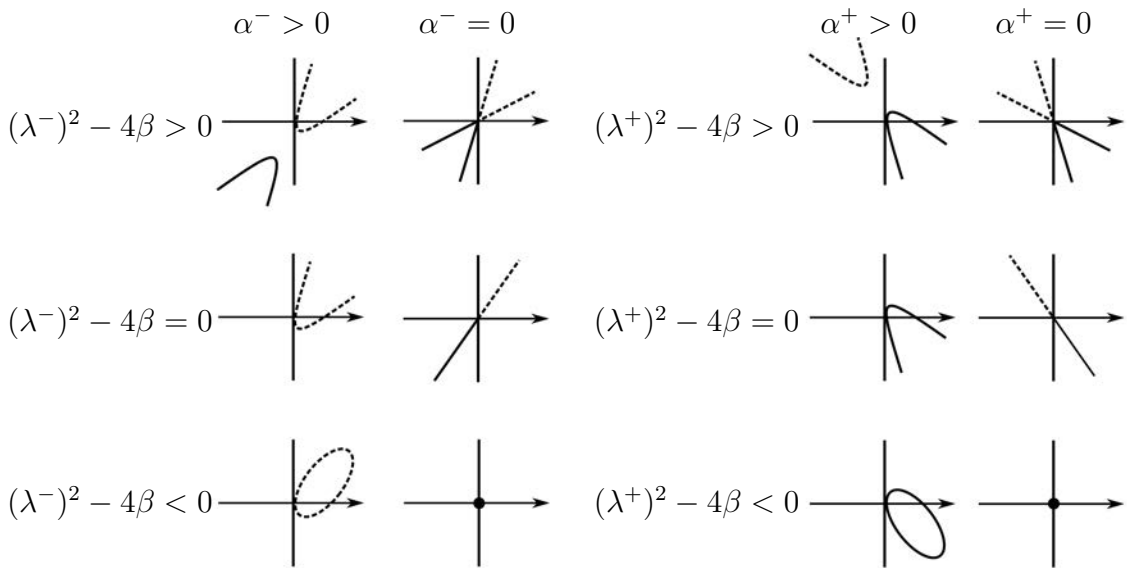


Figure 4.7: The sets, for  $\lambda^- < 0$  and  $\lambda^+ > 0$ , where the piecewise Dulac function (4.5) is not well defined. The branches are depicted in continuous (visible) and dashed (invisible) lines in the respective  $\Sigma^\pm$  zones.

So, we can see, doing a case by case study, that  $\mathbb{R}^2 \setminus ((\{\Lambda^- = 0\} \cap \Sigma^-) \cup (\{\Lambda^+ = 0\} \cap \Sigma^+))$  is formed only by 0-connected or 1-connected regions. In fact, only when  $(\lambda^+)^2 - 4\beta < 0$  we have 1-connected regions.

The last step follows directly computing, using (4.16),  $\operatorname{div}(Z_{B_1}^\pm) = \psi_1^\pm(x) B_1^\pm(x, y)^2$  and using the without contact property together with Theorem 4.2.

We only illustrate two different situations:

- When  $\lambda^- = -1$ ,  $\lambda^+ = 2$ ,  $\alpha^+ = 2$ ,  $\alpha^- = 1$ , and  $\beta = 1/2$ , the zero level curve  $\{\Lambda^- = 0\}$  is an ellipse (totally contained in  $\Sigma^+$ ) and  $\{\Lambda^+ = 0\}$  is a hyperbola. Hence the set  $\{\Lambda^- = 0\} \cap \Sigma^-$  is empty and the set  $\{\Lambda^+ = 0\} \cap \Sigma^+$  is a branch of the hyperbola. See the drawing in Figure 4.8 (left). Clearly, the region  $\mathbb{R}^2 \setminus ((\{\Lambda^- = 0\} \cap \Sigma^-) \cup (\{\Lambda^+ = 0\} \cap \Sigma^+))$  is defined by only two 0-connected regions. Hence we have no limit cycles.

- When  $\lambda^- = -2$ ,  $\lambda^+ = 1/8$ ,  $\alpha^\pm = 1$ , and  $\beta = 1/10$ , the zero level curve  $\{\Lambda^- = 0\}$  is a hyperbola and  $\{\Lambda^+ = 0\}$  is an ellipse. See the drawing in Figure 4.8 (right). So, the region  $\mathbb{R}^2 \setminus ((\{\Lambda^- = 0\} \cap \Sigma^-) \cup (\{\Lambda^+ = 0\} \cap \Sigma^+))$  is defined by three regions, two 0-connected and one 1-connected. Hence, we have at most one limit cycle. The existence, for these values of the parameters, is proved in [LL17].

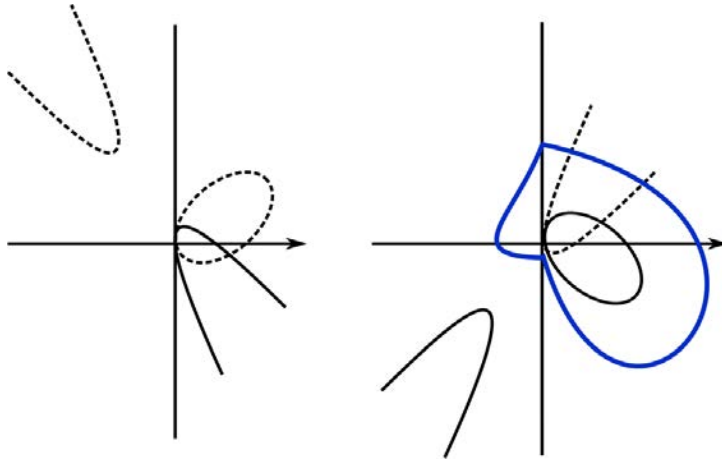


Figure 4.8: Two different situations for system (4.4) with only 0-connected regions (left) or having a 1-connected one (right).

Finally, as the function  $B_1^\pm$  is continuous over  $\Sigma$ , with the sign assumptions for  $\alpha^\pm$  and  $\lambda^\pm$ , Theorem 4.2 proves the hyperbolicity and unstability properties.  $\square$

Before the proof of Proposition 4.5, we show the unstability of the origin and infinity of system (4.8).

**Proposition 4.10.** *Let system (4.8). If  $\lambda^\pm < 0$ , then the origin is the unique singular point which is unstable. Moreover, also the infinity is unstable. So system (4.8) has at least a limit cycle.*

*Proof.* The origin is the unique equilibrium point of systems (4.8) when they are considered in the full  $\mathbb{R}^2$ . In fact, for both, it is unstable because the eigenvalues of the differential matrices at the origin,  $(-\lambda \pm \sqrt{\lambda^2 - 16})/4$  for  $\lambda = \lambda^\pm$ , have positive real parts. See more details on the stability of equilibrium points in piecewise differential systems in [LT14].

The stability of infinity can be studied with the change of variables defined in a neighborhood of the infinity but not on it:  $(x, y) = (R^{-1} \cos \theta, R^{-1} \sin \theta)$ . Then, the derivatives  $\dot{R}$  and  $\dot{\theta}$  are trigonometric rational functions having the same denominator  $(\cos \theta + R)^2 + R^2$ . Which is always positive in our domain,  $R > 0$ . Then, the linear part of system (4.8) becomes  $dR/d\theta = h(\theta)R$  with  $h(\theta) = \cos^2 \theta / (\cos \theta \sin \theta - 1)$ . Notice that it is the same in both sides  $\Sigma^\pm$ , and does not depend on the parameters. As  $R(\theta)$  is a decreasing function, because  $-4/3 \leq h(\theta) \leq 0$ , for any the initial condition  $R(\pi/2) = \rho$  we have  $R(-3\pi/2) > \rho > R(-\pi/2)$ . Consequently, for both equations and also for the system considered in  $\Sigma^\pm$ , the origin is an attracting focus. Hence, recovering the original variables, the infinity is unstable.  $\square$

With the above technical results we can proof the existence of exactly one limit cycle for our rational Liénard family.

*Proof of Proposition 4.5.* Under the conditions of the statement, Proposition 4.10 guaranties the existence of a limit cycle. Only remains to prove that this limit cycle is unique. This is proved checking the hypotheses of Theorem 4.2 for system (4.8) when  $\lambda^\pm < 0$ , following the same procedure as the proof of Proposition 4.3(b). Hence, as the periodic orbits of (4.8) can not cross the pieces of the curves  $\{\Lambda^\pm(x, y) = 0\} \cap \Sigma^\pm$ , we only check that this set defines a 1-connected region and  $\text{div}(Z_{B_3}^\pm)$  have the same sign in  $\Sigma^\pm$ . Here

$$\Lambda^\pm(x, y) = (B_3^\pm(x, y))^{-1} = y^2 - \frac{(x^2 + \lambda^\pm)}{(x \pm 1)^2 + 1} xy + x^2, \quad (4.17)$$

is defined from (4.9).

Straightforward computations show that the divergence

$$\text{div}(Z^\pm) = \frac{-x^4 \mp 4x^3 + (\lambda^\pm - 6)x^2 - 2\lambda^\pm}{((x \pm 1)^2 + 1)^2}$$

is a rational function on  $x$  that changes sign. Because the numerators, using the Descartes rule, have exactly one positive and one negative zeros.

In the first step, we compute

$$\text{div}(Z_{B_3}^\pm) = \psi_3^\pm(x) B_3^\pm(x, y)^2,$$

with  $\psi_3^\pm(x) = 2x^3 \varphi^\pm(x) / ((x \pm 1)^2 + 1)^2$  and  $\varphi^\pm(x) = \mp x^2 + (\lambda^\pm - 2)x \pm \lambda^\pm$ . Clearly,  $x\varphi^+(x) < 0$  for  $x > 0$  because the leading coefficient of  $\varphi^+$  and the values  $\varphi^+(0)$  and  $(\varphi^+)'(0)$  are negative. Similarly,  $x\varphi^-(x) < 0$  for  $x < 0$ . Hence,  $\text{div}(Z_{B_3}^\pm) < 0$  in  $\Sigma^\pm$  and it vanishes only on  $x = 0$ . As the functions  $B_3^\pm$

In the second step, we study the piecewise curves  $\{\Lambda^\pm(x, y) = 0\} \cap \Sigma^\pm$ . We only depict the zero level curve of  $\Lambda^+$ , in (4.17), the other can be obtained with the symmetric change  $(x, y) \rightarrow (-x, -y)$ , because  $\Lambda^-(x, y) = \Lambda^+(-x, -y)$ . We remark that this curve passes through the origin. We draw it from the plots of the two functions, obtained solving it as a

quadratic polynomial in  $y$ ,

$$\eta_{\pm}(\lambda^+) = \frac{x(x^2 + \lambda^+ \pm \sqrt{\Delta(x, \lambda^+)})}{2((x + 1)^2 + 1)},$$

with

$$\Delta(x, \lambda^+) = -(3x^2 + 4x + \lambda^+ + 4)((x + 2)^2 - \lambda^+).$$

As  $\lambda^+ < 0$ , the function  $\Delta(x, \lambda^+)$  is always negative when  $-8/3 < \lambda^+ < 0$  and it is positive for  $x \in ((-2 - \sqrt{-8 - 3\lambda^+})/3, (-2 + \sqrt{-8 - 3\lambda^+})/3)$  when  $\lambda^+ < -8/3$ . The graphics of  $\eta_{\pm}$  remain in  $\Sigma^+$  only when  $-2 + \sqrt{-8 - 3\lambda^+}$  is positive, that is, when  $\lambda^+ < -4$ . Consequently, the level curve  $\{\Lambda^+(x, y) = 0\}$  intersects  $\Sigma^+$  only at the origin when  $\lambda^+ \in [-4, 0)$  and at a curve topologically equivalent to a circle when  $\lambda^+ < -4$ . The different draws of such situations can be seen in Figure 4.9 varying the value of  $\lambda^+$ .

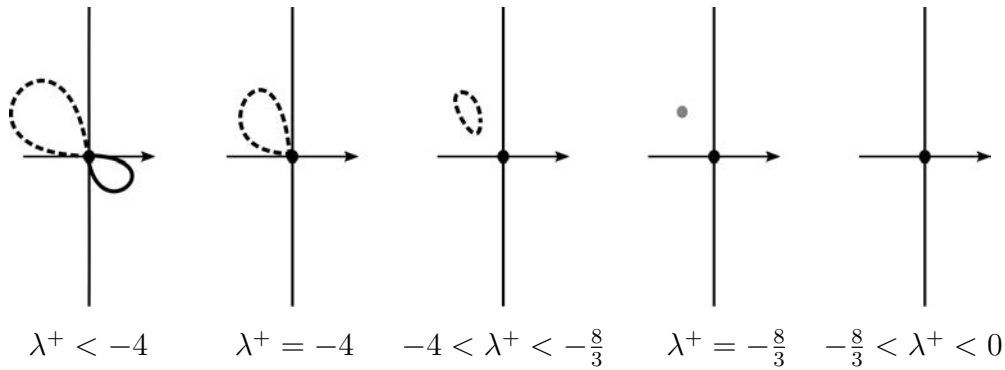


Figure 4.9: The zero level curve of  $\Lambda^+$  in (4.17). The points in  $\Sigma^+$  ( $\Sigma^-$ ) are depicted in continuous (dashed) line.

Finally, a case by case study, using the symmetry of the functions  $\Lambda^{\pm}$  and the pictures in Figure 4.9, proves that all possible draws for the piecewise curves  $\{\Lambda^{\pm}(x, y) = 0\} \cap \Sigma^{\pm}$  define 1-connected regions. See Figure 4.10.

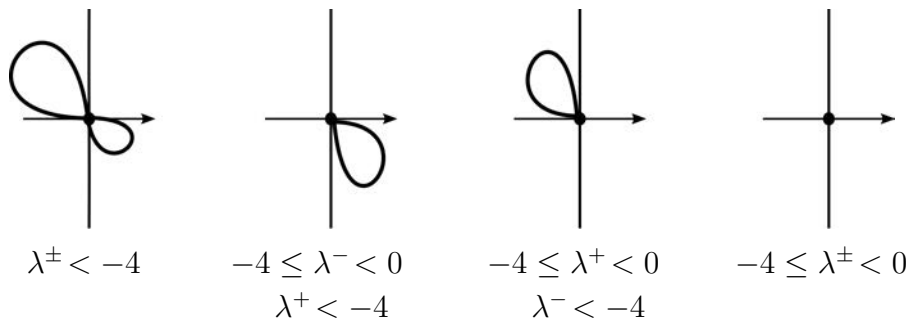


Figure 4.10: The 1-connected regions defined by the zero level curve of  $\Lambda^{\pm}$  in (4.17).

□

## 4.4 A piecewise version of the classical van der Pol oscillator

The main result of this section is stated in Proposition 4.4. It only provides a partial bifurcation diagram of the phase portrait of system (4.6). A complete study depends on the proof of the existence of a bifurcation curve,  $\Upsilon$ , where the phase portrait exhibits a connection between two equilibrium points at infinity. This connection defines a heteroclinic cycle having two semihyperbolic saddles together with a degenerated equilibrium point. These degeneracies make the problem very difficult to be studied. All the results and numerical simulations done in this section are summarized in Figure 4.11. The phase portraits are done in the Poincaré disk for each vector field, see [DLA06].

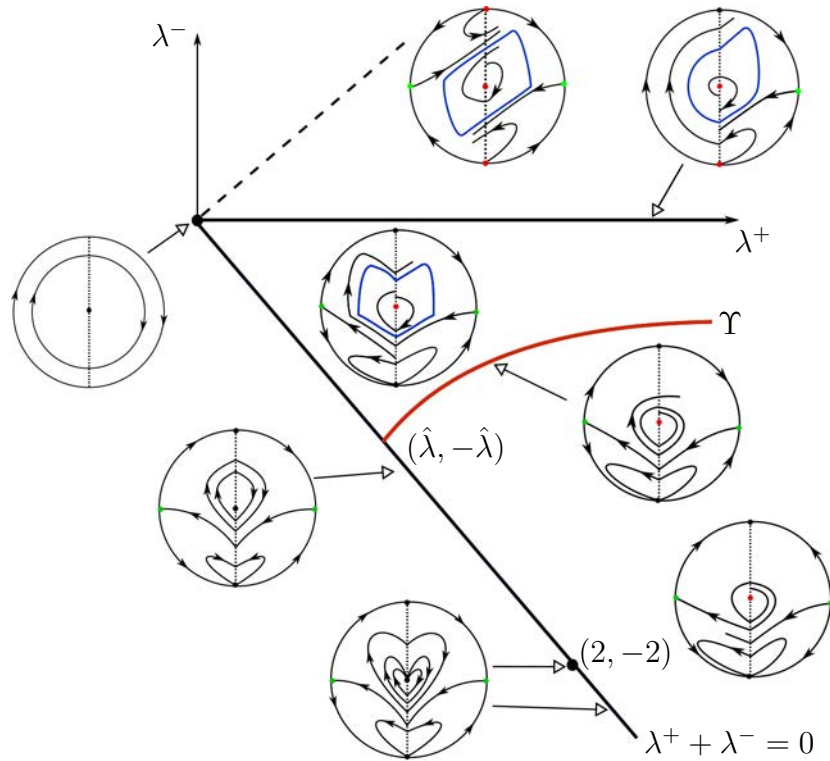


Figure 4.11: Portrait bifurcation of system (4.6).

For simplicity, all the results of this section are written for values  $(\lambda^+, \lambda^-)$  satisfying  $\lambda^+ \geq 0$  and  $-\lambda^+ \leq \lambda^- \leq \lambda^+$ . With the symmetries given in Lemma 4.11 we can cover the full space of parameters. The local phase portrait of the equilibrium points at infinity is done in Lemma 4.12. System (4.6) has only one finite equilibrium point and its stability is given in Lemma 4.13. From all these technical results we can present the proof of the uniqueness of the limit cycle together with the global phase portraits provided by Proposition 4.4. This proves the bifurcation diagram depicted in Figure 4.11 in the region  $\lambda^+ \lambda^- \geq 0$ . By a continuity argument this limit cycle remains near the positive  $\lambda^+$ -axis. This is done in Corollary 4.14. Proposition 4.15 proves the bifurcation diagram when system (4.6) has a center, that is, over the straight line  $\lambda^+ + \lambda^- = 0$ .

The difficulties described above to complete the bifurcation diagram (for  $\lambda^- < 0$ ) are illustrated in Proposition 4.16. This result together with Corollary 4.14 prove, by continuity, Corollary 4.17, which states the existence of at least one point  $(\lambda^+, \lambda^-)$  where the connection exists. Finally, we do some numerical simulations to present what we think that will be the complete bifurcation diagram of system (4.6) in this zone of the parameters. See also Figure 4.11.

**Lemma 4.11.** *System (4.6) is invariant by the following changes of variables:*

$$(a) (x, y, t, \lambda^-, \lambda^+) \rightarrow (-x, -y, t, \lambda^+, \lambda^-).$$

$$(b) (x, y, t, \lambda^-, \lambda^+) \rightarrow (-x, y, -t, -\lambda^+, -\lambda^-).$$

$$(c) (x, y, t, \lambda^-, \lambda^+) \rightarrow (x, -y, -t, -\lambda^-, -\lambda^+).$$

Consequently, we can restrict our analysis to  $\lambda^+ > 0$  and  $-\lambda^+ \leq \lambda^- \leq \lambda^+$ .

*Proof.* The statement follows because, in the parameter space  $(\lambda^-, \lambda^+) \in \mathbb{R}^2$ , the points in the second and third quadrant move with the change (b) to the fourth and first, respectively. Moreover, changes (a) and (c) provides an extra symmetry with respect to the bisectors of the first and fourth quadrants, respectively.  $\square$

**Lemma 4.12.** *Let  $\lambda^+ > 0$ . Then, for  $\lambda^- \in [-\lambda^+, \lambda^+]$ , there are only three topologically conjugated local phase portraits of system (4.6) in a neighborhood of infinity. They are depicted in Figure 4.12.*

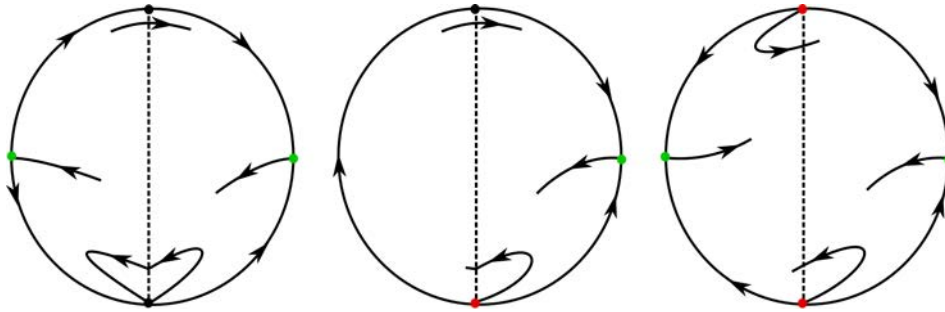


Figure 4.12: Local phase portraits of system (4.6) near the infinity when  $\lambda^+ > 0$  and  $\lambda^- < 0$  (left),  $\lambda^- = 0$  (middle), and  $\lambda^- > 0$  (right).

*Proof.* (a) We start with the local study in the charts  $\mathcal{U}_1$  and  $\mathcal{V}_1$ . We study both systems, for  $\lambda^+$  and  $\lambda^-$ , simultaneously denoting the parameter by  $\lambda$ , when they are non vanishing. With the change  $(x, y, t) = (1/v, u/v, v^2\tau)$ , system (4.6), considered in full space, is transformed to

$$\begin{cases} u' = -\lambda u + A(u, v), \\ v' = B(u, v), \end{cases} \quad (4.18)$$

where  $A(u, v) = \lambda uv^2 - u^2v^2 - v^2$ ,  $B(u, v) = -v^3u$ , and prime denotes the derivative respect to  $\tau$ . This system has a unique equilibrium point at the origin which is a semihyperbolic saddle. Because, by Theorem 2.19 in [DLA06], the solution  $u(v) = -v^2/\lambda - v^4/\lambda + \mathcal{O}(v^6)$  of  $-\lambda u + A(u, v) = 0$  gets  $B(u(v), v) = -v^5/\lambda + \mathcal{O}(v^7)$ . The local phase portraits depend on the sign of  $\lambda$ , see Figure 4.13.

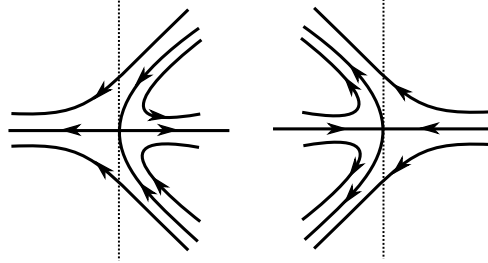


Figure 4.13: The local phase portrait of the origin of system (4.18) for  $\lambda < 0$  (left) and  $\lambda > 0$  (right).

Then, in the chart  $\mathcal{U}_1$ , as  $\lambda^+$  is positive, we have always the local phase portrait as in Figure 4.13 (right). The local phase portraits, in the chart  $\mathcal{V}_1$ , depend on the sign of  $\lambda^-$ . Being as in Figure 4.13 (left) or Figure 4.13 (right) for  $\lambda^- < 0$  or  $\lambda^- > 0$ .

For the remaining case,  $\lambda^- = 0$ , the system (4.6) has a global linear center at the origin. Then, the change to chart  $\mathcal{V}_1$  is not necessary to be done.

With all the above properties, we obtain the local phase portraits depicted in Figure 4.12.

(b) As above, we study both systems simultaneously using  $\lambda$  instead of  $\lambda^+$  or  $\lambda^-$ .

By using the transformation  $(x, y, t) = (u/v, 1/v, v^2\tau)$  system (4.6) is transformed into the system

$$\begin{cases} u' = \lambda(u^3 - uv^2) + v^2 + u^2v^2, \\ v' = v(\lambda(u^2 - v^2) + uv^2), \end{cases} \quad (4.19)$$

where the prime denotes the derivative respect to  $\tau$ . It is easy to check that this system has a unique degenerated equilibrium point at the origin. As it is a nonelementary singularity, we will need some directional blow-ups to prove that it is an attracting ( $\lambda < 0$ ) or a repelling ( $\lambda > 0$ ) node, see Figure 4.14. This is necessary because the differential matrix of (4.19) at the origin vanishes identically. More details about how the local phase portraits of such degenerated equilibrium points can be also found in [DLA06]. As system (4.19) is invariant by the change  $(u, v, t, \lambda) \rightarrow (-u, v, -t, -\lambda)$ , we can restrict our study to  $\lambda > 0$ .

With the weighted blow-up  $(u, v) \rightarrow (u, pu^2)$  and rescaling time (dividing by  $u^2$ ), system (4.19) becomes

$$\begin{cases} u' = \lambda u + u^2p^2(1 - \lambda u + u^2), \\ p' = -\lambda p + up^3(-2 + \lambda u - u^2). \end{cases} \quad (4.20)$$

This system has a unique equilibrium point, which is a saddle. The local phase portrait is given in Figure 4.15 (left).

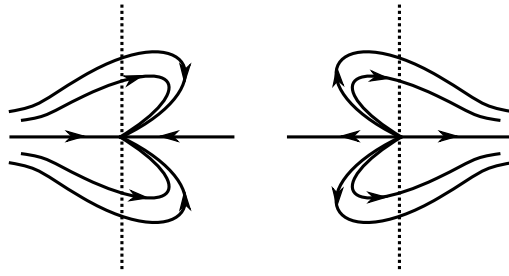


Figure 4.14: The local phase portrait of the origin of system (4.19) for  $\lambda < 0$  (left) or  $\lambda > 0$  (right).

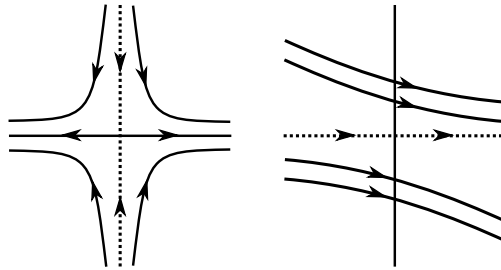


Figure 4.15: The local phase portrait of the origin of systems (4.20) and (4.21) for  $\lambda > 0$ , respectively.

With the blow-up  $(u, v) \rightarrow (qv, v)$  and rescaling time (dividing by  $v$ ) the system (4.19) becomes

$$\begin{cases} q' = 1, \\ v' = v^2(-\lambda + qv + \lambda q^2). \end{cases} \quad (4.21)$$

Which has no singular points. The local phase portrait is given in Figure 4.15 (right). Finally, combining both local figures and using that  $v = 0$  is also a solution and it is the unique that leaves the origin, we can conclude that the origin of system (4.19) is a repelling node. The conclusion for  $\lambda < 0$  follows from the above commented symmetry. The solutions are depicted in Figure 4.14.  $\square$

**Lemma 4.13.** *The bifurcation diagram of the topologically different local phase portraits near the origin of system (4.6), when  $\lambda^+ \geq 0$  and  $-\lambda^+ \leq \lambda^- \leq \lambda^+$ , is depicted in Figure 4.16. Moreover, when  $\lambda^+ > 0$  and  $\max(-2, -\lambda^+) \leq \lambda^- \leq \lambda^+$  the origin is unstable.*

*Proof.* We do a case by case study depending on the eigenvalues of the Jacobian matrices of each system  $Z^\pm$  in (4.6) at the origin. They are

$$\frac{\lambda \pm \sqrt{\lambda^2 - 4}}{2},$$

for  $\lambda = \lambda^+$  and  $\lambda = \lambda^-$ . All cases finish gluing both local pictures in  $Z^\pm$ .

(a) When  $\lambda^\pm = 0$  we have the same global linear center at the origin.

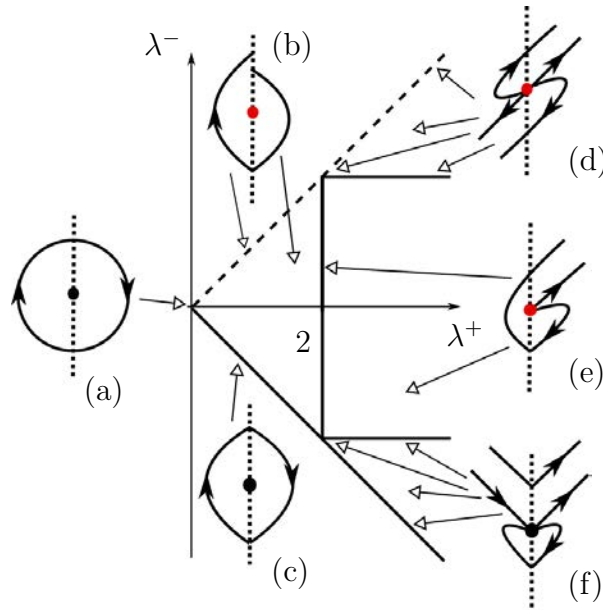


Figure 4.16: The different kinds of equilibrium points in the origin for the system (4.6).

(b) When  $0 < \lambda^+ < 2$  and  $-\lambda^+ < \lambda^- \leq \lambda^+$  we have foci in  $Z^\pm$ . Then, as the singularities are of monodromic type we need to compute the first coefficient of the return map. That is, the first Lyapunov constant. From [CGP01], it is

$$L_1 = \exp\left(\frac{(\lambda^+ + \lambda^-)\pi}{\sqrt{4 - (\lambda^+)^2}\sqrt{4 - (\lambda^-)^2}}\right) - 1.$$

Then, when  $\lambda^+ + \lambda^- > 0$  the origin is a unstable focus.

(c) When  $0 < \lambda^+ < 2$  and  $\lambda^+ + \lambda^- = 0$ , as in the previous case, the origin is a monodromic point. Then, it is center because the system is symmetric with respect to  $x = 0$ . That is, is reversible, or it remains unchanged with respect to the change  $(x, y, t) \rightarrow (-x, y, -t)$ .

(d) When  $2 \leq \lambda^+$  and  $-2 < \lambda^- < 2$ , system  $Z^-$  has a focus at the origin and system  $Z^+$  has a repelling node with both eigenvectors having positive slopes  $(1, (\lambda^+ \pm \sqrt{(\lambda^+)^2 - 4})/2)$ . Then, the origin is an unstable node.

(e) When  $2 \leq \lambda^+$  and  $2 \leq \lambda^- \leq \lambda^+$ , both systems  $Z^\pm$  have repelling nodes at the origin with eigenvectors having positive slopes  $(1, (\lambda^+ \pm \sqrt{(\lambda^+)^2 - 4})/2)$  and  $(1, (\lambda^- \pm \sqrt{(\lambda^-)^2 - 4})/2)$ . Then, the origin is also unstable.

(f) When  $2 \leq \lambda^+$  and  $-\lambda^+ \leq \lambda^- \leq -2$ , system  $Z^+$  (resp.  $Z^-$ ) has a repelling (resp. attracting) node at the origin with eigenvectors having positive (resp. negative) slopes  $(1, (\lambda^+ \pm \sqrt{(\lambda^+)^2 - 4})/2)$  (resp.  $(1, (\lambda^- \pm \sqrt{(\lambda^-)^2 - 4})/2)$ ). Then, we have a point having one hyperbolic and one elliptic sectors.  $\square$

The above two technical lemmas together with the main result of generalization of the Bendixson–Dulac Theorem allow us to proof the main result of this section.

*Proof of Proposition 4.4.* Firstly, as we have commented in the introduction of this section and using Lemma 4.11, we can restrict our proof to values satisfying  $\lambda^+ > 0$ ,  $\lambda^- \geq 0$ . Under these assumptions, the existence of at least one limit cycle follows from the stability of infinity and origin, because both are unstable. See Lemmas 4.12 and 4.13. This follows by the generalization of the Poincaré–Bendixson’s Theorem to piecewise vector fields in  $\mathbb{R}^2$ . See [BCE18].

Secondly, we prove the uniqueness of such periodic orbit. As  $\operatorname{div} Z^\pm$  is positive in the region  $S = \{-1 < x < 1\}$ , from Theorem 4.2, the limit cycles can not be completely contained in  $S$ . In fact, they should contain the 1-connected region defined by the unit circle. Because, as in the proofs of Propositions 4.3 or 4.5, the periodic orbit of (4.4) can not cross the pieces of the curves  $\{\Lambda(x, y) = 0\} \cap \Sigma^\pm$ , where

$$\Lambda^\pm(x, y) = (B_2^\pm(x, y))^{-2} = x^2 + y^2 - 1$$

is defined from (4.7). We point out that they are without contact with the vector field associated to system (4.6). Moreover,  $\operatorname{div}(Z_{B_2}^\pm)$  is negative when  $x^2 + y^2 > 1$ . Then, using also Theorem 4.2, the limit cycle is unique. Moreover, as  $B_2^\pm$  is continuous, it is hyperbolic and stable.

All the global phase portraits in the Poincaré disk given in the statement, follow studying all the possible  $\alpha$  and  $\omega$  limit sets using the generalization of the Poincaré–Bendixson’s Theorem. This is done combining the local phase portrait of the infinity and origin in Lemmas 4.12 and 4.13, and, finally, the uniqueness of the periodic orbit proved above.  $\square$

Next result provides the existence of a limit cycle near the  $\lambda^+$ -axis.

**Corollary 4.14.** *For each  $\lambda^+ > 0$ , there exists  $\varepsilon > 0$  small enough such that system (4.6), for  $\max(-\lambda^+, -\varepsilon) < \lambda^- < 0$ , has at least one limit cycle, which is stable. Moreover, the phase portraits in the Poincaré disk is shown in Figure 4.17, when the limit cycle is unique.*

*Proof.* For the conditions given in the statement, Lemma 4.13 provides the unstability of the origin. For  $\lambda^- = 0$ , from Proposition 4.4, the  $\omega$  limit set of the separatrix of the saddle at infinity for  $Z^+$  is the stable limit cycle. Using the behavior of infinity, for  $\lambda^- < 0$  small enough, given in Lemma 4.12, a continuity argument guaranties the existence of at least a periodic orbit.  $\square$

The values of  $(\lambda^+, \lambda^-)$  where system (4.6) exhibits a center is done in the following result.

**Proposition 4.15.** *When  $\lambda^+ \geq 0$  and  $\lambda^+ + \lambda^- = 0$  system (4.6) has a time-reversible center with respect to the  $y$ -axis. More concretely, when  $\lambda^+ = 0$  it has a global linear center, when  $0 < \lambda^+ < 2$  the inner boundary is the origin which is monodromic, and when  $2 \leq \lambda^+$  the inner boundary is a degenerated equilibrium point having one hyperbolic and one elliptic sectors. Moreover, when  $\lambda^+ \neq 0$  there is a finite solution connecting two saddles at infinity that defines the finite part of the outer boundary. See the respective phase portraits in Figure 4.18.*

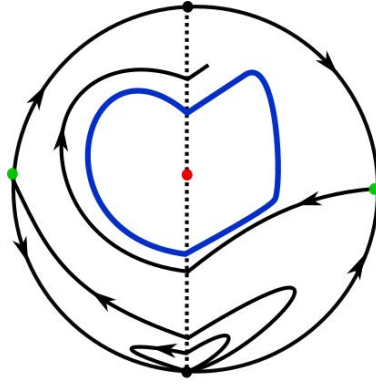


Figure 4.17: Phase portrait of system (4.6) for  $\lambda^+ > 0$  and small enough  $\lambda^- < 0$  if the limit cycle is unique.

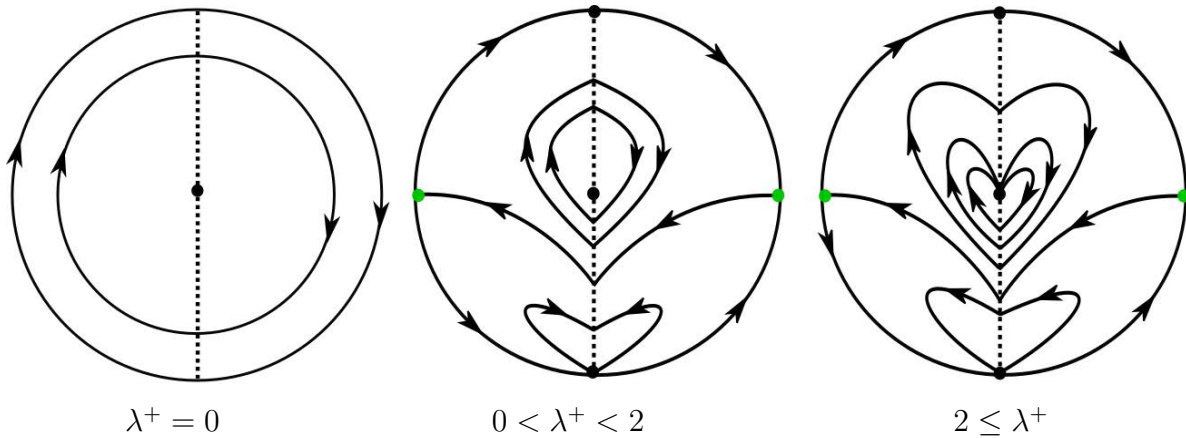


Figure 4.18: Phase portrait of system (4.6)  $\lambda^+ + \lambda^- = 0$ .

*Proof.* The time-reversibility property follows from the condition  $\lambda^+ + \lambda^- = 0$  applying the change  $(x, y, t) \rightarrow (-x, y, -t)$ . Lemma 4.13 provides the local phase portraits of the origin. When  $\lambda^+ = 0$  the local center at the origin is global because in both sides we have the same system. When  $0 < \lambda^+ < 2$  the origin is also a local center, see Figure 4.16(c) but when  $2 \leq \lambda^+$  the origin is a degenerate singularity with one hyperbolic and one elliptic sectors, see Figure 4.16(f). Adding the local phase portrait at infinity, see Figure 4.12 (left), the global picture follows, using the reversibility property, showing that the unstable separatrix of the saddle at infinity of  $Z^+$  crosses the negative  $y$ -axis. See Figure 4.18. In both cases, using Poincaré–Bendixson theorem in the Poincaré disk for piecewise vector fields, see [BCE18], from the sign of the components of the vector field associated to system (4.6) and looking at infinity, any solution starting at a point on the positive  $y$ -axis should arrive to the negative  $y$ -axis crossing the positive  $x$ -axis. Then, also the unstable separatrix should do the same. From the pictures is clear that this separatrix defines a piece of the outer boundary.  $\square$

**Proposition 4.16.** Consider system (4.6) with  $\lambda^+ = 6$  and  $\lambda^- = -4$ . Let  $\Gamma^\pm$  be the pieces of curves defined by the solutions corresponding to the unstable (resp. stable) separatrix of the origin of chart  $\mathcal{U}_1$  (resp.  $\mathcal{V}_1$ ) up to the first intersection with the  $x$ -axis. Then  $\Gamma^- \cap \{x \leq 0\} \subset \{y - \Phi^-(x) > 0\}$  and  $\Gamma^+ \cap \{x \geq 0\} \subset \{y - \Phi^+(x) < 0\}$ , see Figure 4.19. Where

$$\Phi^-(x) = \begin{cases} \Phi_1^-(x) & \text{for } -\frac{11}{10} \leq x \leq 0, \\ \Phi_2^-(x) & \text{for } x \leq -\frac{11}{10}, \end{cases} \quad \Phi^+(x) = \begin{cases} \Phi_1^+(x) & \text{for } 0 \leq x \leq \frac{6}{5}, \\ \Phi_2^+(x) & \text{for } \frac{6}{5} \leq x < \infty, \end{cases}$$

with

$$\begin{aligned} \Phi_1^-(x) &= -\frac{173007133315}{285311670611} - \frac{67406738275}{69202853326} \left(x + \frac{11}{10}\right) \\ &\quad - \frac{702087707035846036257168105708375}{331414880343242169114421852929976} \left(x + \frac{11}{10}\right)^2, \\ \Phi_2^-(x) &= \frac{1}{4x} + \frac{1}{4x^3} + \frac{15}{64x^5} + \frac{11}{64x^7} + \frac{19}{512x^9} - \frac{85}{512x^{11}}, \\ \Phi_2^+(x) &= -\frac{1}{6x} - \frac{1}{6x^3} - \frac{35}{216x^5} - \frac{31}{216x^7} - \frac{133}{1296x^9} - \frac{5}{144x^{11}} \\ &\quad + \frac{15545}{279936x^{13}} + \frac{41381}{279936x^{15}} + \frac{1020679}{5038848x^{17}} + \frac{838775}{5038848x^{19}}, \end{aligned}$$

and  $\Phi_1^+(x)$  the polynomial with minimal degree such that  $y_i = \Phi_1^+(x_i)$  with

$$\begin{aligned} (x_i, y_i) \in & \left\{ \left(0, -\frac{66329}{14331}\right), \left(\frac{6}{35}, -\frac{57983}{16009}\right), \left(\frac{12}{35}, -\frac{37061}{13765}\right), \left(\frac{18}{35}, -\frac{28155}{14903}\right), \right. \\ & \left. \left(\frac{24}{35}, -\frac{17830}{14261}\right), \left(\frac{6}{7}, -\frac{33068}{41763}\right), \left(\frac{36}{35}, -\frac{12900}{26023}\right), \left(\frac{6}{5}, -\frac{1031522014772972842265}{3070471107232407748608}\right) \right\}. \end{aligned}$$

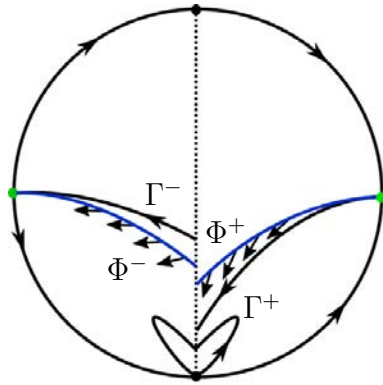


Figure 4.19: Behavior of infinite for  $\lambda^+ = 6$ ,  $\lambda^- = -4$  and the blue curves  $\Phi^\pm$ .

*Proof.* We prove that the curve  $y - \Phi^+(x) = 0$  (resp.  $y - \Phi^-(x) = 0$ ) is piecewise continuous and without contact with respect to the vector fields  $Z^+$  (resp.  $Z^-$ ) when  $x \geq 0$  (resp.  $x \leq 0$ ). Then, checking some other properties of the functions  $\Phi^\pm$ , the geometrical situations of the

points on the curves  $\Gamma^\pm$  with respect to the graph of  $\Phi^\pm(x)$  satisfy the conditions given in the statement. That is, as we have depicted in Figure 4.19.

The piecewise continuity property follows checking only that  $\Phi_1^\pm$  are polynomials,  $\Phi_2^\pm$  are rational functions well defined in the interval of definition, and  $\Phi_1^+(6/5) = \Phi_2^+(6/5)$  and  $\Phi_1^-(-11/10) = \Phi_2^-(-11/10)$ . Straightforward computations show that the function  $\Phi^+(x)$  (resp.  $\Phi^-(x)$ ) is monotonous increasing (resp. decreasing). Moreover, for  $x \geq 0$ ,

$$\langle \nabla(y - \Phi^+(x)), Z^+ \rangle|_{y=\Phi^+(x)} < 0$$

and, for  $x \leq 0$ ,

$$\langle \nabla(y - \Phi^-(x)), Z^- \rangle|_{y=\Phi^-(x)} < 0.$$

These properties follow because all the involved functions, in each considered intervals  $\{(-\infty, -11/10], [-11/10, 0], [0, 6/5], [6/5, \infty)\}$ , write as  $p(x)/x^k$ , being  $p$  polynomials with rational coefficients and  $k \geq 0$  integers. Because,  $\Phi_i^\pm(x)$ , for  $i = 1, 2$  are also functions of this type. Moreover, these polynomials  $p(x)$  have no zeros in the above intervals.

The proof finishes checking that, when  $x$  goes to  $+\infty$  (resp.  $-\infty$ ),  $\Gamma^+ \cap \{x \geq 0\} \subset \{y - \Phi^+(x) < 0\}$  (resp.  $\Gamma^- \cap \{x \leq 0\} \subset \{y - \Phi^-(x) > 0\}$ ). This property holds because, when  $x \nearrow +\infty$ , we have

$$\langle \nabla(y - \widehat{\Phi}_2^+(x)), Z^+ \rangle|_{y=\widehat{\Phi}_2^+(x)} > 0 \quad \text{and} \quad \widehat{\Phi}_2^+(x) < \Phi_2^+(x).$$

Equivalently, when  $x \searrow -\infty$ , we get

$$\langle \nabla(y - \widehat{\Phi}_2^-(x)), Z^- \rangle|_{y=\widehat{\Phi}_2^-(x)} > 0 \quad \text{and} \quad \widehat{\Phi}_2^-(x) > \Phi_2^-(x).$$

Where

$$\begin{aligned} \widehat{\Phi}_2^-(x) &= \Phi_2^-(x) - \frac{5985}{16384x^{13}} - \frac{6381}{16384x^{15}} - \frac{879}{131072x^{17}}, \\ \widehat{\Phi}_2^+(x) &= \Phi_2^+(x) - \frac{838775}{5038848x^{19}}. \end{aligned}$$

Hence, the graph of the curve  $\Gamma^+$  (resp.  $\Gamma^-$ ) is between the graphs of the functions  $\Phi_2^+$  and  $\widehat{\Phi}_2^+$  (resp.  $\Phi_2^-$  and  $\widehat{\Phi}_2^-$ ) when  $x \nearrow +\infty$  (resp.  $x \searrow -\infty$ ). See Figure 4.20.  $\square$

Next, we prove the existence of a point, in the parameter space, exhibiting the connection at infinity.

**Corollary 4.17.** *There exists  $-4 < \lambda^* < 0$  such that system (4.6) for  $(\lambda^+, \lambda^-) = (6, \lambda^*)$  exhibits a connection between the semihyperbolic saddles at infinity.*

*Proof.* The proof follows by continuity taking  $\lambda^+ = 6$  in Corollary 4.14 and Proposition 4.16. Following the notation introduced in Proposition 4.16, the intersection points with the  $x$ -axis of the separatrices  $\Gamma^\pm$  satisfy  $\Phi^+(0) - \Phi^-(0) > 0$  for  $\lambda^- \lesssim 0$  and  $\Phi^+(0) - \Phi^-(0) < 0$  for  $\lambda^- = -4$ . See also Figures 4.17 and 4.19.  $\square$

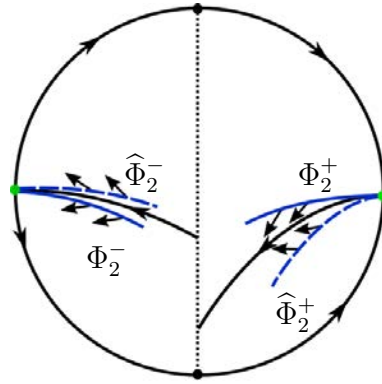


Figure 4.20: The separatrices arriving and scaping from infinity together with the vector field  $Z^\pm$  on the without contact curves  $y - \Phi_2^\pm(x) = 0$  and  $y - \widehat{\Phi}_2^\pm(x) = 0$ .

Next we explain the procedure to provide the functions  $\Phi^\pm$  appearing in the previous results. Other previous works where this kind of mechanism is used are [GSnGG15, GGT10]. The function  $\Phi^+$  is a piecewise continuous function defined by  $\Phi_1^+$  and  $\Phi_2^+$  in two intervals,  $[0, x_1^+]$  and  $[x_1^+, \infty)$ , respectively. Clearly,  $\Phi_1^+(x_1^+) = \Phi_2^+(x_1^+)$ . The function  $\Phi_2^+$  is obtained computing the approximation up to some order  $k$  of the unstable separatrix of the saddle located at the origin of system (4.19), that is, system (4.6) in the chart  $\mathcal{U}_1$ . Although  $\Phi_2^+$  define a curve without contact, it does not cross the  $y$ -axis. This is why we have considered the two pieces. It is necessary that the function  $\Phi_1^+$  maintain the without contact property and such that the graphs arrive to the  $y$ -axis. For simplicity, we have chosen it as a polynomial of some degree  $\ell$ . The function  $\Phi^-$  satisfies equivalent conditions. In Proposition 4.16 we have proposed two different ways to determine such polynomials. In both, the initial value problem defined by the original differential system (4.6) satisfying  $y_1^\pm = \Phi_1^\pm(x_1^\pm)$  is considered. The difference is the mechanism to solve them. One is the power series method at  $x_1^\pm$ . The other is the interpolation polynomial defined by the points obtained with the classical Euler method with some step  $h$ , see [SB02]. Finally, we need to find adequate values for  $k^\pm, \ell^\pm, x_1^\pm, h^\pm$ , such that the relative positions of the graphs of the functions  $\Phi^\pm$  allow us to proof a result like Proposition 4.16.

An improvement of the above results is hard to be done because the described mechanism depend on too many parameters and small variations on them have a big effect on all the involved functions. Moreover, the analytic control of the curves  $\Gamma^\pm$  is very difficult.

Although, the last result provides the existence of a point on the connection curve  $\Upsilon$ , from the above comments it is clear that the proof of the existence of such bifurcation curve, where the limit cycles disappear, is far to be done. We finish doing some numerical simulations to reinforce the idea that, fixed  $\lambda^+$ , there exists only one value  $\lambda^-$  such that the connection holds. Consequently, the connection curve  $\Upsilon$  should be the graph of a function, see Figure 4.11.

Following the notation introduced in Proposition 4.16, we can define the intersection points  $(0, \eta^\pm)$  of the curves  $\Gamma^\pm$  with the discontinuity line  $\Sigma$ , which is in this system the

$y$ -axis. These points define two functions of one variable,  $\eta^\pm(\lambda^\pm)$ . By the symmetries of system (4.6), studied in Lemma 4.11, we have that  $\eta^-(-\lambda) = \eta^+(\lambda)$ . Consequently, we compute numerically only  $\eta^+$ . The computations has been made by numerical continuation of the analytic approximations of high order of the invariant manifold  $\Gamma^+$ , denoted by  $\Phi_2^+$  in Proposition 4.16). The graphs of  $\eta^+$  are depicted in Figure 4.21. The value  $\lambda^+ = \hat{\lambda}$  denotes where the function  $\eta^+$  has its maximum. Notice that  $\eta^+$  is monotonous increasing in  $(0, \hat{\lambda})$  and monotonous decreasing in  $(\hat{\lambda}, \infty)$ .

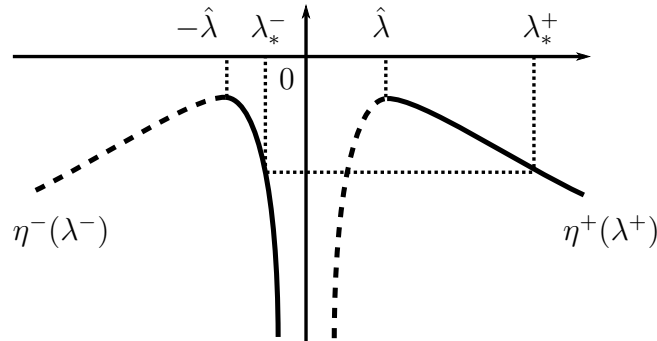


Figure 4.21: The functions  $\eta^\pm$  that define the intersection points of  $\Gamma^\pm$  with  $\Sigma$ .

The bifurcation curve  $\Upsilon$  is defined by the connection of the separatrices  $\Gamma^+$  and  $\Gamma^-$  on the separation curve  $\Sigma$ . The symmetric value  $\hat{\lambda}$ , where the functions  $\eta^\pm$  have a maximum, defines the intersection points of  $\Upsilon$  with the bisector,  $\lambda^+ + \lambda^- = 0$ , of the fourth quadrant. Using the symmetries indicated in Lemma 4.11 and the plot of  $\eta^\pm$  in Figure 4.21, the curve  $\Upsilon$  is obtained from the pairs  $(\lambda^+, \lambda^-)$  for every negative value less or equal than  $\eta^+(\hat{\lambda}) = \eta^-(-\hat{\lambda})$ . We have numerical evidences that there is only one pair for  $\lambda^+ \geq \hat{\lambda}$  and  $-\hat{\lambda} \geq \lambda^- < 0$ . This relation can be seen also in Figure 4.21 where the pairs associated to points on  $\Upsilon$  in Figure 4.11 are depicted as a continuous line and the symmetric part as a dashed line. All the simulations done here indicates that the limit cycle disappears for the values on such bifurcation curve. Finally, we remark that the curve  $\Upsilon$  separates the fourth quadrant in two regions having the infinity and the origin with opposite stability.



# The center and cyclicity problems for quartic linear-like reversible systems

---

---

## Abstract

In this chapter we study the family of quartic linear-like reversible polynomial systems having a nondegenerate center at the origin. This family has degree one with respect to one of the variables. We are interested in systems in this class having two extra nondegenerate centers outside the straight line of symmetry. The geometrical configuration of these centers is aligned or triangular. We solve the center problem in both situations and, in the second case, we start the study of limit cycles obtained from a simultaneous degenerate Hopf bifurcation in the quartic polynomials class.

## 5.1 Introduction

Let us consider a planar analytic system of ordinary differential equations defined in a neighborhood of the origin,  $(\dot{x}, \dot{y}) = (f(x, y), g(x, y))$ . We are interested in the local structure of the solutions near an equilibrium point of nondegenerate center-focus type located at the origin. That is, a point with the Jacobian matrix having nonzero determinant and null trace. More specifically, assuming  $f(0) = g(0) = 0$ , if we write the eigenvalues of the Jacobian matrix of  $(f, g)$  at 0 as  $\alpha \pm i\beta$ , then  $\alpha = 0$  and  $\beta \neq 0$ . So, after a time rescaling, we can assume that  $\beta = 1$ , and we can write the corresponding system in the normal form

$$(\dot{x}, \dot{y}) = (-y + f_n(x, y), x + g_n(x, y)), \quad (5.1)$$

where  $f_n$  and  $g_n$  are polynomials of degree  $n$ , which do not contain constant and linear terms. The problem of distinguishing whether the singular point at the origin of (5.1) is a center or a focus is known as the *Poincaré center problem*, the *center-focus problem*, or just the *center problem*. Even this problem was partially solved by Lyapunov, see [Lia93], it has been studied for some fixed values of the degree  $n$  during more than a century by many authors. The unique family completely solved is the quadratic one. The study of this family was started by Dulac in 1908 in [Dul08], and also performed by Kapteyn some years later, see [Kap11, Kap12]. Up to the work of Frommer ([Fro34]), the necessary and sufficient conditions were not published. This work was done for a quadratic system in real form and the computations were rather difficult. The correct center conditions were published by Saharnikov ([Sah48]) and later by Sibirskiĭ ([Sib54, Sib55]). The center conditions are much simpler to be obtained and the center-focus problem is easily solved if the system is written in complex coordinates, see [Ž94]. For the complete cubic family (when in (5.1)  $n = 3$ ), the problem remains unsolved. Only particular families have been studied, for example the linear plus cubic homogeneous in [Sib65] or cubic with degenerate infinity in [CG96]. Some recent works with other cubic families are [BS06, Coz15, CS98, San12, SN16]. For higher degree systems, nor the homogeneous nonlinearity cases for  $n = 4$  and  $n = 5$  are solved, [CG95]. In last thirty years, there is a big list of published papers studying so many different polynomial families. See, for example, the references in [RS09].

In this chapter we are interested in the limit cycles bifurcating simultaneously from reversible centers with two extra symmetric centers out of the symmetry line. All considered centers are *nondegenerate*. The aim is to do a similar study as the one done by Christopher in [Chr05] or by Prohens and Torregrosa in [PT18]. In this last work, the classification problem for cubics systems having such properties was done. The natural continuation problem is the study of the cyclicity of reversible quartic systems having a center at the origin. These systems can be written as

$$\begin{aligned} \dot{x} &= -y + a_{11}xy + a_{21}x^2y + a_{03}y^3 + a_{31}x^3y + a_{13}xy^3, \\ \dot{y} &= x + a_{20}x^2 + a_{02}y^2 + a_{30}x^3 + a_{12}xy^2 + a_{40}x^4 + a_{22}x^2y^2 + a_{04}y^4. \end{aligned} \quad (5.2)$$

Before to start with the simultaneous bifurcation it is necessary to solve the center-focus

problem for (5.2). This classification problem has been impossible to finish, as similar problems having too many parameters. We remark that the above system has 12 parameters. In order to simplify and convert this problem to some tractable one, we propose a restricted family following the ideas in [LCD<sup>+</sup>97]. We consider the *quartic linear-like reversible systems*, that is, all polynomial systems with degree four, time reversible with respect to the  $x$ -axis, and having degree one also in the variable  $x$ . This family of systems writes as

$$\begin{aligned}\dot{x} &= -y + a_{11}xy + a_{03}y^3 + a_{13}xy^3, \\ \dot{y} &= x + a_{02}y^2 + a_{12}xy^2 + a_{04}y^4.\end{aligned}\tag{5.3}$$

We recall that the above family is invariant with respect to the change of variables  $(x, y, t) \rightarrow (x, -y, -t)$ .

In Section 5.3 we will prove that system (5.3), having two extra symmetric centers out of the symmetry line, can be written in two different normal forms. The first corresponds to the case with three aligned centers over  $x = 0$  and the second with three centers in a triangular position. The following two results provide the answer to the center-focus classification problem.

**Theorem 5.1.** *The reversible quartic system (5.3) having three aligned singularities of center-focus type can be written as*

$$\begin{aligned}\dot{x} &= -y - (2c + b)xy + y^3 + by^3x, \\ \dot{y} &= x - cy^2 - \frac{1}{2}(a^2 + 4c^2 + 2)xy^2 + cy^4,\end{aligned}\tag{5.4}$$

with  $a > 0$  and  $c \geq 0$ . See Figure 5.1 right. Moreover, the above system has three aligned centers at  $(0, 0)$  and  $(0, \pm 1)$  if and only if one the following conditions holds:

$$(\mathcal{A}_1) \quad c = 0;$$

$$(\mathcal{A}_2) \quad b = a^2 - 4c^2 + 2 = 0.$$

**Theorem 5.2.** *The reversible quartic system (5.3) having three singularities of center-focus type in a triangular position can be written as*

$$\begin{aligned}\dot{x} &= -y - \frac{(c+d)xy}{d} + \frac{(b+d)y^3}{d^3} + \frac{(c+b+d)xy^3}{d^3}, \\ \dot{y} &= x + \frac{(a^2d + b^2d + bcd + 2c)y^2}{2cd^2} + \frac{(a^2d + b^2d - 2c)xy^2}{2cd^2} - \frac{(bd+2)y^4}{2d^4},\end{aligned}\tag{5.5}$$

with  $a > 0$ ,  $c \neq 0$ , and  $d > 0$ . See Figure 5.1 left. Moreover, the above system has three centers, one at the origin and two more at  $(-1, \pm d)$ , if and only if one the following conditions holds:

$$(\mathcal{T}_1) \quad a^2d - 2c = b = 0;$$

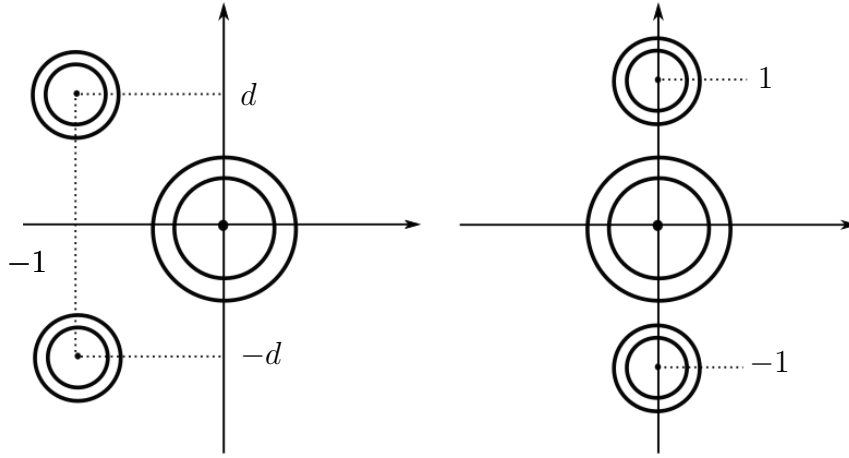


Figure 5.1: The two different configurations of centers of system (5.3)

$$(\mathcal{T}_2) \quad bd + 2 = a^4 + a^2b^2 - a^2c^2 - 2a^2cd - a^2d^2 + 4a^2 + 4b^2 + 4bc - 4 = 0;$$

$$(\mathcal{T}_3) \quad d^2 - bd + cd - 4 = 2(a^2 + b^2) + bc - c^2 - cd = 0;$$

$$(\mathcal{T}_4) \quad d - 2 = c + 1 = a^2 + b^2 - b = 0;$$

$$(\mathcal{T}_5) \quad cd + 4 = b + c + d = a^2 + d^2 - 4 = 0;$$

$$(\mathcal{T}_6) \quad cd + d^2 + 2 = b + c + d = a^2 - 2c^2 + 2d^2 + 10 = 0;$$

$$(\mathcal{T}_7) \quad cd + d^2 - 2 = a^2 + b^2 + bc = 0;$$

$$(\mathcal{T}_8) \quad d - 2 = b - c = a^2 + c^2 - c = 0;$$

$$(\mathcal{T}_9) \quad 2c + 3d = 2b - d = d^2 - 4a^2 - 4 = 0;$$

$$(\mathcal{T}_{10}) \quad b + c + d = a^2d - c^2d - 2cd^2 - d^3 + 2c + 4d = 0;$$

$$(\mathcal{T}_{11}) \quad cd + d^2 - 2 = 2b - d = d^2 - 4a^2 - 4 = 0;$$

$$(\mathcal{T}_{12}) \quad cd + d^2 - 6 = 3b - c - d = 9a^2 - 2c^2 + 2d^2 - 6 = 0;$$

$$(\mathcal{T}_{13}) \quad cd + d^2 - 2 = c^2d - bd^2 - d^3 + 2b + 4d = bc + c^2 - d^2 + 4 = a^2 + b^2 - c^2 + d^2 - 4 = 0;$$

$$(\mathcal{T}_{14}) \quad cd - 2 = b + c - d = a^2 + d^2 - 4 = 0;$$

$$(\mathcal{T}_{15}) \quad c^2d^2 + 2cd^3 + d^4 - cd - 2d^2 - 2 = b + c + d = c^3d - 3cd^3 - 2d^4 + a^2 - 2c^2 - 2cd + 3d^2 + 8 = 0;$$

$$(\mathcal{T}_{16}) \quad cd - 2 = b = a - c = 0;$$

$$(\mathcal{T}_{17}) \quad cd + 2d^2 - 8 = 2b - c = a^2 + d^2 - 4 = 0;$$

$$(\mathcal{T}_{18}) \quad a^2 + cd + d^2 = b + c + d = 0.$$

The chapter is structured as follows, in Section 5.2 we present some preliminary results on the center conditions computation, the Darboux integrability, and the degenerate Hopf bifurcation problem. Section 5.3 is devoted to show the normal forms (5.4) and (5.5). The center classification is done in Section 5.4. Finally, the simultaneous limit cycles bifurcation from some systems listed in the main results is started in Section 5.5.

## 5.2 Preliminaries

This section is devoted to recall some classical concepts, necessary to state and prove the results of this chapter. In Section 5.2.1 we provide the definition and computational algorithm to compute the center conditions to study the center-focus problem. In Section 5.2.2 we explain how the simultaneous degenerate Hopf bifurcations are done for proving the results of Section 5.5. Finally, the necessary Darboux integrability results are given in Section 5.2.3.

### 5.2.1 The center conditions

The approach to characterize when system (5.1) has a center at the origin is based on the well known Poincaré–Lyapunov Theorem, see [Lia47, Poi17]. Before to state it, we recall the definition of *first integral*. We say that a nonconstant analytical function defined in a neighborhood  $\Omega$  of the origin,  $\Phi : \Omega \subset \mathbb{R}^2 \rightarrow \mathbb{R}$ , is a first integral of system (5.1) if it is constant along any solution  $\gamma$  or, equivalently,

$$\dot{x} \frac{\partial \Phi}{\partial x} + \dot{y} \frac{\partial \Phi}{\partial y} \Big|_{\gamma} \equiv 0. \quad (5.6)$$

**Theorem 5.3.** *System (5.1) has a center at the origin if and only if it admits a local analytic first integral of the form*

$$\Phi(x, y) = x^2 + y^2 + \sum_{k+\ell \geq 3} q_{k,\ell} x^k y^\ell. \quad (5.7)$$

*Moreover, the existence of a formal first integral  $\Phi$  of the above form implies the existence of a local analytic first integral of the same form.*

For a proof of this result we refer to [IY08].

The necessary conditions for the existence of a first integral for system (5.1) are obtained looking for a formal series (5.7) satisfying (5.6). To start the computational procedure for finding the first  $N$  conditions for integrability, we write down (5.7) up to order  $2N + 2$

$$\tilde{\Phi}(x, y) = x^2 + y^2 + \sum_{k+\ell \geq 3}^{2N+2} q_{k,\ell} x^k y^\ell. \quad (5.8)$$

Then, for each  $i = 3, \dots, 2N + 2$  we equate to zero the coefficients of terms of degree  $i$  in

the expression

$$\dot{x} \frac{\partial \tilde{\Phi}}{\partial x} + \dot{y} \frac{\partial \tilde{\Phi}}{\partial y} = (-y + f_n(x, y)) \frac{\partial \tilde{\Phi}}{\partial x} + (-x + g_n(x, y)) \frac{\partial \tilde{\Phi}}{\partial y}.$$

Starting at  $i = 3$ , we should solve in a recurrence way each linear system of  $i + 1$  equations with  $i + 1$  variables,  $q_{k,\ell}$  such that  $k + \ell = i$ . All linear systems corresponding to odd degrees,  $i = 2j + 1$ , have a unique solution in terms of previous values of  $q_{k,\ell}$ . As the determinant of the linear system that corresponds to an even degree,  $i = 2j + 2$ , vanishes, we need to add an extra condition in order that the linear system has a unique solution. In fact, at this step, we have one equation more than the number of variables. We add a suitable equation, for the term  $x^{2j+2}$  for example, in order that the derivative over the associated vector field writes as

$$\dot{x} \frac{\partial \tilde{\Phi}}{\partial x} + \dot{y} \frac{\partial \tilde{\Phi}}{\partial y} = L_j x^{2j+2} + \dots . \quad (5.9)$$

Then, when  $L_j$  is different from zero  $\Phi$  it is a Lyapunov function in a neighborhood of the origin. Then, system (5.1) has no first integral and we say that the equilibrium point is a *weak focus* of order  $j$ . In fact this number is known as the  $j$ -th Lyapunov quantity. Moreover, the stability of the origin is given by the sign of  $L_j$ . The condition of the existence of a first integral up to an even order  $i = 2j + 2$  is that  $L_j$  vanishes.

Among other properties, it can be seen in [CGMnMn97] that  $L_j$  are polynomials in the parameters of system (5.1). Clearly, for  $N$  big enough, the above algorithm provides a necessary set of conditions,  $\{L_j = 0 : j = 1, \dots, N\}$ , for system (5.1) to be a center. In other words, we can also say that the polynomials  $L_j$  represent obstacles for the existence of a first integral. In particular, system (5.1) admits a first integral of the form (5.7) if and only if  $L_j = 0$ , for all  $j \geq 1$ . Thus, the simultaneous vanishing of all focus quantities provides conditions which characterize when a system of the form (5.1) has a center at the origin.

The next definition recalls the notion of *Bautin ideal* and the *center variety*.

**Definition 5.4.** *The ideal defined by the real focus quantities,  $\mathcal{B}^{\mathbb{R}} = \langle L_1, L_2, \dots \rangle \subset \mathbb{C}[\lambda]$ , where  $\lambda$  represents all the parameters of system (5.1) is called the real Bautin ideal. The affine variety  $\mathbf{V}^{\mathbb{R}} = \mathbf{V}(\mathcal{B}^{\mathbb{R}})$ , is called the real center variety of system (5.1).*

By the Hilbert Basis Theorem there exists a positive integer  $j$  such that  $\mathcal{B}^{\mathbb{R}} = \mathcal{B}_j^{\mathbb{R}} = \langle L_1, \dots, L_j \rangle$ . The main difficulty is that there is no technique to get  $j$  a priori. Notice that the inclusion  $\mathbf{V}^{\mathbb{R}} = \mathbf{V}(\mathcal{B}^{\mathbb{R}}) \subset \mathbf{V}(\mathcal{B}_j^{\mathbb{R}})$  holds for any  $j \geq 1$ . The opposite inclusion, for a fixed  $j$ , is verified finding the irreducible decomposition of  $\mathbf{V}(\mathcal{B}_j^{\mathbb{R}})$ , see [RS09], such that at any point of each component of the decomposition it corresponds to a system having a center at the origin. To find the irreducible decomposition of  $\mathbf{V}(\mathcal{B}_j^{\mathbb{R}})$ , we perform the computations with the Computer Algebra System SINGULAR ([DGPS18, DPSL18]). In Section 5.4 we explain this procedure more carefully.

### 5.2.2 Degenerate Hopf bifurcation

Roughly speaking, we can say that the (finite) cyclicity of an equilibrium point is the maximum number of isolated periodic orbits bifurcating from it. We are interested only in the limit cycles bifurcating from nondegenerate monodromic points, where the return map is well defined and it is analytic. Moreover, both unperturbed systems and perturbations are polynomials of degree four in the variables  $x, y$ .

With the notation introduced in the above section, the classical known as Hopf bifurcation is the emergence of a limit cycle, varying the trace from zero to a small enough but nonzero value, from a weak-focus of first order. We will denote by  $L_0$  the trace of the perturbed system, clearly  $L_0 = 0$  for the unperturbed one. More concretely, the origin of the unperturbed system is stable (resp. unstable) when  $L_1 < 0$  (resp.  $L_1 > 0$ ). Then, the perturbed system, when  $L_0$  is a small enough positive (resp. negative) real number a small stable (resp. unstable) limit cycle bifurcates from the origin. This is because the monodromic property remains but the local stability of the equilibrium point changes from stable to unstable. The degenerate Hopf bifurcation is the natural generalization of this bifurcation phenomenon when  $k$  small limit cycles appear from a weak-focus of order  $k$ .

In general, the complete unfolding of  $k$  limit cycles near a weak focus of order  $k$  is only guaranteed when the perturbation is analytic, see for example [Rou98]. When the perturbation is restricted to be polynomial of some fixed degree this property is not automatic. This is the case in our problem. Our unperturbed systems (5.3) are of degree four and we are perturbing them in the full quartic polynomial systems. This is the main reason why the problem of finding the cyclicity of a center, like (5.3), is so difficult. A way to avoid this difficulties is to study lower bounds for the cyclicity. This is the aim of the next result due to Christopher in [Chr05] that, as a direct application of the Implicit Function Theorem, it provides necessary conditions to get lower bounds for the cyclicity of a center. In fact, there are similar previous results due to Chicone and Jacobs ([CJ89, CJ91]). Also Han ([Han99]) applies them for Liénard families.

**Theorem 5.5.** *Suppose that  $\mathbf{c}$  is a point on the center variety in the parameter space and that the first  $L_1, \dots, L_k$  Lyapunov quantities have independent linear parts (with respect to the expansion of them with respect all perturbation parameters), then  $\mathbf{c}$  lies on a component of the center variety of codimension at least  $k + 1$ , adding the trace parameter  $L_0$ , and there are bifurcations which produce  $k$  limit cycles locally from the center corresponding to the parameter value  $\mathbf{c}$ .*

In particular, the above result shows the existence of a curve of weak-foci of order  $k$  that unfold  $k$  hyperbolic limit cycles. The existence of this curve is obtained studying the Taylor developments of the varieties  $L_j = 0$ , for  $j = 0, \dots, k$ , that intersect transversally along it but  $L_k$  is nonvanishing.

Finally, in [Chr05] there are results about the existence of such transversal curves studying the homogeneous higher order terms when the previous vanish identically. But they will be used in the future to improve the results of this chapter.

The interest of this chapter is the use of Theorem 5.5 not for studying what is the maximum local cyclicity that a quartic vector field can have inside the quartics class. We are interested in the simultaneous bifurcation of limit cycles in the three center configuration that a system of type (5.3) has. We will explain how we use this result more carefully in Section 5.5.

### 5.2.3 Darboux integrability

A more detailed version of the next result can be found in [DLA06]. For completeness here we only include the statement of Darboux integrability that we will need for proving our classification results, together with some previous concepts and definitions.

Let  $(\dot{x}, \dot{y}) = (P(x, y), Q(x, y))$  be a  $\mathbb{C}$ -polynomial differential system of degree  $m$ . We say that an algebraic curve  $f = 0$  is invariant if the vector field associated to the polynomial differential system is tangent along it. That is

$$P(x, y) \frac{\partial f}{\partial x} + Q(x, y) \frac{\partial f}{\partial y} = K(x, y) f(x, y).$$

The polynomial  $K$  is known as the corresponding *cofactor*. Equivalently,  $\exp(g/h)$  is called an exponential factor, with associated cofactor  $K^e$ , if it satisfies

$$P(x, y) \frac{\partial e^{g/h}}{\partial x} + Q(x, y) \frac{\partial e^{g/h}}{\partial y} = K^e(x, y) e^{g/h}.$$

**Theorem 5.6.** *Suppose that a  $\mathbb{C}$ -polynomial differential system of degree  $m$  admits  $p$  irreducible invariant algebraic curves  $f_i = 0$  with cofactors  $K_i$  for  $i = 1, \dots, p$  and  $q$  exponential factors  $\exp(g_j/h_j)$  with cofactors  $K_j^e$  for  $j = 1, \dots, q$ . Then, there exist complex numbers  $\lambda_i$  and  $\mu_j$  not all zero such that  $\sum_{i=1}^p \lambda_i K_i + \sum_{j=1}^q \mu_j K_j^e = 0$ , if and only if the (multivalued) function*

$$f_1^{\lambda_1} \dots f_p^{\lambda_p} \left( \exp \left( \frac{g_1}{h_1} \right) \right)^{\mu_1} \dots \left( \exp \left( \frac{g_q}{h_q} \right) \right)^{\mu_q}$$

*is a first integral of the  $\mathbb{C}$ -polynomial differential system of degree  $m$ .*

## 5.3 Normal forms

As we have already mentioned, system (5.3) is time-reversible with respect to the  $x$ -axis, and it has a nondegenerate equilibrium point of center-focus type at the origin. Clearly, the reversibility condition and the linear part ensures that the origin will be always a center. As we have explained in the introduction, the aim of this chapter is the study of system (5.3) having two extra nondegenerate centers out of the symmetry line. Then, as they can be located at  $(x_0, \pm y_0)$ , there are two different possibilities,  $x_0 = 0$  and  $x_0 \neq 0$ . In the rest of the section we will proof the first part of the statements of Theorems 5.1 and Theorems 5.2.

In the first case,  $x_0 = 0$ , we can locate the equilibrium points at  $(0, \pm 1)$  after a rescaling. Then, imposing that the determinants of the Jacobian matrix at these points writes as a positive number,  $a^2$ , we get system (5.4). We notice that by the symmetry both determinants

coincide. We can also assume the condition  $c \geq 0$  doing, if necessary, the change  $(x, y) \rightarrow (-x, -y)$ . Hence, with the new variables  $(u, v) = (x, -1 + y)$ , there exists a first integral that writes

$$H(u, v) = (au)^2 + 4(cu - v)^2 + \dots . \quad (5.10)$$

In the second case,  $x_0 \neq 0$ , we can locate the equilibrium points at  $(-1, \pm d)$  after a rescaling, if necessary. The symmetry provides the condition  $d > 0$ . Assuming that the system has an equilibrium point with zero trace we get

$$\begin{aligned} a_{02} &= \frac{d^4 a_{13} + d^2(a_{11} + 2a_{12}) + 4}{2d^2}, \\ a_{03} &= \frac{d^2 a_{13} + a_{11} + 1}{d^2}, \\ a_{04} &= -\frac{d^4 a_{13} + d^2 a_{11} + 2}{2d^4}. \end{aligned}$$

Then, adding that it has positive determinant,  $a^2$ , we obtain

$$a_{12} = -\frac{d^6 a_{13}^2 + 2d^4 a_{11} a_{13} + d^2 a_{11}^2 + a^2 + 2a_{11} + 2}{2d^2(a_{11} + 1)}.$$

Clearly, it is not restrictive if we assume  $a > 0$ . The above denominator never vanishes because, when  $a_{11} = -1$ , the determinant,  $a^2 = -d^2(a_{13}d^2 - 1)^2$ , would be negative. Finally, we introduce two new parameters  $(b, c)$  with the linear change

$$\begin{aligned} a_{11} &= -\frac{c + d}{d}, \\ a_{13} &= \frac{c + b + d}{d^3}. \end{aligned}$$

Hence, with the new variables  $(u, v) = (1 + x, -d + y)$ , there exists a first integral that writes

$$H(u, v) = (adu)^2 + (-bdu + 2cv)^2 + \dots . \quad (5.11)$$

This expression can be easily transformed to (5.8). We remark that the condition  $a_{11} + 1 \neq 0$  is equivalent to  $c \neq 0$ . From all the above transformations the system (5.3) moves to (5.5).

We notice that, although the last parameter change does not seem necessary, it will help to obtain simpler expressions for the center conditions in the next section.

## 5.4 Centers classification

This section is devoted to prove the center classification statement of Theorems 5.1 and 5.2. Because the proof of the second result is quite long we have written it separately in Propositions 5.7 and 5.8. The obtained first integrals are globally defined and their level curves provide, among many others, the three period annuli.

### 5.4.1 Proving the center classification in the aligned case

The reversibility property and the normal form (5.4) ensures that the origin is a center. Then, by the symmetry we only need to study, the equilibrium point  $(0, 1)$ . First we check that the two families of the statement satisfy the center conditions, and second we compute the explicit expressions of the first integrals, which are of Darboux type,  $H_1 = f_1^{\lambda_1} f_2^{\lambda_2} (e^g)^\mu$  and  $H_2 = f_1^{\lambda_1} (e^g)^\mu$ . In both cases  $\mu = 1$ . We will denote by  $K_{f_i}$ ,  $i = 1, 2$ , and  $K_g$  the corresponding cofactors.

The change given to obtain expression (5.10) allow us to use the algorithm described in Section 5.2.1 to compute the first center conditions, that is, the first Lyapunov quantities. Although they are polynomials in the parameters, the change (5.10) introduce some denominators. Straightforward computations show that the denominators of  $L_2$  and  $L_3$  before the usual simplifications are  $a^4(a^2 + 4c^2)^2$  and  $a^8(a^2 + 4c^2)^5$ , respectively, which never vanish because  $a > 0$ . Hence, we can consider only the numerators, modulo positive constants,

$$\begin{aligned} L_1 &= c(a^2b^2 + 2a^2bc + 4b^2c^2 + 8bc^3 - 2a^2 + 8c^2 - 4), \\ L_2 &= -c(a^2 + 4c^2 + 2)(a^2 + 8bc - 4c^2 + 2), \\ L_3 &= c^5(a^2 + 4c^2 + 2)(a^2 - 4c^2 + 2)(6220800a^2c^{14} + 24883200c^{16} + 8121600a^2c^{12} \\ &\quad + 65664000c^{14} + 3124800a^2c^{10} + 51206400c^{12} + 290800a^2c^8 + 13476800c^{10} \\ &\quad - 11200a^2c^6 + 620800c^8 + 600a^2c^4 - 36000c^6 - 52a^2c^2 + 1840c^4 - a^2 + 60c^2). \end{aligned}$$

These values for  $L_i$  are defined when the previous are zero. Moreover,  $L_4, L_5$  also vanish. The necessary part of the statement follows easily checking that the real solutions of  $\{L_1 = L_2 = L_3 = 0\}$  are the families  $\mathcal{A}_1$  and  $\mathcal{A}_2$ .

For the sufficient conditions we only list the functions to get the Darboux first integrals for both families.

◦ Family  $\mathcal{A}_1$  satisfies  $c = 0$ , then

$$\begin{aligned} f_1 &= -2 + (a^2 + 2)y^2, \\ f_2 &= bx + 1, \\ g &= -b(a^2 + 2)((a^2 + 2)x + y^2b), \\ K_{f_1} &= -(a^2 + 2)xy, \\ K_{f_2} &= b(y^2 - 1)y, \\ K_g &= b(a^2 + 2)(a^2bx - (a^2 + 2)y^2 + a^2 + 2)y, \end{aligned}$$

with  $\lambda_1 = a^2b^2$  and  $\lambda_2 = (a^2 + 2)^2$ .

◦ Family  $\mathcal{A}_2$  satisfies  $b = 0$  and  $c = \sqrt{a^2 + 2}$ , then

$$\begin{aligned} f_1 &= -1 - 2\sigma x + 2(a^2 + 2)y^2 + 2\sigma(a^2 + 2)xy^2 - (a^2 + 2)y^4, \\ g &= -2\sigma x, \\ K_{f_1} &= -2\sigma y(1 + \sigma x - y^2), \\ K_g &= 2\sigma y(1 + \sigma x - y^2), \end{aligned}$$

with  $\sigma = \sqrt{a^2 + 2}$  and  $\lambda_1 = 1$ .

This finishes, together with the normal forms proved in Section 5.3, the proof of Theorem 5.1.

## 5.4.2 Proving the center classification in the triangular case

**Proposition 5.7.** *If the equilibrium point  $(-1, \pm d)$  of the quartic system (5.5) is a center then the parameters  $(a, b, c, d)$  satisfy one of the conditions given in the statement of Theorem 5.2.*

*Proof.* As the system (5.5) is reversible with respect to the  $x$ -axis, the center conditions for the point  $(-1, -d)$  are the same as for  $(-1, d)$ . Thus, we only study this point. From the normal form computations done in Section 5.3,  $(-1, d)$  is a nondegenerate equilibrium point of center-focus type, that is, the trace and the determinant of the Jacobian matrix is zero and positive, respectively.

The proof follows computing a few first Lyapunov quantities and then solving them the obtained system to check that all the families are the ones described in the statement.

First, we translate the point to the origin, we do an affine change of coordinates, see (5.11), and rescaling time. Then, we follow the approach described in Section 5.2.1 for the computation of the center conditions  $L_i$  in (5.9). From the affine change, they are rational functions with denominators of the form  $c^k d^\ell$ . As usual, the four parameters,  $(a, b, c, d)$ , appearing in system (5.5) indicate that only the first four Lyapunov quantities will be necessary to be computed, but as we will see, we use the first five. Instead of the complete expression, for simplicity, we denote by  $L_i$  only the numerators of the center conditions, that are polynomials with integer coefficients in  $(a, b, c, d)$ . Because of the size of them, we only show the first one,

$$\begin{aligned} L_1 &= (cd^2 + d^3 - 4d)b^4 + (-8 + d^4 + 2cd^3 + (c^2 - 2)d^2 - 4cd)b^3 + (a^2cd^2 + a^2d^3 \\ &\quad - 2a^2d - 12c)b^2 + (a^2d^4 + 2a^2cd^3 + a^2(c^2 - 2)d^2 - 8a^2 - 4c^2)b + 2a^4d - 4a^2c. \end{aligned}$$

The other 4 numerators are polynomials of degrees 19, 33, 49, and 67 with 317,1524, 4835, and 12152 monomials, respectively.

For the second step, we need to solve the algebraic system of equations  $\mathcal{S} = \{L_1 = L_2 = L_3 = L_4 = L_5 = 0\}$ . Although this system has only 4 variables and 5 equations the usual mechanisms for solving it fails. Instead of finding the solutions directly, we will use the Gianni–Trager–Zacharias algorithm, see [GTZ88], to determine the irreducible components of the variety  $\mathbf{V} = \mathbf{V}(L_1, L_2, L_3, L_4, L_5)$ . The main function used is `minAssGTZ`,

it is implemented in the library `primdec.lib` included on the algebraic computational system SINGULAR, see [DGPS18, DPSL18]. This is also extremely difficult to do in general and also if we work in the finite field  $\mathbb{Z}_p$ , with  $p = 32003$ . as it is usual in SINGULAR. Hence, the irreducible components will be computed considering some auxiliary polynomials obtained from some crossed resultants with respect to one of the parameters, because the new polynomials have less variables but higher degree and contain the solutions that we are interested.

Then, we compute the four resultants with respect to the parameter  $c$ ,  $\text{Res}(L_1, L_2, c)$ ,  $\text{Res}(L_1, L_3, c)$ ,  $\text{Res}(L_1, L_4, c)$ , and  $\text{Res}(L_1, L_5, c)$ . We denote by  $\text{Res}_{12}$ ,  $\text{Res}_{13}$ ,  $\text{Res}_{14}$ , and  $\text{Res}_{15}$ , the corresponding factorized expressions. But leaving only one term, when they have multiplicity bigger than one, and removing the nonvanishing terms, that is the powers of  $a$ ,  $d$ , and  $a^2 + b^2$ . Then, we get

$$\text{Res}_{12} = \mathcal{R} \cdot \mathcal{R}_{12}, \quad \text{Res}_{13} = \mathcal{R} \cdot \mathcal{R}_{13}, \quad \text{Res}_{14} = \mathcal{R} \cdot \mathcal{R}_{14}, \quad \text{Res}_{15} = \mathcal{R} \cdot \mathcal{R}_{15},$$

with the common factor  $\mathcal{R} = \mathcal{R}_1 \mathcal{R}_2 \cdots \mathcal{R}_8$ , where

$$\begin{aligned} \mathcal{R}_1 &= b, \\ \mathcal{R}_2 &= bd + 2, \\ \mathcal{R}_3 &= a^2 d^2 + b^2 d^2 - 2bd + 2d^2 - 8, \\ \mathcal{R}_4 &= a^2 d + b^2 d - bd^2 + 2b, \\ \mathcal{R}_5 &= a^2 d - b^2 d - 2b + 2d, \\ \mathcal{R}_6 &= a^2 d^2 + b^2 d^2 - 4, \\ \mathcal{R}_7 &= a^2 - bd, \\ \mathcal{R}_8 &= a^2 d^2 + (bd + 2)^2 + 2d^2. \end{aligned}$$

We have not written, because of their size, the polynomials  $\mathcal{R}_{12}$ ,  $\mathcal{R}_{13}$ ,  $\mathcal{R}_{14}$ ,  $\mathcal{R}_{15}$ . They have degrees 6, 32, 62, 92 in  $(a, b, d)$  and 9, 293, 1642, and 4803 monomials, respectively.

With the above discussion, and taking into account that the curve  $\mathcal{R}_8 = 0$  has no real points because  $a, d > 0$ , the solution of  $\mathcal{S}$  can be studied solving the eight algebraic systems  $\mathcal{S}_0 = \{L_1 = L_2 = L_3 = L_4 = L_5 = \mathcal{R}_{12} = \mathcal{R}_{13} = \mathcal{R}_{14} = \mathcal{R}_{15} = 0\}$  and  $\mathcal{S}_i = \{L_1 = L_2 = L_3 = L_4 = \mathcal{R}_i = 0\}$  for  $i = 1, \dots, 7$ .

System  $\mathcal{S}_0$  is studied computing the two by two crossed resultants, first with respect to  $d$ , then with respect to  $b$ . In each step we remove, as previously, all the multiple terms and also the powers of the nonvanishing variables or factors ( $d$ ,  $a$ ,  $a^2 + b^2$ ,  $a^2 + 2$ ). Finally, the last two polynomials have only one common factor  $a^2 - 1$ . Next, as  $a > 0$ , we consider the system  $\{\mathcal{R}_{12} = \mathcal{R}_{13} = \mathcal{R}_{14} = \mathcal{R}_{15} = a - 1 = 0\}$ , that has, as also  $d > 0$ , only one solution  $\{a = 1, b = 1/\sqrt{3}, d = \sqrt{3}\}$ . Finally,  $\mathcal{S}_0$  has only two real solutions  $\{a = 1, b = 1/\sqrt{3}, c = 2/\sqrt{3}, d = \sqrt{3}\}$  and  $\{a = 1, b = 1/\sqrt{3}, c = -4/\sqrt{3}, d = \sqrt{3}\}$ . They, satisfy the conditions of cases  $\mathcal{T}_{17}$  and  $\mathcal{T}_5$  of the statement, respectively.

Although some systems can be easily solved, as  $\mathcal{S}_1$  that writes equivalently as the first

family,  $\{b = a^2d - 2c = 0\}$ , most of them need an accurate procedure. We will follow step by step the algorithm described in [RS16].

The 18 families in the statement are obtained solving systems  $\mathcal{S}_i$ , for  $i = 1, \dots, 7$ .

For each  $i$ , except for  $i = 4$ , we use the mentioned Gianni–Trager–Zacharias algorithm and we apply the routine `minAssGTZ` to the ideal  $\mathcal{B}_i = \langle \mathcal{R}_i, L_1, L_2, L_3, L_4 \rangle$ , for simplicity we have not used  $L_5$ . That is, we obtain the necessary conditions to have a center finding the minimal decomposition of the variety of the each ideal  $\mathcal{B}_i$ . We illustrate the procedure only for one family,  $\mathcal{S}_7$ , the other follow similarly.

Working in  $\mathbb{Z}_p[a, b, c, d]$ , with  $p = 32003$ , instead of  $\mathbb{Q}[a, b, c, d]$ , the primary decomposition ideals of  $\mathcal{B}_7$ , provided by SINGULAR, is

$$\begin{aligned} & \langle a, b \rangle, \langle a, d, b - 16001c \rangle, \\ & \langle cd + 2d^2 - 8, b + 16001c, a^2 + d^2 - 4 \rangle, \langle cd - d^2 - 2, b + c, a^2 + d^2 + 2 \rangle, \\ & \langle d^3 + c - 2d, b + d, a^2 + d^2 \rangle, \langle a^2 + cd + d^2, b + c + d \rangle. \end{aligned} \quad (5.12)$$

Next, we use the rational reconstruction algorithm provided by [WGD82] to get a candidate to be the primary decomposition ideal but with rational coefficients. In fact, we should apply the next function to each coefficient of the above polynomials.

```
Rational_Reconstruction(x,p)
u=[1,0,p]
v=[0,1,x]
while sqrt(p/2)<= v[3] do {
  q=floor(u[3]/v[3])
  r=u-qv
  u=v
  v=r
}
if abs(v[2])>= sqrt(p/2) then error()
return(v[3]/v[2])
```

We recall that the *floor function*,  $[x]$ , gives the greatest integer less than or equal to  $x$ . Given an integer  $x$  and a prime  $p$ , the rational reconstruction function defined above, provides a rational number  $y$  such that  $y = x \pmod{p}$  and, in absolute value, the numerator and denominator of  $y$  are less than  $\sqrt{p/2}$ .

In the primary decomposition ideals of  $\mathcal{B}_7$  given in (5.12) all the rational reconstructed values are the same integers except 16001, which is  $-1/2$ . Consequently, the candidate to

be the primary decomposition ideals of  $\mathcal{B}_7$  is

$$\begin{aligned}\tilde{P}_1 &= \langle a, b \rangle, \\ \tilde{P}_2 &= \langle a, d, b + (1/2)c \rangle, \\ \tilde{P}_3 &= \langle cd + 2d^2 - 8, b - (1/2)c, a^2 + d^2 - 4 \rangle, \\ \tilde{P}_4 &= \langle cd - d^2 - 2, b + c, a^2 + d^2 + 2 \rangle, \\ \tilde{P}_5 &= \langle d^3 + c - 2d, b + d, a^2 + d^2 \rangle, \\ \tilde{P}_6 &= \langle a^2 + cd + d^2, b + c + d \rangle.\end{aligned}$$

The next step is to show that  $\sqrt{P_7} = \sqrt{\mathcal{B}_7}$ , where  $P_7 = \bigcap_{k=1}^6 \tilde{P}_k$  in  $\mathbb{Q}[a, b, c, d]$ . We have denoted by  $\sqrt{P}$  the radical of the ideal  $P$ . In general, it is simpler to verify the double inclusion instead of computing the radicals. Adding a new artificial parameter  $w$ , this property can be seen checking that  $\{1\}$  is the Gröbner basis of the next list of ideals,  $\langle 1 - wL_k, P_7 \rangle$ , for  $k = 1, \dots, 4$  and  $\langle 1 - wp, \mathcal{B}_7 \rangle$ , for every  $p \in P_7$ .

In the last step we check which  $\tilde{P}_k$ , for  $k = 1, \dots, 6$ , will appear in the statement. As  $a, d, a^2 + d^2, a^2 + d^2 + 2$  are nonvanishing, only  $\tilde{P}_3$  and  $\tilde{P}_6$  are necessary conditions for system (5.5) be a center. In fact, they are cases  $\mathcal{T}_{17}$  and  $\mathcal{T}_{18}$ , respectively.

Finally, we study family  $\mathcal{S}_4 = \{\mathcal{R}_4, L_1, L_2, L_3, L_4\}$  with another procedure. Because, for the rational reconstructed candidate to be the primary decomposition ideals we have  $\sqrt{P_4} \neq \sqrt{\mathcal{B}_4}$ . As the condition  $b = 0$  has been studied before, here we will assume that  $b \neq 0$ .

We start again computing the four resultants but with respect to the parameter  $a$ ,

$$\text{Res}(\mathcal{R}_4, L_1, a), \quad \text{Res}(\mathcal{R}_4, L_2, a), \quad \text{Res}(\mathcal{R}_4, L_3, a), \quad \text{Res}(\mathcal{R}_4, L_4, a).$$

We denote by  $\widehat{\text{Res}}_1, \widehat{\text{Res}}_2, \widehat{\text{Res}}_3$ , and  $\widehat{\text{Res}}_4$ , the corresponding factorized expressions. But leaving only one term, when they have multiplicity bigger than one, and removing the nonvanishing terms, that are powers of  $b, d$ . Then, we get

$$\widehat{\text{Res}}_1 = \widehat{\mathcal{R}} \cdot \widehat{\mathcal{R}}_1, \quad \widehat{\text{Res}}_2 = \widehat{\mathcal{R}} \cdot \widehat{\mathcal{R}}_2, \quad \widehat{\text{Res}}_3 = \widehat{\mathcal{R}} \cdot \widehat{\mathcal{R}}_3, \quad \widehat{\text{Res}}_4 = \widehat{\mathcal{R}} \cdot \widehat{\mathcal{R}}_4,$$

with the common factor  $\widehat{\mathcal{R}} = cd + d^2 - 2$ . Hence, the solution  $\{L_1 = L_2 = L_3 = L_4 = \widehat{\mathcal{R}}_4 = \widehat{\mathcal{R}} = 0\}$  is case (7).

As we have reduced the set of variables to  $(b, c, d)$ , we can follow as before solving the system  $\{\widehat{\mathcal{R}}_1 = \widehat{\mathcal{R}}_2 = \widehat{\mathcal{R}}_3 = \widehat{\mathcal{R}}_4 = 0\}$  by computing the crossed resultants  $\text{Res}(\widehat{\mathcal{R}}_1, \widehat{\mathcal{R}}_2, b)$ ,  $\text{Res}(\widehat{\mathcal{R}}_1, \widehat{\mathcal{R}}_3, b)$ , and  $\text{Res}(\widehat{\mathcal{R}}_1, \widehat{\mathcal{R}}_4, b)$ . Now, leaving also only one term, when they have multiplicity bigger than one, and removing the nonvanishing terms, that are powers of  $c, d, d^2 + 2, d + 2$ , and  $cd + d^2 - 2$ , we get

$$\widehat{\mathcal{R}}_{12} = \widetilde{\mathcal{R}} \cdot \widetilde{\mathcal{R}}_{12}, \quad \widehat{\mathcal{R}}_{13} = \widetilde{\mathcal{R}} \cdot \widetilde{\mathcal{R}}_{13}, \quad \widehat{\mathcal{R}}_{14} = \widetilde{\mathcal{R}} \cdot \widetilde{\mathcal{R}}_{14},$$

where  $\widetilde{\mathcal{R}} = (d-2)(d^2-2)(2c+3d)(cd+2d^2-4)(d^2-6)$ . As  $\widetilde{\mathcal{R}}_{12} = d^2+6 \neq 0$ , we have to check that, for each factor  $D$  in  $\widetilde{\mathcal{R}}$ , the solution of  $\mathcal{S}_D = \{L_1 = L_2 = L_3 = L_4 = \mathcal{R}_4 = D = 0\}$  is in

one of the cases listed in the statement. For example, for  $d = 2$ , we obtain the two solutions  $\{a^2 + b^2 - b = c + 1 = d - 2 = 0\}$  and  $\{a^2 + b^2 - b = c - b = d - 2 = 0\}$ . The first is (4) and the second is (8). The other factors follows similarly.  $\square$

**Proposition 5.8.** *For each family in the statement of Theorem 5.2, the quartic system (5.5), which is reversible with respect to the  $x$ -axis, has a center at the origin and two centers at the points  $(-1, \pm d)$ .*

*Proof.* The origin of (5.5) is a nondegenerate center-focus point then, by the symmetry property, it is a center. The points  $(-1, \pm d)$  are also nondegenerate equilibria of center-focus type. The proof follows straightforward doing a case by case study. We compute the first integrals, which are of Darboux type, and check that all of them are well defined in a neighborhood of such equilibrium points. In particular, there are only four types of first integrals:

$$H_1 = f_1, \quad H_2 = f_1^{\lambda_1} f_2^{\lambda_2}, \quad H_3 = f_1^{\lambda_1} (e^g)^\mu, \quad \text{and} \quad H_4 = f_1^{\lambda_1} f_2^{\lambda_2} (e^g)^\mu.$$

In the rest of the proof we only show the explicit expressions of the polynomials  $f_1, f_2, g$  and the real numbers  $\lambda_1, \lambda_2$ , because  $\mu = 1$ . We also list the associated cofactors  $K_{f_1}, K_{f_2}$ , and  $K_g$ , when their expressions are not so big. We recall that  $f_1 = 0$  and  $f_2 = 0$  are invariant algebraic curves and  $e^g$  is an exponential factor.

The cases are listed grouped by the expression of the corresponding first integral.

◦ Cases corresponding to the first integral  $H_1 = f_1$  :

( $\mathcal{T}_3$ ) In this case, we have  $a^2 = -(d^2 c^2 + 2d(d^2 - 5)c + (d^2 - 4)^2)$  and  $b = (cd + d^2 - 4)/d$ . Then, as  $a^2$  should be nonnegative, we have that  $(-d^2 + 5 - \sqrt{-2d^2 + 9})/d < c < (-d^2 + 5 + \sqrt{-2d^2 + 9})/d$ , and  $0 < d < 3\sqrt{2}/2$ . We remark that system (5.5) depends quadratically in  $a$ . With this conditions, we get

$$f_1 = 2d^4 x^2 + 2d^4 y^2 + 2d^3(c + d)xy^2 - (cd + 2d^2 - 4)y^4 - 2(cd + d^2 - 2)xy^4.$$

( $\mathcal{T}_8$ ) Here  $a^2 = c - c^2$ ,  $b = c$ , and  $d = 2$ . Hence, when  $0 < c < 1$ , system (5.5) is well defined. Then,

$$f_1 = 16x^2 + 16y^2 + 8(c + 2)xy^2 - (c + 2)y^4 - 2(c + 1)xy^4.$$

( $\mathcal{T}_{12}$ ) In this case, we have  $a^2 = 2(4 - d^2)/d^2$ ,  $b = 2/d$  and  $c = (6 - d^2)/d$ . Thus, when  $0 < d < 2$ , system (5.5) is well defined and we get

$$f_1 = 2d^4 x^2 + 2d^4 y^2 + 12d^2 xy^2 - (d^2 + 2)y^4 - 8xy^4.$$

( $\mathcal{T}_{14}$ ) Here, we have  $a^2 = 4 - d^2$ ,  $b = (d^2 - 2)/d$  and  $c = 2/d$ . So, the condition  $0 < d < 2$  is necessary and we have

$$f_1 = d^4 x^2 + d^4 y^2 + (d^2 + 2)d^2 xy^2 - (d^2 - 1)y^4 - d^2 xy^4.$$

( $\mathcal{T}_{17}$ ) In this case, we have  $a^2 = 4 - d^2$ ,  $b = (4 - d^2)/d$ , and  $c = 2(4 - d^2)/d$ . Here,  $0 < d < 2$  and

$$f_1 = d^4 x^2 + d^4 y^2 - (d^2 - 8)d^2 xy^2 - 2y^4 + (d^2 - 6)xy^4.$$

◦ Cases corresponding to  $H_2 = f_1^{\lambda_1} f_2^{\lambda_2}$  :

( $\mathcal{T}_1$ ) We can write  $b = 0$  and  $c = a^2 d/2$ , for obtaining

$$\begin{aligned} f_1 &= 2d^6 - 8d^4 x - (2a^2 d^2 + 4d^2 + 16)d^2 y^2 + (a^2 d^2 + 2d^2 + 8)y^4, \\ f_2 &= 2 + (a^2 + 2)x, \\ K_{f_1} &= \frac{4}{d^4}(d^2 - y^2)y, \\ K_{f_2} &= -\frac{(a^2 + 2)}{2d^2}(d^2 - y^2)y, \end{aligned}$$

with  $\lambda_1 = d^2(a^2 + 2)$ ,  $\lambda_2 = 8$ .

( $\mathcal{T}_{16}$ ) Here we have  $a = 2/d$ ,  $b = 0$ , and  $c = 2/d$ . Then, we get  $\lambda_1 = 1$ ,  $\lambda_2 = 4/(d^2 + 2)$ , and

$$\begin{aligned} f_1 &= d^6 - 4d^4 x - 2(d^2 + 6)d^2 y^2 + (d^2 + 6)y^4, \\ f_2 &= d^2 + (d^2 + 2)x, \\ K_{f_1} &= \frac{4(d^2 - y^2)y}{d^4}, \\ K_{f_2} &= -\frac{(d^2 + 2)(d^2 - y^2)y}{d^4}. \end{aligned}$$

◦ Cases corresponding to  $H_3 = f_1^{\lambda_1} (e^g)^\mu$ , with  $\mu = 1$  :

( $\mathcal{T}_2$ ) In this case we have  $b = -2/d$  and

$$-a^2 d^2 c^2 - 2a^2 c d^4 - 8c d^2 + a^4 d^2 - a^2 d^4 + 4a^2 d^2 + 4a^2 - 4d^2 + 16 = 0.$$

As  $a > 0$ , the discriminant  $\sigma = (a^2 + 2)^2(a^2 d^2 + 4)$  is positive for all  $a, d$ . Adding an artificial variable,  $e$ , the curve  $\sigma - e^2 = (a^2 + 2)^2 a^2 d^2 - e^2 + (2a^2 + 4)^2 = 0$  is a hyperbola with respect to the variables  $(d, e)$ . Then, we can find a rational parameterization

$$d = \frac{4(a^2 + 2)^2 - t^2}{2at(a^2 + 2)}$$

such that  $\sigma$  is a perfect square. Hence, we can isolate  $b, c$  in terms of  $a, t$ :

$$\begin{aligned} c(a, t) &= -\frac{(t^2 + 2(a^2 + 2)^2 t + 4(a^2 + 2)^2)(t^2 + 4(a^2 + 2)^2)}{2at(4(a^2 + 2)^2 - t^2)(a^2 + 2)}, \\ b(a, t) &= \frac{4at(a^2 + 2)}{t^2 - 4(a^2 + 2)^2}. \end{aligned}$$

Then, we get  $\lambda_1 = -1$  and

$$\begin{aligned} f_1 &= 4(a^2 + 2)^5 t^3 (2a^2 + t + 4)^2 a^2 x y^2 \\ &\quad - 2(a^2 + 2)^3 a^2 t^2 (t^4 - 8(a^2 + 2)^2 (a^2 + 1)t^2 - 16(a^2 + 2)^4) y^2 \\ &\quad - 2(a^2 + 2)^2 t (4(a^2 + 2)^2 - t^2)^2 (t^2 + 2(a^2 + 2)t + 4(a^2 + 2)^2) x \\ &\quad + (2a^2 - t + 4)^4 (t^2 + 2(a^2 + 2)t + 4(a^2 + 2)^2)^2, \\ g &= \frac{4(a^2 + 2)^3 t^2 y^2}{(2a^2 - t + 4)^4} - \frac{2(a^2 + 2)^2 (2a^2 + t + 4)^2 t x}{(2a^2 - t + 4)^2 (t^2 + 2(a^2 + 2)t + 4(a^2 + 2)^2)}. \end{aligned}$$

We remark that without the parameterization the expressions for  $f_1$  and  $g$  are more difficult to be found.

( $\mathcal{T}_4$ ) Here  $a^2 = b(1 - b)$ ,  $c = -1$  and  $d = 2$ . So, system (5.5) is well defined only when  $0 < b < 1$ . Moreover,  $\lambda_1 = 4b$  and

$$\begin{aligned} f_1 &= -4 + (b + 1)y^2, \\ g &= -(b + 1)((2b + 2)x^2 + (b + 2)y^2 + (b + 1)xy^2), \\ K_{f_1} &= -\frac{(b + 1)(y^2 + 4x)y}{8}, \\ K_g &= \frac{b(b + 1)(y^2 + 4x)y}{2}. \end{aligned}$$

( $\mathcal{T}_6$ ) For this case we have  $a^2 = 2(4 - d^2)/d^2$ ,  $b = 2/d$ , and  $c = -(d^2 + 2)/d$ . So, when  $0 < d < 2$  the system (5.5) is well defined. Additionally,

$$\begin{aligned} f_1 &= d^4(2 + d^2)^2 - 8d^4(d^2 + 2)x - 32d^4y^2 + 64d^2xy^2 + 16(d^2 + 2)y^4, \\ g &= \frac{8x}{d^2 + 2}, \\ K_{f_1} &= \frac{8(d^4 - 2d^2x - (d^2 + 2)y^2)y}{(d^2 + 2)d^4}, \\ K_g &= -\frac{8(d^4 - 2d^2x - (d^2 + 2)y^2)y}{(d^2 + 2)d^4}. \end{aligned}$$

and  $\lambda_1 = 1$ .

( $\mathcal{T}_7$ ) Here,  $a^2 = b(d^2 - bd - 2)/d$  and  $c = -(d^2 - 2)/d$ . There are two cases such that system (5.5) is well defined: (i)  $b > 0$ ,  $d < (b - \sqrt{b^2 + 8})/2$  or  $(b + \sqrt{b^2 + 8})/2 < d$ , and (ii)  $b < 0$ ,  $(b - \sqrt{b^2 + 8})/2 < d < (b + \sqrt{b^2 + 8})/2$ . Independently, we have

$$\begin{aligned} f_1 &= -2d^2 + (bd + 2)y^2, \\ g &= -(bd + 2)((bd^3 + 2d^2)x^2 + (2bd + 2d^2)y^2 + (2bd + 4)xy^2), \\ K_{f_1} &= -\frac{(bd + 2)(y^2 + d^2x)y}{d^4}, \\ K_g &= \frac{2b(d^2 - 2)(bd + 2)(y^2 + d^2x)y}{d}, \end{aligned}$$

with  $\lambda_1 = 2bd^3(d^2 - 2)$ .

( $\mathcal{T}_9$ ) In this case,  $a^2 = (d^2 - 4)/4$ ,  $b = d/2$ , and  $c = -3d/2$ . Hence, when  $d > 2$  system (5.5) is well defined. Here we get

$$\begin{aligned} f_1 &= 18d^6 - (12d^6 + 48d^4)x - (4d^6 + 32d^4 + 64d^2)y^2 + (2d^6 + 16d^4 + 32d^2)xy^2 \\ &\quad + (3d^4 + 24d^2 + 48)y^4, \\ g_1 &= 2x(d^2 + 4)/3d^2, \\ K_{f_1} &= \frac{(d^2 + 4)(3y^3 + d^2x - 2d^2)y}{d^4}, \\ K_g &= -\frac{(d^2 + 4)(3y^3 + d^2x - 2d^2)y}{d^4}, \end{aligned}$$

with  $\lambda_1 = 1$ .

( $\mathcal{T}_{10}$ ) The discriminant with respect to  $c$  of the second condition writes as  $\sigma = 4(a^2d^2 + 2d^2 + 1)$ . Similarly, as for family  $\mathcal{T}_2$ , adding an artificial variable,  $e$ , from the rational parameterization of the hyperbola  $\sigma - e^2 = 0$ , we know that

$$a = \frac{-2d^2 + t^2 - 1}{2dt}.$$

Then, the second condition allow us to write

$$\begin{aligned} b &= \frac{2d^2 + t^2 - 2t + 1}{2dt}, \\ c &= -\frac{2d^2t + 2d^2 + t^2 - 2t + 1}{2dt}. \end{aligned}$$

In fact, the other solution is equivalent changing  $t$  by  $-t$ , moreover system (5.5) depends on  $a^2$ . Hence,

$$\begin{aligned} f_1 &= 2d^4t(2d^2(t+1) + (t-1)^2)^2 - 4d^4t(2d^2 + (t+1)^2)(2d^2(t+1) + (t-1)^2)x \\ &\quad - 4d^4t(2d^2 + (t+1)^2)^2y^2 + 2d^2(2d^2 + (t-1)^2)(2d^2 + (t+1)^2)^2xy^2 \\ &\quad + (2d^2(t+1) + (t-1)^2)(2d^2 + (t+1)^2)^2y^4, \\ g &= \frac{2(2d^2 + (t+1)^2)x}{2d^2(t+1) + (t-1)^2}, \\ K_{f_1} &= \frac{(2d^2 + (t+1)^2)(2d^4t - d^2(2d^2 + (t-1)^2)x - (2d^2(ty^2 + 1) + (t-1)^2)y^2)y}{td^4(2d^2(t+1) + (t-1)^2)}, \\ K_g &= -\frac{(2d^2 + (t+1)^2)(2d^4t - d^2(2d^2 + (t-1)^2)x - (2d^2(ty^2 + 1) + (t-1)^2)y^2)y}{td^4(2d^2(t+1) + (t-1)^2)}. \end{aligned}$$

with  $\lambda_1 = 1$ .

( $\mathcal{T}_{11}$ ) In this case, as  $d > 0$ , we have  $b = \sqrt{a^2 + 1}$ ,  $c = -(2a^2 + 1)/\sqrt{a^2 + 1}$ , and  $d = 2\sqrt{a^2 + 1}$ .

Then,

$$\begin{aligned} f_1 &= -4(1 + a^2) + (a^2 + 2)y^2, \\ g &= (a^2 + 2)((2a^4 + 6a^2 + 4)x^2 + (a^2 + 2)xy^2 + (3a^2 + 3)y^2), \\ K_{f_1} &= -\frac{(a^2 + 2)((4a^2 + 4)x + y^2)y}{8(a^2 + 1)^2}, \\ K_g &= -\frac{(2a^2 + 1)(a^2 + 2)((4a^2 + 4)x + y^2)y}{2}, \end{aligned}$$

with  $\lambda_1 = -4(2a^2 + 1)(a^2 + 1)^2$ .

( $\mathcal{T}_{13}$ ) Here we have  $b = 4/d(d^2 - 2)$ ,  $c = -(d^2 - 2)/d$ , and  $(d^2 - 2)^2 a^2 - 4(d^2 - 4) = 0$ . Last condition can be written equivalently as the rational parameterization

$$(a, d) = \left( \frac{8(2t - 1)(2t + 1)t}{16t^4 + 24t^2 + 1}, -\frac{2(4t^2 + 1)}{(2t - 1)(2t + 1)} \right).$$

This expression simplifies the writing of

$$\begin{aligned} f_1 &= -32t^4 - 48t^2 - 2 + (16t^4 - 8t^2 + 1)y^2, \\ g &= -(512t^8 + 512t^6 + 192t^4 + 32t^2 + 2)x^2 - (384t^8 + 384t^6 + 272t^4 + 24t^2 + 3/2)y^2 \\ &\quad - (256t^8 - 32t^4 + 1)xy^2, \\ K_{f_1} &= -\frac{(4t^2 - 1)^2((64t^4 + 32t^2 + 4)xy + (16t^4 - 8t^2 + 1)y^3)}{4(16t^4 + 24t^2 + 1)(4t^2 + 1)^2}, \\ K_g &= \frac{(4t^2 - 1)^2(16t^4 + 24t^2 + 1)((64t^4 + 32t^2 + 4)xy + (16t^4 - 8t^2 + 1)y^3)}{4(4t^2 + 1)^2}, \end{aligned}$$

with  $\lambda_1 = (16t^4 + 24t^2 + 1)^2$ .

( $\mathcal{T}_{15}$ ) In this case, we have two solutions but, as  $a^2 > 0$ , only one corresponds to real values:

$$a^2 = \frac{-2d^2 + \sqrt{4d^2 + 9} + 3}{2d^2}, \quad b = -\frac{1 - \sqrt{4d^2 + 9}}{2d}, \quad c = \frac{-2d^2 + 1 - \sqrt{4d^2 + 9}}{2d}.$$

Then,

$$\begin{aligned} f_1 &= 2d^6 - (\sigma + 3)d^4 + 8(\sigma - 2)d^2 - 12\sigma + 36 - 2d^2(\sigma d^2 - d^2 - 2\sigma + 6)x \\ &\quad - 4d^4 y^2 + 2d^2(\sigma - 1)xy^2 + (2d^2 + \sigma - 1)y^4, \\ g &= \frac{((\sigma + 1)d^2 - 2\sigma - 6)x}{d^4 - 2d^2 - 2}, \\ K_{f_1} &= \frac{(d^4(\sigma d^2 + d^2 - 2\sigma - 6) + 2d^2(-d^4 + \sigma + 3)x - (d^4 - 2d^2 - 2)(\sigma + 3)y^2)y}{(d^4 - 2d^2 - 2)d^4}, \\ K_g &= -\frac{(d^4(\sigma d^2 + d^2 - 2\sigma - 6) + 2d^2(-d^4 + \sigma + 3)x - (d^4 - 2d^2 - 2)(\sigma + 3)y^2)y}{(d^4 - 2d^2 - 2)d^4}, \end{aligned}$$

with  $\sigma = \sqrt{4d^2 + 9}$  and  $\lambda_1 = 1$ .

◦ Cases corresponding to  $H_4 = f_1^{\lambda_1} f_2^{\lambda_2} (e^g)^\mu$ , with  $\mu = 1$  :

( $\mathcal{T}_5$ ) Here, the parameters satisfy  $a^2 = 4 - d^2$ ,  $b = (4 - d^2)/d$ , and  $c = -4/d$ . Thus, the condition  $0 < d < 2$  is necessary in order that system (5.5) is well defined. Then,

$$\begin{aligned} f_1 &= d^4 + d^2(d^2 - 6)x + (d^2 - 6)y^2, \\ f_2 &= 2d^2 + (d^2 - 6)y^2, \\ g &= (d^2 - 6)x, \\ K_{f_1} &= \frac{(d^2 - 6)(d^2x + y^2)y}{d^4}, \\ K_{f_2} &= -\frac{(d^2 - 6)(d^2 - y^2)y}{d^4}, \\ K_g &= -\frac{(d^2 - 6)(d^4 + (d^2 - 4)d^2x - 4y^2)}{d^4}, \end{aligned}$$

with  $\lambda_1 = -d^2$ ,  $\lambda_2 = d^2 - 4$ .

( $\mathcal{T}_{18}$ ) In this case, we have  $b = a^2/d$  and  $c = -(a^2 + d^2)/d$ . Then,

$$\begin{aligned} f_1 &= -d^4 + d^2(a^2 + 2)x + (a^2 + 2)y^2, \\ f_2 &= -2d^2 + (a^2 + 2)y^2, \\ g &= (a^2 + 2)x, \\ K_{f_1} &= \frac{(a^2 + 2)(d^2 - y^2)y}{d^4}, \\ K_{f_2} &= -\frac{(a^2 + 2)(d^2x + y^2)y}{d^4}, \\ K_g &= \frac{(a^2 + 2)(-d^4 + a^2d^2x + (a^2 + d^2)y^2)y}{d^4}, \end{aligned}$$

with  $\lambda_1 = d^2$ ,  $\lambda_2 = a^2$ . □

## 5.5 Simultaneous cyclicity

This section is devoted to study the simultaneous degenerate Hopf bifurcation of system (5.5) for different values of the parameters  $(a, b, c, d)$ . Before to state and prove the main result of this section, we recall in few words the bifurcation scheme presented in [Chr05] for first order perturbations and degree four systems. The unperturbed system (5.5) has three centers located in the vertex of a triangle. As two of them are symmetric with respect to the  $x$ -axis, we study only two simultaneous degenerated Hopf bifurcations. The bifurcation will be done in two steps. First, we consider a perturbation which is symmetric with respect to the  $x$ -axis to get  $n$  symmetric hyperbolic small limit cycles surrounding the symmetric centers using Theorem 5.5. With this first perturbation, the origin remains as a center. Second, we consider a general perturbation to get  $m$  small hyperbolic limit cycles surrounding the origin, also by Theorem 5.5. We obtain in total  $2n + m$  small limit cycles in configuration  $\langle n, m, n \rangle$ .

Recently, the same procedure has been used in [PT18], but with a higher order development, to some systems with degrees up to ten. Improving the best global Hilbert numbers known up to now for polynomial systems from degree four to ten. Here, as in [Chr05], we only study first order developments of the Lyapunov quantities introduced in Section 5.2.2. The study of higher order perturbations will be done in a near future.

**Proposition 5.9.** *There exist polynomial perturbations of degree four such that at least 13 small limit cycles bifurcate from the centers of system (5.5). They present at least two different configurations varying the parameters  $(a, b, c, d)$ :  $\langle 4, 5, 4 \rangle$  and  $\langle 3, 7, 3 \rangle$ . Moreover the phase portraits in the Poincaré disk for the unperturbed systems are also different. See Figure 5.2.*

*Proof.* The proof follows the bifurcation procedure described in the beginning of this section. We will describe only the statement to get the 13 small limit cycles in configuration  $\langle 4, 5, 4 \rangle$ , fixing the values of the parameter of the unperturbed center as  $(a, b, c, d) = (1/2, 1/2, -1, 2)$ . It corresponds to family  $\mathcal{T}_4$ . The same result and configuration can be found in family  $\mathcal{T}_7$ , fixing the parameters to  $(1/2, -1/2, 1, 1)$ . The phase portraits of the unperturbed systems are drawn in the two left pictures in Figure 5.2. In the same way, we can also obtain the 13 small limit cycles bifurcating from the centers of families  $\mathcal{T}_9$  and  $\mathcal{T}_{15}$ , fixing now the parameter values to  $(\sqrt{5}/2, 3/2, -9/2, 3)$  and  $(1, 3\sqrt{7}/7, -13\sqrt{7}/14, \sqrt{7}/2)$ , respectively. The configuration of limit cycles is now  $\langle 3, 7, 3 \rangle$ . The respective phase portraits are drawn in the two right pictures in Figure 5.2.

First we take a perturbation of system (5.5), for the fixed values in  $\mathcal{T}_4$  mentioned above, keeping the reversibility symmetry at the origin,

$$\begin{aligned} \dot{x} &= -y - \frac{1}{2}xy + \frac{5}{16}y^3 + \frac{3}{16}xy^3 + \sum_{k+2\ell+1=1}^4 f_{k,2\ell+1} x^k y^{2\ell+1}, \\ \dot{y} &= x + \frac{1}{4}y^2 - \frac{3}{8}xy^2 - \frac{3}{32}y^4 + \sum_{k+2\ell=1}^4 f_{k,2\ell} x^k y^{2\ell}. \end{aligned} \tag{5.13}$$

It is important to mention that it is not restrictive to assume that the origin remains as an equilibrium point of center type. Then, we do a translation in (5.13) in order that the center  $(-1, 2)$  moves to the origin. Moreover, after the translation, the perturbation should start with terms of degree 2. Because the last limit cycle appears moving the value of the trace at  $(-1, 2)$  in a usual Hopf bifurcation. This fact restrict the values of the perturbation parameters  $f_{k,\ell}$ . Now, we can compute and check that the linear developments of the first four Lyapunov quantities are linearly independent. Hence, we have found at least four small limit cycles surrounding  $(-1, 2)$  and  $(-1, -2)$ , respectively.

Second, it is enough to consider only a perturbation that does not respect the symmetry

around the  $x$ -axis,

$$\begin{aligned} \dot{x} &= -y - \frac{1}{2}xy + \frac{5}{16}y^3 + \frac{3}{16}xy^3 + \sum_{k+2\ell=2}^4 e_{k,2\ell} x^k y^{2\ell}, \\ \dot{y} &= x + \frac{1}{4}y^2 - \frac{3}{8}xy^2 - \frac{3}{32}y^4 + \sum_{k+2\ell+1=2}^4 e_{k,2\ell+1} x^k y^{2\ell+1}. \end{aligned} \quad (5.14)$$

Here we compute and check, as above, that the linear developments of the first 5 Lyapunov quantities are linearly independent. Then, we get five small limit cycles surrounding the origin, via a degenerated Hopf bifurcation. We remark that the last limit cycle also appear moving the trace at the origin from zero to a nonzero value, in a usual Hopf bifurcation.

We remark that the parameters that control both bifurcations, (5.13) and (5.14), are independent. Considering all together we have at least 13 limit cycles in configuration  $\langle 4, 5, 4 \rangle$ .  $\square$

We remark that, in the last result, we have not obtained more limit cycles from a first order analysis because using more Lyapunov quantities we have not more rank to increase the number of limit cycles. Moreover, we have only stated the highest value for the total cyclicity found, studying all the cases listed in Theorem 5.2. We have not done a complete study and we have worked only up to a first order study. We have picked a point  $(a, b, c, d)$  in each of the 18 families and we have obtained which are the ones that provide the highest cyclicity value. The cases with 13 limit cycles, in configuration  $\langle 4, 5, 4 \rangle$ , corresponds to families  $\mathcal{T}_4, \mathcal{T}_7, \mathcal{T}_{11}$ , and  $\mathcal{T}_{13}$  and, in configuration  $\langle 3, 7, 3 \rangle$ , to families  $\mathcal{T}_1, \mathcal{T}_2, \mathcal{T}_6, \mathcal{T}_9, \mathcal{T}_{15}$ , and  $\mathcal{T}_{18}$ . Other families provide less limit cycles. The families  $\mathcal{T}_5, \mathcal{T}_{10}$ , and  $\mathcal{T}_{16}$  exhibit 11 limit cycles in configuration  $\langle 2, 7, 2 \rangle$ . Also 11 appear in configuration  $\langle 3, 5, 3 \rangle$  for families  $\mathcal{T}_8, \mathcal{T}_{14}$ , and  $\mathcal{T}_{17}$ . Finally, family  $\mathcal{T}_{12}$  is the one with less limit cycles, only 9 in configuration  $\langle 2, 5, 2 \rangle$ .

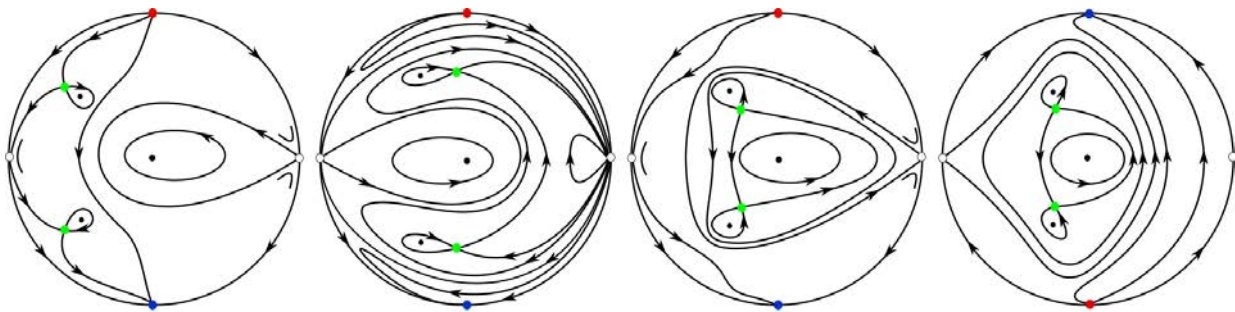


Figure 5.2: Different phase portraits in the Poincaré disc of system (5.5)

The equilibrium points in Figure 5.2 are drawn following the local phase portraits: The centers points in black, the stable nodes in blue, the unstable nodes in red, the saddles in green and the degenerated ones in white. In this last equilibrium points some blowups have been necessary to be done to get the local phase portrait. We remark that the two left centers in Figure 5.2 have three period annulus while the two right ones have four.

# Summary

---

The thesis deals with the study of isolated periodic orbits, the so called limit cycles, in some differential and piecewise differential systems in the plane. This is one of the most important topic in the Qualitative Theory of Differential Equations. The work is structured in an introduction as a first chapter and then four chapters where the results and proofs are developed.

The introduction starts with the most important historical problems studied in qualitative theory of differential equations centered in the main object studied in this work, the limit cycles. It finishes with the summary of the obtained results.

In Chapter 2 we study the number of periodic orbits that bifurcate from a cubic polynomial vector field having two period annuli via piecewise perturbations. The unperturbed cubic planar system simultaneously has a center at the origin and at infinity. We study, up to first order averaging analysis, the bifurcation of periodic orbits from the two period annuli, first separately and second simultaneously. When the polynomial perturbation has degree  $n$ , the inner and outer Abelian integrals are rational functions and we provide an upper bound for the number of simple zeros. The maximum number of limit cycles, up to first order cubic perturbation, from the inner and outer annuli is 9 and 8, respectively. When the simultaneous cubic polynomial bifurcation problem is considered, 12 limit cycles exist. They appear in three configuration types:  $\langle 9, 3 \rangle$ ,  $\langle 6, 6 \rangle$ , and  $\langle 4, 8 \rangle$ . In the non-piecewise scenario, only 5 limit cycles were found.

The number of limit cycles bifurcating from a piecewise quadratic system is studied in Chapter 3. All the differential systems considered are piecewise in two zones separated by a straight line. We prove the existence of 16 crossing limit cycles in this class of systems. As far as we are concerned, this is the best lower bound for the quadratic class. All the limit cycles appear in one nest bifurcating from the period annulus of some isochronous quadratic centers. We do a first and second averaging analysis. This is done perturbing all the isochronous quadratic systems having a birational linearization.

The Bendixson–Dulac Theorem provides a criterion to find upper bounds for the number of limit cycles in analytic differential systems. We extend this classical result to some classes of piecewise differential systems in Chapter 4. This is done in the class of piecewise differential systems where the Green Theorem applies. We apply it to three different Liénard piecewise differential systems. The first is linear, the second is rational and the last corresponds to a particular extension of the cubic van der Pol oscillator. In all cases, the systems present regions in the parameter space with no limit cycles and others having at most one. This extension has no a limit cycle in the full parameters space. It presents a heteroclinic

connection where the limit cycle disappears.

In Chapter 5 we study the family of quartic linear-like time reversible polynomial systems having a nondegenerate center at the origin. This family has degree one with respect to one of the variables. We are interested in systems in this class having also two extra nondegenerate centers outside the straight line of symmetry. The geometrical configuration of these centers is aligned or triangular. We solve the center problem in both situations. When the centers are in a triangular position we study the number of limit cycles appearing by a simultaneous degenerated Hopf bifurcation. Up to a first order analysis we obtain 13 limit cycles in two configuration types:  $\langle 4, 5, 4 \rangle$  and  $\langle 3, 7, 3 \rangle$ .

# Resum

---

La tesi tracta de l'estudi d'òrbites periòdiques aïllades, que anomenarem cicles límits, en alguns sistemes diferencials i diferencials a trossos en el pla. Aquest és un dels temes més importants de la Teoria Qualitativa de les Equacions Diferencials. El treball s'estructura en una introducció com a primer capítol i en quatre capítols on es desenvolupen els resultats i les proves.

La introducció s'inicia amb els problemes històrics més importants estudiats en la teoria qualitativa de les equacions diferencials centrades en l'objecte principal estudiat en aquest treball, els cicles límits. Acaba amb el resum dels resultats obtinguts.

En el capítol 2, estudiem el nombre d'òrbites periòdiques que bifurquen usant pertorbacions a trossos d'un camp vectorial polinòmic cúbic que té dos anells de període. L'origen i l'infinit del sistema no pertorbat és de tipus centre. Estudiem, usant anàlisi del promig a primer ordre, la bifurcació d'òrbites periòdiques en els dos anells, primer separatament i segon simultàniament. Quan la pertorbació polinòmica té un grau  $n$ , les integrals Abelianes internes i externes són funcions racionals i donem una cota superior pel nombre de zeros simples. El nombre màxim de cicles límits, usant una pertorbació cúbica i el mètode del promig a primer ordre, dels anells intern i extern és 9 i 8, respectivament. Quan es considera el problema de bifurcació polinòmica cúbica però de manera simultània, existeixen 12 cicles límit. Aquests es presenten en tres tipus de configuració:  $\langle 9, 3 \rangle$ ,  $\langle 6, 6 \rangle$ , i  $\langle 4, 8 \rangle$ . En l'escenari analític, només es van trobar 5 cicles límit.

El nombre de cicles límits que bifurquen d'un sistema quadràtic definit en dos trossos es desenvolupa en el capítol 3. Es consideren només sistemes diferencials quadràtics definits en dues zones separades per una recta i demostrem l'existència de 16 cicles límit. Pel que sabem, aquest és el millor resultat per a aquesta classe de sistemes. Tots els cicles límits apareixen en un sol niu, tot bifurcant de l'anell de període d'alguns centres quadràtics isòcrons. Usem el mètode del promig de primer i segon ordre. Això es fa pertorbant tots els sistemes quadràtics isòcrons que tenen una linealització biracional.

El Teorema de Bendixson-Dulac proporciona un criteri per a trobar cotes superiors pel nombre de cicles límits en sistemes diferencials analítics. Extenem aquest resultat a algunes classes de sistemes diferencials a trossos en el Capítol 4. Això es fa per sistemes diferencials a trossos pels que el Teorema de Green té validesa. Ho apliquem a tres tipus diferents de sistemes diferencials de Liénard. El primer és lineal, el segon és racional i l'últim correspon a una extensió particular de l'oscil·lador cúbic de van der Pol. En tots els casos, els sistemes presenten regions en l'espai de paràmetres sense cicles límits i altres que en tenen com a màxim un. Aquesta extensió no té sempre exhibeix un cicle límit. A més, presenta una

connexió heteroclina on desapareix el cicle límit.

En el capítol 5 estudiem una família de sistemes diferencials polinòmics reversibles de grau 4, que tenen un centre no degenerat a l'origen. Aquesta família té grau un respecte a una de les variables. Ens interessen els sistemes d'aquesta classe que tenen també dos centres no degenerats fora de la recta de simetria. La configuració geomètrica d'aquests centres és alineada o triangular. Resolem el problema de centre en ambdues situacions. Quan els centres es troben en una posició triangular, estudiem el nombre de cicles límits que apareixen per una bifurcació degenerada de Hopf simultània. Fent una anàlisi de primer ordre obtenim 13 cicles de límit en dos tipus de configuració:  $\langle 4, 5, 4 \rangle$  i  $\langle 3, 7, 3 \rangle$ .

# Resumo

---

A tese trata do estudo de órbitas periódicas isoladas, os chamados ciclos limite, em alguns sistemas diferenciais e diferenciais por partes no plano. Este é um dos tópicos mais importantes da Teoria Qualitativa das Equações Diferenciais. O trabalho é estruturado em uma introdução com um primeiro capítulo e, em seguida, quatro capítulos onde os resultados e as provas são desenvolvidos.

A introdução parte dos problemas históricos mais importantes estudados na teoria qualitativa das equações diferenciais centradas no objeto principal estudado neste trabalho, os ciclos limite. Termina com o resumo dos resultados obtidos.

No Capítulo 2, estudamos o número de órbitas periódicas que se bifurcam a partir de um campo vetorial polinomial cúbico com dois anéis de período por meio de perturbações por partes. O sistema planar cúbico não perturbado possui simultaneamente um centro na origem e no infinito. Estudamos, até a análise da média de primeira ordem, a bifurcação de órbitas periódicas dos dois anéis de período, primeiro separadamente e segundo simultaneamente. Quando a perturbação polinomial tem grau  $n$ , as integrais Abelianas internas e externas são funções racionais e fornecemos um limite superior para o número de zeros simples. O número máximo de ciclos limite, até a perturbação cúbica de primeira ordem, dos anéis interno e externo é 9 e 8, respectivamente. Quando o problema simultâneo de bifurcação polinomial cúbica é considerado, existem 12 ciclos limite. Eles aparecem em três tipos de configuração:  $\langle 9, 3 \rangle$ ,  $\langle 6, 6 \rangle$ , e  $\langle 4, 8 \rangle$ . No cenário analítico, apenas 5 ciclos limite foram encontrados.

O número de ciclos limite bifurcando a partir de um sistema quadrático por partes é estudado no Capítulo 3. Todos os sistemas diferenciais por partes considerados são em duas zonas separadas por uma linha reta. Provamos a existência de 16 ciclos limite nesta classe de sistemas. No que nos diz respeito, esse é o melhor limite inferior para a classe quadrática. Todos os ciclos limites aparecem em um ninho bifurcando-se a partir do anel de período de alguns centros quadráticos isócronos. Nós fazemos uma análise da média de primeira e segunda ordem. Isto é feito perturbando todos os sistemas quadráticos isócronos tendo uma linearização biracional.

O Teorema de Bendixson-Dulac fornece um critério para encontrar limites superiores para o número de ciclos limite em sistemas diferenciais analíticos. Extendemos esse resultado clássico para algumas classes de sistemas diferenciais por partes no Capítulo 4. Isso é feito na classe de sistemas diferenciais por partes onde o Teorema de Green se aplica. Nós aplicamos a três sistemas diferenciais diferentes de Liénard. O primeiro é linear, o segundo é racional e o último corresponde a uma extensão particular do oscilador cúbico de van der Pol. Em todos os casos, os sistemas apresentam regiões no espaço de parâmetros sem ciclos limite e

outros tendo no máximo um. Esta extensão não possui um ciclo limite para todos os valores dos parâmetros. Apresenta uma conexão heteroclínica onde o ciclo limite desaparece.

No Capítulo 5, estudamos a família de sistemas polinomiais reversíveis quártico com um centro não degenerado na origem. Esta família tem grau um em relação a uma das variáveis. Nós estamos interessados ??em sistemas nesta classe tendo também dois centros extra também não degenerados fora da reta de simetria. A configuração geométrica desses centros é alinhada ou triangular. Nós resolvemos o problema de centro em ambas situações. Quando os centros estão em uma posição triangular, estudamos o número de ciclos limite que aparecem por uma bifurcação de Hopf degenerada simultânea. Até uma análise de primeira ordem, obtemos 13 ciclos limite em dois tipos de configuração:  $\langle 4, 5, 4 \rangle$  e  $\langle 3, 7, 3 \rangle$ .

# Bibliography

---

- [ABB11] V. Acary, O. Bonnefon, and B. Brogliato. *Nonsmooth modeling and simulation for switched circuits*, volume 69 of *Lecture Notes in Electrical Engineering*. Springer, Dordrecht, 2011.
- [Bau54] N. N. Bautin. On the number of limit cycles which appear with the variation of coefficients from an equilibrium position of focus or center type. *American Math. Soc. Translation*, 1954(100):19, 1954.
- [BCE18] C. A. Buzzi, T. Carvalho, and R. D. Euzébio. On Poincaré–Bendixson theorem and non-trivial minimal sets in planar nonsmooth vector fields. *Publ. Mat.*, 62(1):113–131, 2018.
- [BGT18] C. A. Buzzi, A. Gasull, and J. Torregrosa. Algebraic limit cycles in piecewise linear differential systems. *Internat. J. Bifur. Chaos Appl. Sci. Engrg.*, 28(03):1850039, 2018.
- [BL04] A. Buică and J. Llibre. Averaging methods for finding periodic orbits via Brouwer degree. *Bull. Sci. Math.*, 128(1):7–22, 2004.
- [BPT13] C. Buzzi, C. Pessoa, and J. Torregrosa. Piecewise linear perturbations of a linear center. *Discrete Contin. Dyn. Syst.*, 33(9):3915–3936, 2013.
- [BS06] Y. L. Bondar and A. P. Sadovskii. Solution of the center and focus problem for a cubic system that reduces to the Liénard system. *Differ. Uravn.*, 42(1):11–22, 141, 2006.
- [CG95] J. Chavarriga and J. Giné. Integrability of a linear center perturbed by homogeneous polynomial. In *Proceedings of the 2nd Catalan Days on Applied Mathematics (Odeillo, 1995)*, Collect. Études, pages 61–75. Presses Univ. Perpignan, Perpignan, 1995.
- [CG96] J. Chavarriga and J. Giné. Integrability of cubic systems with degenerate infinity. In *XIV CEDYA/IV Congress of Applied Mathematics (Spanish)(Vic, 1995)*, page 12. Univ. Barcelona, Barcelona, 1996.
- [CGMnMn97] A. Cima, A. Gasull, V. Mañosa, and F. Mañosas. Algebraic properties of the Liapunov and period constants. *Rocky Mountain J. Math.*, 27(2):471–501, 1997.

- [CGP01] B. Coll, A. Gasull, and R. Prohens. Degenerate Hopf bifurcations in discontinuous planar systems. *J. Math. Anal. Appl.*, 253(2):671–690, 2001.
- [CH82] S. N. Chow and J. K. Hale. *Methods of bifurcation theory*, volume 251 of *Grundlehren der Mathematischen Wissenschaften [Fundamental Principles of Mathematical Science]*. Springer-Verlag, New York-Berlin, 1982.
- [Che97] L. A. Cherkas. The Dulac function for polynomial autonomous systems on a plane. *Differ. Uravn.*, 33(5):689–699, 719, 1997.
- [Chi06] C. Chicone. *Ordinary differential equations with applications*, volume 34 of *Texts in Applied Mathematics*. Springer, New York, second edition, 2006.
- [Chr05] C. Christopher. Estimating limit cycle bifurcations from centers. In *Differential equations with symbolic computation*, Trends Math., pages 23–35. Birkhäuser, Basel, 2005.
- [CJ89] C. Chicone and M. Jacobs. Bifurcation of critical periods for plane vector fields. *Trans. Amer. Math. Soc.*, 312(2):433–486, 1989.
- [CJ91] C. Chicone and M. Jacobs. Bifurcation of limit cycles from quadratic isochrones. *J. Differential Equations*, 91(2):268–326, 1991.
- [CL95] C. J. Christopher and N. G. Lloyd. Polynomial systems: a lower bound for the Hilbert numbers. *Proc. Roy. Soc. London Ser. A*, 450(1938):219–224, 1995.
- [CL07] C. Christopher and C. Li. *Limit cycles of differential equations*. Advanced Courses in Mathematics. CRM Barcelona. Birkhäuser Verlag, Basel, 2007.
- [CLP09] B. Coll, C. Li, and R. Prohens. Quadratic perturbations of a class of quadratic reversible systems with two centers. *Discrete Contin. Dyn. Syst.*, 24(3):699–729, 2009.
- [CLYZ18] X. Cen, C. Liu, L. Yang, and M. Zhang. Limit cycles by perturbing quadratic isochronous centers inside piecewise polynomial differential systems. *J. Differential Equations*, 2018. In press.
- [CNT18] L. P. C. Cruz, D. D. Novaes, and J. Torregrosa. New lower bound for the Hilbert number in piecewise quadratic differential systems. Preprint, 2018.
- [Coz15] D. Cozma. The problem of the center for cubic systems with two parallel invariant straight lines and one invariant cubic. *Romai J.*, 11(2):63–75, 2015.
- [CRT18] L. P. C. Cruz, V. Romanovsky, and J. Torregrosa. The center and cyclicity problems for quartic linear-like reversible systems. Work in progress, 2018.

- [CS98] D. Cozma and A. Subua. The solution of the problem of center for cubic differential systems with four invariant straight lines. *An. Științ. Univ. Al. I. Cuza Iași. Mat. (N.S.)*, 44(suppl.):517–530 (2000), 1998. *Math. Anal. Appl.* (Iași, 1997).
- [CS99] J. Chavarriga and M. Sabatini. A survey of isochronous centers. *Qual. Theory Dyn. Syst.*, 1(1):1–70, 1999.
- [CT18a] L. P. C. Cruz and J. Torregrosa. A Bendixson–Dulac theorem for some piecewise systems. Preprint, 2018.
- [CT18b] L. P. C. Cruz and J. Torregrosa. Simultaneous bifurcation of limit cycles from a cubic piecewise center with two period annuli. *J. Math. Anal. Appl.*, 461(1):248–272, 2018.
- [dBCK08] M. di Bernardo, C. J. Budd, A. R. Champneys, and P. Kowalczyk. *Piecewise-smooth dynamical systems*, volume 163 of *Applied Mathematical Sciences*. Springer-Verlag London, Ltd., London, 2008. Theory and applications.
- [DGPS18] W. Decker, G.-M. Greuel, G. Pfister, and H. Schönemann. SINGULAR 4-1-1 — A computer algebra system for polynomial computations. <http://www.singular.uni-kl.de>, 2018.
- [DL03] F. Dumortier and C. Li. Perturbation from an elliptic Hamiltonian of degree four. IV. Figure eight-loop. *J. Differential Equations*, 188(2):512–554, 2003.
- [DLA06] F. Dumortier, J. Llibre, and J. C. Artés. *Qualitative theory of planar differential systems*. Universitext. Springer-Verlag, Berlin, 2006.
- [DPSL18] W. Decker, G. Pfister, H. Schönemann, and S. Laplagne. `primdec.lib` a SINGULAR 4-1-1 library for computing the primary decomposition and radical ideals, 2018.
- [Dul08] H. Dulac. Détermination et intégration d’une certaine class d’équations différentielles ayant pour point singulier un centre. *Bull. Sci. Math.*, 32(2):230–252, 1908.
- [Fat28] P. Fatou. Sur le mouvement d’un système soumis à des forces à courte période. *Bull. Soc. Math. France*, 56:98–139, 1928.
- [Fil52] A. F. Filippov. A sufficient condition for the existence of a stable limit cycle for an equation of the second order. *Mat. Sbornik N.S.*, 30(72):171–180, 1952.
- [Fil88] A. F. Filippov. *Differential equations with discontinuous righthand sides*, volume 18 of *Mathematics and its Applications (Soviet Series)*. Kluwer Academic Publishers Group, Dordrecht, 1988. Translated from the Russian.

- [FPT12] E. Freire, E. Ponce, and F. Torres. Canonical discontinuous planar piecewise linear systems. *SIAM J. Appl. Dyn. Syst.*, 11(1):181–211, 2012.
- [FPT14] E. Freire, E. Ponce, and F. Torres. The discontinuous matching of two planar linear foci can have three nested crossing limit cycles. *Publ. Mat.*, 58(suppl.):221–253, 2014.
- [Fro34] M. Frommer. Über das Auftreten von Wirbeln und Strudeln (geschlossener und spiraliiger Integralkurven) in der Umgebung rationaler Unbestimmtheitsstellen. *Math. Ann.*, 109(1):395–424, 1934.
- [GG10] A. Gasull and H. Giacomini. Upper bounds for the number of limit cycles of some planar polynomial differential systems. *Discrete Contin. Dyn. Syst.*, 27(1):217–229, 2010.
- [GG13] A. Gasull and H. Giacomini. Some applications of the extended Bendixson–Dulac theorem. In *Progress and challenges in dynamical systems*, volume 54 of *Springer Proc. Math. Stat.*, pages 233–252. Springer, Heidelberg, 2013.
- [GGJ08] A. Garijo, A. Gasull, and X. Jarque. Simultaneous bifurcation of limit cycles from two nests of periodic orbits. *J. Math. Anal. Appl.*, 341(2):813–824, 2008.
- [GGT10] A. Gasull, H. Giacomini, and J. Torregrosa. Some results on homoclinic and heteroclinic connections in planar systems. *Nonlinearity*, 23(12):2977–3001, 2010.
- [GLT12] A. Gasull, J. T. Lázaro, and J. Torregrosa. Upper bounds for the number of zeroes for some Abelian integrals. *Nonlinear Anal.*, 75(13):5169–5179, 2012.
- [GLV96] H. Giacomini, J. Llibre, and M. Viano. On the nonexistence, existence and uniqueness of limit cycles. *Nonlinearity*, 9(2):501–516, 1996.
- [GSnGG15] J. D. García-Saldaña, A. Gasull, and H. Giacomini. Bifurcation values for a family of planar vector fields of degree five. *Discrete Contin. Dyn. Syst.*, 35(2):669–701, 2015.
- [GT03] A. Gasull and J. Torregrosa. Center-focus problem for discontinuous planar differential equations. *Internat. J. Bifur. Chaos Appl. Sci. Engrg.*, 13(7):1755–1765, 2003. *Dynamical systems and functional equations (Murcia, 2000)*.
- [GTZ88] P. Gianni, B. Trager, and G. Zacharias. Gröbner bases and primary decomposition of polynomial ideals. *J. Symbolic Comput.*, 6(2-3):149–167, 1988. *Computational aspects of commutative algebra*.
- [Han99] M. Han. Liapunov constants and Hopf cyclicity of Liénard systems. *Ann. Differential Equations*, 15(2):113–126, 1999.

- [HK91] J. K. Hale and H. Koçak. *Dynamics and bifurcations*, volume 3 of *Texts in Applied Mathematics*. Springer-Verlag, New York, 1991.
- [HY12] S.-M. Huan and X.-S. Yang. On the number of limit cycles in general planar piecewise linear systems. *Discrete Contin. Dyn. Syst.*, 32(6):2147–2164, 2012.
- [ILN17] J. Itikawa, J. Llibre, and D. D. Novaes. A new result on averaging theory for a class of discontinuous planar differential systems with applications. *Rev. Mat. Iberoam.*, 33(4):1247–1265, 2017.
- [Ily02] Y. Ilyashenko. Centennial history of Hilbert’s 16th problem. *Bull. Amer. Math. Soc. (N.S.)*, 39(3):301–354, 2002.
- [IY08] Y. Ilyashenko and S. Yakovenko. *Lectures on analytic differential equations*, volume 86 of *Graduate Studies in Mathematics*. American Mathematical Society, Providence, RI, 2008.
- [Kap11] W. Kaptyn. On the midpoints of integral curves of differential equations of the first degree. *Nederl. Adak. Wetensch. Verslag. Afd. Natuurk. Koninkl.*, pages 1446–1457, 1911.
- [Kap12] W. Kaptyn. New investigations on the midpoints of integral of differential equations of the first degree. *Nederl. Adak. Wetensch. Verslag. Afd. Natuurk. Koninkl.*, 20:1354–1365, 1912.
- [Kho84] A. Khovanskii. Cycles of dynamical systems on the plane and Rolle’s theorem. *Siberian Mathematical Journal*, 25(3):502–506, 1984.
- [KS66] S. Karlin and W. J. Studden. *Tchebycheff systems: With applications in analysis and statistics*. Pure and Applied Mathematics, Vol. XV. Interscience Publishers John Wiley & Sons, New York-London-Sydney, 1966.
- [Kul97] W. Kulpa. The Poincaré–Miranda theorem. *Amer. Math. Monthly*, 104(6):545–550, 1997.
- [LCD+97] N. G. Lloyd, C. J. Christopher, J. Devlin, J. M. Pearson, and N. Yasmin. Quadratic-like cubic systems. *Differential Equations Dynam. Systems*, 5(3-4):329–345, 1997. Planar nonlinear dynamical systems (Delft, 1995).
- [LdMP77] A. Lins, W. de Melo, and C. C. Pugh. On Liénard’s equation. In *Geometry and topology (Proc. III Latin Amer. School of Math., Inst. Mat. Pura Aplicada CNPq, Rio de Janeiro, 1976)*, pages 335–357. Lecture Notes in Math., Vol. 597. Springer, Berlin, 1977.
- [Li03] J. Li. Hilbert’s 16th problem and bifurcations of planar polynomial vector fields. *Internat. J. Bifur. Chaos Appl. Sci. Engrg.*, 13(1):47–106, 2003.

- [Lia93] A. M. Liapunov. Investigation of one of the special cases of the stability of motion. *Mat. Sb.*, 17:253–333, 1893.
- [Lia47] A. M. Liapunov. *Problème Général de la Stabilité du Mouvement*. Annals of Mathematics Studies, no. 17. Princeton University Press, Princeton, N. J.; Oxford University Press, London, 1947.
- [LL12] C. Li and J. Llibre. Uniqueness of limit cycles for Liénard differential equations of degree four. *J. Differential Equations*, 252(4):3142–3162, 2012.
- [LL17] S. Li and J. Llibre. Phase portraits of piecewise linear continuous differential systems with two zones separated by a straight line. Preprint, December 2017.
- [LLY09] C. Li, C. Liu, and J. Yang. A cubic system with thirteen limit cycles. *J. Differential Equations*, 246(9):3609–3619, 2009.
- [LM14] J. Llibre and A. C. Mereu. Limit cycles for discontinuous quadratic differential systems with two zones. *J. Math. Anal. Appl.*, 413(2):763–775, 2014.
- [LMN15] J. Llibre, A. C. Mereu, and D. D. Novaes. Averaging theory for discontinuous piecewise differential systems. *J. Differential Equations*, 258(11):4007–4032, 2015.
- [LNT15a] J. Llibre, D. D. Novaes, and M. A. Teixeira. Limit cycles bifurcating from the periodic orbits of a discontinuous piecewise linear differentiable center with two zones. *Internat. J. Bifur. Chaos Appl. Sci. Engrg.*, 25(11):1550144, 11, 2015.
- [LNT15b] J. Llibre, D. D. Novaes, and M. A. Teixeira. On the birth of limit cycles for non-smooth dynamical systems. *Bull. Sci. Math.*, 139(3):229 – 244, 2015.
- [Lou64] W. S. Loud. Behavior of the period of solutions of certain plane autonomous systems near centers. *Contributions to Differential Equations*, 3:21–36, 1964.
- [LP03] J. Llibre and E. Ponce. Piecewise linear feedback systems with arbitrary number of limit cycles. *Internat. J. Bifur. Chaos Appl. Sci. Engrg.*, 13(4):895–904, 2003.
- [LP12] J. Llibre and E. Ponce. Three nested limit cycles in discontinuous piecewise linear differential systems with two zones. *Dyn. Contin. Discrete Impuls. Syst. Ser. B Appl. Algorithms*, 19(3):325–335, 2012.
- [LPdRR01] J. Llibre, J. S. Pérez del Río, and J. A. Rodríguez. Averaging analysis of a perturbed quadratic center. *Nonlinear Anal.*, 46(1, Ser. A: Theory Methods):45–51, 2001.

- [LPT08] J. Llibre, E. Ponce, and F. Torres. On the existence and uniqueness of limit cycles in Liénard differential equations allowing discontinuities. *Nonlinearity*, 21(9):2121–2142, 2008.
- [LR97] J.-M. Lion and J.-P. Rolin. Théorème de préparation pour les fonctions logarithmico-exponentielles. *Ann. Inst. Fourier (Grenoble)*, 47(3):859–884, 1997.
- [LT14] J. Llibre and A. E. Teruel. *Introduction to the qualitative theory of differential systems*. Birkhäuser Advanced Texts: Basler Lehrbücher. [Birkhäuser Advanced Texts: Basel Textbooks]. Birkhäuser/Springer, Basel, 2014.
- [LT16] J. Llibre and Y. Tang. Limit cycles of discontinuous piecewise quadratic and cubic polynomial perturbations of a linear center. Preprint, 2016.
- [MH09] H. Ma and M. Han. Limit cycles of a  $Z_3$ -equivariant near-Hamiltonian system. *Nonlinear Anal.*, 71(9):3853–3871, 2009.
- [MHL09] H. Ma, M. Han, and C. Lhotka. Limit cycles of some  $Z_3$ -equivariant near-Hamiltonian systems of degrees 3 and 4. *Ann. Differential Equations*, 25(2):170–178, 2009.
- [MRT95] P. Mardešić, C. Rousseau, and B. Toni. Linearization of isochronous centers. *J. Differ. Equations*, 121(1):67–108, 1995.
- [MT15] J. C. Medrado and J. Torregrosa. Uniqueness of limit cycles for sewing piecewise linear systems. *J. Math. Anal. Appl.*, 431:529–544, 2015.
- [NT17] D. D. Novaes and J. Torregrosa. On extended Chebyshev systems with positive accuracy. *J. Math. Anal. Appl.*, 448(1):171–186, 2017.
- [PGT14] S. Pérez-González and J. Torregrosa. Simultaneous bifurcation of limit cycles from a linear center with extra singular points. *Bull. Sci. Math.*, 138(1):124–138, 2014.
- [Poi17] H. Poincaré. Mémoire sur les courbes définies par une équation différentielle. Sér.3)7(1881), 375–422; Sér.(3)8(1882),251–296; Sér.(4)1(1885),167–244; Sér.(4)2(1886), 151–217.
- [PT14] R. Prohens and J. Torregrosa. Periodic orbits from second order perturbation via rational trigonometric integrals. *Phys. D*, 280/281:59–72, 2014.
- [PT18] R. Prohens and J. Torregrosa. New lower bounds for the Hilbert numbers using reversible centers. Preprint, 2018.
- [Rou98] R. Roussarie. *Bifurcation of planar vector fields and Hilbert’s sixteenth problem*, volume 164 of *Progress in Mathematics*. Birkhäuser Verlag, Basel, 1998.

- [RS09] V. G. Romanovski and D. S. Shafer. *The center and cyclicity problems: a computational algebra approach*. Birkhäuser Boston, Inc., Boston, MA, 2009.
- [RS16] V. G. Romanovski and D. S. Shafer. Centers and limit cycles in polynomial systems of ordinary differential equations. In *School on real and complex singularities in São Carlos, 2012*, volume 68 of *Adv. Stud. Pure Math.*, pages 267–373. Math. Soc. Japan, [Tokyo], 2016.
- [Sah48] N. A. Saharnikov. On Frommer’s conditions for the existence of a center. *Akad. Nauk SSSR. Prikl. Mat. Meh.*, 12:669–670, 1948.
- [San12] B. Sang. Center-focus problems for two classes of cubic differential systems. *J. Nanjing Norm. Univ. Nat. Sci. Ed.*, 35(2):16–21, 2012.
- [SB02] J. Stoer and R. Bulirsch. *Introduction to numerical analysis*, volume 12 of *Texts in Applied Mathematics*. Springer-Verlag, New York, 3rd edition, 2002.
- [Shi80] S. L. Shi. A concrete example of the existence of four limit cycles for plane quadratic systems. *Sci. Sinica*, 23(2):153–158, 1980.
- [Sib54] K. S. Sibirskiĭ. On conditions for the presence of a center and a focus. *Kišinev. Gos. Univ. Uč. Zap.*, 11:115–117, 1954.
- [Sib55] K. S. Sibirskiĭ. The principle of symmetry and the problem of the center. *Kišinev. Gos. Univ. Uč. Zap.*, 17:27–34, 1955.
- [Sib65] K. S. Sibirskiĭ. On the number of limit cycles in the neighborhood of a singular point. *Differencialnye Uravnenija*, 1:53–66, 1965.
- [Sma98] S. Smale. Finding a horseshoe on the beaches of Rio. *Math. Intelligencer*, 20(1):39–44, 1998.
- [SN16] B. Sang and C. Niu. Solution of center-focus problem for a class of cubic systems. *Chin. Ann. Math. Ser. B*, 37(1):149–160, 2016.
- [WGD82] P. S. Wang, M. J. T. Guy, and J. H. Davenport. P-adic reconstruction of rational numbers. *SIGSAM Bull.*, 16(2):2–3, 1982.
- [Xio16] Y. Xiong. The number of limit cycles in perturbations of polynomial systems with multiple circles of critical points. *J. Math. Anal. Appl.*, 440(1):220–239, 2016.
- [Ż94] H. Żołądek. Quadratic systems with center and their perturbations. *J. Differential Equations*, 109(2):223–273, 1994.
- [Ż95] H. Żołądek. Eleven small limit cycles in a cubic vector field. *Nonlinearity*, 8(5):843–860, 1995.

- [Ż16] H. Żołądek. The CD45 case revisited. In *Mathematical Sciences with Multidisciplinary Applications*, pages 595–625, Cham, 2016. Springer International Publishing.
- [ZDHD92] Z. F. Zhang, T. R. Ding, W. Z. Huang, and Z. X. Dong. *Qualitative theory of differential equations*, volume 101 of *Translations of Mathematical Monographs*. American Mathematical Society, Providence, RI, 1992.